DESIGN, SYNTHESIS, AND APPLICATION OF AZADIBENZOCYCLOOCTYNE DERIVATIVES FOR TISSUE ENGINEERING AND NANOMATERIAL SCIENCE

by

CHEN ZHAO

(Under the Direction of Vladimir Popik)

ABSTRACT

Azadibenzocyclooctyne (ADIBO) is an efficient reagent for strain-promoted azide-alkyne cycloaddition (SPAAC) with long shelf life and high reactivity towards azides even in aqueous solutions. This dissertation is focused on the design, synthesis, and application of ADIBO derivatives. Alginates are a family of natural linear polysaccharides that become extremely important due to their ability to form hydrogels under mild conditions. Alginate hydrogels are widely used for cell culture and wound dressing as drug delivery system. A bis-ADIBO crosslinker was designed to achieve *in situ* crosslinking of azide-decorated alginate. The resulting hydrogels showed the potential application in tissue engineering. A cyclopropenone-masked ADIBO (photo-ADIBO) has also been developed, which can be deprotected by UV irradiation and revealed the ADIBO. A photo-ADIBO-ADIBO crosslinker was built to initiate the azide-decorated alginate crosslinking by photo-activation. The resulting hydrogels might be used for cell culture and wound dressing material. The ADIBO was also decorated with O-

Naphthoquinone Methide Precursors (o-NQMP) to synthesize photocleavable amphiphilic block polymer. This material can be a potential candidate for the development of drug delivery micelles.

INDEX WORDS: ADIBO, SPAAC, Alginate, Hydrogel, Photo-ADIBO, o-NQMP, Amphiphilic block copolymer.

DESIGN, SYNTHESIS, AND APPLICATION OF AZADIBENZOCYCLOOCTYNE DERIVATIVES FOR TISSUE ENGINEERING AND NANOMATERIAL SCIENCE

by

CHEN ZHAO

BS, NANKAI UNIVERSITY, CHINA, 2016

A Dissertation Submitted to the Graduate Faculty of the University of Georgia in Partial Fulfillment of the Requirements for the Degree

DOCTOR OF PHILOSOPHY

ATHENS, GEORGIA

2022

DESIGN, SYNTHESIS, AND APPLICATION OF AZADIBENZOCYCLOOCTYNE DERIVATIVES FOR TISSUE ENGINEERING AND NANOMATERIAL SCIENCE

by

CHEN ZHAO

Major Professor: Vladimir Popik

Committee: Robert S. Phillips

Jason Locklin

Electronic Version Approved:

Ron Walcott

Vice Provost for Graduate Education and Dean of the Graduate School

The University of Georgia

May 2022

ACKNOWLEDGEMENTS

I would like to express my most profound appreciation to my major professor Dr. Popik. He is an excellent academic advisor and provides encouragement and patience throughout my projects. His enthusiasm for scientific research inspires me to keep pursuing the beauty of chemistry. The completion of my dissertation would not have been possible without the support of Dr. Popik. I would also like to extend my deepest gratitude to my committee members, Dr. Robert S. Phillips, and Dr. Jason Locklin. They have invaluable insight into the chemistry and provide ingenious suggestions for my projects. I would also like to thank all my former and current group members, Dr. Nannan Lin, Dr. Kun Wang, Dr. Chris McNitt, Zichun Ren, Chris Molnar, Rohan Bhavsar, Shrey Patel, Shubham Sharma, Ayesha Nisathar, Patrick Foster. It was a pleasure to work with all of you. I must also thank my family members, especially my parents. They never waiver in their support and never hesitate to give the best to me. I love you so much. Thanks also to my boyfriend Yutian, he is always there whenever I need help, and we share a pleasant memory at the University of Georgia.

TABLE OF CONTENTS

LIST OF FIGURES

LIST OF SCHEMES

LIST OF TABLES

CHAPTER 1

INTRODUCTION

1.1 Strain-Promoted Azide-Alkyne Cycloaddition (SPAAC)

Arthur Michael discovered the cycloaddition reaction between alkynes and organic azides.[1] The Copper-Catalyzed Azide-Alkyne Cycloaddition reaction (CuAAC) has become instrumental click chemistry, a term introduced in 2001 by K.B. Sharpless to describe a range of "near-perfect" bond-forming reactions.[2] CuAAC reaction was reported simultaneously by the groups of Meldal and Sharpless.[3] The Bertozzi group further developed one of Huisgen's copper-free click reactions to overcome the cytotoxicity of the CuAAC reaction by introducing alkyne in a strained difluorooctyne (DIFO).[4] This Strain-Promoted Azide-Alkyne Cycloaddition (SPAAC) reaction proceeds as a concerted [3+2] cycloaddition by the exact mechanism as the Huisgen 1,3-dipolar cycloaddition.[5] The [3 + 2] cycloaddition of azides and cyclooctyne derivatives (Scheme 1. 1) exhibits high selectivity, high functional group tolerance, and straightforward reaction conditions. It is also compatible with protic, aprotic, and aqueous solvent systems and has a rapid rate with high yields. Moreover, this reaction is catalyst-free.

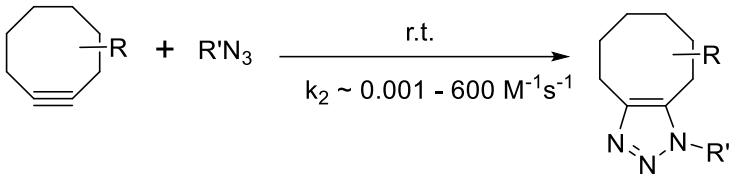

Scheme 1. 1 Strain-Promoted Azide-Alkyne Cycloaddition Between Cyclooctynes and Azides

A range of different cyclooctynes (Figure 1. 1) has been prepared for SPAAC. The first-generation cyclooctynes do not contain fused rings, fluorine substituents, or heteroatoms in the ring structure. The representative first-generation cyclooctyne **1.1** has a rate constant of $1.2 \cdot 10^{-3}$ $M^{-1} \cdot s^{-1}$ when reacts with benzyl azide in deuterated acetonitrile.[4] The second-generation cyclooctynes introduce high electronegative fluorine substituents to improve the SPAAC reactivity. The reaction rate constant of monofluorinated cyclooctyne **1.2** is increased to $4.3 \cdot 10^{-3}$ $M^{-1} \cdot s^{-1}$.[4] The monobenzodifluorocyclooctyne **1.3** has an even higher rate constant as $5.2 \cdot 10^{-2}$ $M^{-1} \cdot s^{-1}$.[6] Besides, dibenzocyclooctynes were prepared to enhance the reactivity of cyclooctynes. The reaction rate constant of compound **1.4** is $5.7 \cdot 10^{-2}$ $M^{-1} \cdot s^{-1}$ when it reacts with benzyl azide.[7] A cyclopropane ring introduction could also enhance cyclooctyne reactivity. The representative bicyclo[6.1.0]nonynes **1.5** exhibits as high as 0.14 $M^{-1} \cdot s^{-1}$ rate constant.[8] Heterocyclic cyclooctynes have also been prepared, such as azacyclooctynes, thiacyclooctynes, and oxacyclooctynes. The representative oxacyclooctyne **1.6** exhibits the reaction rate constant as 7.9 $M^{-1} \cdot s^{-1}$.[9]

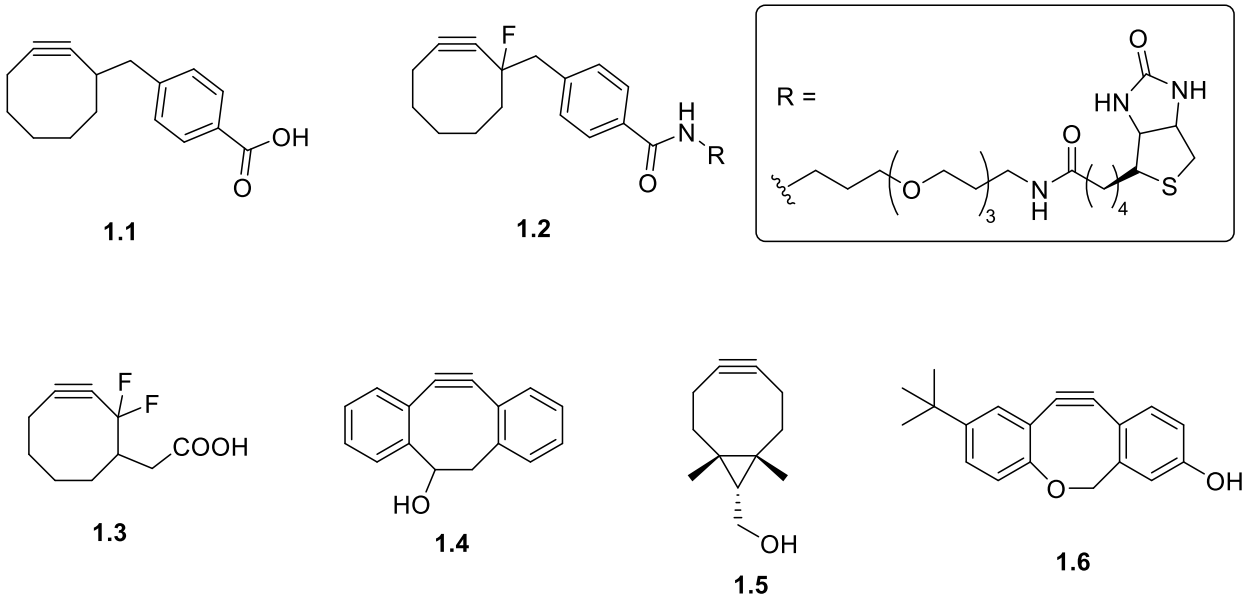

Figure 1. 1 Cylooctyne Derivatives

Strain-promoted azide-alkyne cycloaddition (SPAAC) has become an essential and powerful tool since its discovery. It has been widely applied in bioconjugation, polymer synthesis, and self-regenerative material production. Exploration on SPAAC as an essential click chemistry tool will be continued in the future.

1.2 Azadibenzocyclooctyne (ADIBO)

Dibenzocyclooctyne's synthesis is much more accessible among reactive cyclooctynes. The cyclooctynes' reactivity was vastly improved when a nitrogen atom substituted one of the saturated carbons in the cyclooctyne ring. Azadibenzocyclooctyne (ADIBO) is one of the most reactive cyclooctyne species (Figure 1. 2).[6, 10-14] The reaction kinetics of representative ADIBO **1.7** and benzyl azide was determined in methanol and the rate constant was 0.31 $M^{-1} \cdot s^{-1}$.[11]

Moreover, ADIBO could be easily synthesized starting from the inexpensive precursor.[15] ADIBO exhibits excellent aqueous stability and long shelf-life. These properties make ADIBO a popular SPAAC tool.

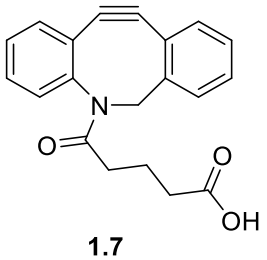

1.7

Figure 1. 2 Azadibenzocyclooctyne (ADIBO)

1.3 Cyclopropenone-Based Photoinduced Click Chemistry

Light-triggered click chemistry offers unique spatiotemporal control. In 2009, our group developed the cyclopropenone-masked dibenzocyclooctynes **1.8** for photoinduced, copper-free azide-alkyne cycloaddition reaction.[16] Cyclopropenones are unreactive toward azides under ambient conditions in the dark, while the UV irradiation could rapidly reveal the reactive strained alkynes **1.9** (Scheme 1. 2). This photo-triggered click reaction has been successfully utilized in several applications, including glycan labeling, surface functionalization, nanoparticles functionalization, hydrogel derivatization, and synthesis of hetero-bivalent agents.[9, 17-24]

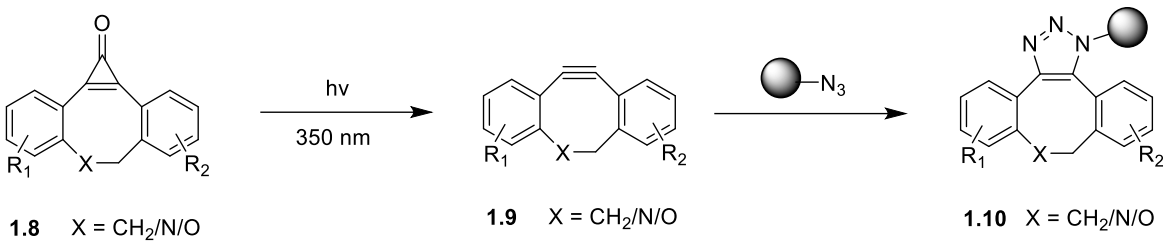

Scheme 1. 2 Light-Induced Strain-Promoted Azide-Alkyne Cycloaddition

1.4 Alginate

Alginates are linear polysaccharides consisting of 1→4 linked β-D-mannuronic acid (M) and α-L-guluronic acid (G) (Figure 1. 3).[25] The most general arrangement is long sequences of G residues and M residues inserted between mixed G and M residues. The salt of alginates is extracted from brown seaweed.

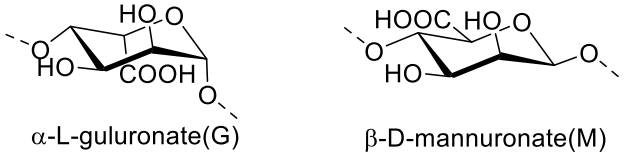

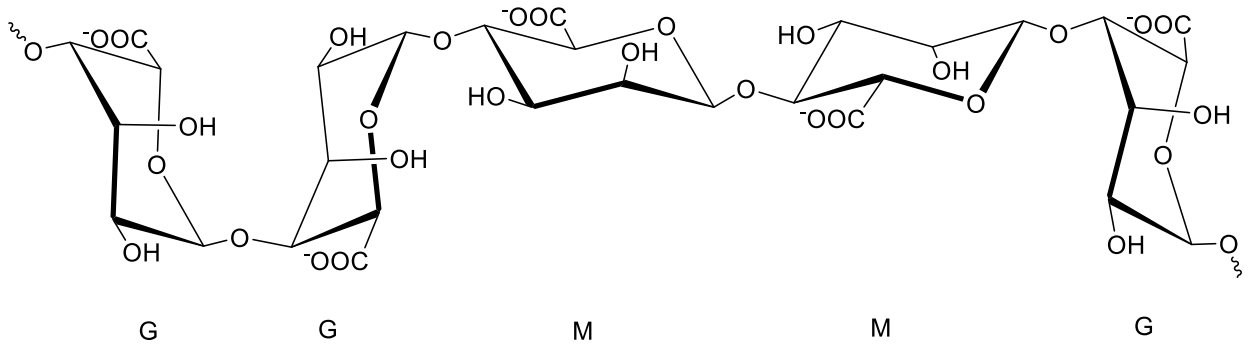

Figure 1. 3 Chemical Structures of α-L-guluronic acid (G), β-D-mannuronic acid (M), and General Chain Conformation

Divalent cations can crosslink alginate. Ca^{2+} is the most used one to induce alginate solution's gelation. The driving force of ionic crosslinking is the interactions between G-blocks which associate to form tightly held junctions in the presence of divalent cations.[26] The general gelation mechanism of alginate is well known as the "egg-box" model, which was proposed by Dr. Grant in 1973 to describe the Ca^{2+} mediated gelation (Figure 1. 4).[27] In addition to G-blocks, MG blocks could also participate. Alginate with high G content can form brittle and robust gels, while alginate rich in M blocks makes softer and more elastic gels.

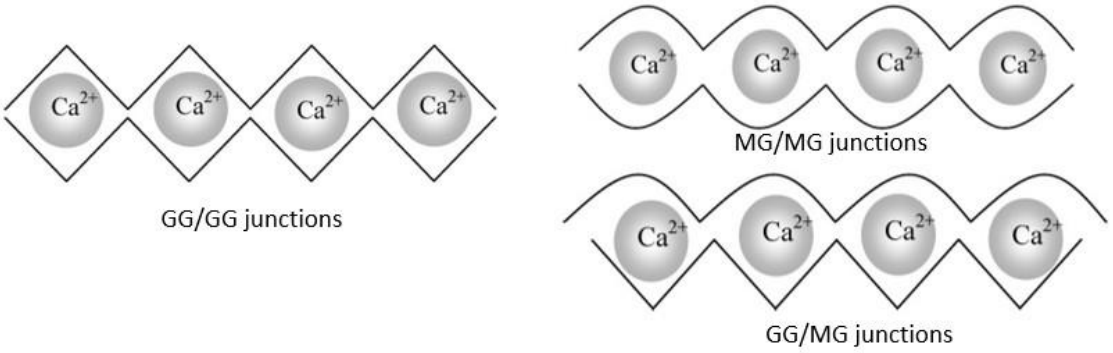

Figure 1. 4 Ionic Crosslinked Alginate Hydrogel

Alginate could also be crosslinked covalently to generate non-reversible and robust chemical bonds. Furthermore, introducing covalent crosslinking enables the control of mechanical properties in alginate hydrogels. Covalently crosslinked hydrogels can be synthesized via various reactions, including Schiff base reaction, click chemistry, and photo-induced thiol-ene reaction (Scheme 1. 3).[28-30]

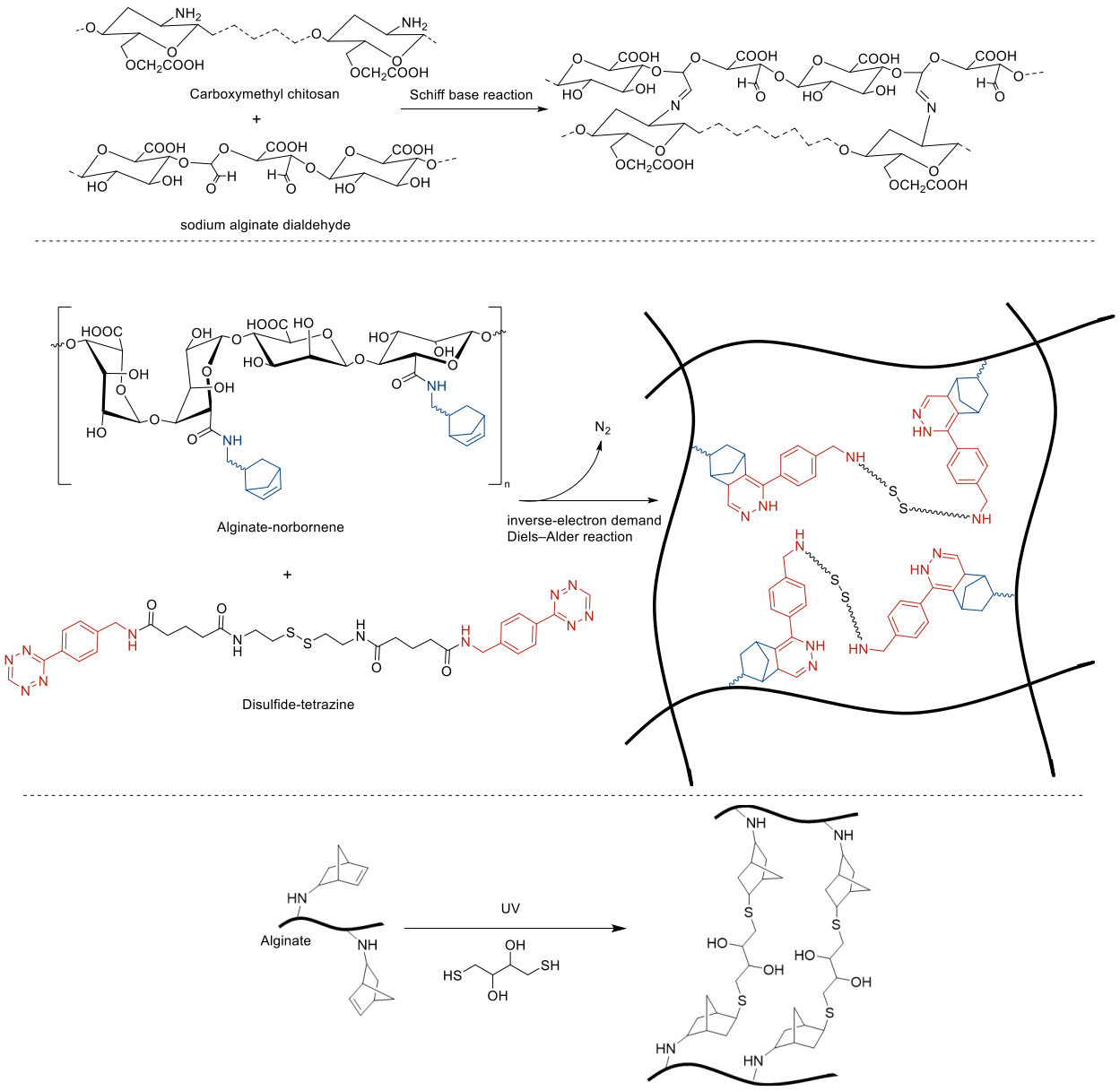

Scheme 1. 3 Covalent Crosslinked Alginate Hydrogel

Alginate-based hydrogels' three-dimensional interconnected structure shows high water absorption ability and permits the unhindered passage of nutrients, oxygen, and therapeutic factor. These properties broaden alginate hydrogel applications in many areas like three-dimensional cell culture, wound dressing tissue, and drug delivery system.[25, 31, 32]

1.5 Naphthoquinone Methide Precursor (o-NQMP)

Photochemical generation of a reactive diene can be done in physiological conditions while not requiring a catalyst or generating any byproducts. Thus, this reaction has been widely explored in biological studies and material chemistry. Appropriate precursors can be photoactivated to generate reactive heterodienes such as o-quinone methides, which are involved in the hetero-Diels-Alder reaction.

Our group has reported a photo-click platform for the facile and efficient light-induced hetero-Diels-Alder reaction. The naphthoquinone methide precursor **1.11** can be activated using UV light to generate o-naphthoquinone methide (o-NQM) **1.12** in high quantum yield ($\Phi = 0.17 \pm 0.02$). The reactive o-NQM undergoes facile hetero-Diels-Alder reaction with vinyl ethers or enamines to afford photostable derivatives of benzo[g]chromans **1.13** in high yields. With rapid hydration, the unreacted o-NQM regenerates starting **1.11** (Scheme 1. 4).[33] The efficient ligation under ambient conditions in an aqueous solution could be achieved by this method, and the fast kinetics allows for the high spatial and temporal resolution.

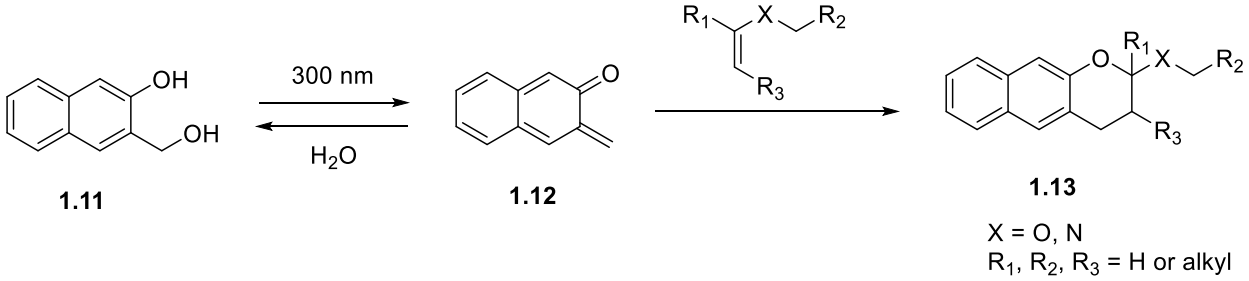

Scheme 1. 4 Light-Induced Hetero-Diels-Alder Cycloaddition Between o- Naphthoquinone

Methide Precursor and Electron-Rich Polarized Olefins

Notably, o-NQM exhibits selectivity when generated in the presence of water, alcohol, or thiol. The aliphatic vinyl ethers like **1.15** and enamines could be successfully added to o-NQM in aqueous solutions while hydration of o-NQM to **1.14** outcompetes cycloaddition for other alkenes (Scheme 1. 5).

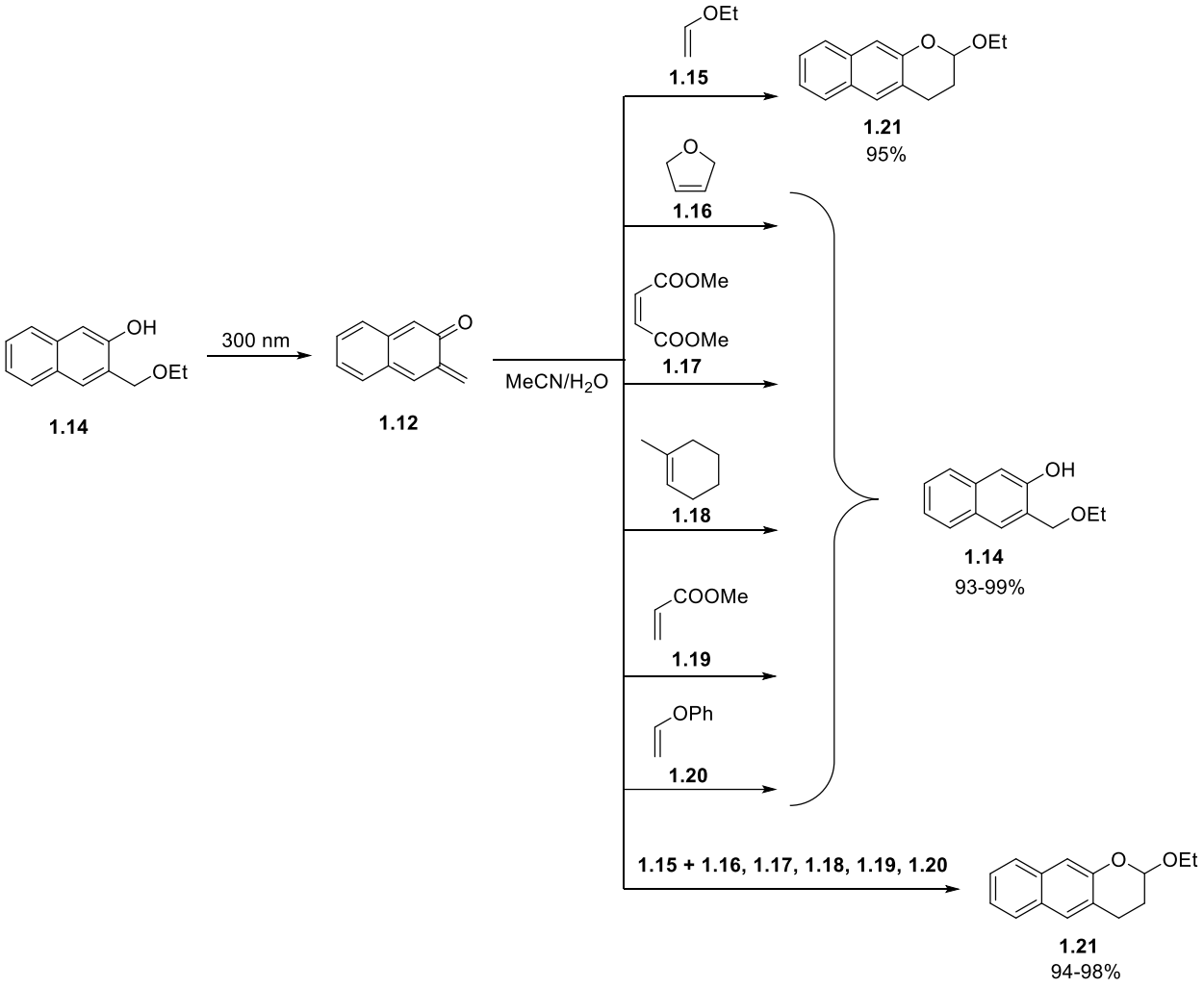

Scheme 1. 5 Competitions Between Hydration and Cycloaddition

Various functional groups were decorated on the 8-position of the o-NQMP naphthalene ring

(Figure 1. 5). It has been demonstrated that these 8-position substituents of o-NQMPs remain intact under the Diels-Alder photo-click conditions.

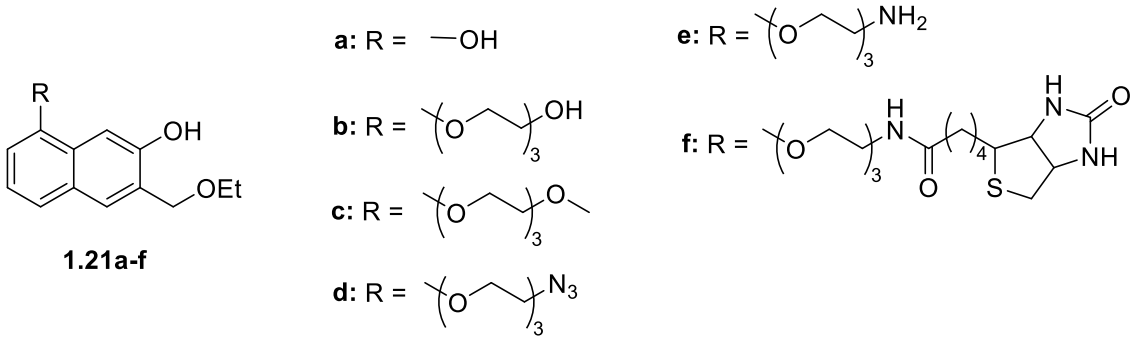

Figure 1. 5 o-NQMPs with Substituent in 8-Position

This photo-click platform has been utilized for surface derivatization, surface patterning, and spatiotemporal controlled DNA-protein interactions.[34-36]

1.6 References

1. Michael, A.; Auf, U. D. E. V. D., Acetylendicarbonsäuremethylester. *Journal für praktische Chemie* **1893,** *48*, 94-95.

2. Hein, J. E.; Fokin, V. V., Copper-catalyzed azide-alkyne cycloaddition (CuAAC) and beyond: new reactivity of copper(I) acetylides. *Chemical Society Reviews* **2010,** *39* (4), 1302-1315.

3. Rostovtsev, V. V.; Green, L. G.; Fokin, V. V.; Sharpless, K. B., A stepwise huisgen cycloaddition process: copper(I)-catalyzed regioselective "ligation" of azides and terminal alkynes. *Angewandte Chemie (International ed. in English)* **2002,** *41* (14), 2596-9.

4. Agard, N. J.; Baskin, J. M.; Prescher, J. A.; Lo, A.; Bertozzi, C. R., A Comparative Study of Bioorthogonal Reactions with Azides. *ACS Chemical Biology* **2006,** *1* (10), 644-648.

5. Huisgen, R., 1, 3-dipolar cycloadditions. Past and future. *Angewandte Chemie International Edition in English* **1963,** *2* (10), 565-598.

6. Codelli, J. A.; Baskin, J. M.; Agard, N. J.; Bertozzi, C. R., Second-Generation Difluorinated Cyclooctynes for Copper-Free Click Chemistry. *Journal of the American Chemical Society* **2008,** *130* (34), 11486-11493.

7. Ning, X.; Guo, J.; Wolfert, M. A.; Boons, G.-J., Visualizing Metabolically Labeled Glycoconjugates of Living Cells by Copper-Free and Fast Huisgen Cycloadditions. *Angewandte Chemie International Edition* **2008,** *47* (12), 2253-2255.

8. Dommerholt, J.; Schmidt, S.; Temming, R.; Hendriks, L. J. A.; Rutjes, F. P. J. T.; van Hest, J. C. M.; Lefeber, D. J.; Friedl, P.; van Delft, F. L., Readily accessible bicyclononynes for bioorthogonal labeling and three-dimensional imaging of living cells. *Angewandte Chemie (International ed. in English)* **2010,** *49* (49), 9422-9425.

9. McNitt, C. D.; Popik, V. V., Photochemical generation of oxa-dibenzocyclooctyne (ODIBO) for metal-free click ligations. *Organic & Biomolecular Chemistry* **2012,** *10* (41), 8200-8202.

10. Sletten, E. M.; Bertozzi, C. R., A Hydrophilic Azacyclooctyne for Cu-Free Click Chemistry. *Organic Letters* **2008,** *10* (14), 3097-3099.

11. Debets, M. F.; van Berkel, S. S.; Schoffelen, S.; Rutjes, F. P. J. T.; van Hest, J. C. M.; van Delft, F. L., Aza-dibenzocyclooctynes for fast and efficient enzyme PEGylation via copper-

free (3+2) cycloaddition. *Chemical Communications* **2010,** *46* (1), 97-99.

12. Ning, X.; Guo, J.; Wolfert, M. A.; Boons, G. J., Visualizing metabolically labeled glycoconjugates of living cells by copper-free and fast huisgen cycloadditions. *Angewandte Chemie (International ed. in English)* **2008,** *47* (12), 2253-5.

13. Jewett, J. C.; Sletten, E. M.; Bertozzi, C. R., Rapid Cu-Free Click Chemistry with Readily Synthesized Biarylazacyclooctynones. *Journal of the American Chemical Society* **2010,** *132* (11), 3688-3690.

14. Baskin, J. M.; Prescher, J. A.; Laughlin, S. T.; Agard, N. J.; Chang, P. V.; Miller, I. A.; Lo, A.; Codelli, J. A.; Bertozzi, C. R., Copper-free click chemistry for dynamic in vivo imaging. *Proceedings of the National Academy of Sciences of the United States of America* **2007,** *104* (43), 16793-7.

15. Kuzmin, A.; Poloukhtine, A.; Wolfert, M. A.; Popik, V. V., Surface Functionalization Using Catalyst-Free Azide−Alkyne Cycloaddition. *Bioconjugate Chemistry* **2010,** *21* (11), 2076-2085.

16. Poloukhtine, A. A.; Mbua, N. E.; Wolfert, M. A.; Boons, G.-J.; Popik, V. V., Selective Labeling of Living Cells by a Photo-Triggered Click Reaction. *Journal of the American Chemical Society* **2009,** *131* (43), 15769-15776.

17. Starke, F.; Walther, M.; Pietzsch, H.-J., A novel dibenzo-azacyclooctyne precursor for application in regioselective copper-free click chemistry, obtained by an innovative 3-step synthesis. *Archive for Organic Chemistry* **2010,** *2010* (11), 350-359.

18. Orski, S. V.; Poloukhtine, A. A.; Arumugam, S.; Mao, L.; Popik, V. V.; Locklin, J., High Density Orthogonal Surface Immobilization via Photoactivated Copper-Free Click Chemistry. *Journal of the American Chemical Society* **2010,** *132* (32), 11024-11026.

19. Laradji, A. M.; McNitt, C. D.; Yadavalli, N. S.; Popik, V. V.; Minko, S., Robust, Solvent-Free, Catalyst-Free Click Chemistry for the Generation of Highly Stable Densely Grafted Poly(ethylene glycol) Polymer Brushes by the Grafting To Method and Their Properties. *Macromolecules* **2016,** *49* (20), 7625-7631.

20. Bjerknes, M.; Cheng, H.; McNitt, C. D.; Popik, V. V., Facile Quenching and Spatial Patterning of Cyloоctynes via Strain-Promoted Alkyne–Azide Cycloaddition of Inorganic Azides. *Bioconjugate Chemistry* **2017,** *28* (5), 1560-1565.

21. Luo, W.; Gobbo, P.; McNitt, C. D.; Sutton, D. A.; Popik, V. V.; Workentin, M. S., "Shine & Click" Photo-Induced Interfacial Unmasking of Strained Alkynes on Small Water-Soluble Gold Nanoparticles. *Chemistry – A European Journal* **2017,** *23* (5), 1052-1059.

22. Sun, L.; Gai, Y.; McNitt, C. D.; Sun, J.; Zhang, X.; Xing, W.; Li, Z.; Popik, V. V.; Zeng, D., Photo-Click-Facilitated Screening Platform for the Development of Hetero-Bivalent Agents with High Potency. *The Journal of Organic Chemistry* **2020,** *85* (9), 5771-5777.

23. Luo, W.; Legge, S. M.; Luo, J.; Lagugné-Labarthet, F.; Workentin, M. S., Investigation of Au SAMs Photoclick Derivatization by PM-IRRAS. *Langmuir* **2020,** *36* (4), 1014-1022.

24. Friscourt, F.; Fahrni, C. J.; Boons, G.-J., A Fluorogenic Probe for the Catalyst-Free Detection of Azide-Tagged Molecules. *Journal of the American Chemical Society* **2012,** *134*

(45), 18809-18815.

25. Pawar, S. N.; Edgar, K. J., Alginate derivatization: A review of chemistry, properties and applications. *Biomaterials* **2012,** *33* (11), 3279-3305.

26. Hu, C.; Lu, W.; Mata, A.; Nishinari, K.; Fang, Y., Ions-induced gelation of alginate: Mechanisms and applications. *International Journal of Biological Macromolecules* **2021,** *177*, 578-588.

27. Sikorski, P.; Mo, F.; Skjåk-Bræk, G.; Stokke, B. T., Evidence for Egg-Box-Compatible Interactions in Calcium−Alginate Gels from Fiber X-ray Diffraction. *Biomacromolecules* **2007,** *8* (7), 2098-2103.

28. Xu, W.; Liu, K.; Li, T.; Zhang, W.; Dong, Y.; Lv, J.; Wang, W.; Sun, J.; Li, M.; Wang, M.; Zhao, Z.; Liang, Y., An in situ hydrogel based on carboxymethyl chitosan and sodium alginate dialdehyde for corneal wound healing after alkali burn. *Journal of Biomedical Materials Research Part A* **2019,** *107* (4), 742-754.

29. Siboro, S. A. P.; Anugrah, D. S. B.; Ramesh, K.; Park, S.-H.; Kim, H.-R.; Lim, K. T., Tunable porosity of covalently crosslinked alginate-based hydrogels and its significance in drug release behavior. *Carbohydrate Polymers* **2021,** *260*, 117779.

30. Handrea-Dragan, M.; Botiz, I., Multifunctional Structured Platforms: From Patterning of Polymer-Based Films to Their Subsequent Filling with Various Nanomaterials. *Polymers* **2021,** *13* (3).

31. Balakrishnan, B.; Mohanty, M.; Umashankar, P. R.; Jayakrishnan, A., Evaluation of an in

situ forming hydrogel wound dressing based on oxidized alginate and gelatin. *Biomaterials* **2005,** *26* (32), 6335-6342.

32. García-Astrain, C.; Avérous, L., Synthesis and evaluation of functional alginate hydrogels based on click chemistry for drug delivery applications. *Carbohydrate Polymers* **2018,** *190*, 271-280.

33. Arumugam, S.; Popik, V. V., Light-Induced Hetero-Diels−Alder Cycloaddition: A Facile and Selective Photoclick Reaction. *Journal of the American Chemical Society* **2011,** *133* (14), 5573-5579.

34. Arumugam, S.; Popik, V. V., Patterned Surface Derivatization Using Diels–Alder Photoclick Reaction. *Journal of the American Chemical Society* **2011,** *133* (39), 15730-15736.

35. Arumugam, S.; Orski, S. V.; Locklin, J.; Popik, V. V., Photoreactive Polymer Brushes for High-Density Patterned Surface Derivatization Using a Diels–Alder Photoclick Reaction. *Journal of the American Chemical Society* **2012,** *134* (1), 179-182.

36. Richter, S. N.; Maggi, S.; Mels, S. C.; Palumbo, M.; Freccero, M., Binol Quinone Methides as Bisalkylating and DNA Cross-Linking Agents. *Journal of the American Chemical Society* **2004,** *126* (43), 13973-13979.

CHAPTER 2

IN SITU CROSS-LINKABLE HYDROGEL VIA STRAIN-PROMOTED AZIDE-ALKYNE CYCLOADDITION

2.1 Introduction

Alginate hydrogels are versatile, thanks to the simple crosslinking process. These hydrogels can be easily prepared by ionic or covalent gelation. They exhibit excellent biocompatibility, tunable porosity, and mechanical properties. These features give alginate hydrogel applications in many areas such as three-dimensional cell culture,[1-3] cartilage tissue engineering,[4, 5] wound healing materials,[6-8] and drug delivery systems.[9-11]

This project designed a clickable alginate hydrogel that enables covalent, catalyst-free crosslinking. The sodium alginates were chemically modified with azide groups to yield Alg-azide (**Alg-A**). And a water-soluble bis-ADIBO crosslinker was designed to achieve the gelation of **Alg-A**. The mechanical properties of the resulting hydrogels could be easily tuned by varying the ratio between azide groups on alginate backbones and crosslinkers. We followed the gelation process by monitoring storage and loss modulus change to determine the gel points and saturation storage modulus. The water absorption behavior of the hydrogels was also studied, and the swollen hydrogels' morphology was determined by scanning electron microscopy (SEM).

2.2 Bis-ADIBO Crosslinker and Alginate Derivatives Design and Synthesis

The strain-promoted azide-alkyne cycloaddition (SPAAC) has become an ideal coupling approach to induce gelation. Azadibenzocyclooctyne (ADIBO) is one of the most reactive cyclooctyne derivatives towards azides. Thus, we have designed a water-soluble bis-ADIBO crosslinker 2.1 to achieve the alginate gelation in this project. **ADIBO-NH$_2$** was prepared by previously published procedure by Popik group[12] with slight modifications. The synthesis started from the commercially available dibenzosuberenone, which was converted to oxime **2.2** using hydroxylamine hydrochloride. And then, Eaton's reagent (5.5% P_2O_5 in methanesulfonic acid) was used to perform Beckmann rearrangement. The resulting amide **2.3** was reduced to amine **2.4** using lithium aluminium hydride. A linker **2.5** with protected amine was synthesized and coupled with compound **2.4** using DCC (N,N'-dicyclohexylcarbodiimide) and DMAP (4-dimethylaminopyridine) to yield compound **2.6,** which was brominated and eliminated to yield cyclooctyne **2.7**. The amine was deprotected to give **ADIBO-NH$_2$**, which was coupled by ethylenediaminetetraacetic acid (EDTA) dianhydride to produce water-soluble bis-ADIBO **2.1** (Scheme 2. 1). The aqueous solubility of **2.1** was determined as 0.43 mM by UV.

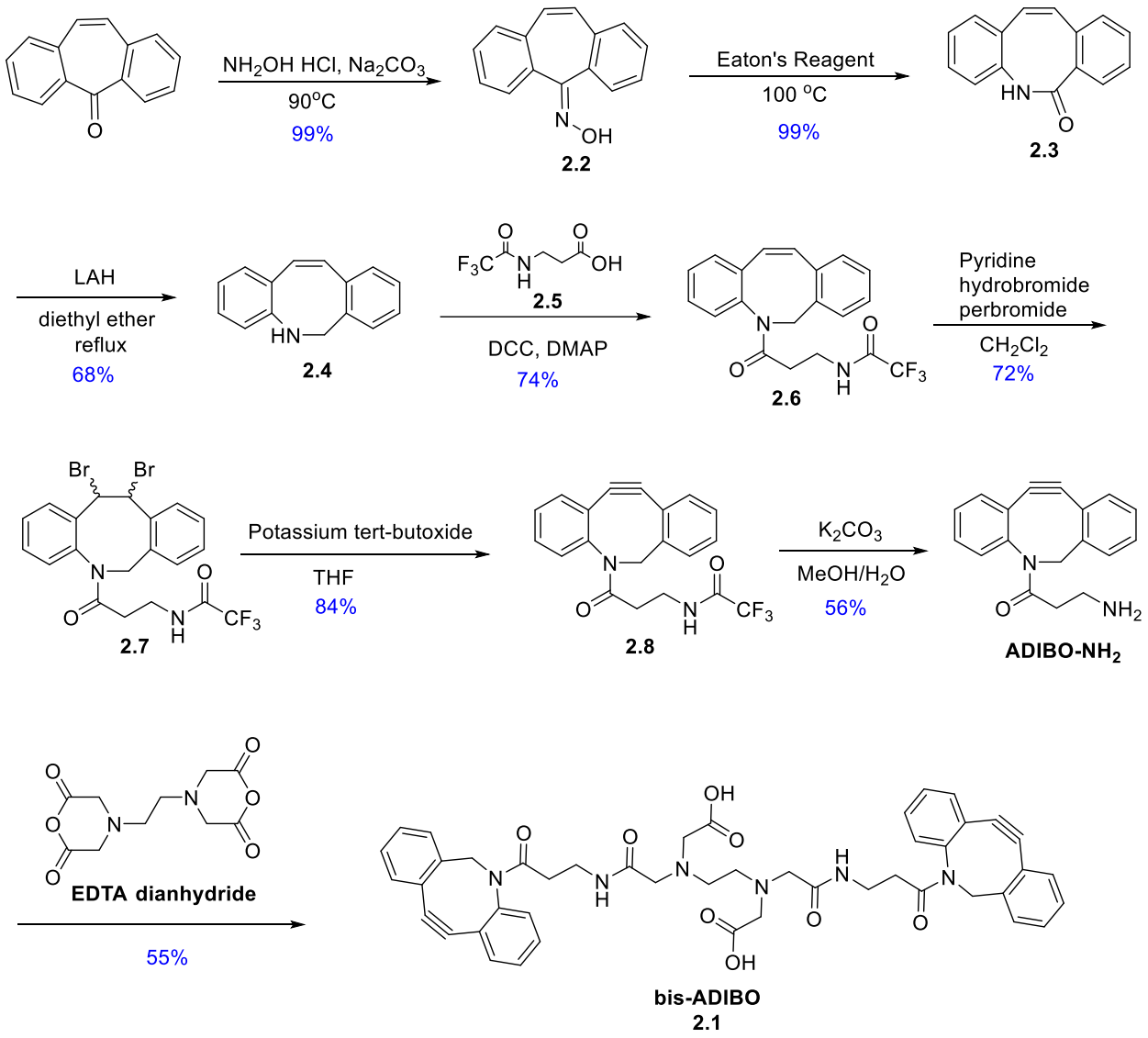

Scheme 2. 1 Synthesis of bis-ADIBO 2.1

We designed an azide linker **2.11** for the alginate backbone to make it cross-linkable via SPAAC. The synthesis started from the commercially available tetraethylene glycol, which was mesylated by methanesulfonyl chloride to yield dimesylated product **2.9**. Sodium azide was utilized to convert **2.9** to bis-azide functionalized product **2.10**. One of the azide groups was reduced to the amine group by Staudinger reaction to yield linker **2.11** (Scheme 2. 2).

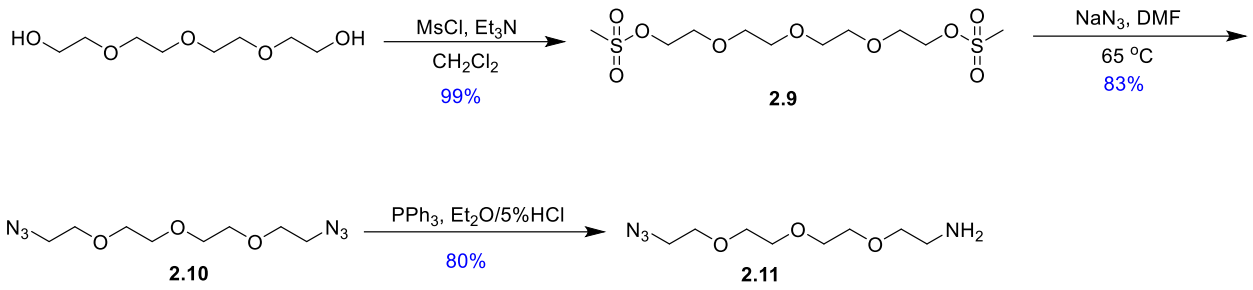

Scheme 2. 2 Synthesis of Linker 2.11

The linker **2.11** was conjugated on commercially available ultra-low viscosity alginate acid sodium salt via carbodiimide coupling to yield azide functionalized alginate **Alg-A** (Scheme 2. 3). Different degree of substitution (DS) was achieved by varying the ratio between alginate and 1-ethyl-3-(3′-dimethylaminopropyl)carbodiimide · HCl (EDC · HCl). We successfully synthesized 16% (**Alg-A1**), 20% (**Alg-A2**), and 24% (**Alg-A3**) azide substituted alginate. The DS was calculated from the elementary analysis results.

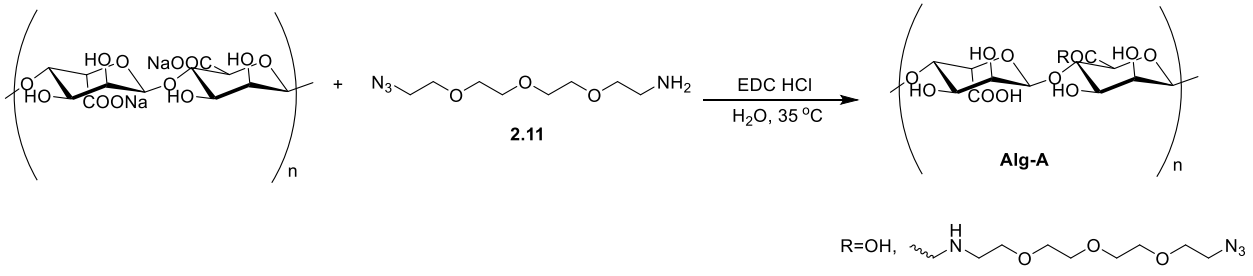

Scheme 2. 3 Synthesis of Alg-A

Infrared spectroscopy (IR) was used to characterize **Alg-A**. The existence of an absorbance band at 2113 cm^{-1} proves the success of azide functionalization (Figure 2. 1).

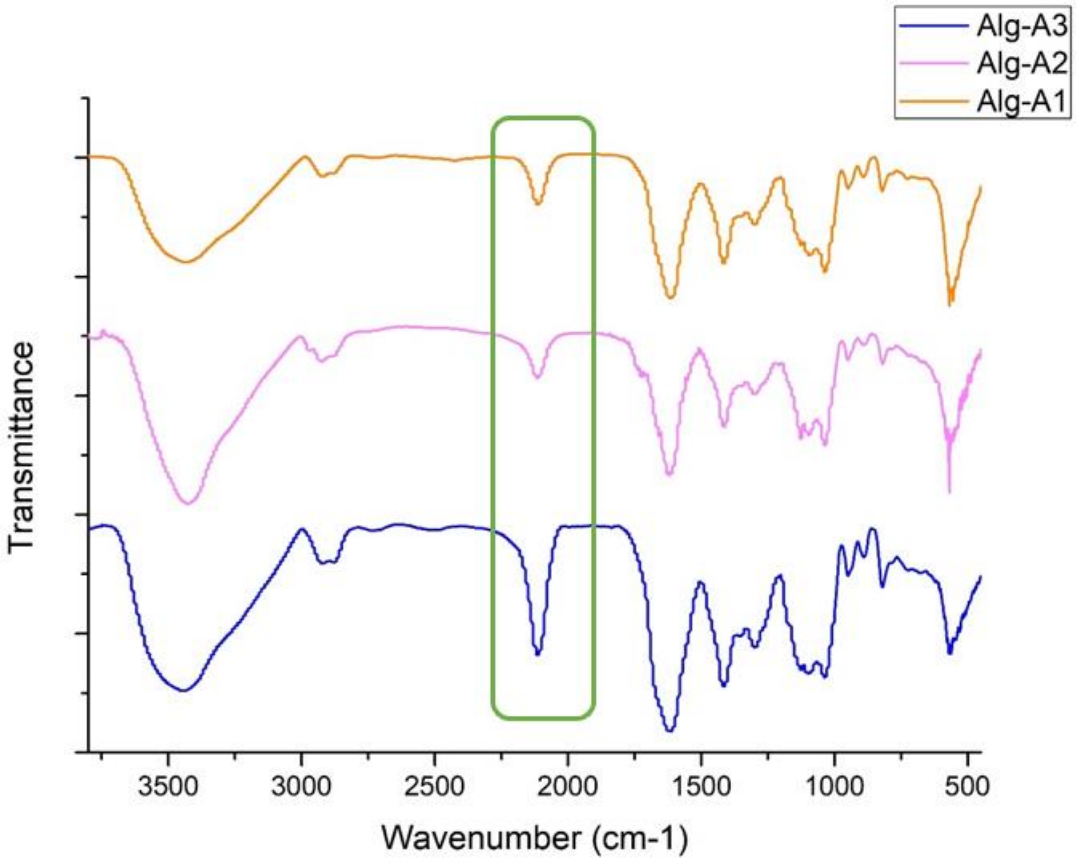

Figure 2. 1 IR Spectra of Alg-A

2.3 Preparation of Alginate Hydrogel

The **Alg-A** was crosslinked by **2.1** in DMSO/H_2O (1:4, v:v) solution. The **Alg-A** was dissolved in DI water to a concentration of 53 mg/mL (w/v) and bis-ADIBO **2.1** was dissolved in DMSO/H_2O just before use. These two solutions were mixed to yield hydrogels with 4% (w/w) **Alg-A** (Scheme 2. 4).

There are two cyclooctyne units in each bis-ADIBO **2.1** molecule, and each equivalent of cyclooctyne unit can react with the same equivalent of azide. Thus, hydrogels with azide/bis-

ADIBO **2.1** molar ratios 1:0.3 and 1:0.45 should have unreacted azides after gelation. These two hydrogels were prepared to explore how the bis-ADIBO **2.1** amount affects the hydrogel properties in the presence of unreacted azides. While hydrogel with azide/bis-ADIBO **2.1** molar ratio 1:0.75 should have unreacted cyclooctyne units after gelation, and this hydrogel was prepared to demonstrate how the hydrogel properties change in the presence of excess cyclooctyne units.

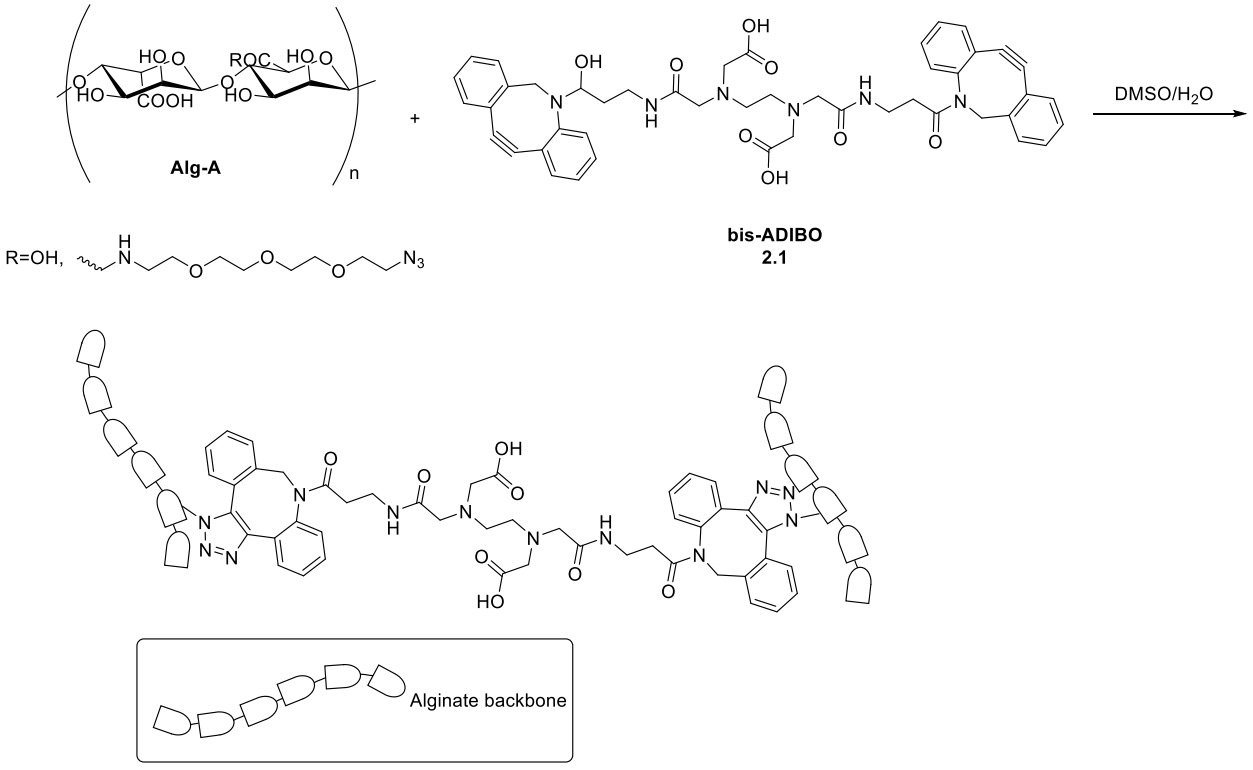

Scheme 2. 4 Alginate Hydrogel Preparation

2.4 Rheology Analysis and Absorption Behavior Tests

Alginate hydrogels rheological characterization was performed using a DHR2 rheometer.

The **Alg-A** and **2.1** solutions were mixed at 0 °C to slow down the crosslinking reaction during the mixing step. The temperature was then increased to 25 °C at 20.0 °C/min ramp rate, and the storage and loss modulus were monitored starting from this step. The temperature was maintained at 25 °C and the storage and loss modulus were monitored in the following 30 min. The experiment was repeated three times for each sample.

The temperature ramp and time sweep data for three different DS 4% **Alg-A** with azide/bis-ADIBO **2.1** = 1/0.30 were collected (Figure 2. 2). In all three DS **Alg-A** samples, we observed the loss modulus (G'') was higher than the storage modulus (G') at the beginning of the temperature ramp. This scenario indicates the solution showed fluid flow-like behavior. G' increased sharply subsequently, which can be considered as a result of the sol-gel transition. The cross-over point of G' and G'' is defined as gel point. The gel point formation indicates the solution has transitioned from fluid flow-like behavior to solid elastic behavior. G' reached a plateau within 8 min for each sample which shows the rapid gel formation. The gel point happened earlier with increasing azide substitution on the alginate backbone. The maximum value of G' also increased with the increasing azide substitution on the alginate backbone, which shows the ability to manipulate hydrogel mechanical properties by controlling the azide substitution.

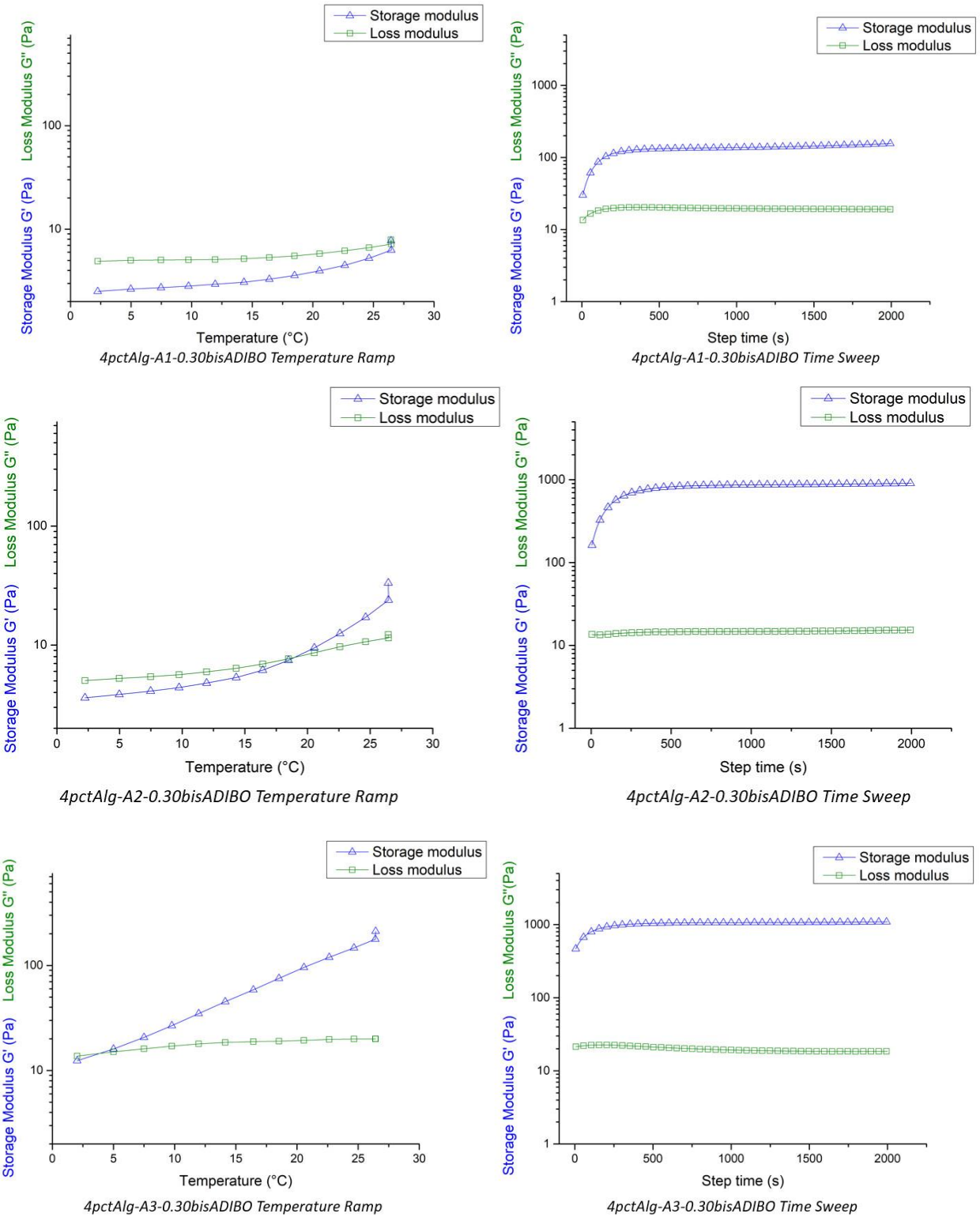

Figure 2. 2 Gelation Rheology of 4% Alg-A with azide/bis-ADIBO 2.1 = 1/0.30

We then explored the gelation rheology for three different DS 4% **Alg-A** with azide/bis-ADIBO **2.1** = 1/0.45 (Figure 2. 3). The starting G'' was higher than starting G' for the **Alg-A1** sample and **Alg-A2** sample while the beginning G' was higher than the beginning G'' for the **Alg-A3** sample. The gel point for the **Alg-A3** sample happened before the temperature ramp and this sample exhibited the fastest gelation. The maximum value of G' increased with increasing azide substitution on the alginate backbone.

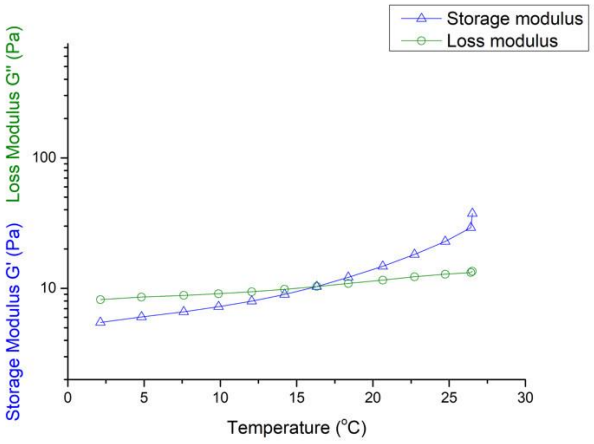

4pctAlg-A1-0.45bisADIBO Temperature Ramp

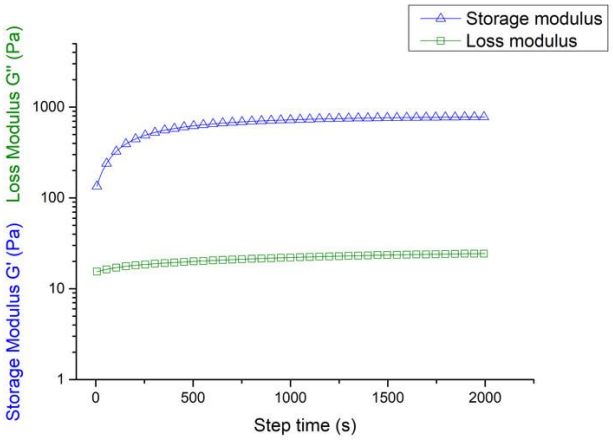

4pctAlg-A1-0.45bisADIBO Time Sweep

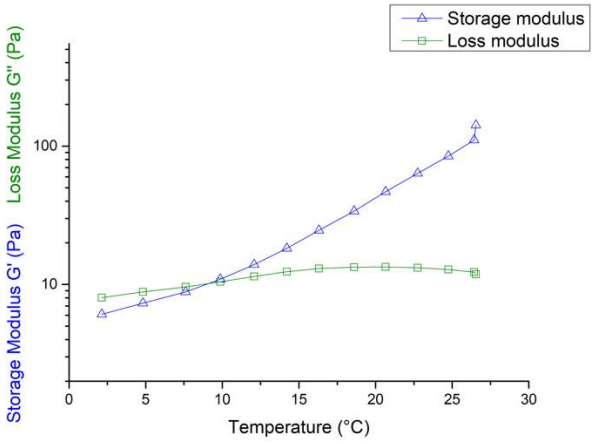

4pctAlg-A2-0.45bisADIBO Temperature Ramp

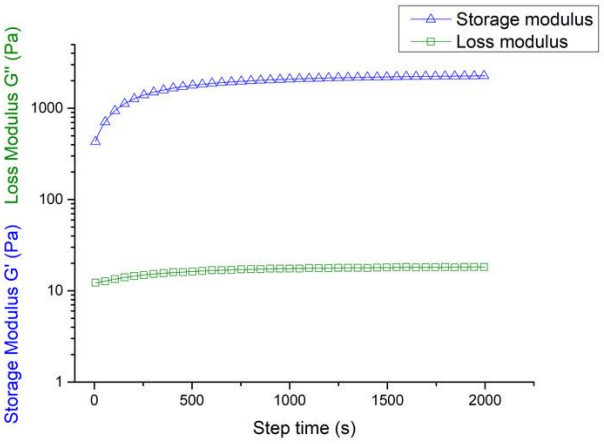

4pctAlg-A2-0.45bisADIBO Time Sweep

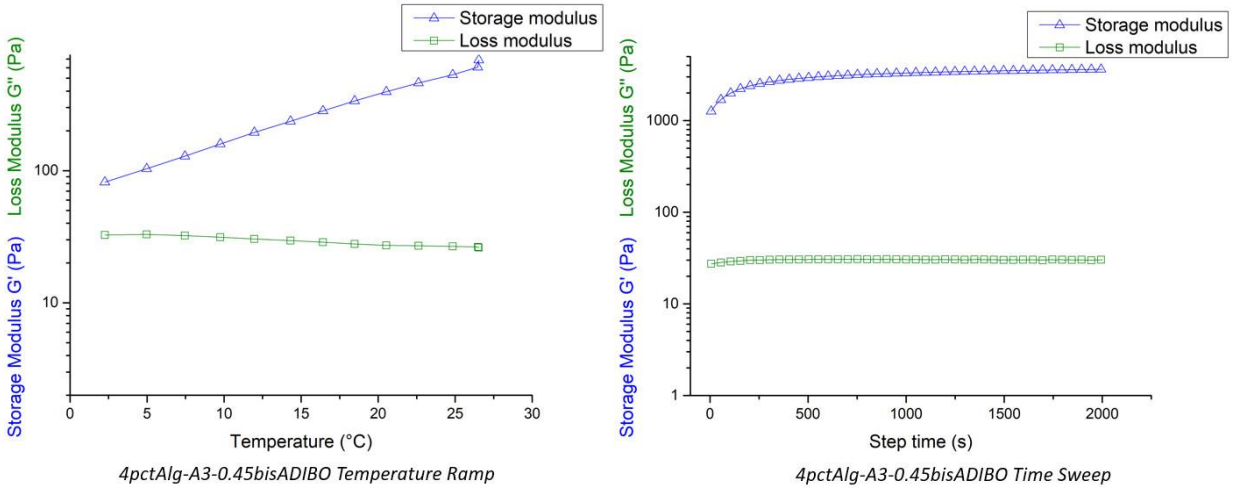

Figure 2. 3 Gelation Rheology of 4% Alg-A with azide/bis-ADIBO 2.1 = 1/0.45

The gelation rheology for three different DS 4% **Alg-A** with azide/bis-ADIBO **2.1** = 1/0.75 (Figure 2. 4) was also explored. The hydrogel became more rigid when using a higher azide substituted alginate backbone. And the gelation process was shortened when higher azide substituted alginate was used.

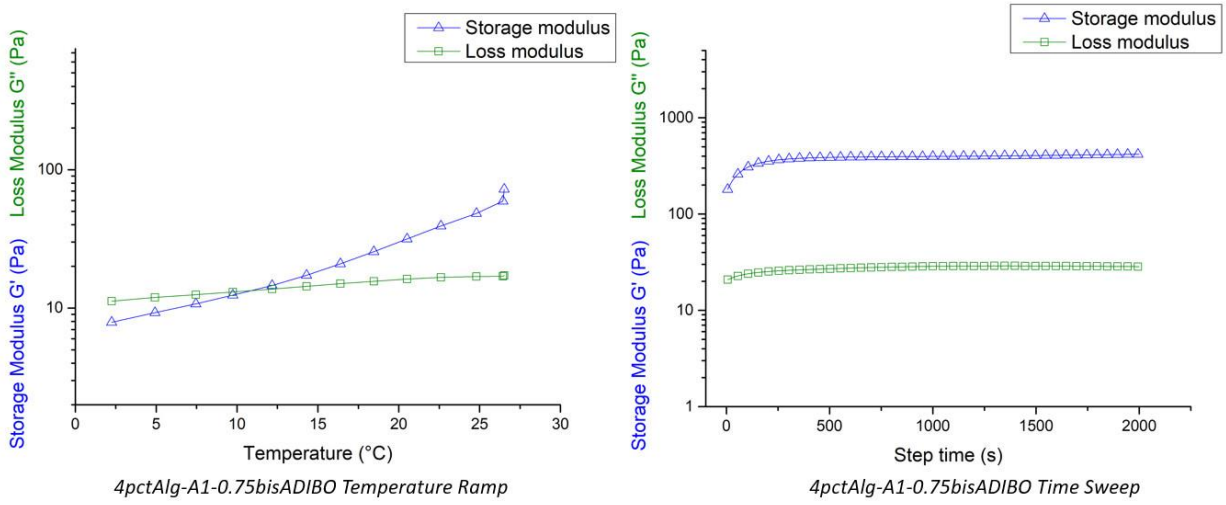

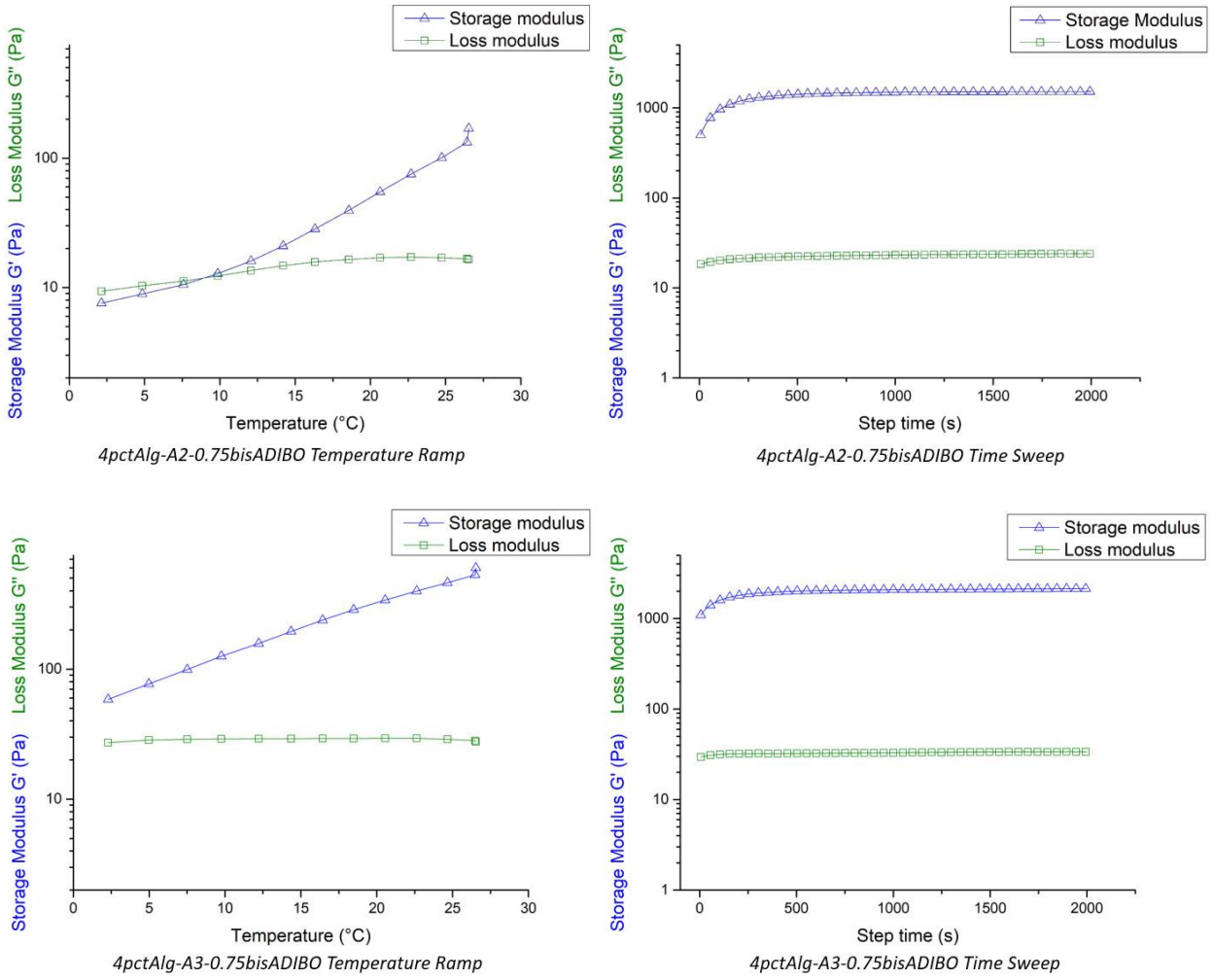

Figure 2. 4 Gelation Rheology of 4% Alg-A with azide/bis-ADIBO 2.1 = 1/0.75

The G' at a plateau for each hydrogel sample was summarized (Figure 2. 5). We found that hydrogels shared the same azide/bis-ADIBO ratio tend to have higher maximum G' when the azide substitution on the alginate backbone increased. The maximum value of G' could also be increased by increasing the crosslinker amount when the system has unreacted azides after gelation. However, the maximum G' was decreased when the system has unreacted cyclooctyne units after gelation. This may be because one of the cyclooctyne units in bis-ADIBO **2.1** reacts

rapidly with azides on the alginate backbone and leaves much fewer available azides to conjugate the other cyclooctyne units in the crosslinker. This scenario results in the decrease of crosslinking points when the system has unreacted cyclooctyne units after gelation.

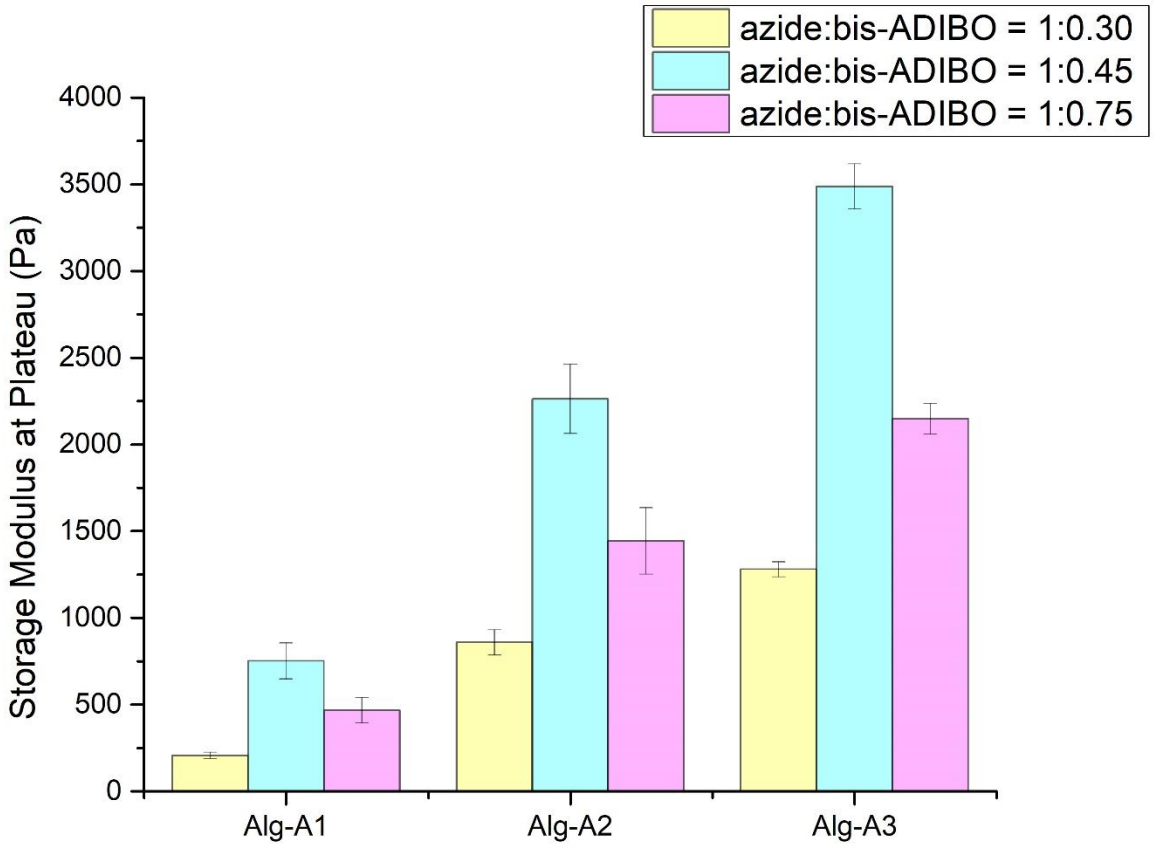

Figure 2. 5 Alginate Hydrogels Storage Modulus at Plateau

The absorption behavior for hydrogels was also determined. The freshly made hydrogel samples were weighed as W_0 before soaking in phosphate buffer (pH = 7.4) overnight and the weight was determined as W_1. The swelling ratio was calculated using the below equation.

$$Q = (W_1 - W_0)/W_0$$

The swelling ratio for each hydrogel sample was summarized (Figure 2. 6). The swelling ratio is closely related to saturation G'. Hydrogels with azide:bis-ADIBO **2.1** = 1:0.3 exhibit the best absorption capacity in each DS **Alg-A**. The hydrogels with larger saturation G' tend to have a smaller swelling ratio, which may result from the higher crosslinking density limits the flexibility of the alginate backbone.

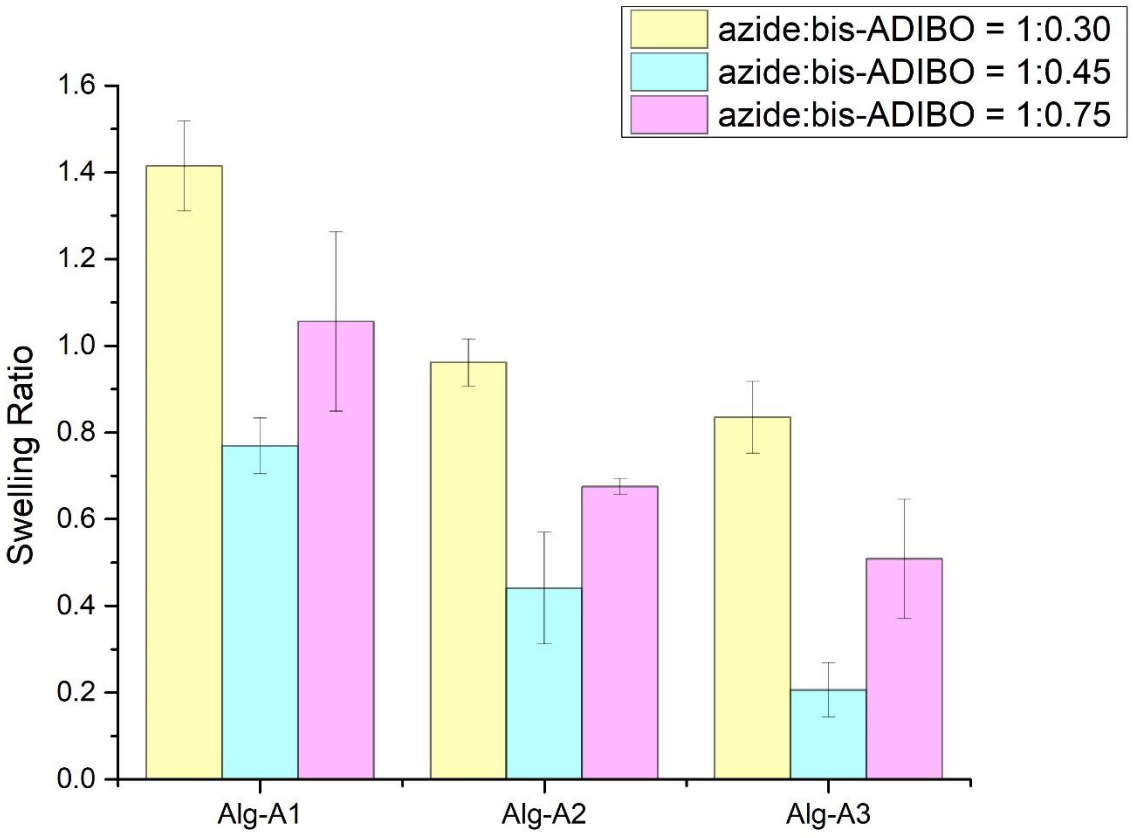

Figure 2. 6 Alginate Hydrogels Swelling Ratio

2.5 Morphological Characterizations

The hydrogels morphologies and microstructures were characterized by SEM. The freshly made hydrogels were swollen in DI water overnight before freezing in liquid nitrogen for 2 min. The samples were then freeze-dried overnight before collecting SEM images (Figure 2. 7). The lyophilized alginate hydrogels have a loose 3D network structure with pore sizes in the range of 10 µm – 100 µm.

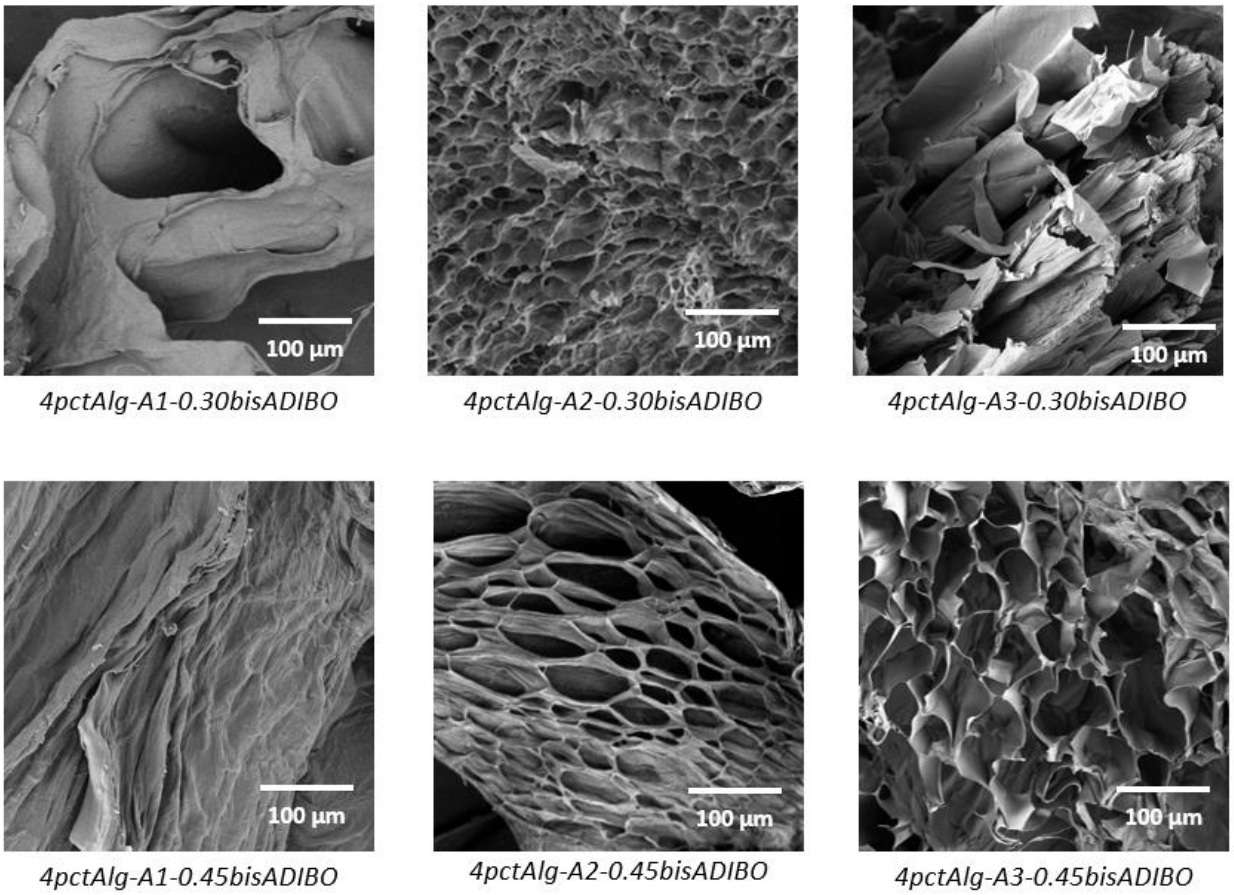

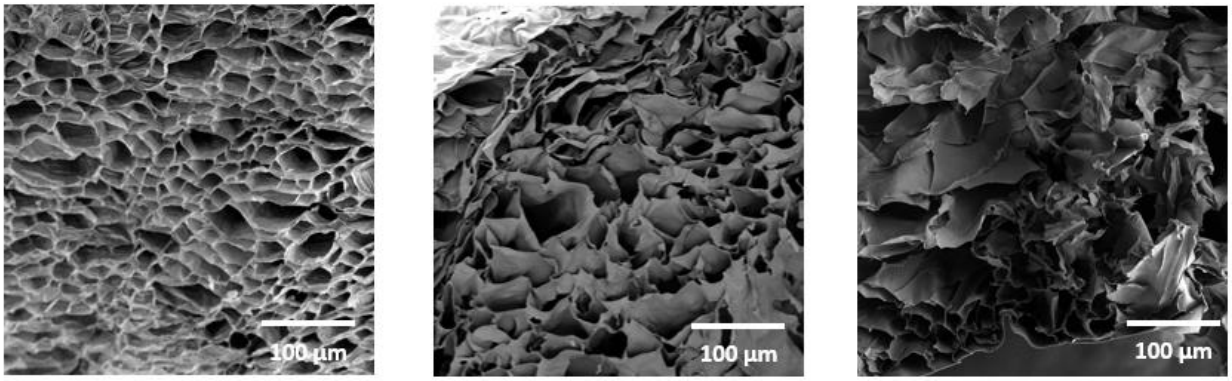

Figure 2. 7 Alginate Hydrogels SEM Images

2.6 Post-Modification Tests

The alginate hydrogels with azide:bis-ADIBO **2.1** molar ratio as 1:0.75 have unreacted cyclooctyne units in the system which should have the ability to be post-modified using azide substance. 5-FAM-azide was chosen for the post-modification. The 5-FAM-azide could be easily dissolved in an aqueous solution at neutral conditions, and it exhibits strong absorbance at 493 nm. In this project, 11.3 µM 5-FAM-azide solution was prepared in 0.1% DMSO/phosphate buffer (pH = 7.46) to accomplish hydrogels post-modification. This initial concentration was determined by UV spectroscopy as C_0.

The hydrogel for post-modification was prepared by dissolving **Alg-A3** in DI water at a concentration of 80 mg/mL (w:v) and bis-ADIBO **2.1** was dissolved in DMSO/H_2O just before use. These two solutions were mixed in silicon mold to yield hydrogels with 4% **Alg-A3**. Hydrogels with azide/bis-ADIBO **2.1** = 1/0.75 were prepared for post-modification. The

resulting hydrogel sheet was cut into the cylinder by biopsy punch and the weight was determined as W_h. The chemical absorption capacity is 21.00 μmol/g when every cyclooctyne unit is reacted with azide substances. The hydrogel cylinders were separated into the experiment group and control group. The control group was soaked in 10 mL 10 mM NaN_3 solution in 0.1% DMSO/phosphate buffer (pH = 7.46) for overnight to deactivate remaining cyclooctynes on hydrogel and the experiment group was immersed in 0.1%DMSO/phosphate buffer to swell overnight. All hydrogels were removed from the swelling solution and immersed in 10 mL 11.3 μM 5-FAM-azide solution for 2 h (the total 5-FAM-azide amount was below the hydrogel's chemical absorption capacity), then the 5-FAM-azide solution was collected. The hydrogel was then washed three times with 0.1% DMSO/phosphate buffer (Figure 2. 8). The last wash solutions UV-Vis spectra were collected and there was no absorbance beyond 250 nm wavelength, which indicates the washing is complete. All the washed solutions were collected and combined with a previous 5-FAM-azide solution; the concentration (C_e) was determined by UV spectroscopy.

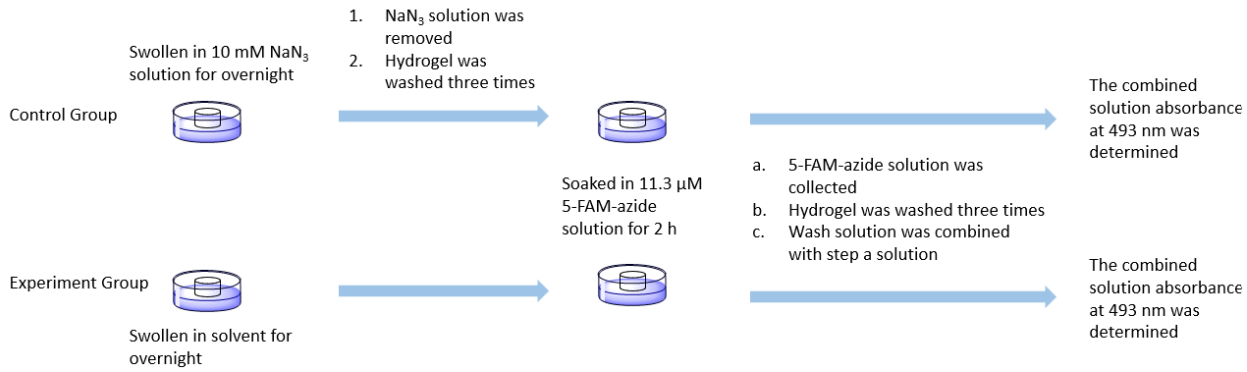

Figure 2. 8 Hydrogel Post-Modification by 5-FAM-azide

The experiment group FAB-hydrogel showed green fluorescence under handheld UV light (Figure 2. 9a) while the control group hydrogel did not exhibit fluorescence at the same condition (Figure 2. 9b).

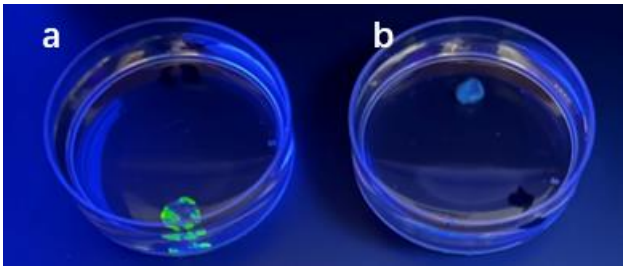

Figure 2. 9 Fluorescence Behavior under Handheld UV light

The hydrogel chemical absorption capacity in 2 h ($Q_{FAM\text{-}2\ h}$), was calculated by the equation:

$$Q_{FAM-2\,h} = \frac{C_0\,V_{dye} - C_e\left(V_{dye} + V_{wash}\right)}{W_0}$$

The control group barely showed 5-FAM-azide absorption while the experiment group had $Q_{FAM\text{-}2\ h}$ as 0.13 μmol/g (Figure 2. 10). This indicates that the hydrogel we built has the post-modification ability. The modification could be rapidly done at a low concentration.

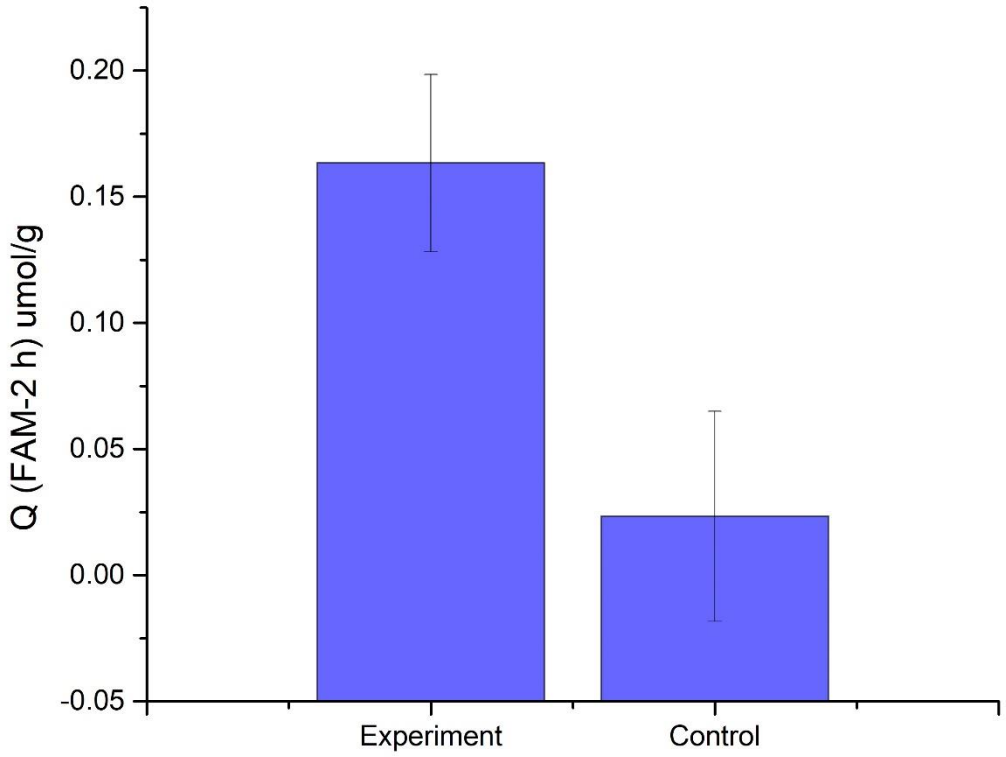

Figure 2. 10 Chemical Absorption Capacity in 2 h

We then designed a Rhodamine B based azide substance **2.12** to test the multiple modifications capability of the alginate hydrogels (azide:bis-ADIBO = 1:0.75). The functionalization of Rhodamine B was achieved by coupling with linker **2.11** with the help of EDC · HCl (Scheme 2. 5). Rhodamine-N_3 **2.12** extinction coefficient was determined in DI water containing 0.2% DMSO, the hydrochloric acid solution was also added to improve **2.12** solubility. The resulting solution concentration was 88.3 μM and the pH was determined as 3.23. The extinction coefficient at 560 nm was determined as 3603.9 $M^{-1} \cdot cm^{-1}$.

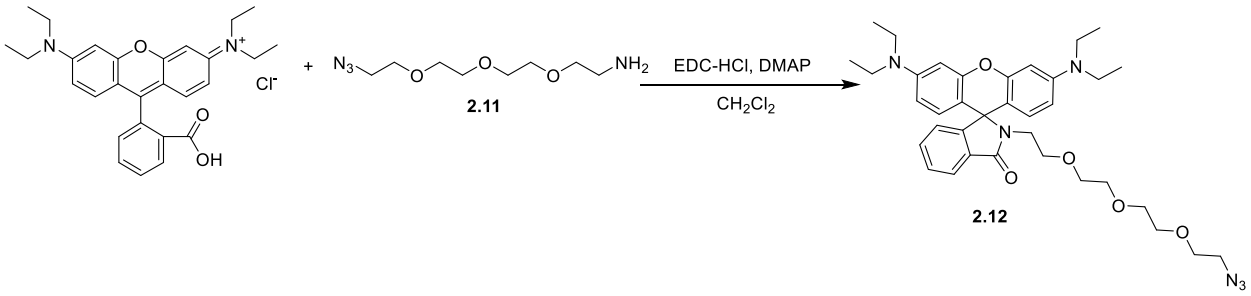

Scheme 2. 5 Synthesis of Rhodamine-N_3 2.12

Rhodamine **2.12** does not show fluorescence under neutral condition and exhibits pink fluorescence under acidic condition (Scheme 2. 6). 5-FAM-N_3 shows green fluorescence under neutral or basic condition and does not exhibit fluorescence under acidic condition (Scheme 2. 6). This feature allows us to examine the hydrogel multiple modifications' ability under different pH conditions.

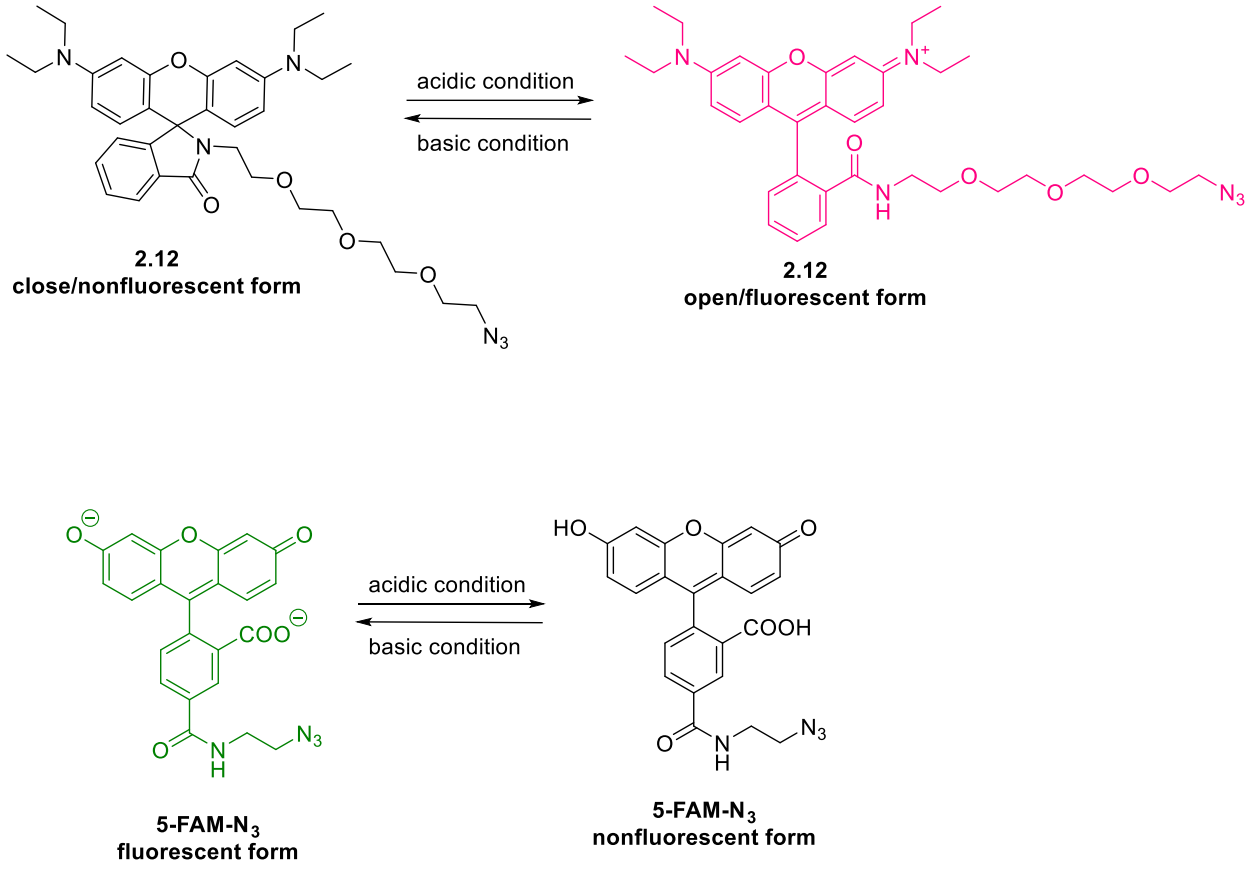

Scheme 2. 6 Rhodamine-N_3 2.12 and 5-FAM-N_3 Fluorescence Behaviors under Different pH Conditions

0.2% DMSO/HCl/H_2O (pH = 3.23) solution was used as solvent in this modification. The FAB-hydrogel was soaked in solvent overnight before being immersed in 10 mL 93.2 μM **Rhodamine-N_3 2.12** for 2.5 h (the total Rhodamine-N_3 **2.12** amount was below the hydrogel's chemical absorption capacity). The hydrogel was then washed three times, the last wash solution UV-Vis spectra was collected and there was no absorbance above 250 nm, which indicates the washing is complete. The hydrogel showed pink color after Rhodamine modification (Figure 2. 11a). The hydrogel was then soaked in 0.1% DMSO/phosphate buffer (pH = 7.46) for 2 h. The

hydrogel fluorescence changed from pink to green (Figure 2. 11b), which proves the FAM modification was untouched after the second modification. The hydrogel was then soaked in acidic buffer (0.2% DMSO/HCl/H_2O; pH = 3.23) overnight and the hydrogel showed strong pink fluorescence under handheld UV light (Figure 2. 11c) which proves the existence of Rhodamine modification. This phenomenon indicates that the hydrogel has the ability of multiple modifications, and the FAM-RB-hydrogel might be a good candidate for pH indicator.

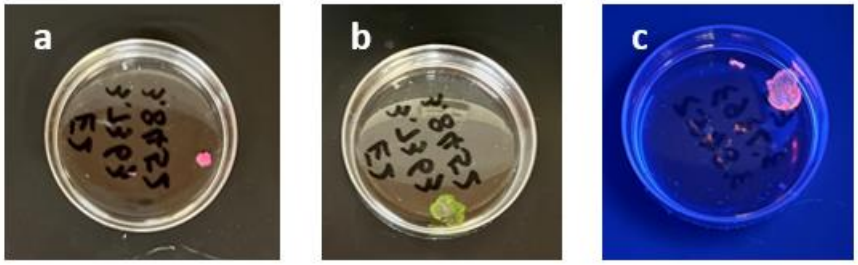

Figure 2. 11 FAM-RB-Hydrogel

2.7 Stability

The hydrogel's stability was tested using FAM-hydrogel by soaking the hydrogel in 0.1% DMSO/phosphate buffer (pH = 7.46) and following the fluorophore release over 20 days (Figure 2. 12). There was no significant fluorophore release in 20 days, which indicates FAM-hydrogels are stable under neutral conditions.

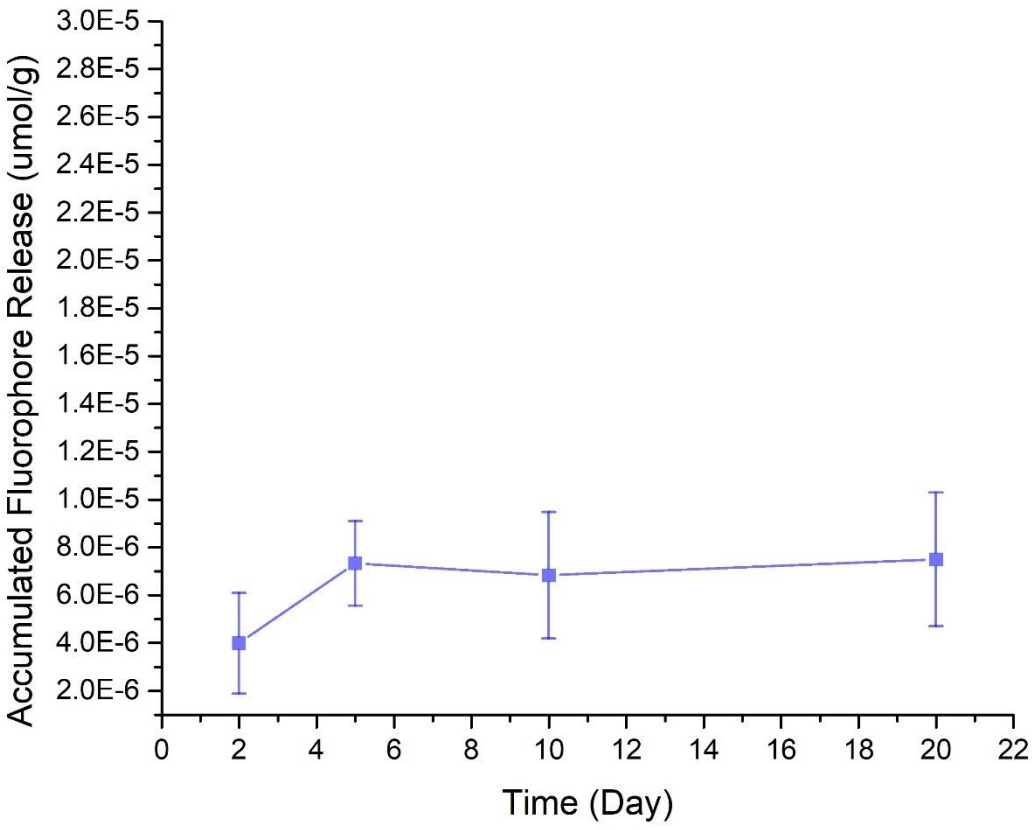

Figure 2. 12 Accumulated Fluorophore Release within 20 Days

2.8 Conclusion

We designed a water-soluble bis-ADIBO crosslinker **2.1** to accomplish the efficient gelation between azide functionalized alginate **Alg-A**. The hydrogels were more rigid when azide substitution on the alginate backbone was increased. The maximum storage modulus could also be manipulated by controlling the ratio between azide substitution and bis-ADIBO **2.1**. When azide:bis-ADIBO molar ratio is larger than 1:0.5, the hydrogel showed higher stiffness if higher

ratio content of bis-ADIBO **2.1** was used. However, the hydrogels were softer when azide:bis-ADIBO molar ratio was less than 1:0.5. All the alginate hydrogel samples showed very good water absorption capability and the SEM images prove the sponge-like structure of these hydrogels. Moreover, the hydrogel with azide:bis-ADIBO molar ratio of 1:0.75 retained a significant amount of reactive cyclooctyne in the system which is capable to be modified after gelation. We also demonstrated that the FAM modified hydrogels remain stable over 20 days. The post-modification ability might be useful when the hydrogels are applied in tissue engineering or cell culture.

2.9 Experimental Section

Compound **2.2 – 2.8** and **ADIBO-NH$_2$** were prepared following the previously published procedure by Popik group[12] with slight modifications.

5*H*-Dibenzo[a,d][7]annulen-5-one oxime (2.2): hydroxylamine hydrochloride (20.22 g, 291.3 mmol) and Na_2CO_3 (11.58 g, 109.2 mmol) was added to 5H-dibenzo[a,d][7]annulen-5-one (15.00 g, 72.9 mmol) in 90 mL ethanol. The reaction was then refluxed for 24 h. Then the reaction mixture was cooled to room temperature and poured into 50 mL ice-cold 1 M HCl. The solution was then filtered and washed with 3*50 mL 1M HCl and 3*50 mL DI water. The crude product was left to dry in air for 1 h and then in vacuum for overnight to give the product as white solid (14.83 g, 99%). ^{1}H NMR (400 MHz, Chloroform-*d*) δ 7.73 (s, 1H), 7.50 (d, 1H), 7.33 (m, 1H), 7.28 – 7.13 (m, 5H), 7.08 (d, 1H), 6.99 (d, 1H), 6.87 (d,1H).

(Z)-Dibenzo[b,f]azocin-6(5H)-one 2.3: 63 mL Eaton's reagent was added to **2.2** (14.83 g, 71.9 mmol). The reaction was heated in an oil bath to 100 °C for 30 min. The reaction mixture color changed from light yellow to dark brown. The hot reaction mixture was poured into 314 g crushed ice and mixed with a glass stirring rod to fully quench the Eaton's reagent. The slurry was then filtered and washed with 1200 mL DI water until the filtrate was neutral. The filter cake was dried in vacuum, the product was collected as off-white powder (15.49 g, 97%). ^{1}H NMR (400 MHz, $CDCl_3$) δ 7.79 (s, 1H), 7.50 (dd, *J* = 7.6, 1.4 Hz, 1H), 7.36 – 7.29 (m, 2H), 7.26 – 7.14 (m, 4H), 7.09 (d, *J* = 7.6 Hz, 1H), 6.99 (d, *J* = 11.7 Hz, 1H), 6.87 (d, *J* = 11.6 Hz, 1H).

(Z)-5,6-Dihydrodibenzo[b,f]azocine 2.4: 2.3 (8.81 g, 39.8 mmol) in 54 mL anhydrous ethyl ether was slowly added to a solution of $LiAlH_4$ (3.03 g, 79.8 mmol) in 234 mL anhydrous ethyl ether at 0 °C. The mixture was refluxed at 40 °C overnight. And then the reaction was diluted with 27 mL methylene chloride and cooled to 0 °C for 30 min before being quenched by 4 mL water and kept cool for 15 min. Then 4 mL 4 M NaOH aqueous solution and 10 mL water were slowly added to the mixture. Sodium sulfate was added after 30 min stirring until the liquid layer appeared clear. The reaction mixture was then filtered, and the solids were washed with EtOAc to remove the adsorbed product. The filtrate was evaporated to remove solvent and purified on a silica gel column using 10% EtOAc in hexanes to yield the pure product as light-yellow solid (5.64 g, 68%). ^{1}H NMR (400 MHz, $CDCl_3$) δ 7.43 – 7.29 (m, 1H), 7.17 – 7.04 (m, 4H), 6.91 (d, *J* = 7.4 Hz, 1H), 6.84 (t, *J* = 7.6 Hz, 1H), 6.58 (t, *J* = 7.2 Hz, 1H), 6.53 – 6.47 (m, 2H), 6.34 (d, *J* = 13.0 Hz, 1H), 4.51 (d, *J* = 17.2 Hz, 2H).

3-(2,2,2-Trifluoroacetamido)propanoic acid 2.5: 12.6 mL triethylamine (90 mmol, 1.5 equiv.) was added to a solution of β-alanine (5.24 g, 60 mmol), ethyl trifluoroacetate (10.8 mL, 90 mmol, 1.5 equiv.) in 240 mL MeOH. The reaction was then concentrated under vacuum, and the residue was co-evaporated with EtOH (20 mL * 3) to remove triethylamine. And then the mixture was dried under high vacuumed overnight. The residue was re-dissolved in EtOAc, washed with 0.1 M NaH_2PO_4 (200 mL * 3), brine (100 mL * 2). The organic layer was dried over Na_2SO_4 and concentrated to product as yield white solid (3.18 g, 29%). ^{1}H NMR (400 MHz, D_2O) δ 3.47 (t, *J* = 6.3 Hz, 2H), 2.56 (t, *J* = 6.5 Hz, 2H).

(Z)-N-(3-(Dibenzo[b,f]azocin-5(6H)-yl)-3-oxopropyl)-2,2,2-trifluoroacetamide 2.6: DCC (2.80 g, 13.7 mmol) and catalytic amount of DMAP were added to a solution of **2.5** (2.30 g, 12.3 mmol) in 75 mL methylene chloride. The mixture was stirred 10 min before a solution of **2.4** (2.55 g, 12.3 mmol) in 5 mL methylene chloride was added. The reaction was stirred overnight and then washed with water and brine. The organic layer was dried over Na_2SO_4 and concentrated, purified on a silica gel column using 40% EtOAc in hexanes to yield product as orange solid (3.40 g, 74%). ^{1}H NMR (400 MHz, $CDCl_3$) δ 7.34 (m, 4H), 7.24 – 7.13 (m, 4H), 6.81 (d, *J* = 13.0 Hz, 1H), 6.59 (d, *J* = 12.9 Hz, 1H), 5.56 (d, *J* = 15.3 Hz, 1H), 4.31 (d, *J* = 15.2 Hz, 1H), 3.59 – 3.42 (m, 2H), 2.35 – 2.26 (m, 1H), 2.07 – 1.97 (m, 1H).

N-(3-(11,12-Dibromo-11,12-dihydrodibenzo[b,f]azocin-5(6H)-yl)-3-oxopropyl)-2,2,2-trifluoroacetamide 2.7: pyridium hydrobromide perbromide (3.40 g, 10.5 mmol) was added to a solution of **2.6** (3.40 g, 9.1 mmol) in 14 mL methylene chloride. The reaction was stirred at room

temperature overnight, and then diluted with 230 mL methylene chloride. The organic layer was washed by 5% HCl aqueous solution and concentrated $Na_2S_2O_3$. The organic layer was then dried over Na_2SO_4 and concentrated, purified on a silica gel column using methylene chloride as eluent to yield crude product as white flake (4.38 g). The crude product was then recrystallized using EtOAc to yield product as white crystals (3.50 g, 72%). ^{1}H NMR (400 MHz, $CDCl_3$) δ 7.76 (d, *J* = 7.8 Hz, 1H), 7.62 (s, 1H), 7.27 – 7.17 (m, 2H), 7.09 (t, *J* = 8.2 Hz, 2H), 6.99 (d, *J* = 7.3 Hz, 1H), 6.93 (d, *J* = 5.5 Hz, 1H), 5.86 (m, 2H), 5.19 (d, *J* = 10.0 Hz, 1H), 4.22 (d, *J* = 14.8 Hz, 1H), 3.64 (m, 2H), 2.68 (m, 1H), 2.40 (m, 1H).

2.8: a solution of 1 M potassium tert-butoxide in anhydrous tetrahydrofuran (10.9 mmol, 10.9 mL, 3.3 equiv.) was added dropwise using addition funnel to a solution of **2.7** (1.75 g, 3.3 mmol) in 8 mL anhydrous tetrahydrofuran at 0 °C. The reaction mixture was then warmed to room temperature and stirred overnight before being diluted with ethyl acetate. The mixture was washed with brine and the aqueous layer was extracted by EtOAc twice. The organic layers were combined and dried over Na_2SO_4 before being concentrated under vacuum. The crude product was purified on a silica gel column using 30% EtOAc in hexanes to yield the product as orange solid (1.03 g, 84%). ^{1}H NMR (400 MHz, $CDCl_3$) δ 7.70 (d, *J* = 7.7 Hz, 1H), 7.47 – 7.31 (m, 7H), 7.16 (s, 1H), 5.17 (d, *J* = 13.8 Hz, 1H), 3.76 (d, *J* = 14.0 Hz, 1H), 3.53 (m, 1H), 3.30 (m, 1H), 2.55 (m, 1H), 2.00 (m, 1H).

ADIBO-NH$_2$: a solution of K_2CO_3 (0.20 g, 1.44 mmol, 5.5 equiv.) in 0.8 mL water was added to a solution of **2.8** (0.10 g, 0.26 mmol) in 2.0 mL MeOH. The reaction was stirred at

room temperature for overnight. The solvent was then removed under vacuum and residue was separated between methylene chloride/EtOAc (1:4) and water. The organic layer was washed with brine, dried and concentrated, purified on a silica gel column using 5%-10% MeOH in methylene chloride to yield the product as yellow oil (0.04 g, 56%). ^{1}H NMR (400 MHz, $CDCl_3$) δ 8.37 (s, 2H), 7.64 (d, *J* = 8.0 Hz, 1H), 7.54 – 7.29 (m, 7H), 5.12 (d, *J* = 14.3 Hz, 1H), 3.74 (d, *J* = 13.8 Hz, 1H), 3.17 – 2.89 (m, 3H), 2.03 (m, 1H), 1.42 (m, 1H).

Bis-ADIBO (2.1): EDTA dianhydride (0.09 g, 0.34 mmol) was added to a solution of **ADIBO-NH₂** (0.20 g, 0.71 mmol, 2.1 equiv.) in 11 mL chloroform. The reaction was stirred at room temperature for overnight. Then the solvent was removed under vacuum. The crude product was purified on a silica gel column using 50% MeOH in CH_2Cl_2 to yield product as yellow solid (0.15 g, 55%). ESI-MS (negative) Calcd. for $C_{46}H44N_6O_8$ $[M - H]^-$: 807.31479. Found: 807.31488. ^{1}H NMR (600 MHz, DMSO) δ 8.47 (s, 2H), 7.59 (m, 4H), 7.48 (m, 2H), 7.43 (m, 2H), 7.35 (m, 4H), 7.29 (m, 2H), 7.17 (m, 2H), 5.03 (d, *J* = 14.1 Hz, 2H), 3.62 (d, *J* = 14.1 Hz, 2H), 3.22 – 3.13 (m, 2H), 3.03 (m, 4H), 2.91 (m, 2H), 2.76 (m, 2H), 2.71 – 2.55 (m, 4H), 2.33 (m, 4H), 1.81 (m, 2H). ^{13}C NMR (151 MHz, DMSO) δ 173.52, 170.21, 148.78, 132.88, 128.90, 128.76, 128.61, 128.52, 127.24, 125.68, 122.87, 62.66, 58.79, 55.43, 55.38, 54.63, 40.20, 35.74, 34.20.

((Oxybis(ethane-2,1-diyl))bis(oxy))bis(ethane-2,1-diyl) dimethanesulfonate (2.9): a solution of methanesulfonyl chloride (17.60 g, 154.5 mmol, 11.9 mL, 3.0 equiv.) in 90 mL methylene chloride was slowly added to a mixture of triethylamine (19.8 mL, 15.60 g, 154.5

mmol, 3.0 equiv.) and tetraethylene glycol (10.00 g, 51.5 mmol) in 30 mL methylene chloride. The mixture was stirred at 0°C for 2 h and then at room temperature for overnight. The reaction was then washed with 3% HCl aqueous solution (130 mL) and then brine (130 mL), extracted with methylene chloride (130 mL). The procedure was repeated 3 times, the organic layer was dried over Na_2SO_4 and then in vacuum to yield dimesylated product as yellow oil (18.05 g, 100%). ^{1}H NMR (400 MHz, $CDCl_3$) δ 4.31 (m, 4H), 3.73 – 3.68 (m, 4H), 3.61 – 3.55 (m, 8H), 3.01 (s, 6H). ^{13}C NMR (101 MHz, $CDCl_3$) δ 70.67, 70.54, 69.21, 69.05, 37.69.

1-Azido-2-(2-(2-(2-azidoethoxy)ethoxy)ethoxy)ethane (2.10): sodium azide (9.42 g, 144.0 mmol, 5.0 equiv.) was added to a solution of **2.9** (10.00 g, 28.5 mmol) in 170 mL dimethylformamide. The reaction was stirred at 65°C overnight before being diluted with 270 mL EtOAc and washed with water and brine. The organic layer was dried over Na_2SO_4 and concentrated to yield the product as pale oil (5.79 g, 83%). ^{1}H NMR (400 MHz, $CDCl_3$) δ 3.64 – 3.57 (m, 12H), 3.32 (t, J = 5.0 Hz, 4H). ^{13}C NMR (101 MHz, $CDCl_3$) δ 70.74, 70.05, 50.71.

2-(2-(2-(2-Azidoethoxy)ethoxy)ethoxy)ethan-1-amine (2.11): 113 mL 5% HCl aqueous solution was added with vigorous stirring to a solution of **2.10** (11.10 g, 45.7 mmol) in 53 mL Et_2O at room temperature. A solution of triphenyl phosphine (10.72 g, 41.1 mmol, 0.9 equiv.) in 53 mL Et_2O was slowly added to the mixture using an addition funnel. The mixture was then allowed to react at room temperature for 24 h. The reaction mixture was washed with EtOAc (200 mL*3) to remove the unreacted starting materials and triphenylphosphine oxide that was formed during the reaction. The aqueous layer was collected, cooled to 0°C, and concentrated

before KOH aqueous solution was added to it until the pH of the solution was basic (pH ~12). The product was extracted from the aqueous layer by washing with methylene chloride three times. The organic layer was dried over Na_2SO_4 and concentrated under vacuum to yield the product as pale-yellow oil (7.18 g, 80%). ESI-MS (positive) Calcd. for $C_8H_{18}N_4O_3$ $[M + H]^+$: 219.14517. Found: 219.14513. ^{1}H NMR (400 MHz, $CDCl_3$) δ 3.71 – 3.61 (m, 12H), 3.52 (t, *J* = 5.2 Hz, 2H), 3.40 (t, *J* = 5.0 Hz, 2H), 2.87 (t, *J* = 5.2 Hz, 2H). ^{13}C NMR (101 MHz, $CDCl_3$) δ 73.44, 70.73, 70.68, 70.66, 70.30, 70.05, 50.70, 41.80.

Alg-A: sodium alginate (very low viscosity) (2.00 g, 9.8 mmol) was dissolved in 65 mL DI water to a concentration of 3.0 wt.%. The pH of the solution was adjusted to 3.4 using 0.4 M HCl aqueous solution (~5 mL), and the solution was then diluted to 2.0 wt.% using DI water. Next, an aqueous solution of EDC · HCl ($N_{EDC\ HCl}/N_{NaAlg}$ = 0.5, 0.7, 0.9) (0.94 g, 4.9 mmol;1.32 g, 6.9 mmol; 1.69 g, 8.8 mmol) in 2 mL DI water and catalytic amount of DMAP were slowly added to the system, and the pH of the reaction was maintained at 3.4 by the addition of 0.4 M HCl aqueous solution (~4 mL). After 5 min reaction, a solution of **2-3** ($N_{2\text{-}3}/N_{NaAlg}$ = 2.0) (4.33 g, 19.6 mmol) in 5 mL DI water was added and the mixture was stirred at 35 °C for 24 h. The product was precipitated three times using acetone before being freeze-dried for 24 h to yield the product as white powder (1.56 g).

2-(2-(2-(2-(2-Azidoethoxy)ethoxy)ethoxy)ethyl)-3',6'-bis(diethylamino)spiro[isoindoline-1,9'-xanthen]-3-one (2.12): EDC · HCl (0.81 g, 4.2 mmol, 2.0 equiv.) and catalytic amount of DMAP (0.26 g, 2.1 mmol, 1.0 equiv.) were added to a

solution of Rhodamine B (1.00 g, 2.1 mmol) and **2.11** (0.92 g, 4.2 mmol, 2.0 equiv.) in 30 mL anhydrous methylene chloride. The reaction was stirred at room temperature for overnight before washed with 1 M HCl, 1 M $NaHCO_3$ and brine. The organic layer was dried over Na_2SO_4 and concentrated under vacuum to yield product as purple oil (0.75 g, 56%). ESI-MS (positive) Calcd. for $C_{36}H_{46}N_6O_5$ $[M + H]^+$: 643.3603. Found: 643.3595. ^{1}H NMR (600 MHz, $CDCl_3$) δ 7.89 (dd, *J* = 5.5, 2.8 Hz, 1H), 7.44 – 7.40 (m, 2H), 7.06 (dd, *J* = 5.5, 2.7 Hz, 1H), 6.43 (d, *J* = 8.7 Hz, 2H), 6.37 (s, 2H), 6.26 (d, *J* = 8.0 Hz, 2H), 3.64 – 3.61 (m, 2H), 3.61 – 3.57 (m, 4H), 3.51 – 3.48 (m, 2H), 3.40 – 3.37 (m, 2H), 3.36 – 3.31 (m, 12H), 3.17 (t, *J* = 7.4 Hz, 2H), 1.16 (t, *J* = 6.9 Hz, 12H). ^{13}C NMR (151 MHz, $CDCl_3$) δ 168.20, 153.20, 148.72, 132.47, 132.19, 130.95, 128.89, 128.71, 128.06, 127.76, 123.92, 123.57, 122.70, 108.10, 107.93, 105.49, 97.84, 97.64, 77.21, 77.00, 76.79, 70.60, 70.46, 69.93, 67.76, 50.63, 44.34, 39.24, 12.79, 12.65, 12.52, 12.38.

Alg-A Gelation: 80.0 mg **Alg-A** was dissolved in 1.5 mL DI water to a concentration of 53 mg/mL (w/v). Bis-ADIBO **2.1** was dissolved in 0.4 mL DMSO and then diluted with 0.1 mL DI water just before use. These two solutions were mixed in a 3:1 (v/v) ratio to yield hydrogels with 4% (w/w) **Alg-A**. The amount for each reagent is listed below (Table 2. 1, Table 2. 2, Table 2.3).

Table 2. 1 Reagents Amount (Alg-A with azide/bis-ADIBO 2.1 = 1:0.3)

	Alg-A Repeating Units (mmol)	Azides on **Alg-A** (mmol)	Bis-ADIBO **2.1** (mg)	Bis-ADIBO **2.1** (mmol)

Alg-A1	0.286	0.044	8.1	0.010
Alg-A2	0.293	0.057	13.8	0.017
Alg-A3	0.271	0.064	15.6	0.019

Table 2. 2 Reagents Amount (Alg-A with azide/bis-ADIBO 2.1 = 1:0.45)

	Alg-A Repeating Units (mmol)	Azides on **Alg-A** (mmol)	Bis-ADIBO **2.1** (mg)	Bis-ADIBO **2.1** (mmol)
Alg-A1	0.286	0.044	16.1	0.020
Alg-A2	0.293	0.057	20.9	0.026
Alg-A3	0.271	0.064	23.4	0.029

Table 2. 3 Reagents Amount (Alg-A with azide/bis-ADIBO 2.1 = 1:0.75)

	Alg-A Repeating Units (mmol)	Azides on **Alg-A** (mmol)	Bis-ADIBO **2.1** (mg)	Bis-ADIBO **2.1** (mmol)
Alg-A1	0.286	0.044	26.7	0.033
Alg-A2	0.293	0.057	34.6	0.043
Alg-A3	0.271	0.064	38.8	0.048

Rheometer Setups: Rheological characterization was performed using a DHR2 rheometer

fitted with 25.0 mm parallel plate. 363 μL **Alg-A** solution and 121 μL bis-ADIBO **2.1** solutions were introduced on the bottom plate. A solvent trap was used to prevent sample dehydration. The solutions were mixed at 200.0 1/s shear rate for 60 s at 0 °C. The sample was equilibrated for 5 s before the temperature ramp was performed at 20.0 °C/min ramp rate, 10.0 rad/s angular frequency, and 10.0 % strain. The sample was equilibrated for 10 s before the time sweep was performed at 10.0 rad/s angular frequency, 10.0 % strain, 25 °C, and 1000 μm gap distance. These parameters are within the linear viscoelastic range for this hydrogel.

2.10 References

1. Wang, X.; Wang, W.; Ma, J.; Guo, X.; Yu, X.; Ma, X., Proliferation and Differentiation of Mouse Embryonic Stem Cells in APA Microcapsule: A Model for Studying the Interaction between Stem Cells and Their Niche. *Biotechnology Progress* **2006,** *22* (3), 791-800.

2. Utech, S.; Prodanovic, R.; Mao, A. S.; Ostafe, R.; Mooney, D. J.; Weitz, D. A., Microfluidic Generation of Monodisperse, Structurally Homogeneous Alginate Microgels for Cell Encapsulation and 3D Cell Culture. *Advanced Healthcare Materials* **2015,** *4* (11), 1628-33.

3. Richardson, T.; Barner, S.; Candiello, J.; Kumta, P. N.; Banerjee, I., Capsule stiffness regulates the efficiency of pancreatic differentiation of human embryonic stem cells. *Acta Biomaterialia* **2016,** *35*, 153-65.

4. Bencherif, S. A.; Sands, R. W.; Bhatta, D.; Arany, P.; Verbeke, C. S.; Edwards, D. A.; Mooney, D. J., Injectable preformed scaffolds with shape-memory properties. *Proceedings of the*

National Academy of Sciences **2012,** *109* (48), 19590.

5. Wang, L.; Shansky, J.; Borselli, C.; Mooney, D.; Vandenburgh, H., Design and Fabrication of a Biodegradable, Covalently Crosslinked Shape-Memory Alginate Scaffold for Cell and Growth Factor Delivery. *Tissue Engineering Part A* **2012,** *18* (19-20), 2000-2007.

6. Wang, T.; Zheng, Y.; Shi, Y.; Zhao, L., pH-responsive calcium alginate hydrogel laden with protamine nanoparticles and hyaluronan oligosaccharide promotes diabetic wound healing by enhancing angiogenesis and antibacterial activity. *Drug Delivery and Translational Research* **2019,** *9* (1), 227-239.

7. Mirani, B.; Pagan, E.; Currie, B.; Siddiqui, M. A.; Hosseinzadeh, R.; Mostafalu, P.; Zhang, Y. S.; Ghahary, A.; Akbari, M., An Advanced Multifunctional Hydrogel-Based Dressing for Wound Monitoring and Drug Delivery. *Advanced Healthcare Materials* **2017,** *6* (19).

8. Kong, X.; Fu, J.; Shao, K.; Wang, L.; Lan, X.; Shi, J., Biomimetic hydrogel for rapid and scar-free healing of skin wounds inspired by the healing process of oral mucosa. *Acta Biomaterialia* **2019,** *100*, 255-269.

9. Yu, L.; Sun, Q.; Hui, Y.; Seth, A.; Petrovsky, N.; Zhao, C.-X., Microfluidic formation of core-shell alginate microparticles for protein encapsulation and controlled release. *Journal of Colloid and Interface Science* **2019,** *539*, 497-503.

10. Gamboa, A.; Araujo, V.; Caro, N.; Gotteland, M.; Abugoch, L.; Tapia, C., Spray Freeze-Drying as an Alternative to the Ionic Gelation Method to Produce Chitosan and Alginate Nano-Particles Targeted to the Colon. *Journal of Pharmaceutical Sciences* **2015,** *104* (12), 4373-

4385.

11. Zhang, C.; Wu, Y.; Liu, T.; Zhao, Y.; Wang, X.; Wang, W.; Yuan, Z., Antitumor activity of drug loaded glycyrrhetinic acid modified alginate nanoparticles on mice bearing orthotopic liver tumor. *Journal of Controlled Release* **2011,** *152*, e111-e113.

12. Kuzmin, A.; Poloukhtine, A.; Wolfert, M. A.; Popik, V. V., Surface Functionalization Using Catalyst-Free Azide−Alkyne Cycloaddition. *Bioconjugate Chemistry* **2010,** *21* (11), 2076-2085.

CHAPTER 3

IN SITU CROSS-LINKABLE HYDROGEL VIA PHOTO-CLICK CHEMISTRY

3.1 Introduction

Covalently crosslinked hydrogels offer advantages such as tunable porosity, long-term stability, and ease of functionalization. Photo-induced crosslinking has attracted great attention among all the covalent gelation methods because of its unique features.[1-3] Photochemistry permits a high production rate, mild conditions, and accurate spatio-temporal control.[4, 5] Photo-initiated polymerization and photo-click chemistry are two significant types of photo-induced gelation. However, the photo-initiated polymerization requires the addition of a photoinitiator which might have potential toxicity of cell activity. Photo-click chemistry provides high selectivity and rapid reaction rate without adding catalyst or generation of by-product. This crosslinking strategy has been used for a lot of applications such as cell culture,[6, 7] drug delivery,[8] wound dressing material.[9, 10]

In this project, we covalently linked azadibenzocyclooctyne (ADIBO) and cyclopropenone-masked dibenzocyclooctyne to make a photo-induced crosslinker for azide functionalized alginate (**Alg-A**). The crosslinker could be decorated on the alginate backbone before gelation, thus the mixing could be avoided before crosslinking. This photosensitive crosslinker could be

activated under 350 nm UV light to reveal the reactive cyclooctyne. The crosslinking density can be easily controlled by the duration of irradiation or light intensity. The resulting hydrogels are promising candidates for cell culture and wound dressing materials.

3.2 Photo-Induced Crosslinker Design and Synthesis

A reactive cyclooctyne unit and a cyclopropenone masked cyclooctyne unit were conjugated to build a photo-induced crosslinker. We synthesized the crosslinker by covalent conjugating **ADIBO-NH$_2$** and cyclopropenone masked ADIBO. The preparation of photo-ADIBO **3.4** followed the procedure published before.[11] The synthesis started from the indirect reductive amination using commercially available 3-methoxybenzaldehyde and 3-methoxyaniline to give **3.1**, which is further coupled with **3.5** to yield **3.2**. The carboxylic acid is deprotected by hydrolysis before the double Friedel-Crafts alkylation with tetrachlorocyclopropene in the presence of aluminum chloride to yield **3.4**. The **ADIBO-NH$_2$** was coupled with **3.4** by carbodiimide chemistry to yield crosslinker **3.6** (Scheme 3. 1).

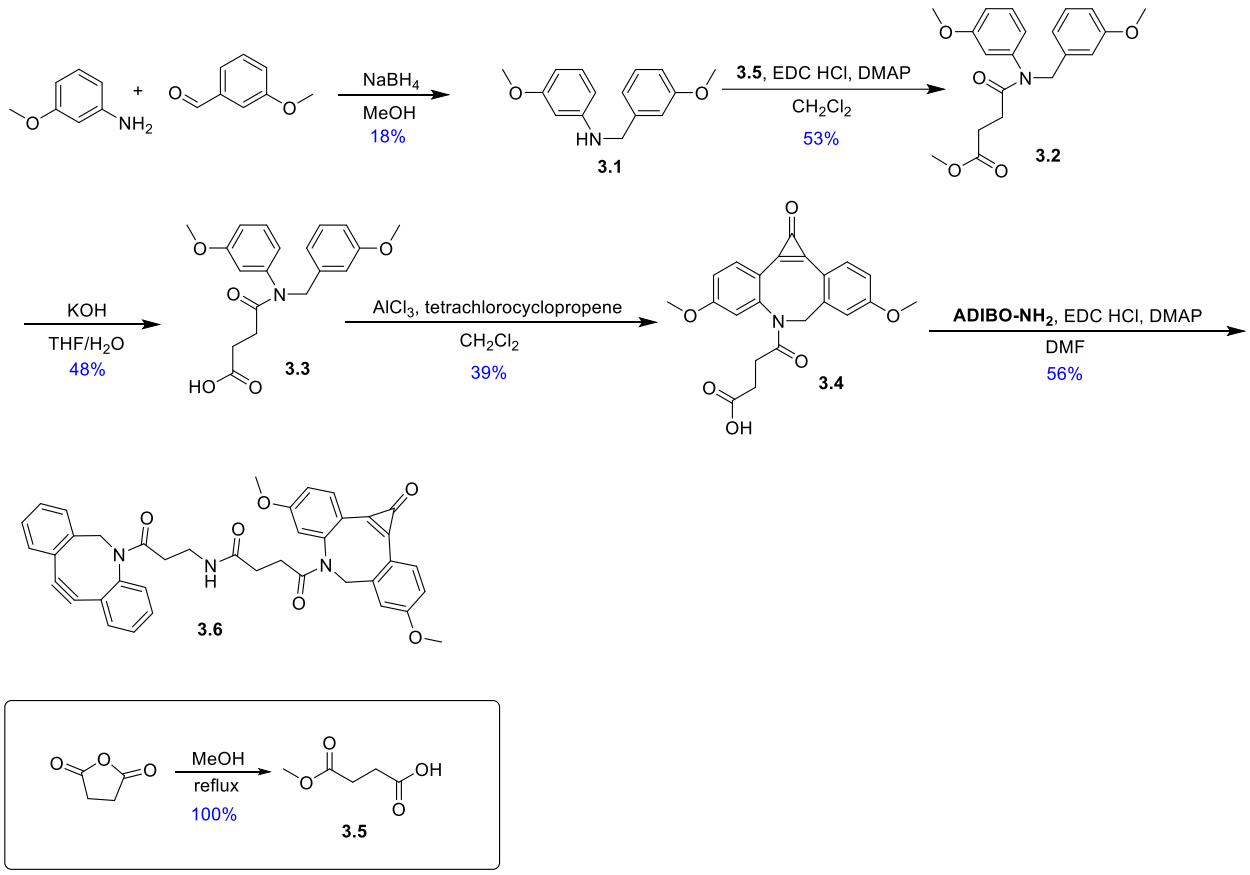

Scheme 3. 1 Synthesis of 3.6

3.3 Photo-Induced Alginate Gelation

The photo-induced gelation of **Alg-A** started from the conjugation with **3.6** to yield **photo-ADIBO-Alg**. The **Alg-A** solution in DI water and the **3.6** solution in DMSO/DI water were stirred at room temperature overnight before lyophilization (Scheme 3. 2).

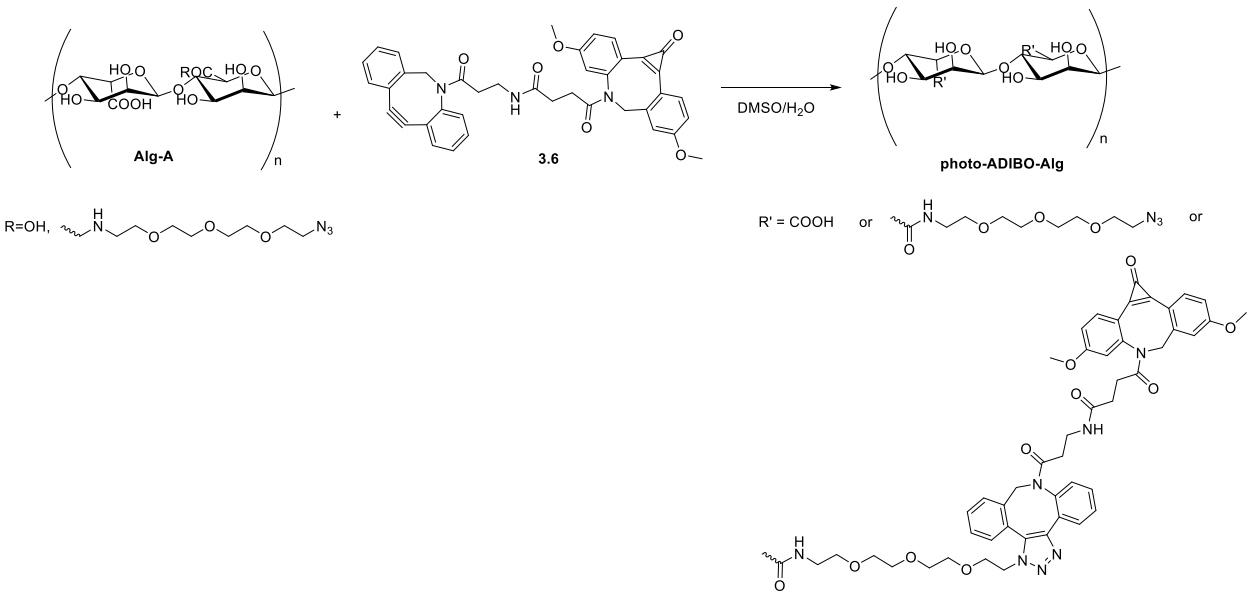

Scheme 3. 2 Synthesis of Photo-ADIBO-Alg

The lyophilized **photo-ADIBO-Alg** was redissolved in DI water to make a 2% (w/w) alginate solution for the photo-induced gelation (Scheme 3. 3).

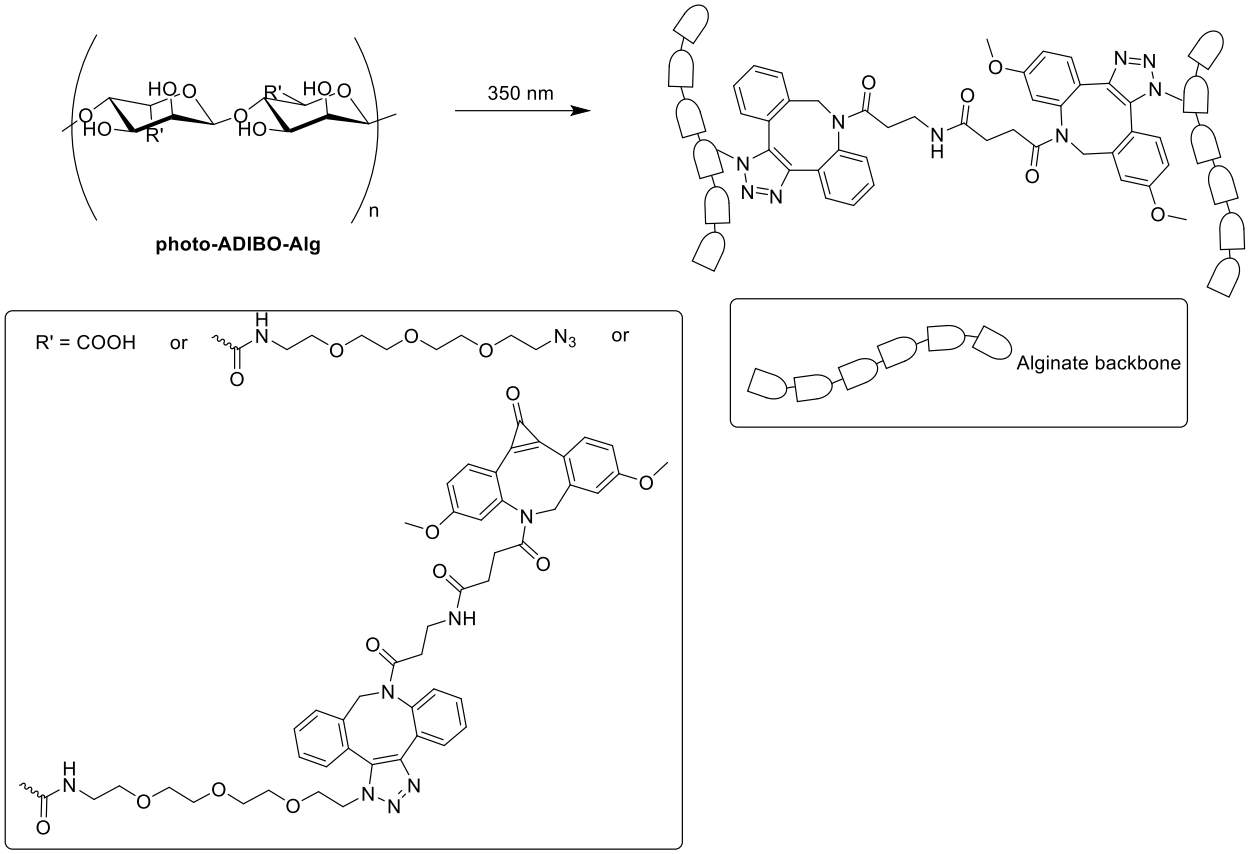

Scheme 3. 3 Photo-Induced Alginate Gelation

The **photo-ADIBO-Alg** solution was irradiated by 350 nm UV light followed by 3 min incubation at r.t. to complete the gelation (Figure 3. 1).

Figure 3. 1 Photo-Induced Alginate Gelation

3.4 Future Work and Conclusion

We built a photo-induced crosslinker to achieve the alginate gelation. This crosslinking strategy could avoid the non-homogenous gelation. The organic solvent can also be avoided in crosslinking. The crosslinking density of this hydrogel could be controlled by the crosslinker's ratio, and the duration of irradiation or light intensity. This photo-induced hydrogel is a good candidate for the wound dressing material. The hydrogel mechanical properties and morphology, as well as swelling, are under investigation.

3.5 Experiment Section

Compound **3.1 – 3.4** were prepare following the procedure published before.[11]

3-Methoxy-N-(3-methoxybenzyl)aniline 3.1: 3-methoxybenzaldehyde (22.12 g, 162.0 mmol) was added to a solution of 3-methoxyaniline (20.00 g, 162.0 mmol) in 460 mL MeOH. After stirring for 3 h at room temperature, $NaBH_4$ (18.39 g, 486.0 mmol, 3.0 equiv.) was slowly added at 0 °C. The resulting solution was stirred at 0 °C for another 30 minutes. The solvent was then removed by vacuum to give brown oil which was redissolved in ethyl acetate before being washed by saturated ammonium chloride aqueous solution. The organic layer was then dried over Na_2SO_4 and concentrated in vacuum before being purified on a silica gel column using 10% EtOAc in hexanes to give the product as clear oil (25.6 g, 65%). ^{1}H NMR (400 MHz, $CDCl_3$) δ 10.00 (s, 2H), 7.50 – 7.45 (m, 4H), 7.42 (d, J = 2.1 Hz, 2H), 7.20 (m, 2H), 3.89 (s, 6H).

Methyl 4-((3-methoxybenzyl)(3-methoxyphenyl)amino)-4-oxobutanoate 3.2: EDC · HCl (0.81 g, 4.2 mmol, 2 equiv.) and catalytic amount of DMAP were added to a solution of **3.5** (0.55 g, 4.2 mmol, 2 equiv.) in 8.1 mL methylene chloride. The mixture was stirred 10 min before a solution of **3.1** (0.50 g, 2.1 mmol) in 4.6 mL methylene chloride was added. The reaction was stirred at room temperature for overnight before washing by brine. The organic layer was then dried over Na_2SO_4 and concentrated under vacuum before purified on a silica gel column using 50% EtOAc in hexanes to yield product as clear oil (0.40 g, 53%). ^{1}H NMR (400 MHz, $CDCl_3$) δ 7.20 – 7.07 (m, 2H), 6.77 (m, 1H), 6.70 (m, 3H), 6.58 (d, *J* = 7.8 Hz, 1H), 6.51 (s, 1H), 4.77 (s, 2H), 3.69 (s, 3H), 3.65 (s, 3H), 3.60 (s, 3H), 2.57 (t, *J* = 6.7 Hz, 2H), 2.33 (t, *J* = 6.6 Hz, 2H).

4-((3-Methoxybenzyl)(3-methoxyphenyl)amino)-4-oxobutanoic acid 3.3: a solution of potassium hydroxide (0.12 g, 2.2 mmol, 2 equiv.) in 2.2 mL DI water was added to a solution of **3.2** (0.40 g, 1.1 mmol) in 1.7 mL tetrahydrofuran. The reaction was stirred at room temperature for 1 h before being quenched by 1 M HCl aqueous solution until the pH was under 7 and extracted by EtOAc. The organic layer was washed by brine, dried over Na_2SO_4, and concentrated under vacuum before being purified on a silica gel column using 50% acetone in hexanes to yield the product as clear oil (0.18 g, 48%). ^{1}H NMR (400 MHz, $CDCl_3$) δ 7.30 – 7.16 (m, 2H), 6.88 (m, 1H), 6.83 – 6.76 (m, 3H), 6.67 – 6.62 (m, 1H), 6.57 (m, 1H), 4.87 (s, 2H), 3.76 (s, 3H), 3.74 (s, 3H), 2.72 – 2.66 (m, 2H), 2.47 – 2.40 (m, 2H).

4-(4,9-Dimethoxy-1-oxo-1,7-dihydro-6H-dibenzo[b,f]cyclopropa[d]azocin-6-yl)-4-oxobutanoic acid 3.4: tetrachlorocyclopropene (1.43 mL, 2.07 g, 11.5 mmol, 1.0 equiv.) was

added to a suspension of aluminum chloride (5.37 g, 40.3 mmol, 3.5 equiv.) in 247 mL CH_2Cl_2 and stirred in room temperature for 10 min. The suspension was transferred to -78 °C and stirred for further 5 min before a solution of **3.3** (4.00 g, 11.5 mmol) in 13 mL CH_2Cl_2 was added dropwise. The reaction mixture was stirred at -78 °C for 4 h followed by stirring at room temperature for overnight. The reaction was then quenched by 165 mL 5% HCl aqueous solution, washed with water and brine and concentrated under vacuum. The crude product was then purified on a silica gel column using acetone and recrystallized using EtOAc to yield pure product as white solid (1.75 g, 39%). ^{1}H NMR (400 MHz, DMSO) δ 7.93 (dd, *J* = 8.5, 4.5 Hz, 1H), 7.76 (d, *J* = 8.5 Hz, 1H), 7.36 (d, *J* = 2.5 Hz, 1H), 7.26 (d, *J* = 2.4 Hz, 1H), 7.20 (dd, *J* = 8.6, 2.5 Hz, 1H), 7.07 (dd, *J* = 8.5, 2.6 Hz, 1H), 5.04 (d, *J* = 14.5 Hz, 1H), 4.26 (d, *J* = 14.4 Hz, 1H), 3.91 (s, 3H), 3.89 (s, 3H), 2.70 – 2.60 (m, 1H), 2.34 (m, 2H), 1.89 (m, 1H).

4-Methoxy-4-oxobutanoic acid (3.5): succinic anhydride (15.00 g, 149.9 mmol) in 75 mL MeOH was refluxed overnight. The solvent was removed under vacuum to yield the product as white crystal. The product was used for the next step without further purification. ^{1}H NMR (400 MHz, $CDCl_3$) δ 3.64 (d, *J* = 3.0 Hz, 3H), 2.65 – 2.61 (m, 2H), 2.57 (m, 2H).

3.6: EDC · HCl (0.18 g, 1.0 mmol, 1.2 equiv.) and catalytic amount of DMAP were added to a solution of **3.4** (0.38 g, 1.0 mmol, 1.2 equiv.) in 4 mL methylene chloride. The mixture was stirred at room temperature for 10 min before a solution of **ADIBO-NH$_2$** (0.22 g, 0.8 mmol) in 6 mL methylene chloride and 10 mL DMF before stirring at room temperature overnight. The solvent was removed under vacuum, and the residue was redissolved in methylene chloride

before being washed by brine. The organic layer was dried over Na_2SO_4, purified on a silica gel column using 5% MeOH in CH_2Cl_2 to yield the product as yellow oil (0.17 g, 26%). ESI-MS: m/z = 652.2 $[M + H]^+$, 674.2 $[M + Na]^+$, 690.2 $[M + K]^+$.

3.6 References

1. Kahveci, M. U.; Ciftci, M.; Evran, S.; Timur, S.; Yagci, Y., Photoinduced in situ formation of clickable PEG hydrogels and their antibody conjugation. *Designed Monomers and Polymers* **2015,** *18* (2), 129-136.

2. La, Y.-H.; McCloskey, B. D.; Sooriyakumaran, R.; Vora, A.; Freeman, B.; Nassar, M.; Hedrick, J.; Nelson, A.; Allen, R., Bifunctional hydrogel coatings for water purification membranes: Improved fouling resistance and antimicrobial activity. *Journal of Membrane Science* **2011,** *372* (1), 285-291.

3. Sautrot-Ba, P.; Razza, N.; Breloy, L.; Andaloussi, S. A.; Chiappone, A.; Sangermano, M.; Hélary, C.; Belbekhouche, S.; Coradin, T.; Versace, D. L., Photoinduced chitosan–PEG hydrogels with long-term antibacterial properties. *Journal of Materials Chemistry B* **2019,** *7* (42), 6526-6538.

4. Xue, Y.; Xiao, H.; Zhang, Y., Antimicrobial Polymeric Materials with Quaternary Ammonium and Phosphonium Salts. *International Journal of Molecular Sciences* **2015,** *16* (2).

5. Fouassier, J.-P.; Lalevée, J., *Photoinitiators for polymer synthesis: scope, reactivity, and efficiency*. John Wiley & Sons: 2012.

6. Alge, D. L.; Azagarsamy, M. A.; Donohue, D. F.; Anseth, K. S., Synthetically tractable click hydrogels for three-dimensional cell culture formed using tetrazine-norbornene chemistry. *Biomacromolecules* **2013,** *14* (4), 949-53.

7. Jia, W.; Gungor-Ozkerim, P. S.; Zhang, Y. S.; Yue, K.; Zhu, K.; Liu, W.; Pi, Q.; Byambaa, B.; Dokmeci, M. R.; Shin, S. R.; Khademhosseini, A., Direct 3D bioprinting of perfusable vascular constructs using a blend bioink. *Biomaterials* **2016,** *106*, 58-68.

8. Shih, H.; Lin, C. C., Photoclick Hydrogels Prepared from Functionalized Cyclodextrin and Poly(ethylene glycol) for Drug Delivery and in Situ Cell Encapsulation. *Biomacromolecules* **2015,** *16* (7), 1915-23.

9. Yang, Y.; Liu, X.; Li, Y.; Wang, Y.; Bao, C.; Chen, Y.; Lin, Q.; Zhu, L., A postoperative anti-adhesion barrier based on photoinduced imine-crosslinking hydrogel with tissue-adhesive ability. *Acta Biomaterialia* **2017,** *62*, 199-209.

10. Zhang, J.; Zheng, Y.; Lee, J.; Hua, J.; Li, S.; Panchamukhi, A.; Yue, J.; Gou, X.; Xia, Z.; Zhu, L.; Wu, X., A pulsatile release platform based on photo-induced imine-crosslinking hydrogel promotes scarless wound healing. *Nature Communications* **2021,** *12* (1), 1670.

11. Li, Z.; Kosuri, S.; Foster, H.; Cohen, J.; Jumeaux, C.; Stevens, M. M.; Chapman, R.; Gormley, A. J., A Dual Wavelength Polymerization and Bioconjugation Strategy for High Throughput Synthesis of Multivalent Ligands. *Journal of the American Chemical Society* **2019,** *141* (50), 19823-19830.

CHAPTER 4

PHOTOCLEAVABLE AMPHIPHILIC BLOCK COPOLYMERS

4.1 Introduction

Interest is growing in the design of light-responsive amphiphilic block copolymers (BCP).[1-4] Block copolymers contain two or more covalently linked homopolymer subunits. The amphiphilic block copolymers tend to self-assemble into various types of morphologies including micelles in aqueous solution. The driving force of micelles formation is the hydrophobic effect induced by hydrophobic blocks in an aqueous solution.[5-7] These nanostructures have been grown for use in drug encapsulation and controlled delivery.[8-11] Recently, photocleavable nanostructures have gained growing attention.[12-17] The photo-responsive system could be selectively degraded by incorporation of the photocleavable units in the block copolymers. And light triggering promises the precise temporal and spatial control over other stimuli.

In this project, we designed a photo-cleavable linker as the amphiphilic copolymers joint point. The linker was built by incorporating propargyl group decorated o-naphthoquinone methides precursor (o-NQMP) and azadibenzocyclooctyne (ADIBO). The azide functionalized polymers could then be easily installed sequentially by copper(I)-catalyzed azide-alkyne

cycloaddition (CuAAC) and strain-promoted azide-alkyne cycloaddition (SPAAC). The resulting copolymers could be cleaved by UV light at ambient conditions. This block copolymer system could be a good candidate for drug-loaded micelles to achieve photo-responsive drug release.

4.2 Photocleavable Linker Design and Synthesis

In this project, the synthesis procedure of ADIBO acid **4.4** was modified from the previously published procedure (Scheme 4. 1).[18] The EDC coupling between compound **2.4** and compound **3.5** yielded compound **4.1**. The carboxylic acid was deprotected by potassium hydroxide to provide compound **4.2**, which was then brominated to deliver **4.3**. ADIBO acid **4.4** was synthesized by eliminating **4.3**. The last step of this synthesis pathway requires extremely pure potassium tert-butoxide, which increases the synthesis difficulty for this scheme.

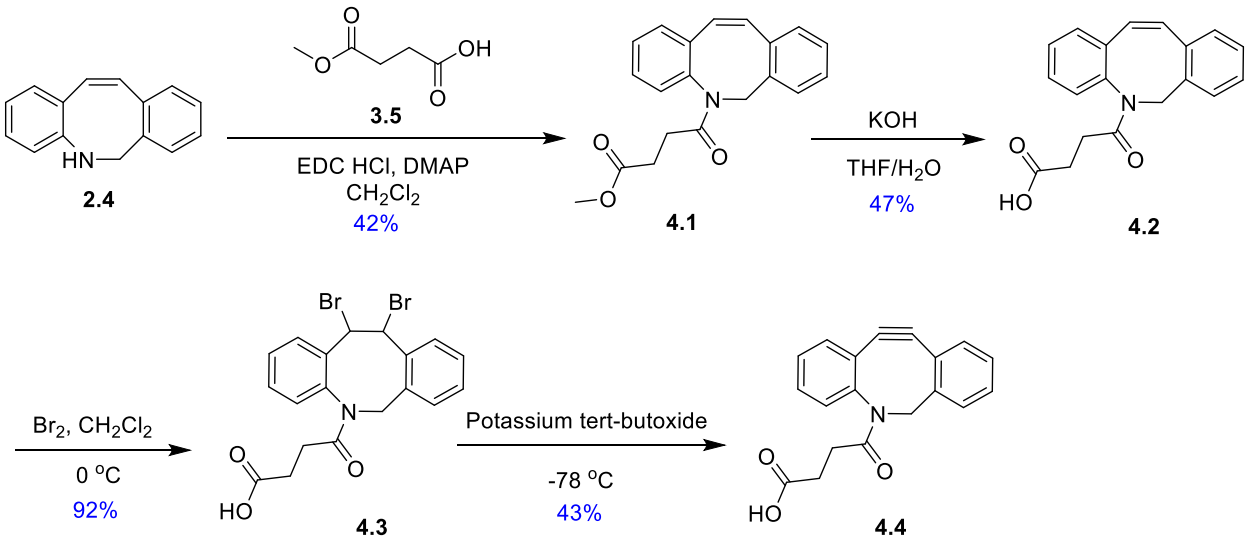

Scheme 4. 1 Synthesis of ADIBO Acid 4.4

The o-naphthoquinone methides precursor (o-NQMP) was incorporated with the propargyl

group in this project. A linker **4.6** was synthesized for the o-NQMP functionalization. Tetraethylene glycol was decorated with the propargyl group before tosylation to yield the linker **4.6**. The o-NQMP was prepared from 3,5-dihydroxy-2-naphthoic acid methylation to yield compound **4.7**. Lithium aluminium hydride (LAH) reduction was followed to give diol **4.8** which was protected using 2,2-dimethoxypropane (DMP) to yield compound **4.9**. The linker **4.6** was installed on **4.9** to yield a propargyl group decorated **4.10**. The protected diol was then revealed by Amberlyst-15 before diethylene glycol was incorporated. The compound **4.12** was brominated before azide substitution. The resulting **4.15** was synthesized in a high yield by reducing compound **4.14** with the help of LAH (Scheme 4. 2). This part of the synthesis collaborated with Dr. Nannan Lin.

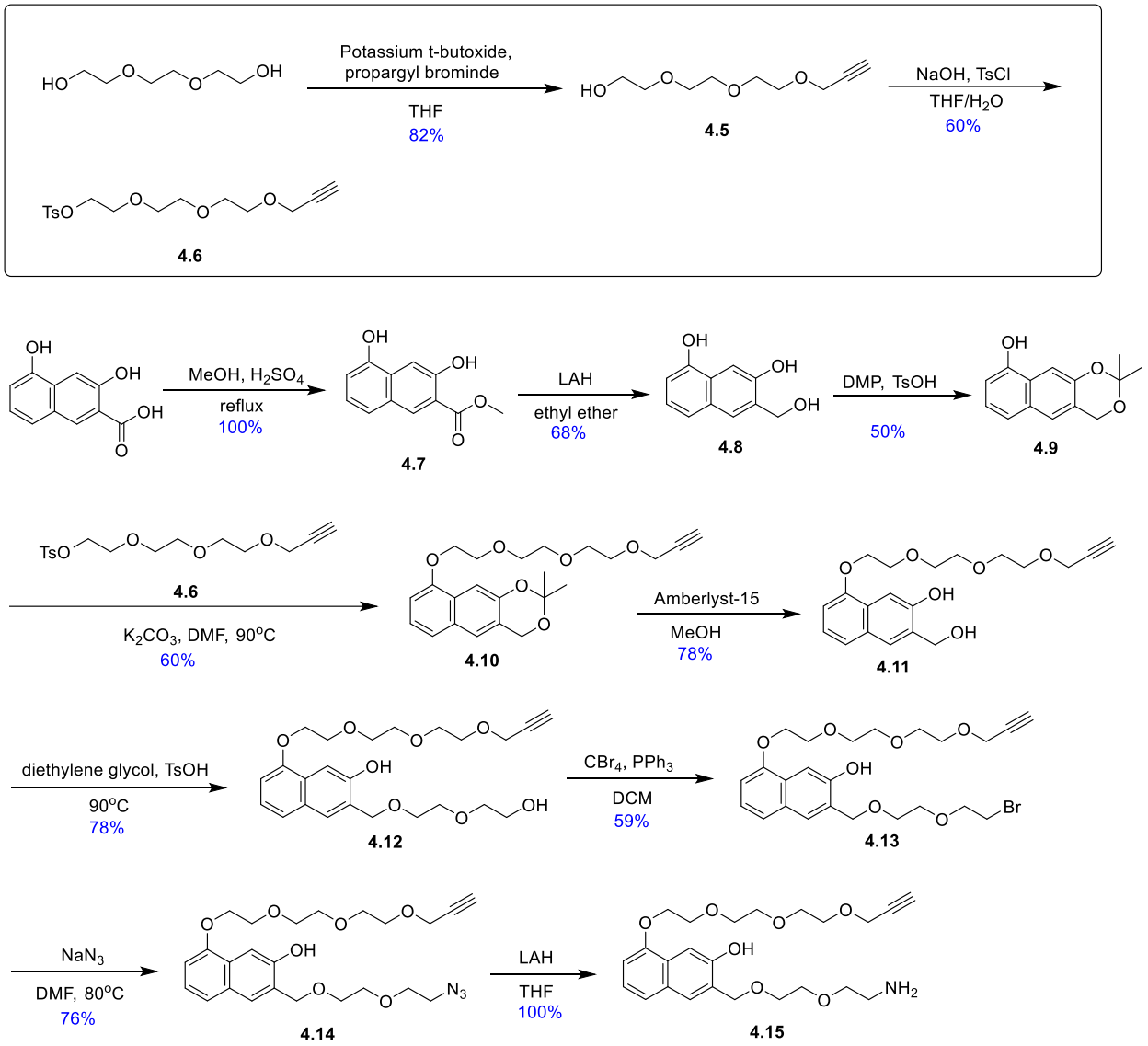

Scheme 4. 2 Synthesis of 4.16

The photocleavable linker was synthesized by incorporating propargyl functionalized o-NQMP **4.15** and ADIBO acid **4.4** via carbodiimide coupling (Scheme 4. 3).

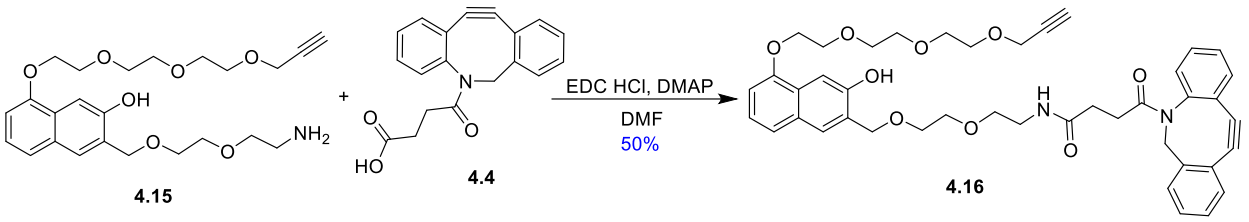

Scheme 4. 3 Synthesis of Photocleavable Linker 4.16

4.3 Hydrophilic and Hydrophobic Polymer Design and Synthesis

Poly(ethylene glycol) monomethyl ether (mPEG) was chosen as the hydrophilic polymer in this project. PEG has been approved by the United States Food and Drug Administration (FDA) for medical use and it shows high aqueous solubility, low protein absorption, and low cell adhesion.[19] The PEG was decorated with azide groups for the installation on a photocleavable linker (Scheme 4. 4). The **mPEG-OH** was mesylated to yield **mPEG-OMs** before the azide substitution to afford **mPEG-N$_3$**.

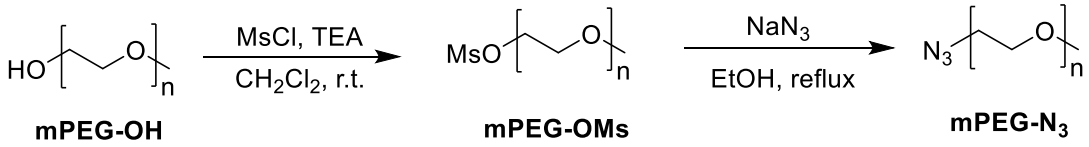

Scheme 4. 4 Synthesis of mPEG-N$_3$

Polycaprolactone (PCL) was chosen as the hydrophobic polymer for this project. The synthesis of **PCL-N$_3$** started from ring-opening polymerization (ROP) using Tin (II) 2-ethylhexanoate followed by azide functionalization (Scheme 4. 5). This part of the synthesis collaborated with Dr. Yutian Ke.

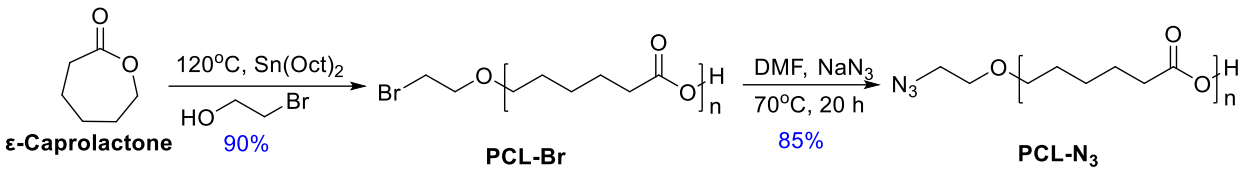

Scheme 4. 5 Synthesis of PCL-N_3

4.4 Photocleavable Block Copolymer Design and Synthesis

mPEG-N_3 was clicked on **4.16** by mixing in dark for overnight and the resulting **4.17** was precipitated out using ethyl ether. The next equivalent of **mPEG-N_3** will be clicked on **4.17** with the help of the Cu (I) catalyst in future work (Scheme 4. 6).

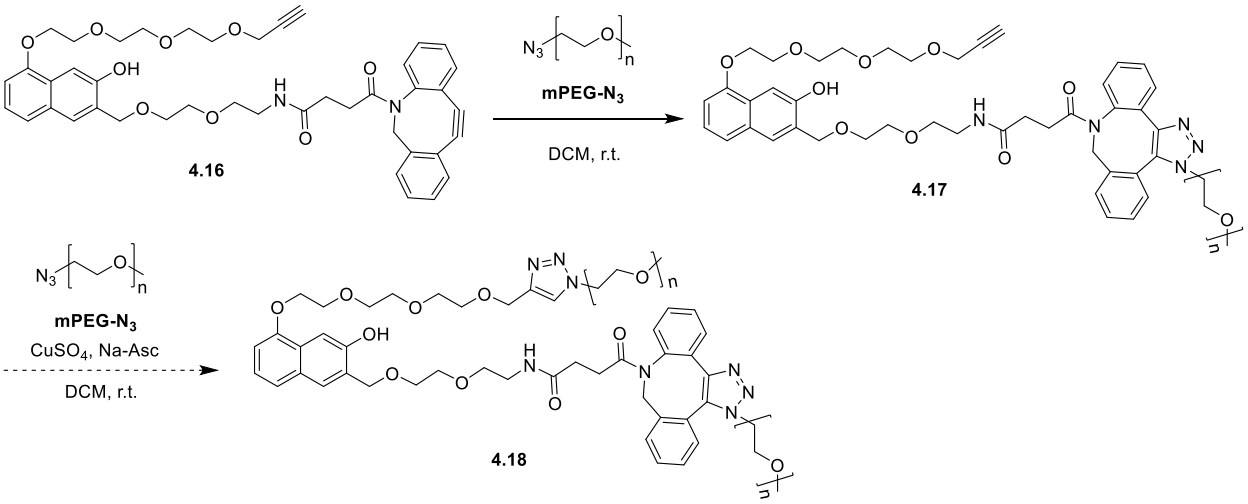

Scheme 4. 6 Photo Cleavable Block Copolymer Synthesis

4.5 Future Work and Conclusion

We successfully synthesized a photocleavable linker for amphiphilic copolymers installation.

CuAAC.

The amphiphilic block copolymer synthesis and the copolymer's photocleavage behavior are still under investigation.

4.6 Experiment Section

Compound **4.1 – 4.4** were prepared following published procedure.[18]

Methyl (Z)-4-(dibenzo[b,f]azocin-5(6H)-yl)-4-oxobutanoate 4.1: EDC · HCl (10.30 g, 53.8 mmol, 2.0 equiv.) and catalytic amount of DMAP was added to a solution of **3.5** (7.11 g, 53.8 mmol, 2.0 equiv.) in 53 mL CH_2Cl_2. The mixture was stirred for 10 min before a solution of **2.4** (5.60 g, 27.0 mmol) in 53 mL CH_2Cl_2 was added. The reaction was stirred at room temperature for overnight before washed by brine. The organic layer was dried over Na_2SO_4 before purified on a silica gel column using 10%-30% EtOAc in hexanes to yield product as white crystals (3.65 g, 42%). ^{1}H NMR (400 MHz, $CDCl_3$) δ 7.20 – 7.03 (m, 8H), 6.73 (d, J = 12.9 Hz, 1H), 6.55 (d, J = 12.9 Hz, 1H), 5.45 (d, J = 15.0 Hz, 1H), 4.19 (d, J = 15.1 Hz, 1H), 3.55 (s, 3H), 2.58 – 2.49 (m, 1H), 2.38 (m, 2H), 1.94 (m, 1H). ^{13}C NMR (101 MHz, $CDCl_3$) δ 173.50, 170.92, 140.55, 136.53, 135.89, 134.63, 132.71, 131.88, 130.92, 130.22, 128.61, 128.32, 128.08, 127.36, 127.01, 54.55, 51.70, 29.61, 29.08.

(Z)-4-(Dibenzo[b,f]azocin-5(6H)-yl)-4-oxobutanoic acid 4.2: A solution of potassium hydroxide (0.39 g, 7.0 mmol, 2.0 equiv.) in 7.0 mL DI water was added to a solution of **4.1** (1.13 g, 3.5 mmol) in 5.4 mL tetrahydrofuran. The reaction was stirred at room temperature for 1 h

before quenched by 1 M HCl until the pH was under 7 and extracted by EtOAc. The organic layer was washed by brine, dried over Na_2SO_4, and concentrated under vacuum before purified on a silica gel column using 66% EtOAc in hexanes to yield product as colorless oil (0.51 g, 47%). ^{1}H NMR (400 MHz, $CDCl_3$) δ 7.25 – 7.20 (m, 3H), 7.19 – 7.03 (m, 5H), 6.76 – 6.71 (m, 1H), 6.57 – 6.52 (m, 1H), 5.46 (d, *J* = 15.1 Hz, 1H), 4.23 (d, *J* = 15.1 Hz, 1H), 2.58 – 2.44 (m, 2H), 2.43 – 2.30 (m, 1H), 1.98 (m, 1H). ^{13}C NMR (101 MHz, $CDCl_3$) δ 176.14, 171.92, 140.01, 136.44, 135.82, 134.06, 132.95, 131.81, 130.85, 130.15, 128.75, 128.41, 128.02, 127.45, 127.24, 124.16, 54.62, 29.73, 29.57.

4-(11,12-Dibromo-11,12-dihydrodibenzo[b,f]azocin-5(6H)-yl)-4-oxobutanoic acid 4.3: a solution of Br_2 (0.16 mL, 0.50 g, 3.2 mmol, 1.3 equiv.) in 0.6 mL CH_2Cl_2 was slowly added to a solution of **4.2** (0.72 g, 2.4 mmol) in 10.1 mL CH_2Cl_2 at 0 °C. The reaction was stirred at 0 °C for 1 h (the reaction was followed by ^{1}H NMR and monitored the disappearance of the peak at ~ 6.7 ppm) before being worked up by being quenched with Na_2SO_3 aqueous solution (0.20 g in 1.44 mL DI water) and washed with water. The organic layer was washed with 1 M H_3PO_4, brine, and dried over Na_2SO_4. The solvent was removed under vacuum to yield the product as green foam (1.03 g, 92%). The crude product was put into the next step without any further purification. Since compound **4.3** is unstable, it should be eliminated on the same day as it is prepared.

4.4: A solution of **4.3** (1.03 g, 2.2 mmol) in 4.4 mL anhydrous tetrahydrofuran was cooled at -78 °C for 5 min before the addition of 4 M KOtBu solution in anhydrous tetrahydrofuran (2.8

mL, 11.0 mmol, 5.0 equiv., pre-cooled in -78 °C). The reaction was stirred at -78 °C for 2 h before diluted with 8 mL ethyl ether and washed with 1 M H_3PO_4, brine, dried over Na_2SO_4, and filtered. The solvent was then removed by rotary evaporation without a heating bath. Once most of the solvent has been removed, **4.4** began to precipitate into the solution as off-white crystals. At the onset of crystal formation, the flask was removed from the rotary evaporator and 8 mL ethyl ether was added, and the product was left to crystallize at -20 °C overnight. The product was then filtered and washed with small aliquots of ice-cold ethyl ether to yield **4.4** as white crystals (0.29 g, 43%). ^{1}H NMR (400 MHz, DMSO) δ 11.99 (s, 1H), 7.65 (m, 2H), 7.56 – 7.45 (m, 3H), 7.41 – 7.25 (m, 3H), 5.04 (d, *J* = 14.0 Hz, 1H), 3.63 (d, *J* = 14.0 Hz, 1H), 2.60 (dt, *J* = 16.6, 7.0 Hz, 1H), 2.30 (dt, *J* = 17.1, 6.9 Hz, 1H), 2.19 (m, 1H), 1.84 – 1.73 (m, 1H).

2-(2-(2-(Prop-2-yn-1-yloxy)ethoxy)ethoxy)ethan-1-ol 4.5: potassium t-butoxide (1.57 g, 14.0 mmol, 0.7 equiv.) was added to a solution of triethylene glycol (3.00 g, 20.0 mmol) in 80 mL anhydrous tetrahydrofuran at 0 °C. The mixture was stirred at 0 °C for 30 min before a solution of propargyl bromide (2.0 mL, 2.67 g, 80% in toluene, 18.0 mmol, 0.9 equiv.) in 27 mL anhydrous tetrahydrofuran was added dropwise. The reaction was stirred at room temperature for overnight before filtered by celite and purified on a silica gel column using EtOAc to yield product as yellow oil (2.15 g, 82%). ESI-MS: m/z = 189.2 $[M+H]^+$, 211.2 $[M+Na]^+$. ^{1}H NMR (400 MHz, $CDCl_3$) δ 4.19 (d, *J* = 2.4 Hz, 2H), 3.73 – 3.63 (m, 11H), 3.59 (dd, *J* = 5.3, 3.8 Hz, 2H), 2.73 (s, 1H).

2-(2-(2-(Prop-2-yn-1-yloxy)ethoxy)ethoxy)ethyl 4-methylbenzenesulfonate 4.6: a

solution of NaOH (1.60 g, 40.0 mmol) in 26 mL water was added to a solution of **4.5** (2.15 g, 11.4 mmol) in 17 mL tetrahydrofuran at 0 °C. And then a solution of TsCl (3.91 g, 20.5 mmol, 1.8 equiv.) in 9 mL tetrahydrofuran was added to the mixture. The reaction was then warmed to room temperature and stirred overnight. The reaction was extracted by 176 mL EtOAc and washed by water and brine. The organic layer was dried over Na_2SO_4, concentrated under vacuum to yield product as light-yellow oil (2.33 g**,** 60%). ESI-MS: m/z = 343.2 $[M+H]^+$, 365.2 $[M+Na]^+$, 381.3 $[M+K]^+$. ^{1}H NMR (400 MHz, $CDCl_3$) δ 7.76 – 7.71 (m, 2H), 7.28 (m, 2H), 4.16 – 4.08 (m, 4H), 3.68 – 3.56 (m, 8H), 2.38 (s, 3H). ^{13}C NMR (101 MHz, $CDCl_3$) δ 144.79, 133.05, 129.83, 128.00, 79.64, 74.55, 70.76, 70.57, 70.45, 69.24, 69.10, 68.71, 58.41, 21.65.

Methyl 3,5-dihydroxy-2-naphthoate 4.7: 10 mL concentrated H_2SO_4 was added drop wisely to a solution of 3,5-dihydroxy-2-naphthoic acid (8.00 g, 39.2 mmol) in 200 mL MeOH. The mixture was refluxed for 2 d before being precipitated in 1 L ice water. The precipitates were collected via suction filtration as yellow solid (8.40 g, 100%). ^{1}H NMR (400 MHz, $CDCl_3$) δ 10.36 (s, 1H), 8.40 (s, 1H), 7.56 (s, 1H), 7.35 (d, J = 8.3 Hz, 1H), 7.09 (t, J = 7.9 Hz, 1H), 6.78 (d, J = 7.4 Hz, 1H), 5.14 (s, 1H), 3.96 (s, 3H). ^{13}C NMR (101 MHz, $CDCl_3$) δ 170.27, 156.13, 150.03, 132.22, 129.12, 128.30, 123.74, 121.92, 114.63, 111.18, 106.26, 52.63.

6-(Hydroxymethyl)naphthalene-1,7-diol 4.8: a solution of **4.7** (5.00 g, 22.9 mmol) in 50 mL anhydrous ethyl ether was slowly added to a solution of LAH (2.17 g, 57.3 mmol, 2.0 equiv.) in 47 mL anhydrous ethyl ether at 0°C. The reaction was slowly warmed up to room temperature and stirred overnight before being quenched by 1 M HCl and extracted with EtOAc. The organic

layer was washed by brine, dried over Na_2SO_4, concentrated, and purified on a silica gel column using 10% MeOH in CH_2Cl_2 to yield the product as yellow solid (2.97 g, 68%). ESI-MS: m/z = 189.0 $[M-H]^-$. ^1H NMR (400 MHz, DMSO) δ 9.74 (s, 1H), 9.67 (s, 1H), 7.70 (s, 1H), 7.36 (s, 1H), 7.19 (t, *J* = 5.6 Hz, 1H), 7.05 – 7.00 (m, 1H), 6.73 – 6.69 (m, 1H), 4.61 (s, 2H). ^{13}C NMR (101 MHz, DMSO) δ 152.58, 152.06, 132.16, 129.55, 125.52, 125.16, 123.25, 118.61, 107.83, 103.47, 59.08.

2,2-Dimethyl-4H-naphtho[2,3-d][1,3]dioxin-9-ol 4.9: 2,2-dimethoxypropane (1.7 mL, 1.41 g, 13.5 mmol, 2.7 equiv.) and catalytic amount of TsOH was added to a solution of **4.8** (0.95 g, 5.0 mmol) in 30 mL anhydrous acetone. The mixture was stirred at room temperature for overnight before being neutralized with 1.5 mL triethylamine. The solvent was then removed under vacuum and the residue was redissolved in 30 mL EtOAc and washed with water and brine, dried over Na_2SO_4, concentrated, and purified on a silica gel column using 20% EtOAc in hexanes to yield product as light brown solid (0.58 g, 50%). ESI-MS: m/z = 229.0 $[M-H]^-$. ^1H NMR (400 MHz, $CDCl_3$) δ 7.57 (s, 1H), 7.47 (s, 1H), 7.34 (d, *J* = 8.3 Hz, 1H), 7.17 (dd, *J* = 8.2, 7.5 Hz, 1H), 6.76 (dd, *J* = 7.4, 0.6 Hz, 1H), 5.10 (m, 2H), 1.63 (s, 6H). ^{13}C NMR (101 MHz, $CDCl_3$) δ 150.40, 149.51, 129.77, 124.86, 123.68, 123.37, 121.72, 120.10, 108.33, 106.38, 99.88, 61.21, 24.98.

2,2-Dimethyl-9-(2-(2-(2-(prop-2-yn-1-yloxy)ethoxy)ethoxy)ethoxy)-4H-naphtho[2,3-d][1,3]dioxine 4.10: K_2CO_3 (0.94 g, 6.8 mmol, 2.0 equiv.) and a solution of **4.6** (1.30 g, 3.8 mmol, 1.1 equiv.) in 5 mL DMF were added to a solution of **4.9** (0.79 g, 3.4 mmol) in 17 mL

DMF. The mixture was stirred at 90 °C for overnight. The reaction was then separated between EtOAc and water. The organic layer was washed with water and brine, dried over Na_2SO_4, concentrated, and purified on a silica gel column using 20% EtOAc in hexanes to yield product as brown oil (0.82 g, 60%). ESI-MS: m/z = 423.3 $[M+Na]^+$. ^1H NMR (400 MHz, $CDCl_3$) δ 7.68 (s, 1H), 7.45 (s, 1H), 7.32 (d, *J* = 8.3 Hz, 1H), 7.25 – 7.20 (m, 1H), 6.75 (d, *J* = 7.4 Hz, 1H), 5.09 (s, 2H), 4.32 – 4.28 (m, 2H), 4.23 (d, *J* = 2.4 Hz, 2H), 4.03 – 3.98 (m, 2H), 3.83 (dd, *J* = 5.8, 3.5 Hz, 2H), 3.76 – 3.72 (m, 6H), 2.44 (t, *J* = 2.4 Hz, 1H), 1.62 (s, 6H).

3-(Hydroxymethyl)-8-(2-(2-(2-(prop-2-yn-1-yloxy)ethoxy)ethoxy)ethoxy)naphthalen-2-ol 4.11: 0.22 g amberlyst-15 ion exchange resin was added to a solution of **4.10** (0.22 g, 0.5 mmol) in 3 mL MeOH. The reaction was stirred at room temperature for overnight. The solid phase was removed by filtration before concentrated and purified on a silica gel column using 40% EtOAc in hexanes to yield product as yellow oil (0.14 g, 78%). ESI-MS: m/z = 359.2 $[M-H]^-$. ^1H NMR (400 MHz, $CDCl_3$) δ 7.74 (s, 1H), 7.60 (s, 1H), 7.38 (d, *J* = 8.2 Hz, 1H), 7.25 – 7.20 (m, 1H), 6.83 (d, *J* = 7.1 Hz, 1H), 4.96 (s, 2H), 4.30 (m, 2H), 4.27 (d, *J* = 2.4 Hz, 2H), 3.94 – 3.91 (m, 2H), 3.84 – 3.75 (m, 8H), 2.48 – 2.44 (m, 1H).

3-((2-(2-Hydroxyethoxy)ethoxy)methyl)-8-(2-(2-(2-(prop-2-yn-1-yloxy)ethoxy)ethoxy)ethoxy)naphthalen-2-ol 4.12: catalytic amount of p-TsOH was added to a solution of **4.11** (0.14 g, 0.4 mmol) in 6 mL diethylene glycol. The reaction was stirred at 90 °C for overnight before cooled down and separated between EtOAc and water. The organic layer was then washed with brine, dried over Na_2SO_4, concentrated, and purified on a silica gel

column using 80% EtOAc in hexanes to yield product as yellow oil (0.14 g, 78%). ESI-MS: m/z = 447.2 $[M-H]^-$, 483.2 $[M+Cl]^-$. ^1H NMR (400 MHz, $CDCl_3$) δ 7.59 (s, 1H), 7.45 (s, 1H), 7.23 (d, *J* = 8.2 Hz, 1H), 7.10 (t, *J* = 7.9 Hz, 1H), 6.66 (d, *J* = 7.5 Hz, 1H), 4.75 (s, 2H), 4.19 – 4.15 (m, 2H), 4.11 (d, *J* = 2.4 Hz, 2H), 3.89 – 3.85 (m, 2H), 3.73 – 3.67 (m, 6H), 3.65 – 3.58 (m, 8H), 3.55 – 3.50 (m, 2H), 2.36 (t, *J* = 2.4 Hz, 1H).

3-((2-(2-Bromoethoxy)ethoxy)methyl)-8-(2-(2-(2-(prop-2-yn-1-yloxy)ethoxy)ethoxy)ethoxy)naphthalen-2-ol 4.13: a solution of PPh_3 (0.11 g, 0.4 mmol, 1.0 equiv.) in 3.7 mL anhydrous CH_2Cl_2 was slowly added to a mixture of CBr_4 (0.14 g, 0.4 mmol, 1.0 equiv.) and **4.12** (0.19 g, 0.4 mmol) in 9.5 mL anhydrous CH_2Cl_2 at 0 °C. The reaction was warmed to room temperature and stirred for overnight before concentrated and purified on a silica gel column using (50% EtOAc/Hexanes) yield product as light-yellow gel (0.12 g, 59%). ESI-MS: m/z = 509.1 $[M-H]^-$, 545.1 $[M+Cl]^-$. ^1H NMR (400 MHz, $CDCl_3$) δ 7.62 (s, 1H), 7.48 (s, 1H), 7.26 (d, *J* = 8.3 Hz, 1H), 7.13 (t, *J* = 7.9 Hz, 1H), 6.70 (d, *J* = 7.4 Hz, 1H), 4.82 (s, 2H), 4.24 – 4.19 (m, 2H), 4.14 (t, *J* = 2.9 Hz, 2H), 3.93 – 3.88 (m, 2H), 3.79 – 3.73 (m, 4H), 3.70 – 3.65 (m, 10H), 3.45 (t, *J* = 6.3 Hz, 2H), 2.36 (t, *J* = 2.4 Hz, 1H).

3-((2-(2-Azidoethoxy)ethoxy)methyl)-8-(2-(2-(2-(prop-2-yn-1-yloxy)ethoxy)ethoxy)ethoxy)naphthalen-2-ol 4.14: NaN_3 (0.44 g, 6.8 mmol, 4.0 equiv.) was added to a solution of **4.13** (0.87 g, 1.7 mmol) in 22 mL DMF. The mixture was stirred at 80 °C for overnight before cooled down to room temperature and separated between EtOAc and water. The organic layer was washed with brine, dried over Na_2SO_4, concentrated, and purified on a

silica gel column using 50% EtOAc in hexanes to yield product as clear gel (0.61 g, 76%). ESI-MS: m/z = 472.2 $[M-H]^-$. ^1H NMR (400 MHz, $CDCl_3$) δ 7.71 (s, 1H), 7.57 (s, 1H), 7.34 (d, *J* = 8.3 Hz, 1H), 7.24 – 7.17 (m, 1H), 6.79 (d, *J* = 7.2 Hz, 1H), 4.90 (s, 2H), 4.32 – 4.28 (m, 2H), 4.23 (d, *J* = 2.4 Hz, 2H), 4.01 – 3.96 (m, 2H), 3.86 – 3.68 (m, 16H), 3.49 – 3.45 (m, 2H), 2.45 (t, *J* = 2.4 Hz, 1H).

3-((2-(2-Aminoethoxy)ethoxy)methyl)-8-(2-(2-(2-(prop-2-yn-1-yloxy)ethoxy)ethoxy)ethoxy)naphthalen-2-ol 4.15: a solution of **4.14** (0.61 g, 1.3 mmol) in 10 mL anhydrous tetrahydrofuran was added dropwise in a suspension of LAH (0.48 g, 12.6 mmol, 9.7 equiv.) in 75 mL anhydrous tetrahydrofuran at 0 °C. The reaction was then warmed to room temperature and stirred for overnight before being quenched with 32 mL methanol and followed with 1 M HCl/MeOH solution (60 mL). The suspension was filtrated through celite and the filtrate was concentrated under vacuum. The residue was then purified on a silica gel column using 3% - 27% - 70% TEA/MeOH/EtOAc to yield product as orange solid (0.60 g, 100%). ESI-MS (positive) Calcd. for $C_{24}H_{33}NO_7$ $[M+H]^+$: 448.23298. Found: 448.23299. ^1H NMR (400 MHz, DMSO) δ 7.74 (s, 1H), 7.50 (s, 1H), 7.36 (d, *J* = 8.2 Hz, 1H), 7.16 (t, *J* = 7.9 Hz, 1H), 6.85 (d, *J* = 7.6 Hz, 1H), 4.63 (s, 2H), 4.26 – 4.21 (m, 2H), 4.13 (d, *J* = 2.3 Hz, 2H), 3.91 – 3.86 (m, 2H), 3.68 (m, 8H), 3.60 – 3.51 (m, 8H), 3.43 (t, *J* = 2.3 Hz, 1H).

4.16: EDC · HCl (0.17 g, 0.9 mmol, 1.2 equiv.) and catalytic amount of DMAP were added to a solution of **4.4** (0.29 g, 0.9 mmol, 1.2 equiv.) in 9 mL degassed DMF before a solution of **4.15** (0.34 g, 0.8 mmol) in 21 mL degassed DMF was added. The reaction was stirred at room

temperature for overnight before solvent was removed under vacuum, the residue was redissolved in CH_2Cl_2 and washed with brine, dried over Na_2SO_4 and purified on a silica gel column using EtOAc to yield product as yellow oil (0.29 g, 50%). ESI-MS: m/z = 735.4 $[M+H]^+$, 757.4 $[M+Na]^+$. ^1H NMR (400 MHz, $CDCl_3$) δ 7.64 (d, *J* = 8.1 Hz, 1H), 7.56 (s, 1H), 7.49 – 7.45 (m, 2H), 7.32 (m, 4H), 7.23 (m 3H), 7.18 – 7.08 (m, 2H), 6.70 (d, *J* = 7.4 Hz, 1H), 6.33 (s, 1H), 5.10 (dd, *J* = 13.9, 4.5 Hz, 1H), 4.75 (d, *J* = 4.0 Hz, 1H), 4.20 (dd, *J* = 10.7, 5.2 Hz, 2H), 4.11 (t, *J* = 2.6 Hz, 2H), 3.90 – 3.86 (m, 2H), 3.69 – 3.65 (m, 4H), 3.63 – 3.59 (m, 6H), 3.56 (dd, *J* = 5.3, 3.1 Hz, 2H), 3.45 – 3.37 (m, 2H), 3.31 (m, 2H), 2.83 – 2.72 (m, 1H), 2.48 – 2.40 (m, 1H), 2.34 (dd, *J* = 5.4, 3.0 Hz, 1H), 2.17 – 2.10 (m, 1H), 1.88 (m, 1H).

mPEG-OMs: mPEG-OH (5.00 g, 1.0 mmol, 1.0 equiv.) was dried over high vacuum overnight through a drying tube with P_2O_5. Then dissolved in anhydrous 8.3 mL CH_2Cl_2. The solution was cooled in an ice-water bath before adding triethylamine (0.31 mL, 0.23 g, 2.3 mmol, 2.3 equiv.) followed by MsCl (0.26 mL, 0.39 g, 3.4 mmol, 3.4 equiv.) and the reaction could warm to room temperature and stir for 14 h. The solution was diluted with 33.3 mL CH_2Cl_2, washed with 2M HCl : brine (1:1 v/v, 3*10 mL, 0.5 g PEG/mL), brine (1*10 mL, 0.5 g PEG/mL) , dried with Na_2SO_4 and then diluted by 20 mL CH_2Cl_2 and precipitated by the addition of excess Et_2O (10* v/v, 200 mL). The precipitation was stored at -4 °C for 12h before the solids were collected by vacuum filtration and washed with additional Et_2O. The product was dried under reduced pressure to yield mPEG-OMs as a white solid (4.29 g, 84%).

mPEG-N_3: sodium azide (0.56 g, 8.4 mmol, 10.0 equiv.) was added to a solution of **mPEG-**

OMs (4.29 g, 0.84 mmol) in 54 mL ethanol. The suspension was refluxed overnight before being concentrated under vacuum. The crude product was cooled to room temperature before being suspended in 34 mL CH_2Cl_2:MeOH (10:1, v/v, 0.125 g/mL), filtrated through a short plug of $SiO_2/MgSO_4$, and washed by additional 34 mL CH_2Cl_2:MeOH (10:1, v/v). The filtrate was concentrated under vacuum to a volume of 17 mL (0.25 g PEG/mL) before the addition of 171 mL Et_2O. The precipitation was stored at -4 °C for overnight before the solids were collected by vacuum filtration and washed with additional Et_2O. The product was dried under reduced pressure to yield **mPEG-N_3** as a white solid (3.65 g, 86%).

4.17: mPEG-N_3 (0.55 g, 0.11 mmol, 1.0 equiv.) and **4.16** (0.08 g, 0.11 mmol, 1.0 equiv.) were dissolved in 1.4 mL CH_2Cl_2 in a small glass vial. The reaction mixture was stirred at dark for 24 h before being diluted by 1.4 mL CH_2Cl_2 (0.20 g PEG/mL) and precipitated by the addition of excess 28 mL Et_2O. The precipitation was stored at - 4°C for 12 h before the solids were collected by suction filtration and washed with additional Et_2O and dried under reduced pressure to yield the product as light-yellow solid (0.32 g, 51%).

PCL-Br: a round-bottom flask equipped with a nitrogen inlet and septum was carefully flamed under nitrogen and purged with nitrogen (3 times). The initiator 2-bromoethanol (0.12g, 1.0 mmol, 1 eq.) and Tin (II) 2-ethylhexanoate (0.05g, 1%wt to monomer) were dissolved in 1 mL toluene and injected into the flask. The monomer ε-caprolactone (4.79g, 43.0 mmol, 43 equiv.) was added and heated to 120 ºC under vigorous stirring for 24 hours. The crude product was cooled to room temperature and dissolved in 10 mL tetrahydrofuran and precipitated into 50

mL hexanes. The polymer powders were isolated by filtration, redissolved in 10 mL tetrahydrofuran, precipitated into 50 mL hexanes twice. The product was dried under reduced pressure to yield the product as a white solid (4.30 g, 90%).

PCL-N_3: a round-bottom flask fitted with a condenser was charged with **PCL-Br** (4.5 g, 1 equiv.), 10 mL DMF, and then sodium azide (0.60 g, 10 equiv.). The suspension was heated to 70 ^oC and stirred overnight. The mixture was rapidly filtered through a short plug of $SiO_2/MgSO_4$, washed by an additional 2 mL DMF. The filtrate was precipitated into 50 mL hexanes. The polymer powders were isolated by filtration, washed with additional hexanes (20 mL *3). The product was dried under reduced pressure to yield the product as a white solid (3.83 g, 85%).

4.7 References

1. Jochum, F. D.; Theato, P., Thermo- and light responsive micellation of azobenzene containing block copolymers. *Chemical Communications* **2010,** *46* (36), 6717-6719.

2. Han, D.; Tong, X.; Zhao, Y., Fast Photodegradable Block Copolymer Micelles for Burst Release. *Macromolecules* **2011,** *44* (3), 437-439.

3. Schumers, J. M.; Fustin, C. A.; Gohy, J. F., Light-responsive block copolymers. *Macromolecular Rapid Communications* **2010,** *31* (18), 1588-607.

4. Babin, J.; Pelletier, M.; Lepage, M.; Allard, J. F.; Morris, D.; Zhao, Y., A new two-photon-sensitive block copolymer nanocarrier. *Angewandte Chemie (International ed. in English)* **2009,** *48* (18), 3329-32.

5. Chen, Z.; Wang, X.; Zhang, L.; He, L., Vesicles from the self-assembly of coil–rod–coil triblock copolymers in selective solvents. *Polymer* **2014,** *55* (12), 2921-2927.

6. Cui, J.; Han, Y.; Jiang, W., Asymmetric vesicle constructed by AB/CB diblock copolymer mixture and its behavior: a Monte Carlo study. *Langmuir* **2014,** *30* (30), 9219-27.

7. Jiménez, Z. A.; Yoshida, R., Temperature Driven Self-Assembly of a Zwitterionic Block Copolymer That Exhibits Triple Thermoresponsivity and pH Sensitivity. *Macromolecules* **2015,** *48* (13), 4599-4606.

8. Onaca, O.; Enea, R.; Hughes, D. W.; Meier, W., Stimuli-responsive polymersomes as nanocarriers for drug and gene delivery. *Macromolecular Bioscience* **2009,** *9* (2), 129-39.

9. Yan, B.; Tong, X.; Ayotte, P.; Zhao, Y., Light-responsive block copolymer vesicles based on a photo-softening effect. *Soft Matter* **2011,** *7* (21), 10001-10009.

10. Torchilin, V. P., Micellar nanocarriers: pharmaceutical perspectives. *Pharmaceutical Research* **2007,** *24* (1), 1-16.

11. Klaikherd, A.; Nagamani, C.; Thayumanavan, S., Multi-Stimuli Sensitive Amphiphilic Block Copolymer Assemblies. *Journal of the American Chemical Society* **2009,** *131* (13), 4830-4838.

12. Cabane, É.; Malinova, V.; Meier, W. P., Synthesis of Photocleavable Amphiphilic Block Copolymers: Toward the Design of Photosensitive Nanocarriers. *Macromolecular Chemistry and Physics* **2010,** *211*, 1847-1856.

13. Lee, R. S.; Li, Y. C.; Wang, S. W., Synthesis and characterization of amphiphilic

photocleavable polymers based on dextran and substituted-ε-caprolactone. *Carbohydrate Polymers***2015,** *117*, 201-210.

14. Yamamoto, S.; Yamada, T.; Kubo, G.; Sakurai, K.; Yamaguchi, K.; Nakanishi, J., Preparation of a Series of Photoresponsive Polymersomes Bearing Photocleavable a 2-nitrobenzyl Group at the Hydrophobic/Hydrophilic Interfaces and Their Payload Releasing Behaviors. *Polymers* **2019,** *11* (8).

15. Gungor, E.; Armani, A. M., Photocleavage of Covalently Immobilized Amphiphilic Block Copolymer: From Bilayer to Monolayer. *Macromolecules* **2016,** *49* (16), 5773-5781.

16. Wang, J.; Ouyang, Y.; Li, S.; Wang, X.; He, Y., Photocleavable amphiphilic diblock copolymer with an azobenzene linkage. *RSC Advances* **2016,** *6* (62), 57227-57231.

17. Shrivastava, S.; Matsuoka, H., Photocleavable amphiphilic diblock copolymer micelles bearing a nitrobenzene block. *Colloid and Polymer Science* **2016,** *294*.

18. McNelles, S. A.; Pantaleo, J. L.; Adronov, A., Highly Efficient Multigram Synthesis of Dibenzoazacyclooctyne (DBCO) without Chromatography. *Organic Process Research & Development* **2019,** *23* (12), 2740-2745.

19. Rijcken, C. J.; Soga, O.; Hennink, W. E.; van Nostrum, C. F., Triggered destabilisation of polymeric micelles and vesicles by changing polymers polarity: an attractive tool for drug delivery. *Journal of Controlled Release* **2007,** *120* (3), 131-48.

APPENDICES

1. ^{1}H and ^{13}C NMR Spectra

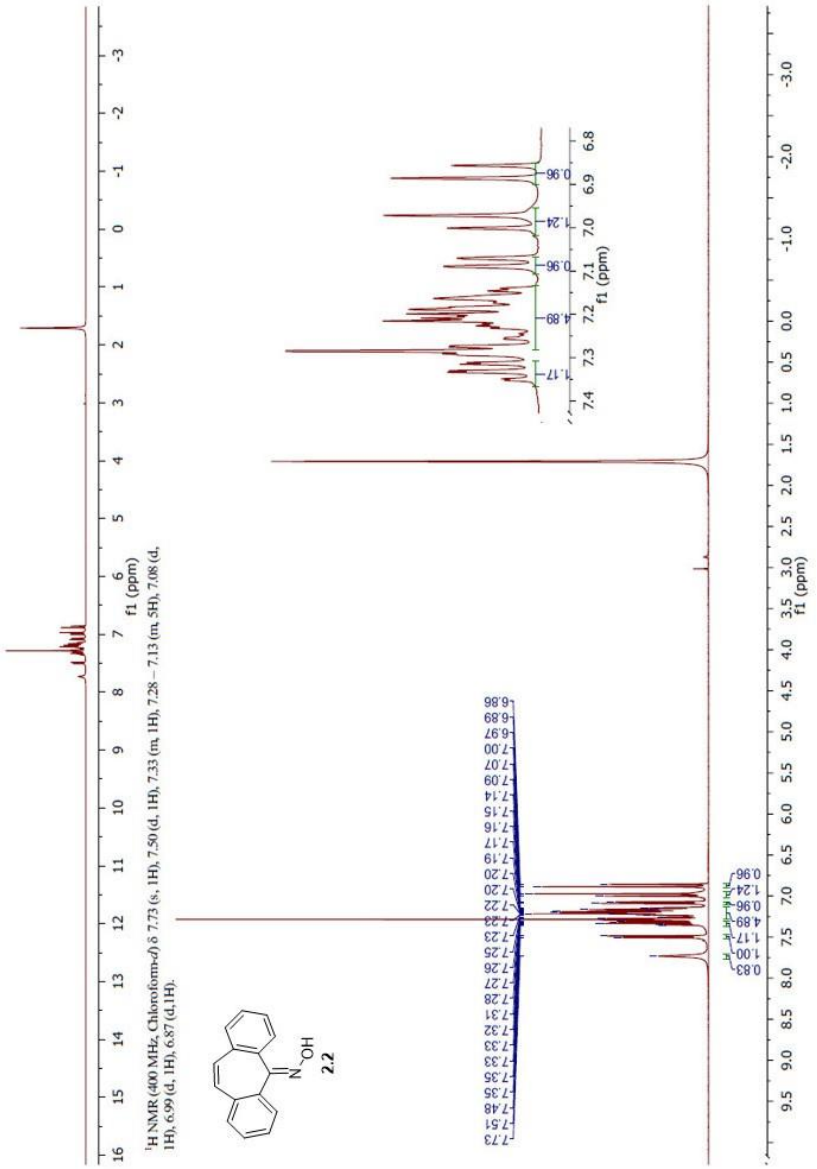

2.2 ^{1}H NMR Spectra

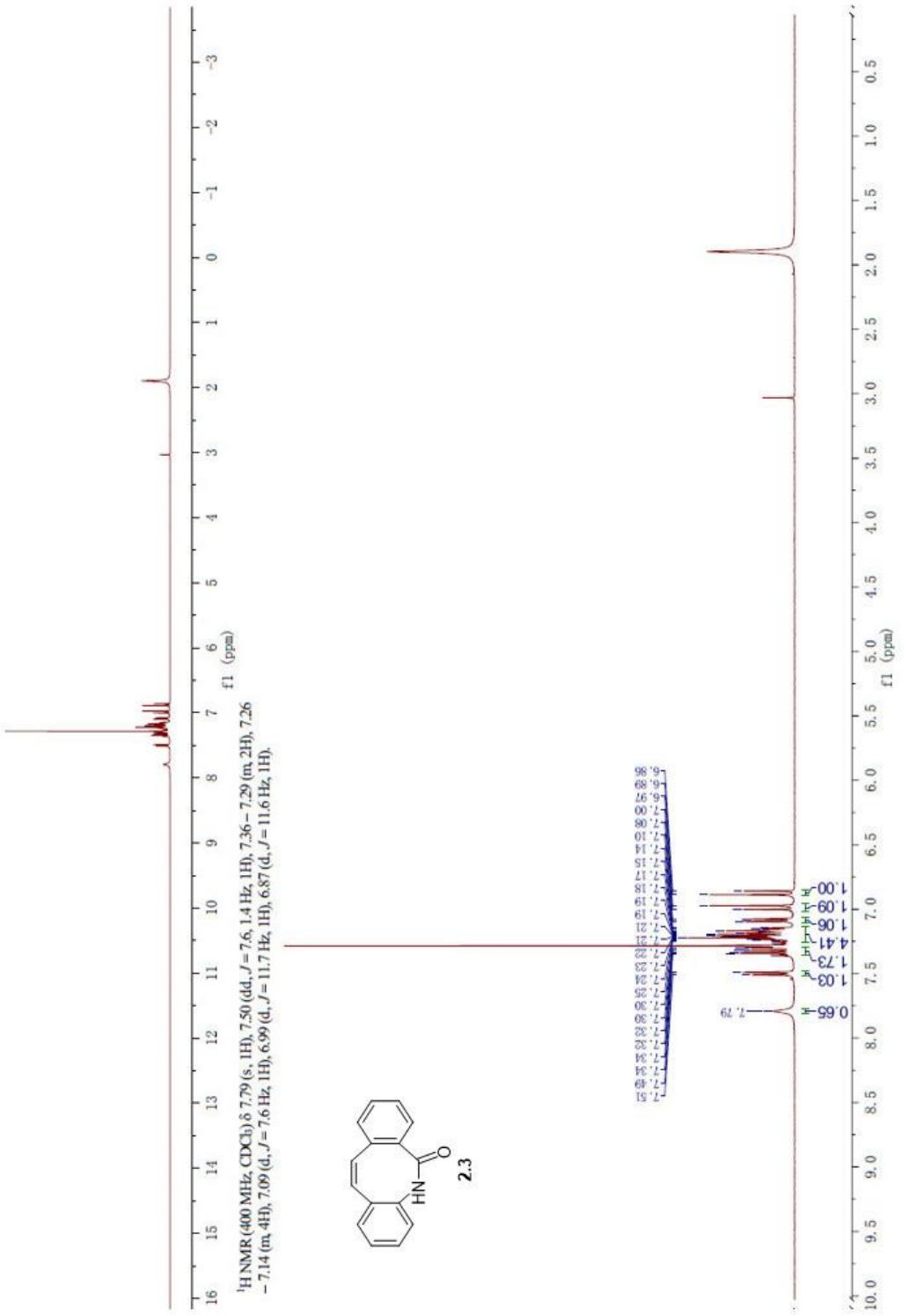

2.3 ^{1}H NMR Spectra

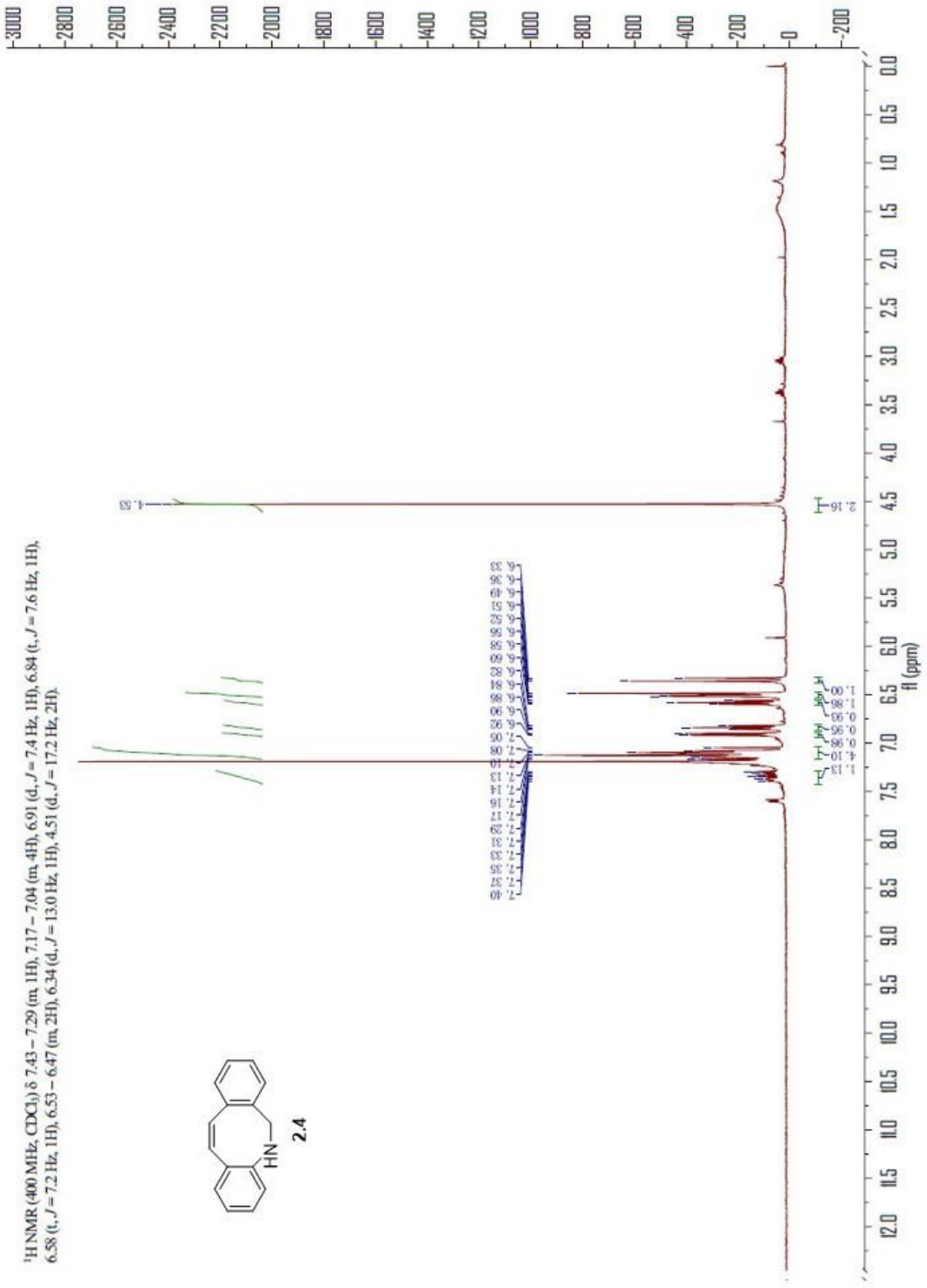

2.4 ^{1}H NMR Spectra

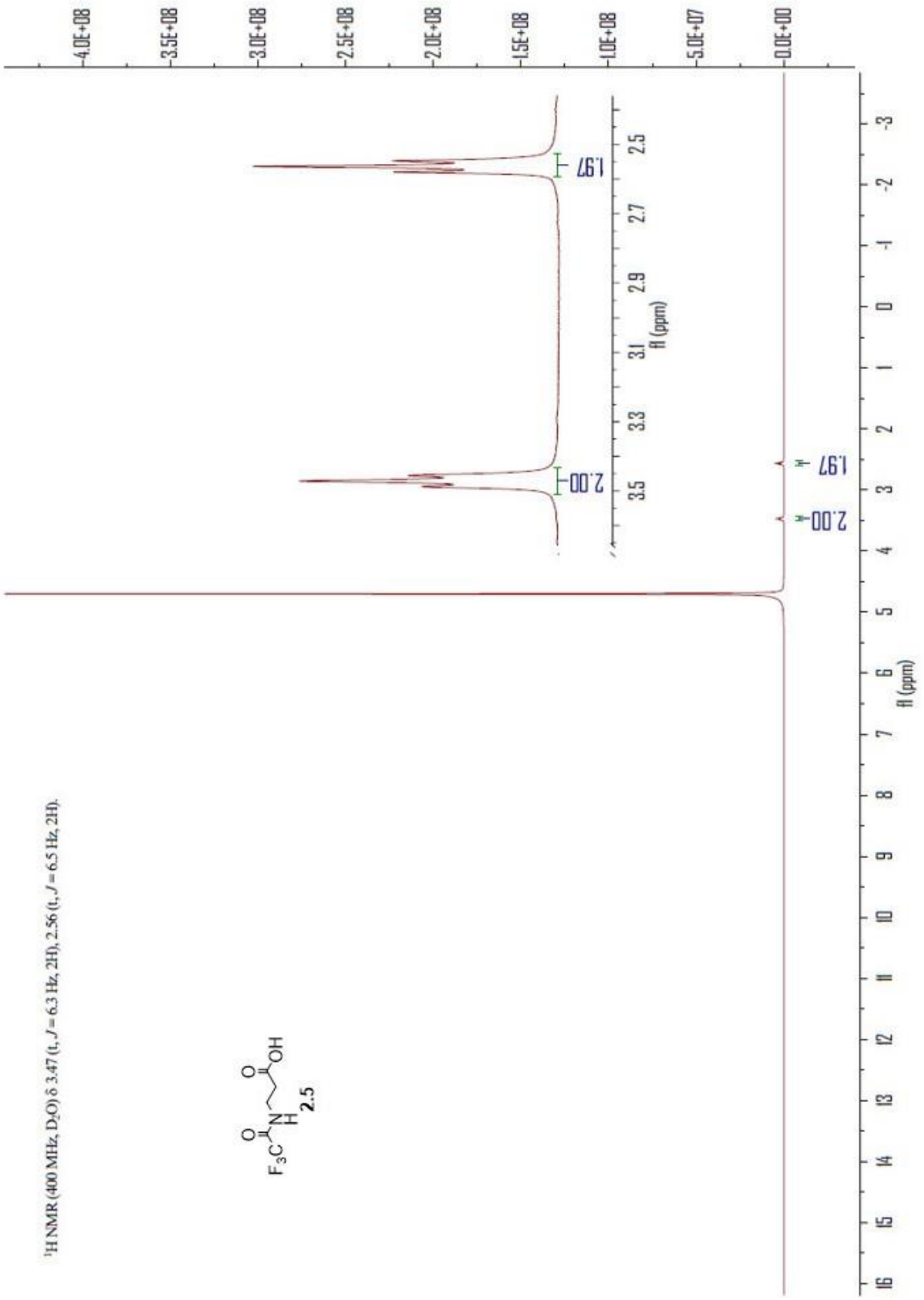

2.5 ^{1}H NMR Spectra

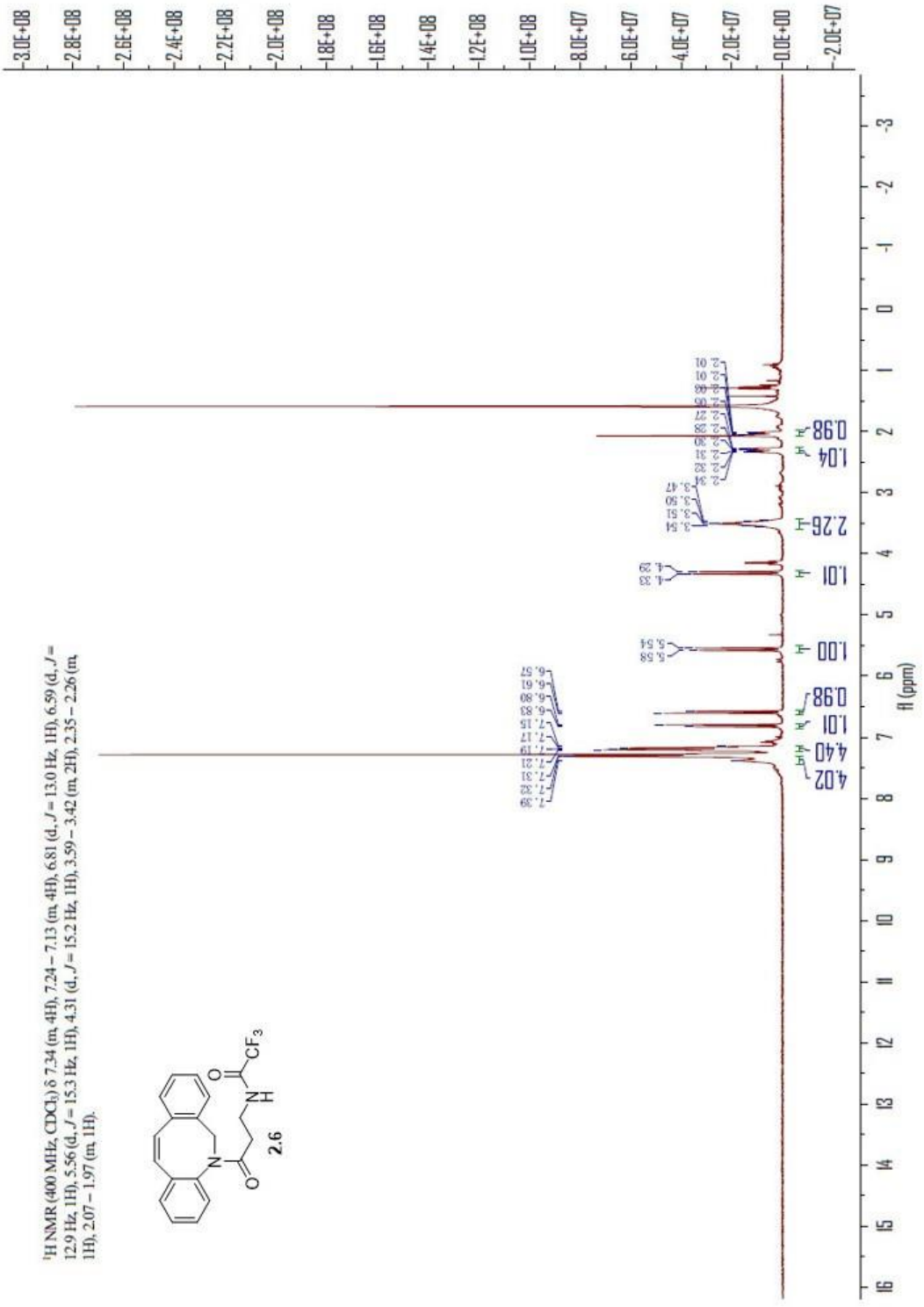

^{1}H NMR (400 MHz, $CDCl_3$) δ 7.34 (m, 4H), 7.24 – 7.13 (m, 4H), 6.81 (d, J = 13.0 Hz, 1H), 6.59 (d, J = 12.9 Hz, 1H), 5.56 (d, J = 15.3 Hz, 1H), 4.31 (d, J = 15.2 Hz, 1H), 3.59 – 3.42 (m, 2H), 2.35 – 2.26 (m, 1H), 2.07 – 1.97 (m, 1H).

2.6

2.6 ^{1}H NMR Spectra

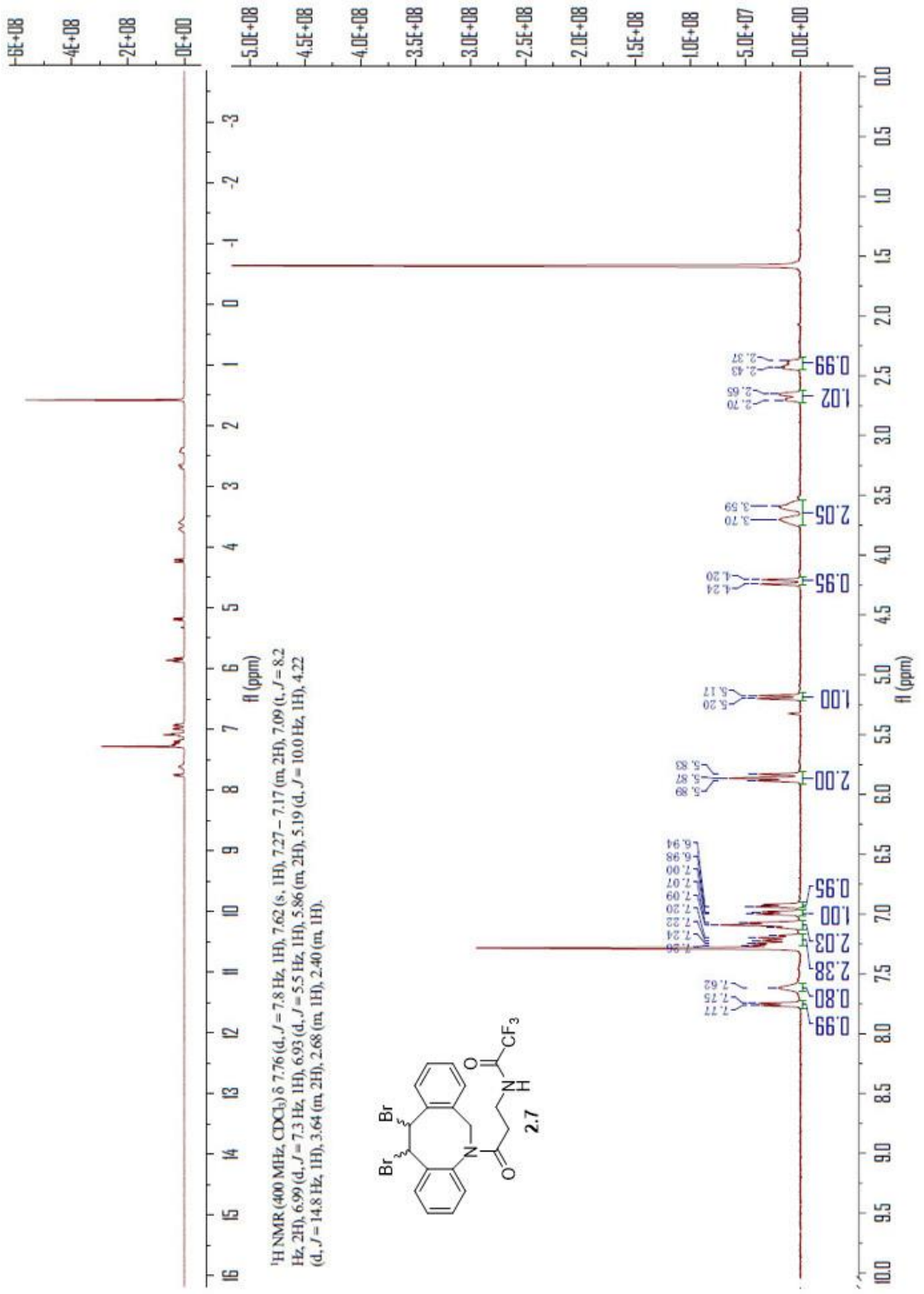

^{1}H NMR (400 MHz, $CDCl_3$) δ 7.76 (d, J = 7.8 Hz, 1H), 7.62 (s, 1H), 7.27 – 7.17 (m, 2H), 7.09 (t, J = 8.2 Hz, 2H), 6.99 (d, J = 7.3 Hz, 1H), 6.93 (d, J = 5.5 Hz, 1H), 5.86 (m, 2H), 5.19 (d, J = 10.0 Hz, 1H), 4.22 (d, J = 14.8 Hz, 1H), 3.64 (m, 2H), 2.68 (m, 1H), 2.40 (m, 1H).

2.7 ^{1}H NMR Spectra

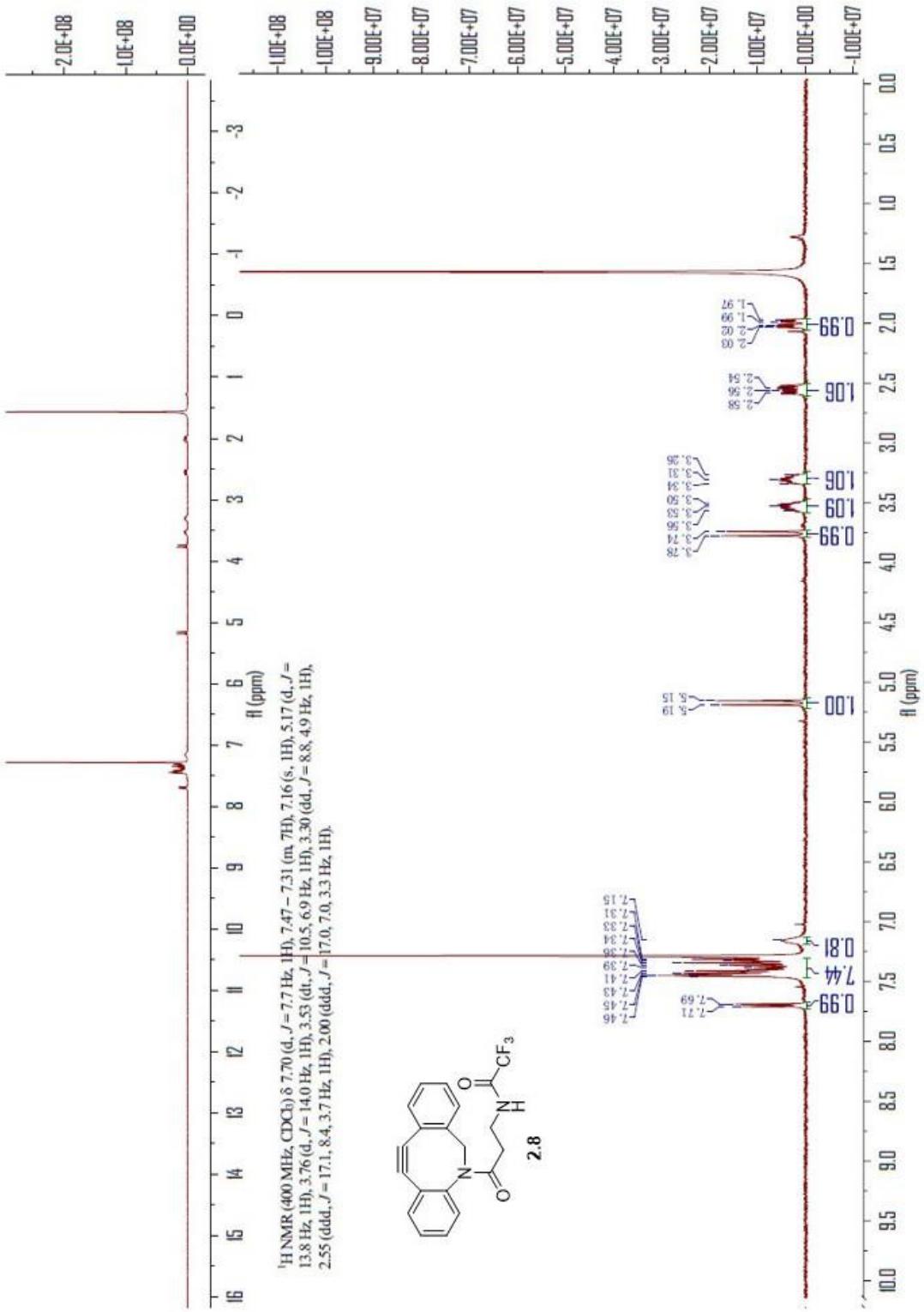

2.8 ^{1}H NMR Spectra

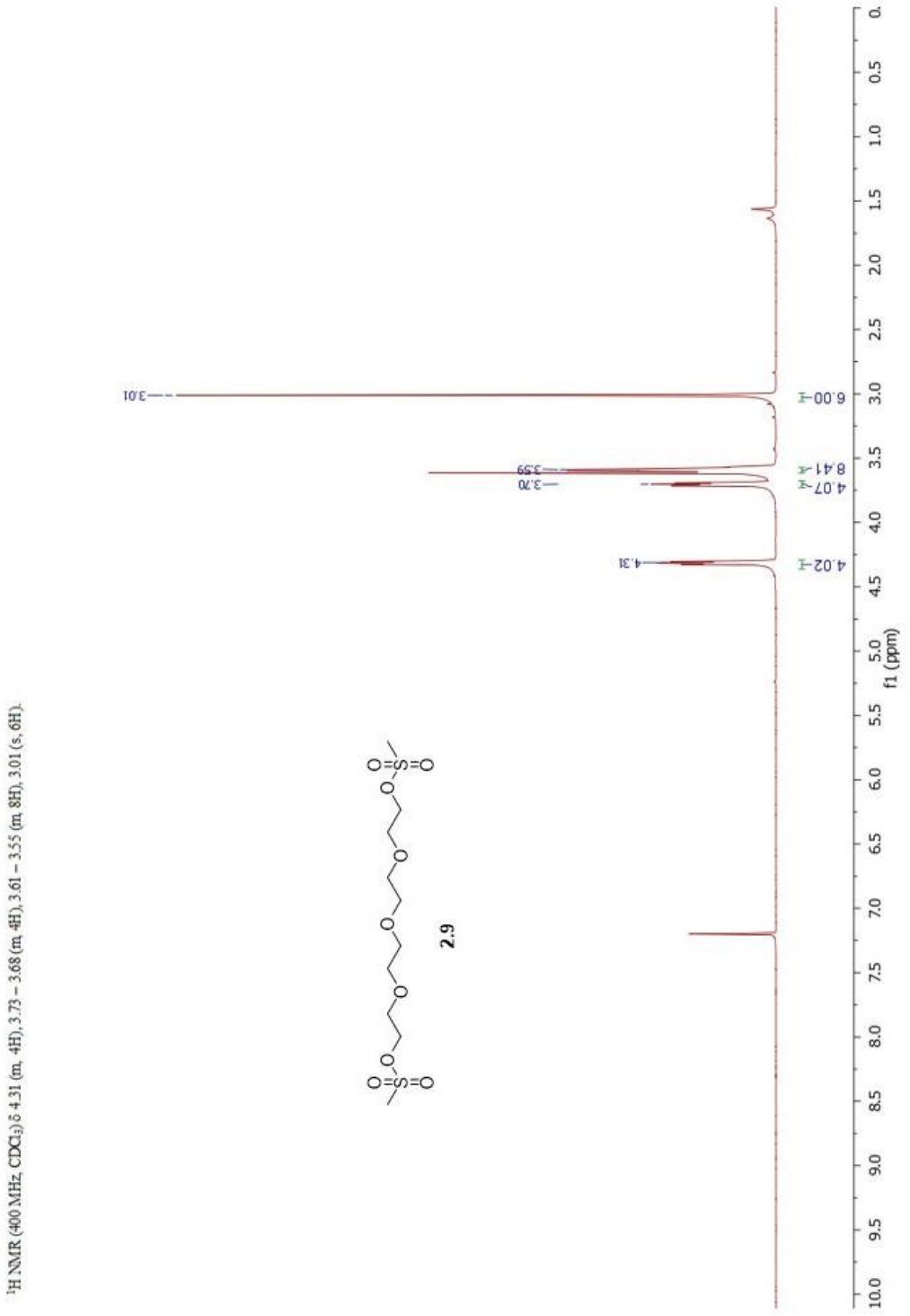

^{1}H NMR (400 MHz, $CDCl_3$) δ 4.31 (m, 4H), 3.73 – 3.68 (m, 4H), 3.61 – 3.55 (m, 8H), 3.01 (s, 6H).

2.9 ^{1}H NMR Spectra

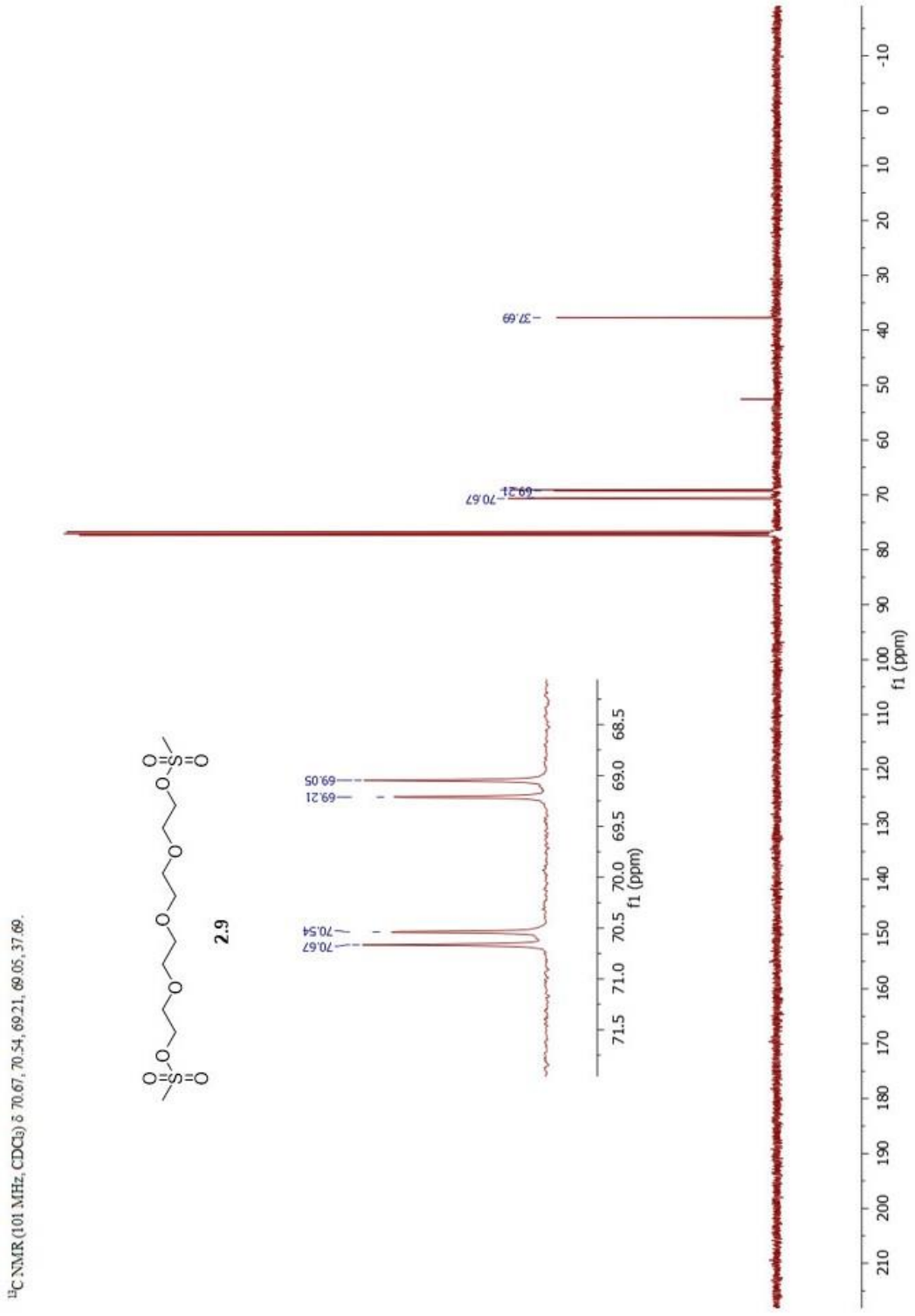

2.9 ^{13}C NMR Spectra

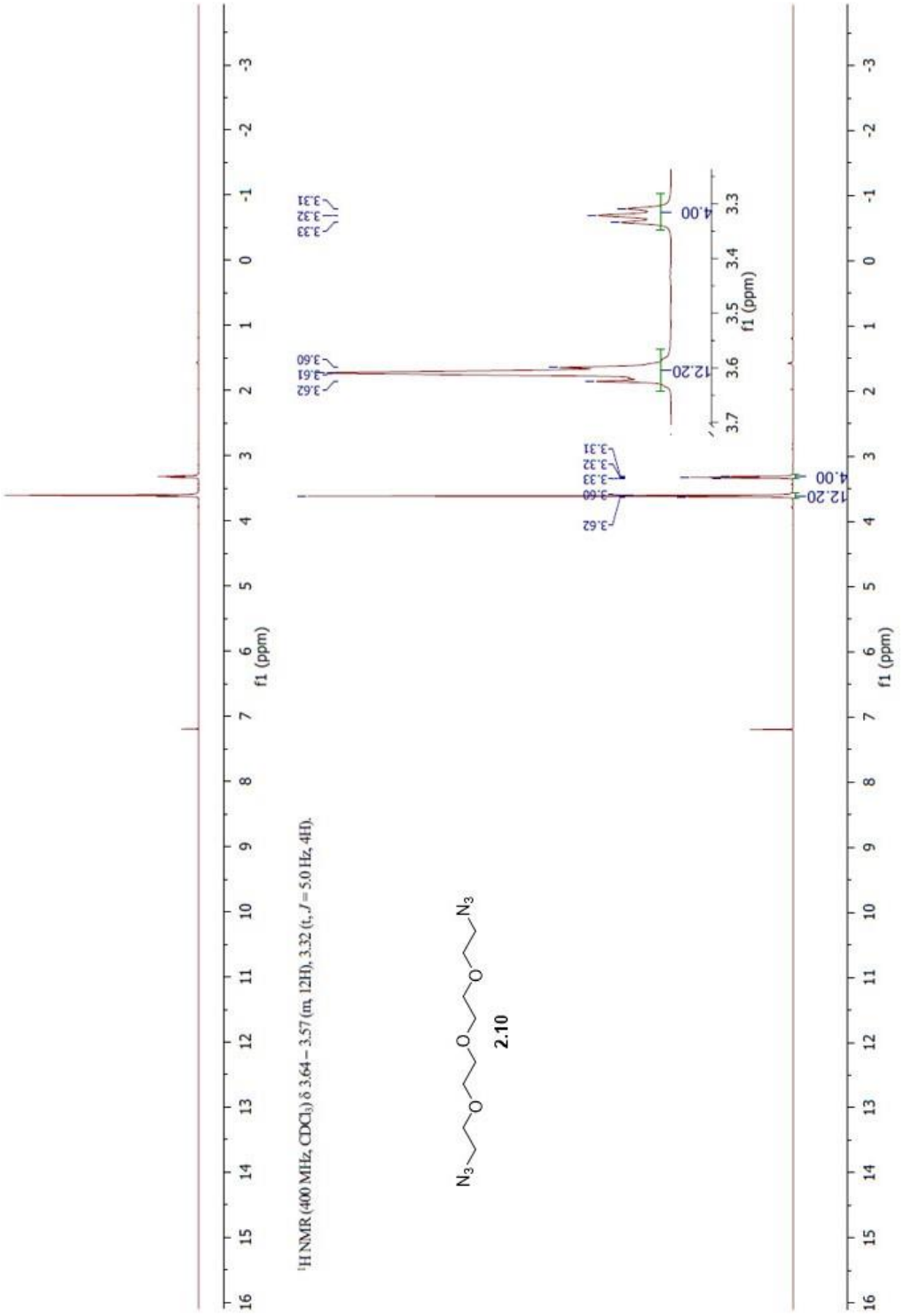

2.10 ^{1}H NMR Spectra

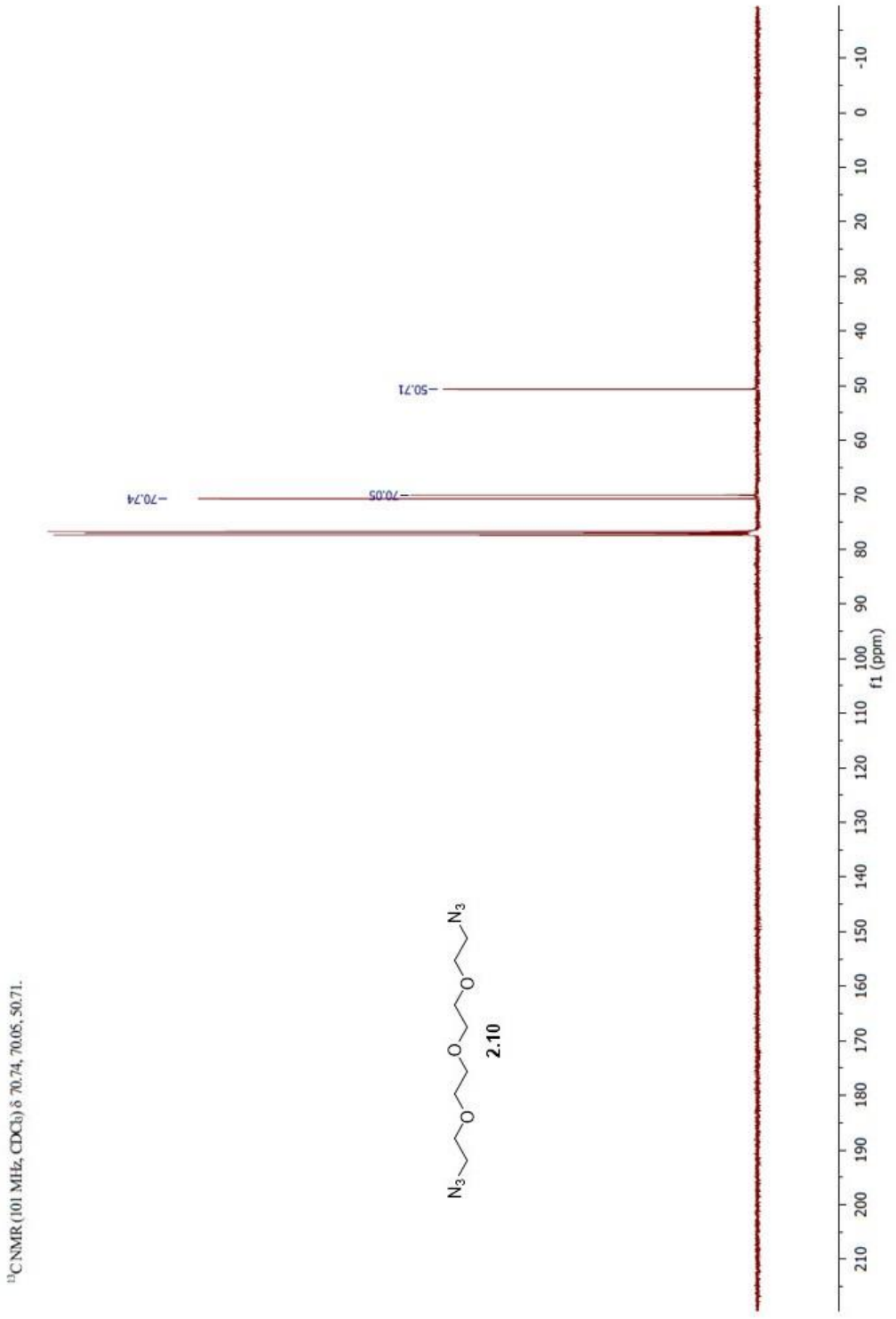

2.10 ^{13}C NMR Spectra

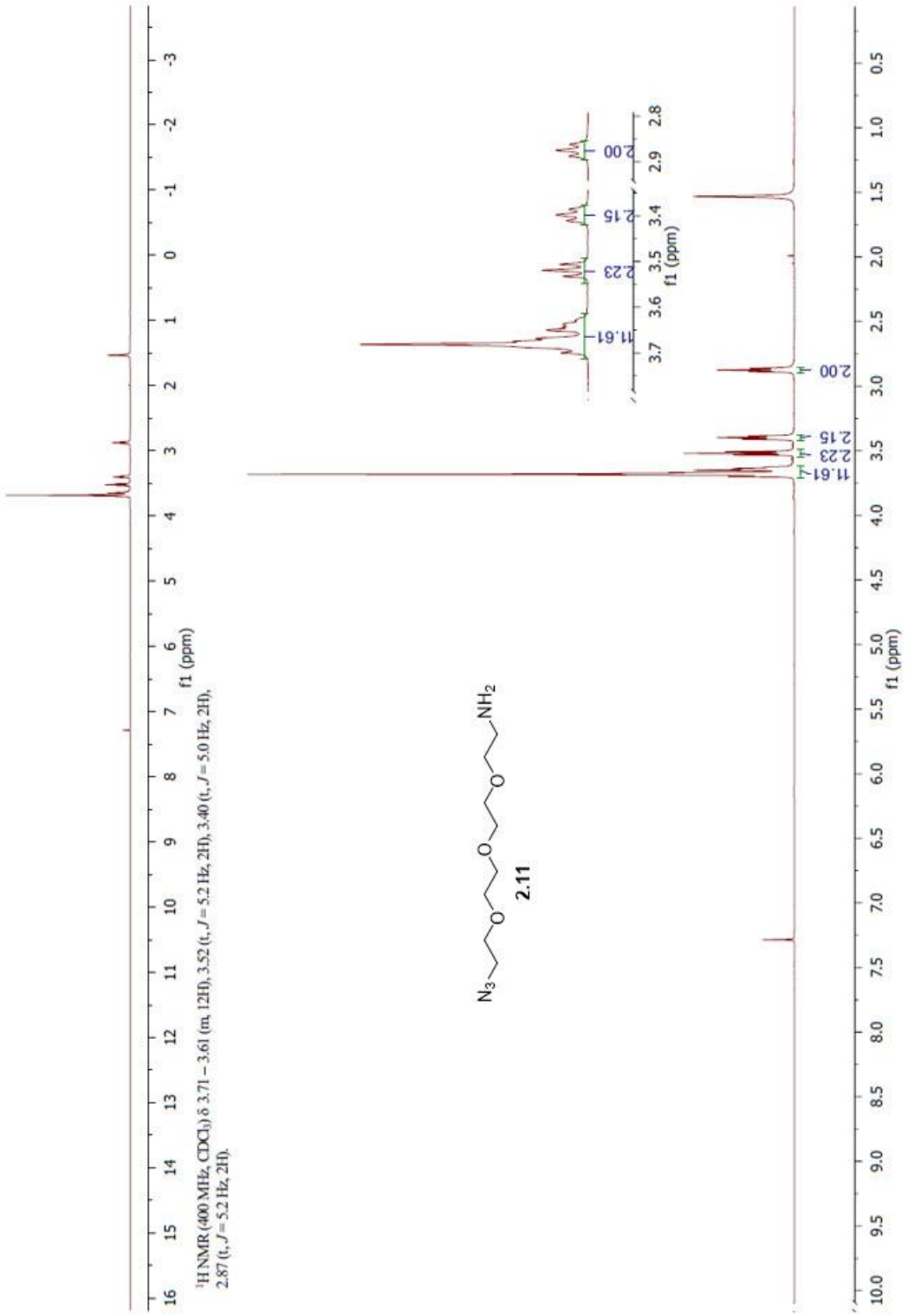

2.11 ^{1}H NMR Spectra

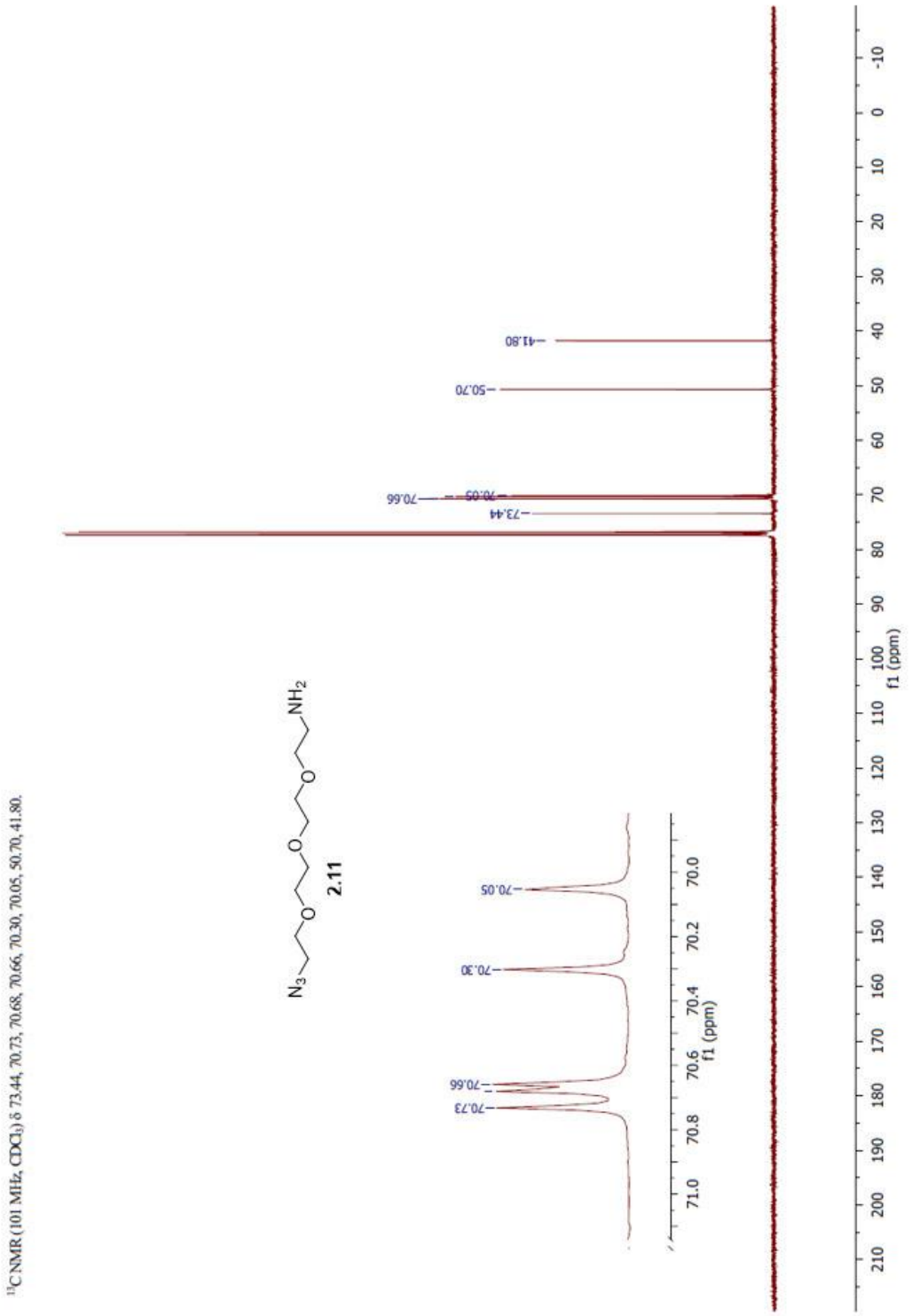

2.11 ^{13}C NMR Spectra

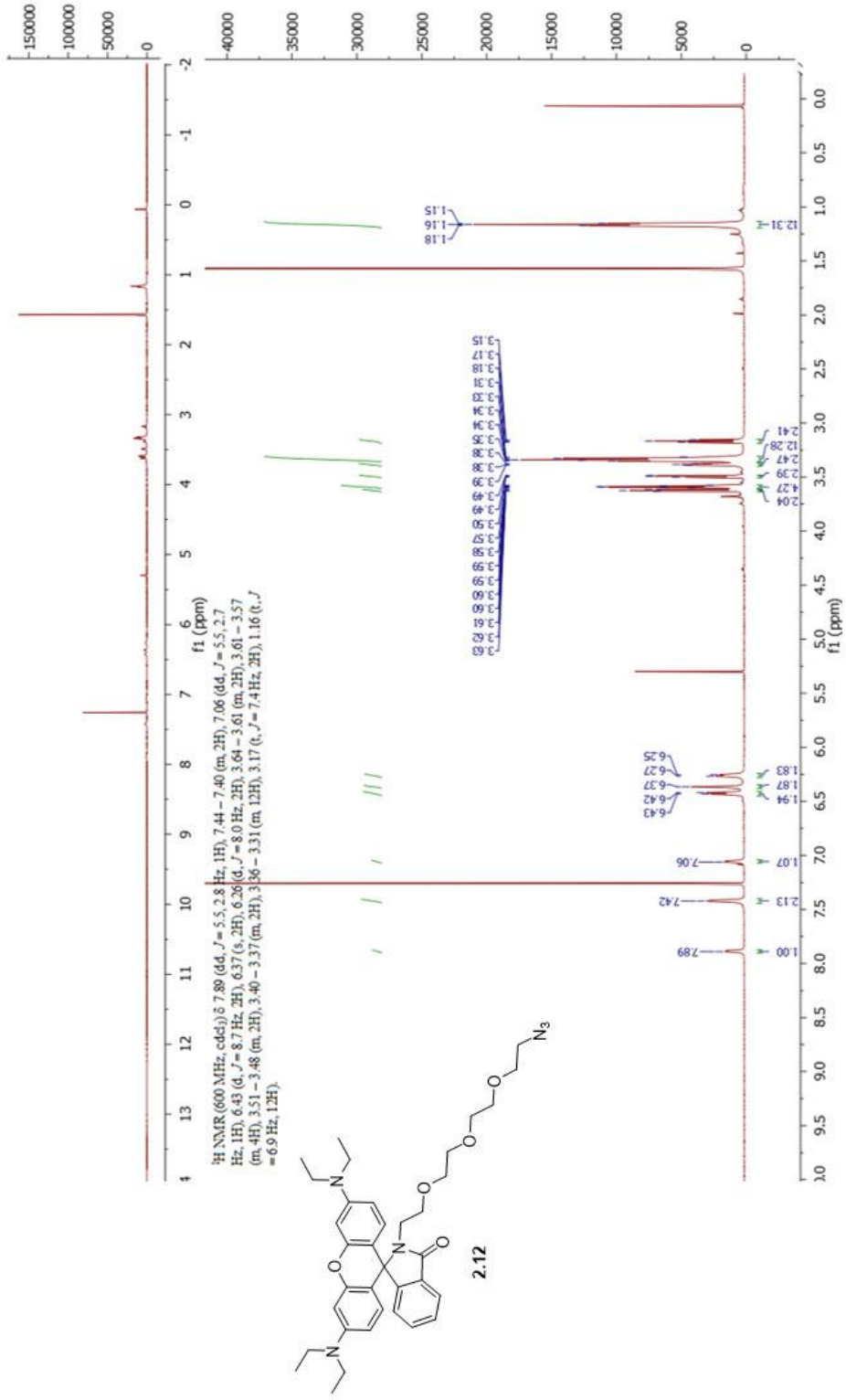

2.12 ^{1}H NMR Spectra

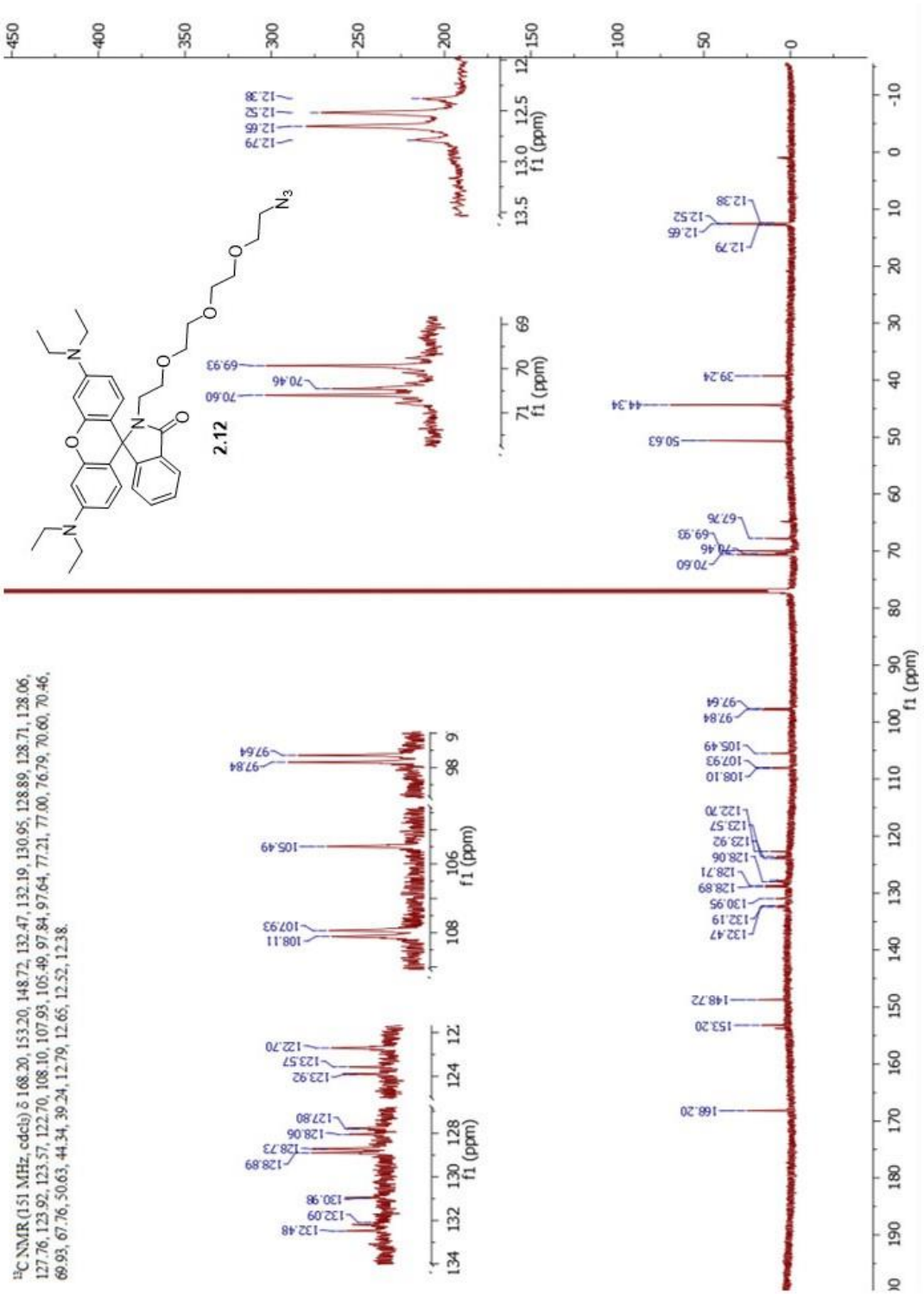

2.12 ^{13}C NMR Spectra

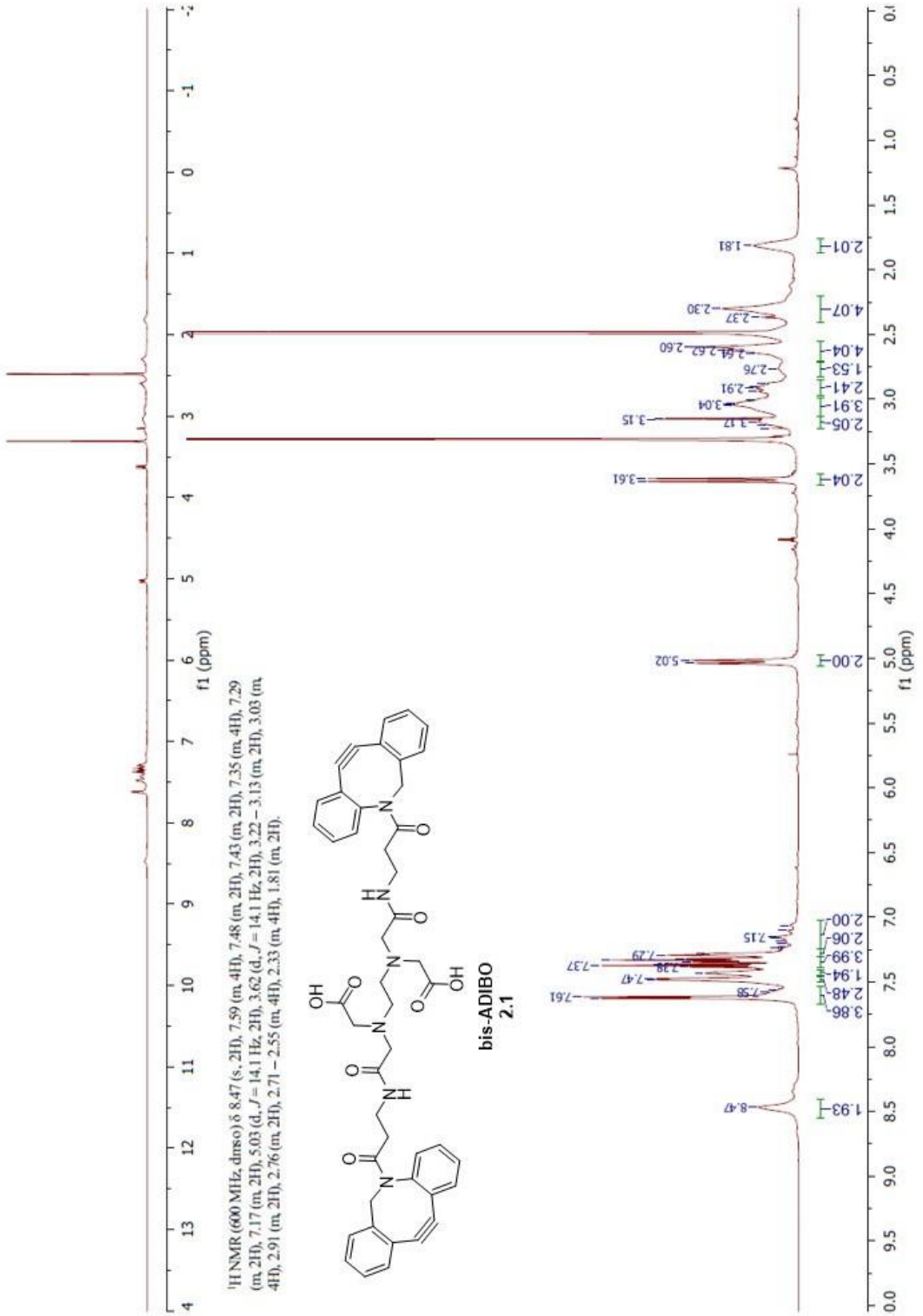

2.1 ^{1}H NMR Spectra

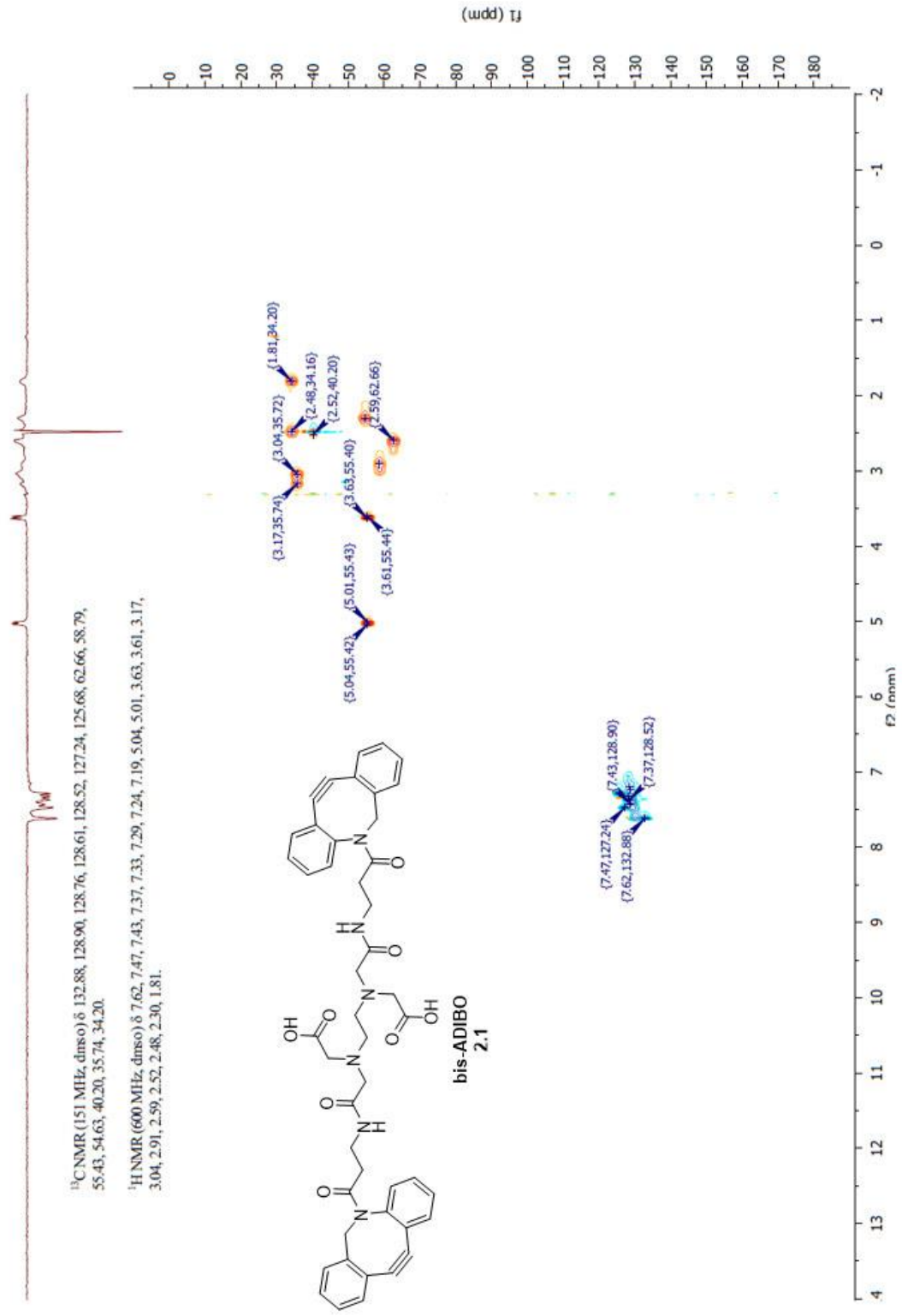

2.1 HSQC Spectra

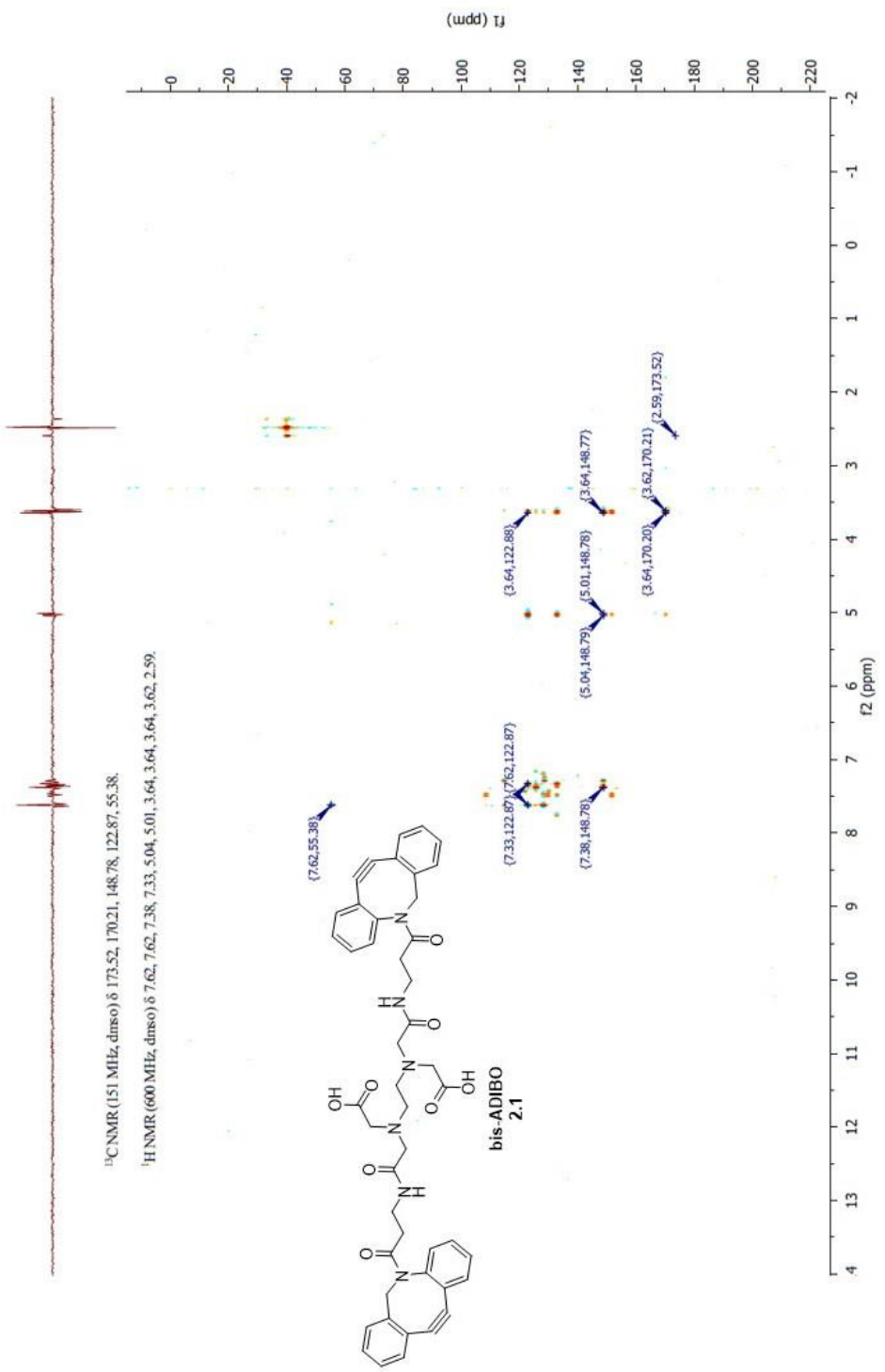

^{13}C NMR (151 MHz, dmso) δ 173.52, 170.21, 148.78, 122.87, 55.38.

^{1}H NMR (600 MHz, dmso) δ 7.62, 7.62, 7.38, 7.33, 5.04, 5.01, 3.64, 3.64, 3.64, 3.64, 3.62, 2.59.

2.1 HMBC Spectra

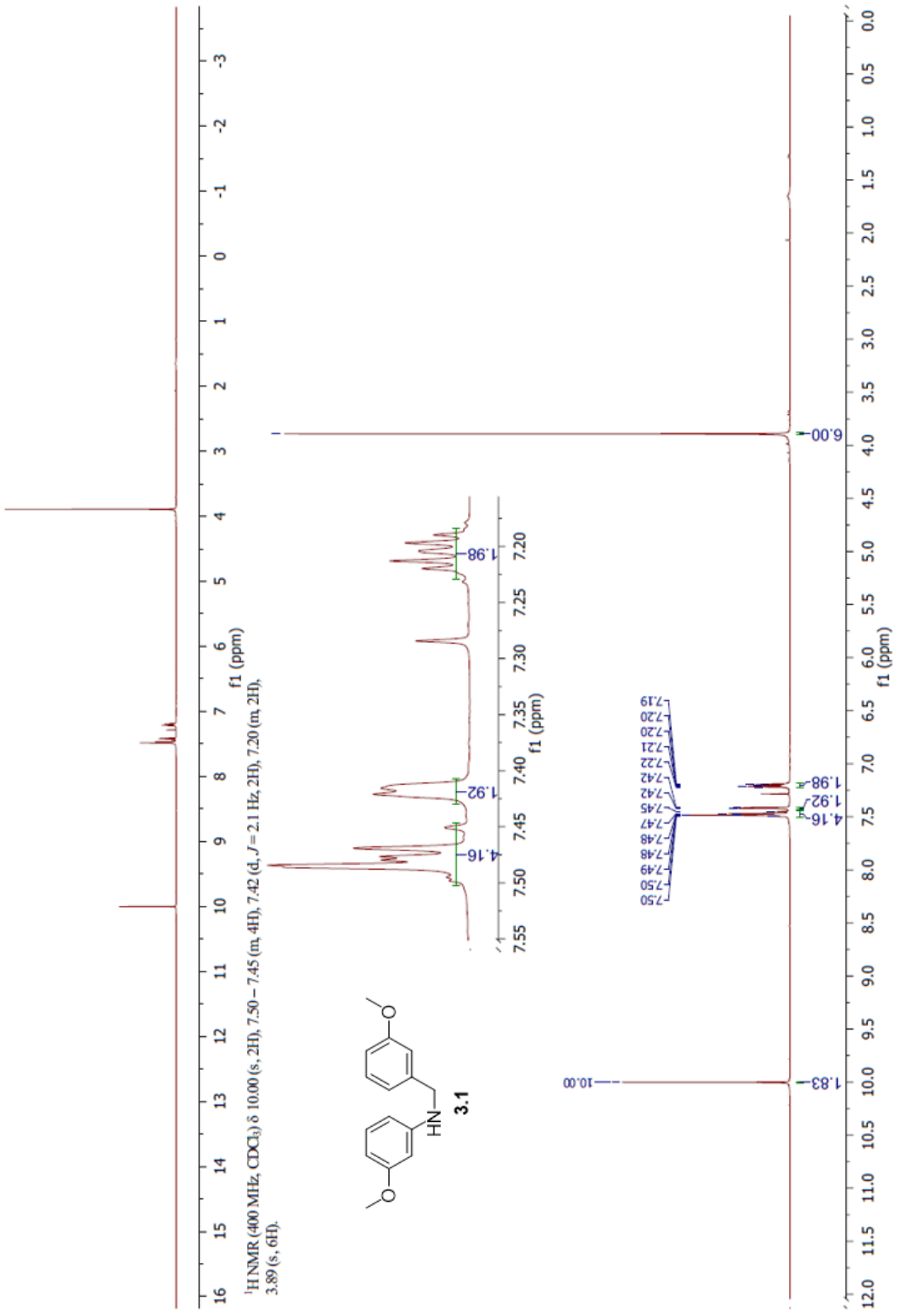

3.1 ^{1}H NMR Spectra

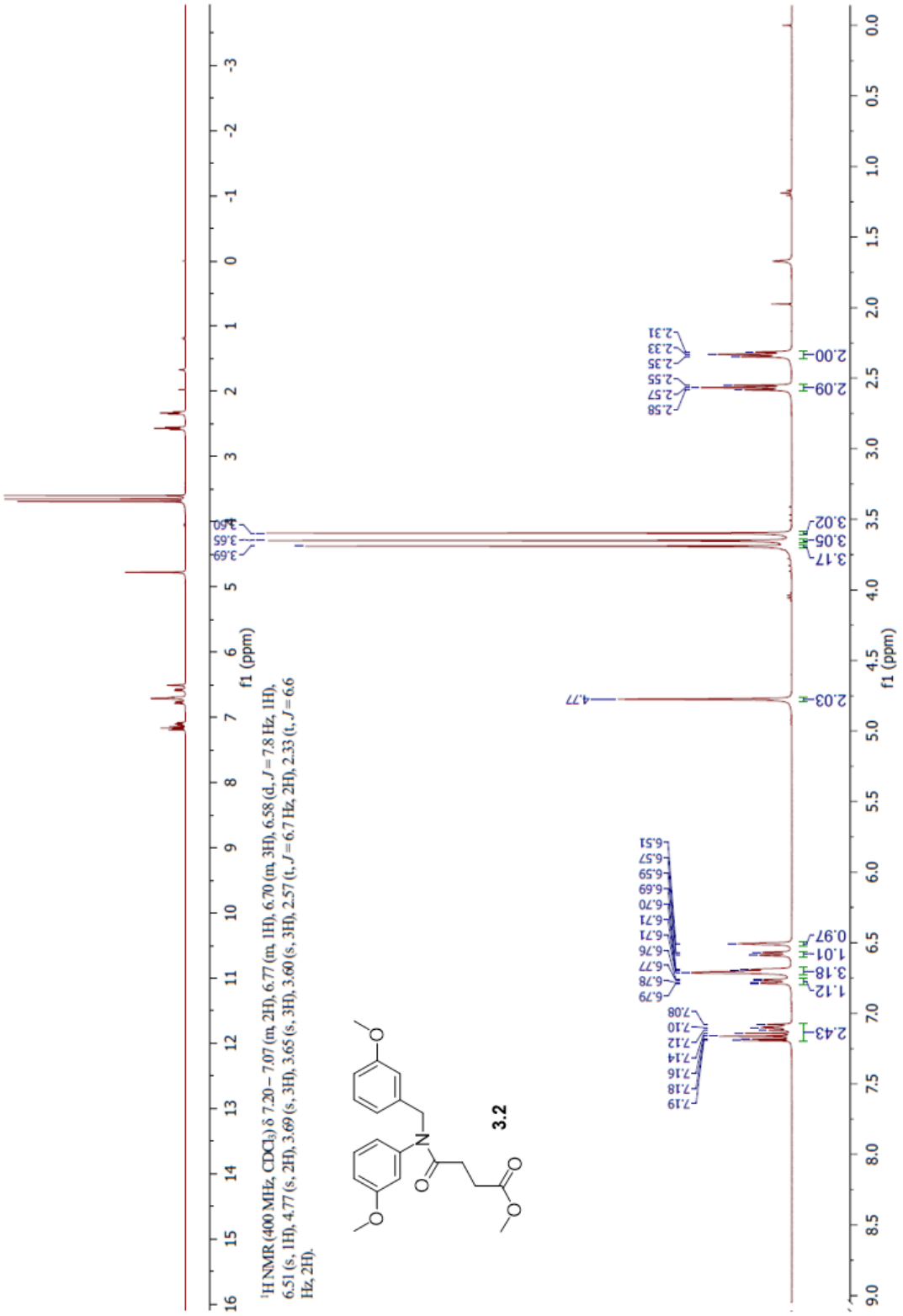

^{1}H NMR (400 MHz, $CDCl_3$) δ 7.20 – 7.07 (m, 2H), 6.77 (m, 1H), 6.70 (m, 3H), 6.58 (d, J = 7.8 Hz, 1H), 6.51 (s, 1H), 4.77 (s, 2H), 3.69 (s, 3H), 3.65 (s, 3H), 3.60 (s, 3H), 2.57 (t, J = 6.7 Hz, 2H), 2.33 (t, J = 6.6 Hz, 2H).

3.2 ^{1}H NMR Spectra

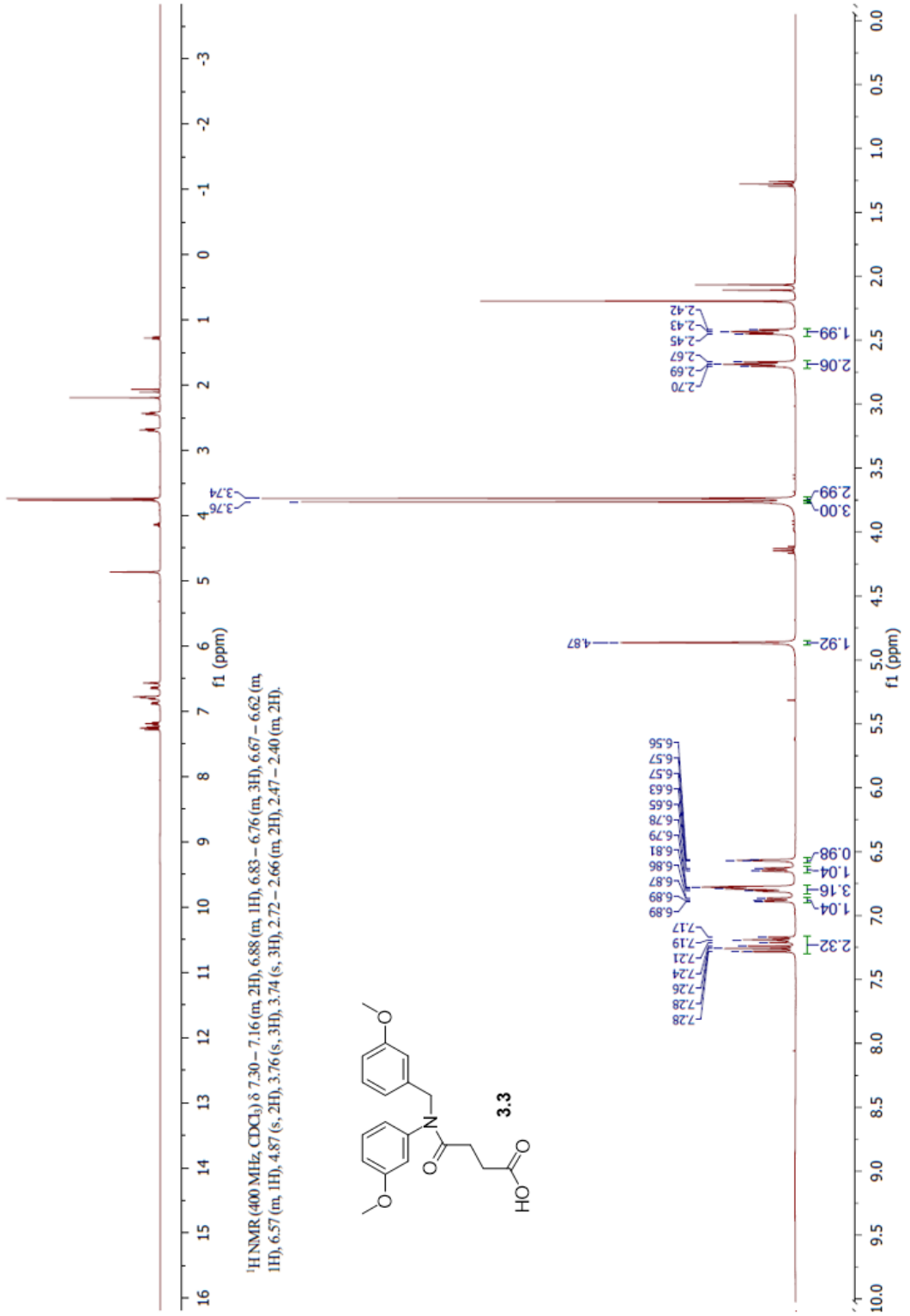

[1]H NMR (400 MHz, $CDCl_3$) δ 7.30 – 7.16 (m, 2H), 6.88 (m, 1H), 6.83 – 6.76 (m, 3H), 6.67 – 6.62 (m, 1H), 6.57 (m, 1H), 4.87 (s, 2H), 3.76 (s, 3H), 3.74 (s, 3H), 2.72 – 2.66 (m, 2H), 2.47 – 2.40 (m, 2H).

3.3 ^{1}H NMR Spectra

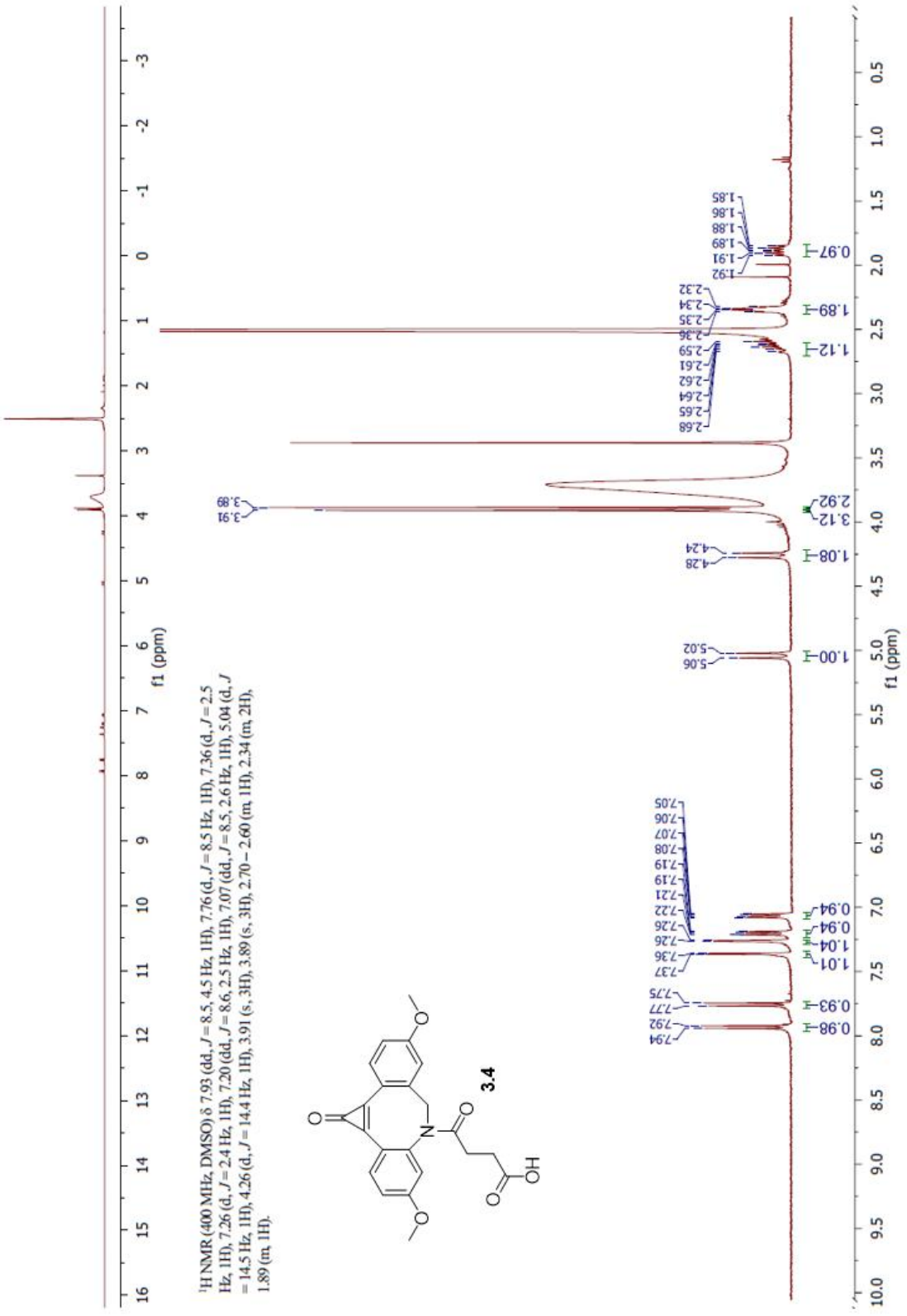

^{1}H NMR (400 MHz, DMSO) δ 7.93 (dd, J = 8.5, 4.5 Hz, 1H), 7.76 (d, J = 8.5 Hz, 1H), 7.36 (d, J = 2.5 Hz, 1H), 7.26 (d, J = 2.4 Hz, 1H), 7.20 (dd, J = 8.6, 2.5 Hz, 1H), 7.07 (dd, J = 8.5, 2.6 Hz, 1H), 5.04 (d, J = 14.5 Hz, 1H), 4.26 (d, J = 14.4 Hz, 1H), 3.91 (s, 3H), 3.89 (s, 3H), 2.70 – 2.60 (m, 1H), 2.34 (m, 2H), 1.89 (m, 1H).

3.4 ^{1}H NMR Spectra

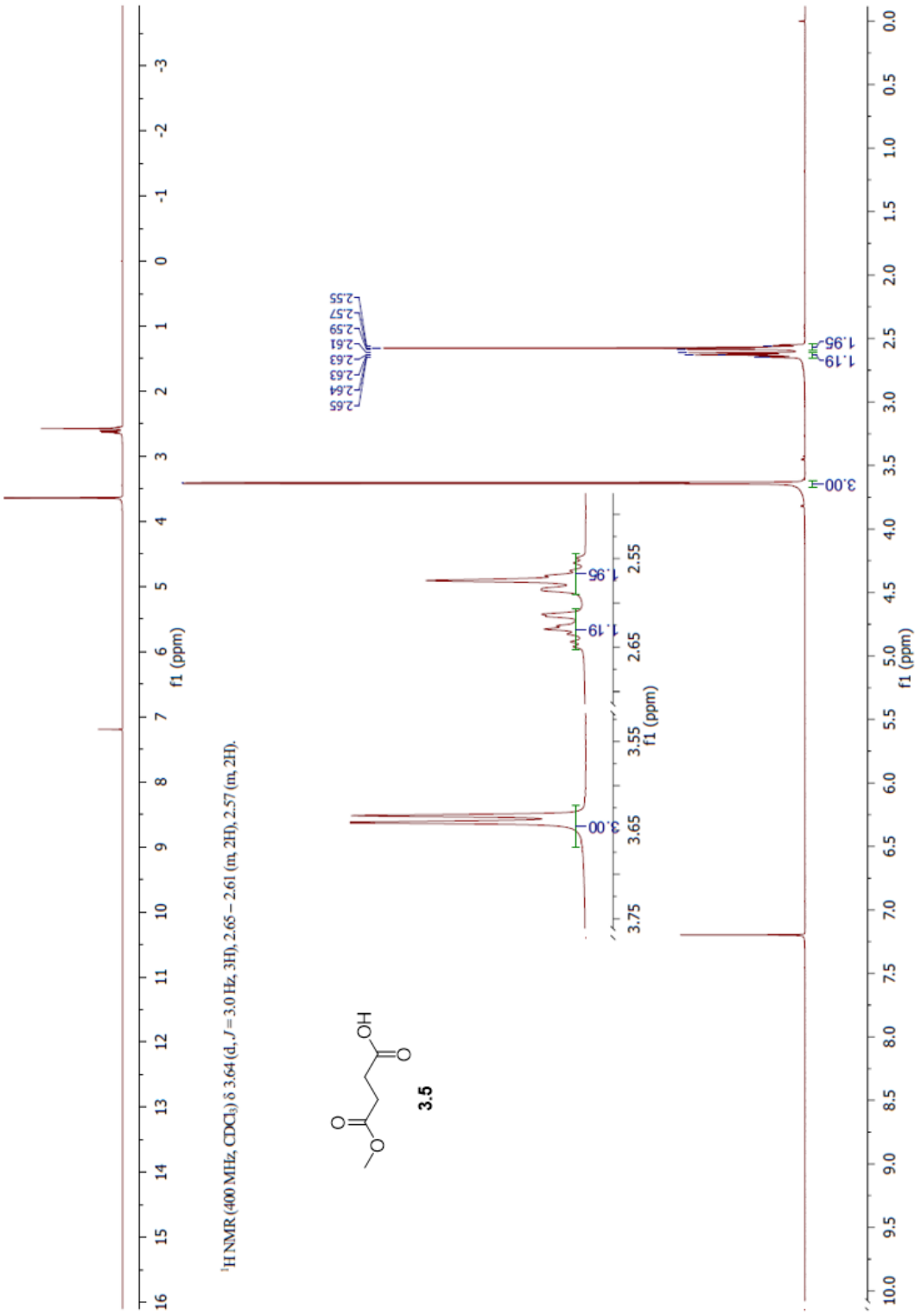

3.5 ^{1}H NMR Spectra

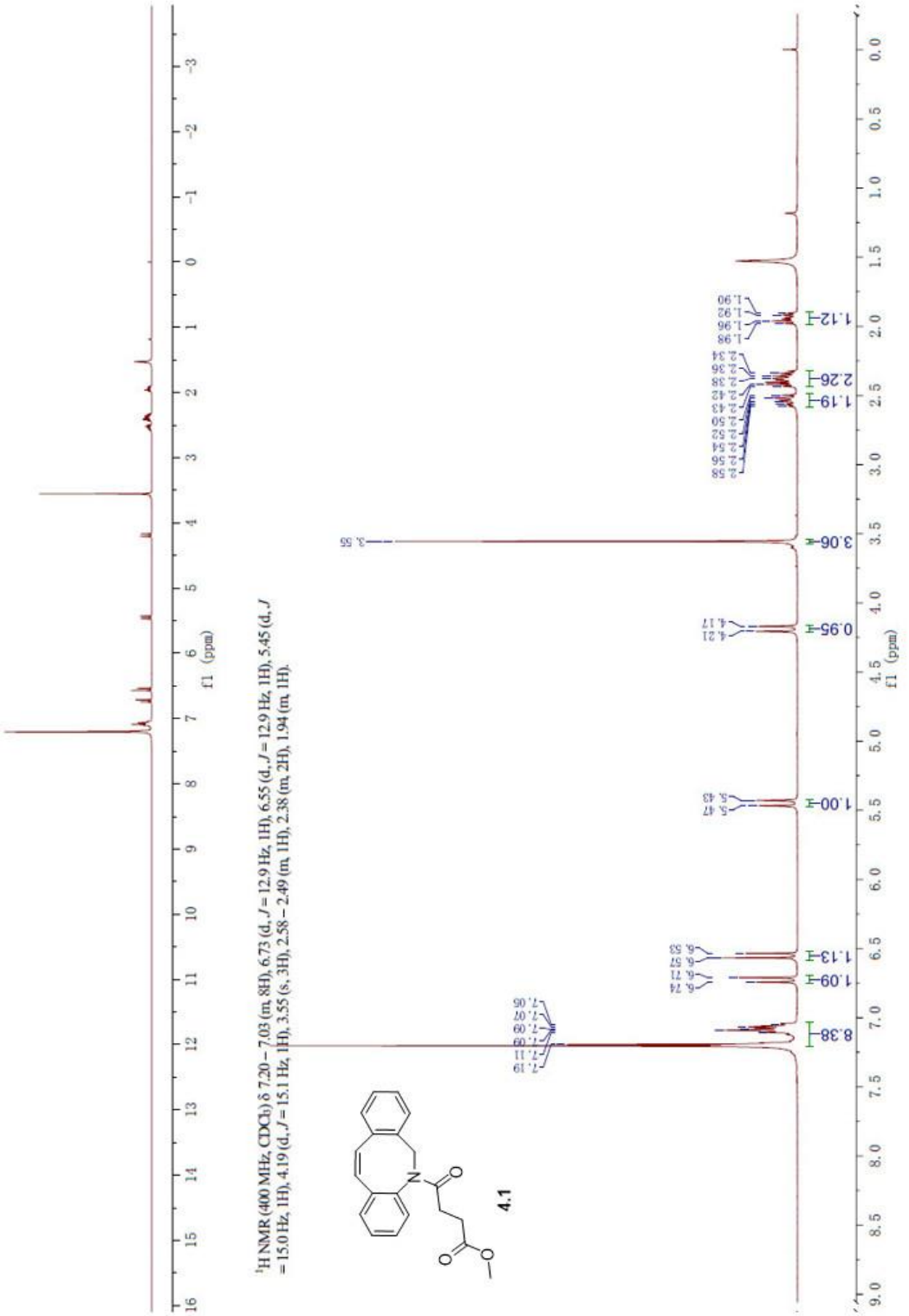

4.1 ^{1}H NMR Spectra

^{13}C NMR (101 MHz, $CDCl_3$) δ 173.50 , 170.92, 140.55, 136.53, 135.89 , 134.63, 132.71, 131.88, 130.92, 130.22 , 128.61, 128.32, 128.08, 127.36, 127.01, 54.55, 51.70, 29.61, 29.08.

4.1 ^{13}C NMR Spectra

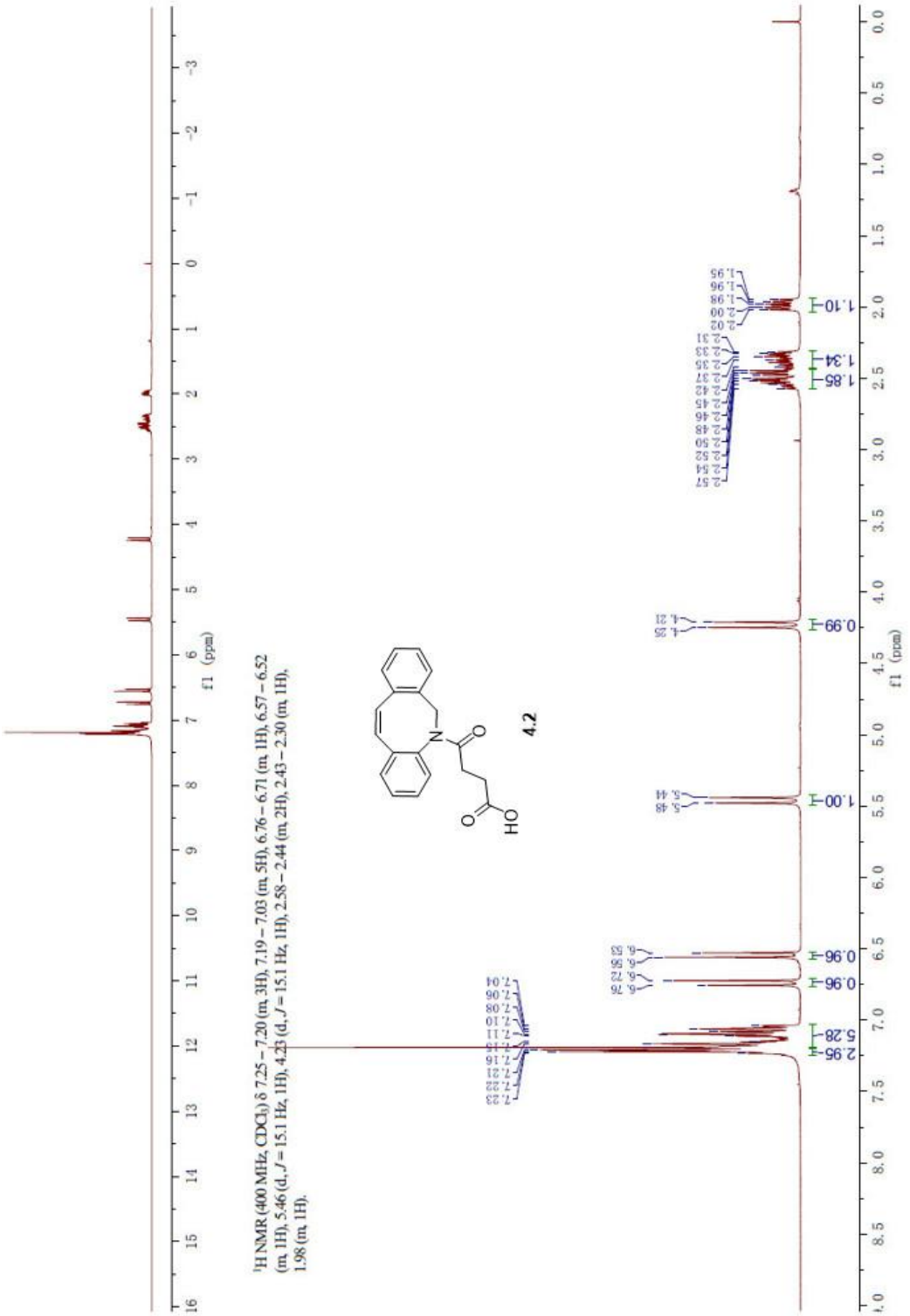

4.2 ^{1}H NMR Spectra

4.2 ^{13}C NMR Spectra

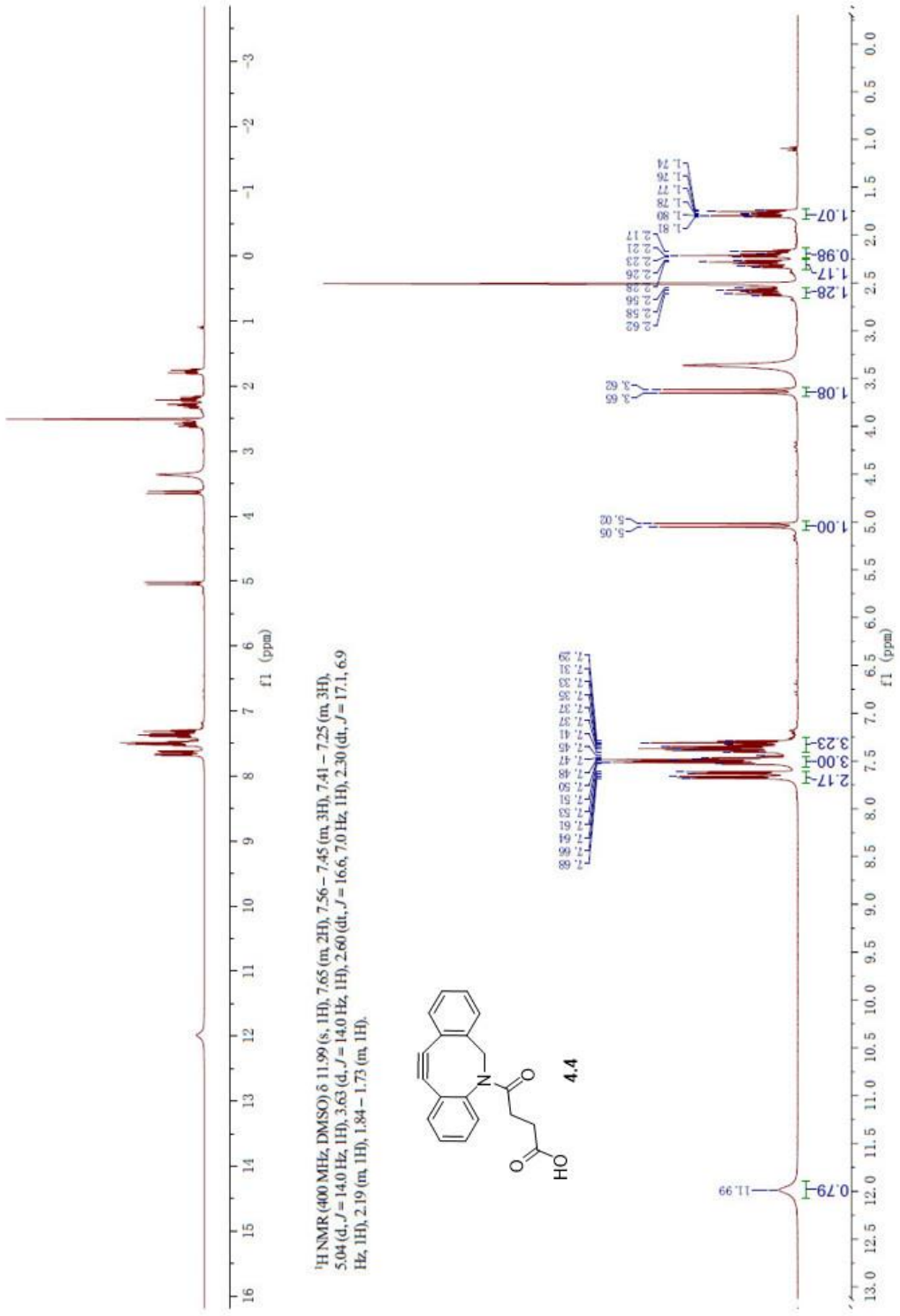

4.4 ^{1}H NMR Spectra

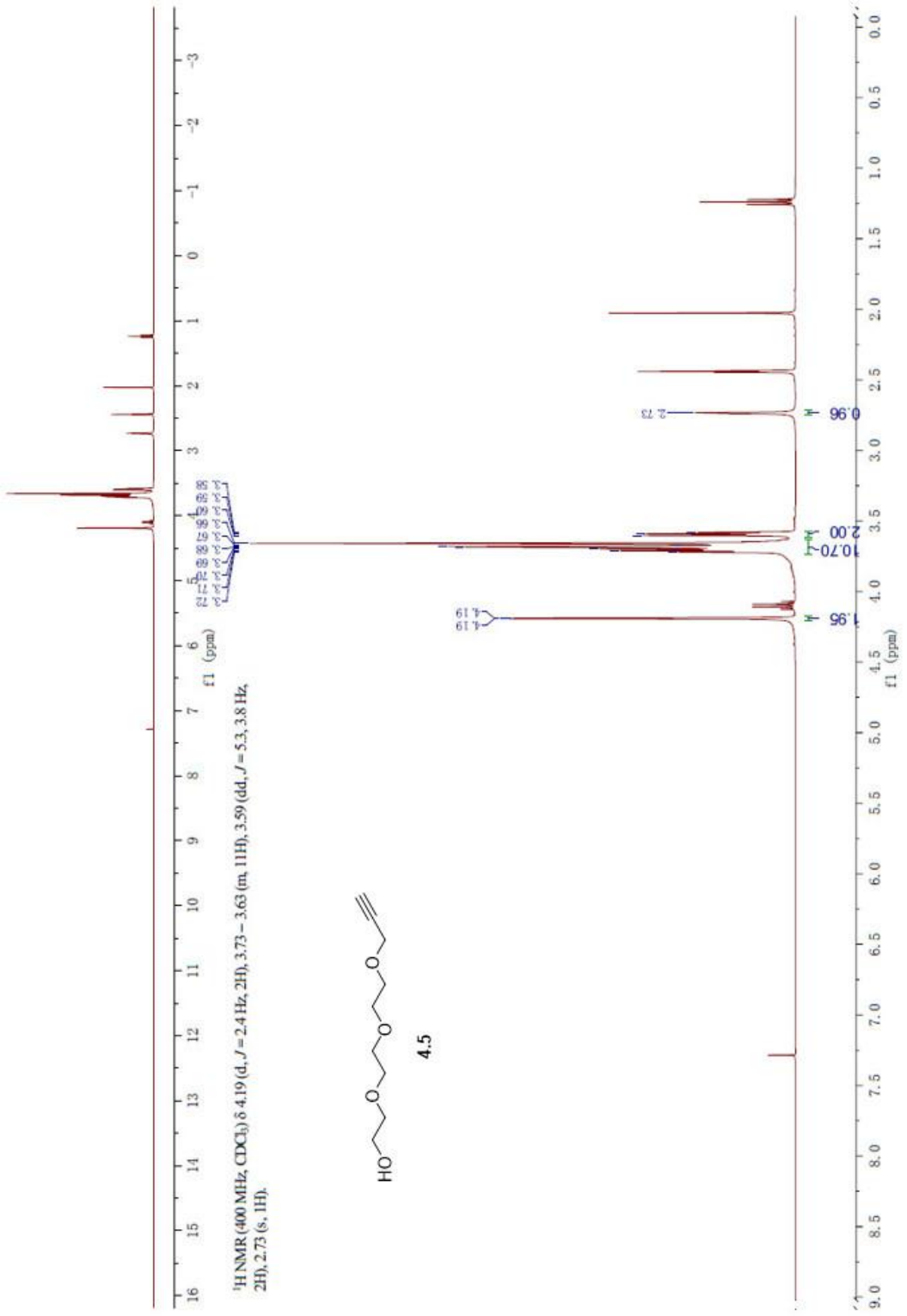

^{1}H NMR (400 MHz, $CDCl_3$) δ 4.19 (d, J = 2.4 Hz, 2H), 3.73 – 3.63 (m, 11H), 3.59 (dd, J = 5.3, 3.8 Hz, 2H), 2.73 (s, 1H).

4.5 ^{1}H NMR Spectra

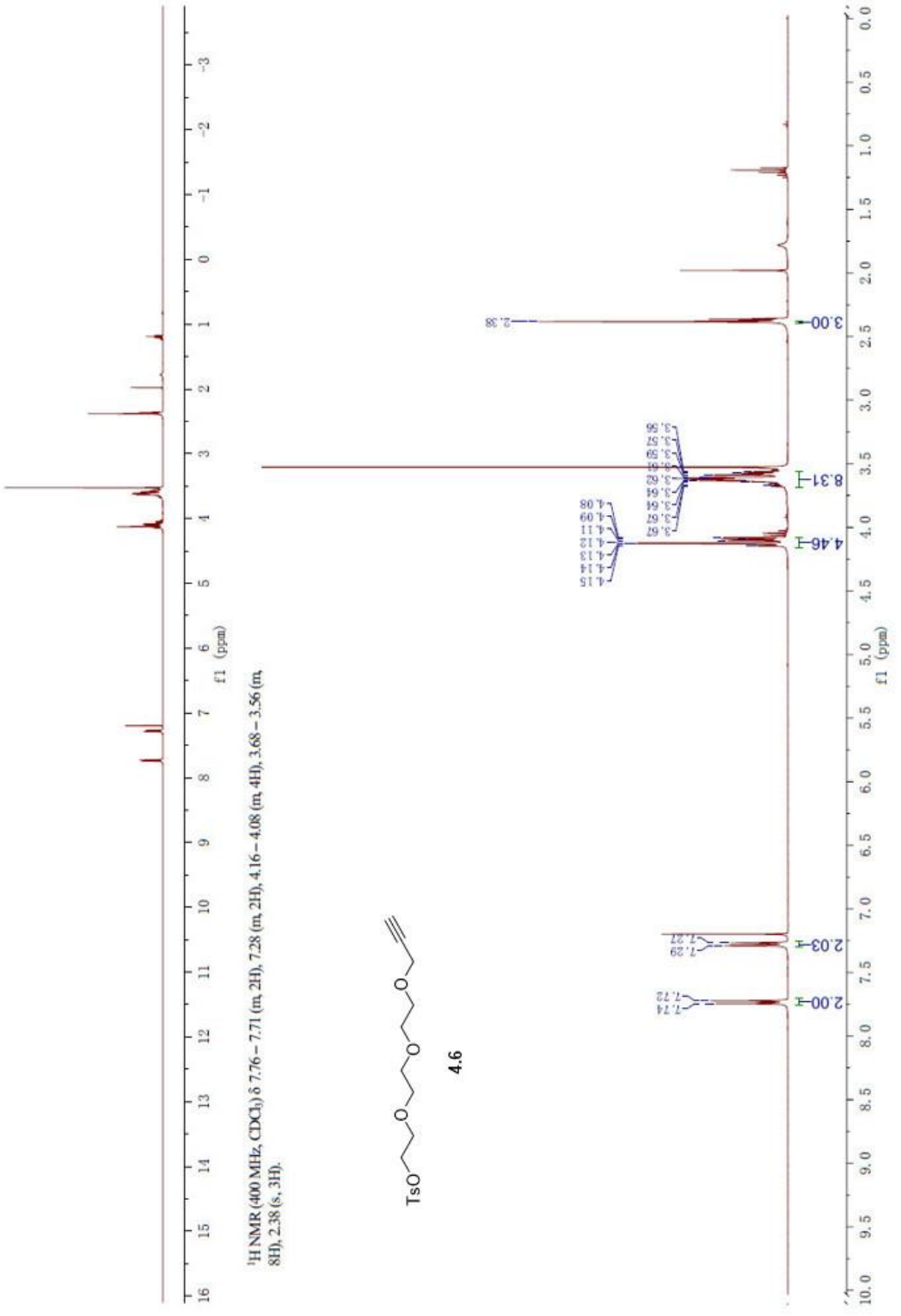

^{1}H NMR (400 MHz, $CDCl_3$) δ 7.76 – 7.71 (m, 2H), 7.28 (m, 2H), 4.16 – 4.08 (m, 4H), 3.68 – 3.56 (m, 8H), 2.38 (s, 3H).

4.6 ^{1}H NMR Spectra

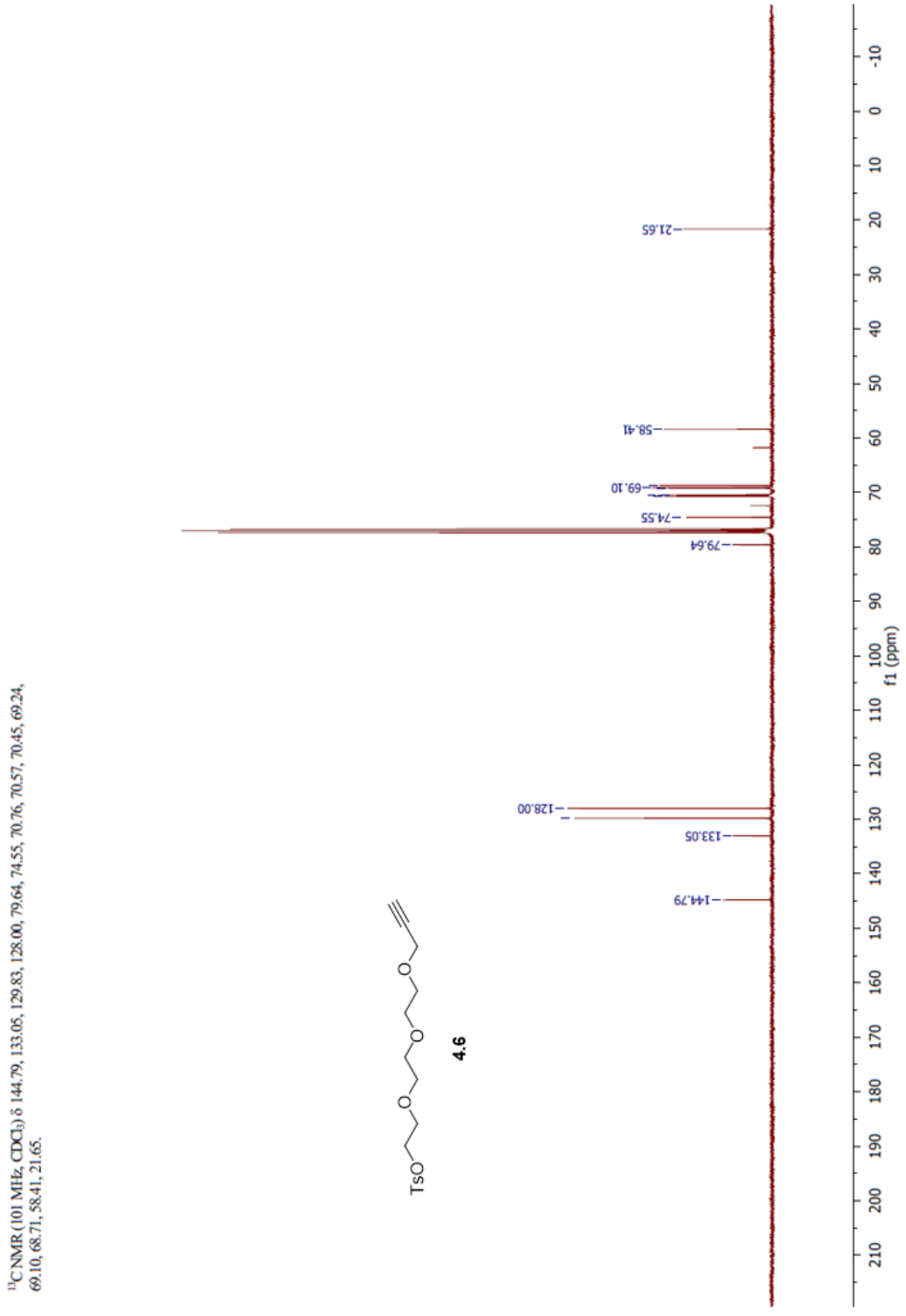

4.6 ^{13}C NMR Spectra

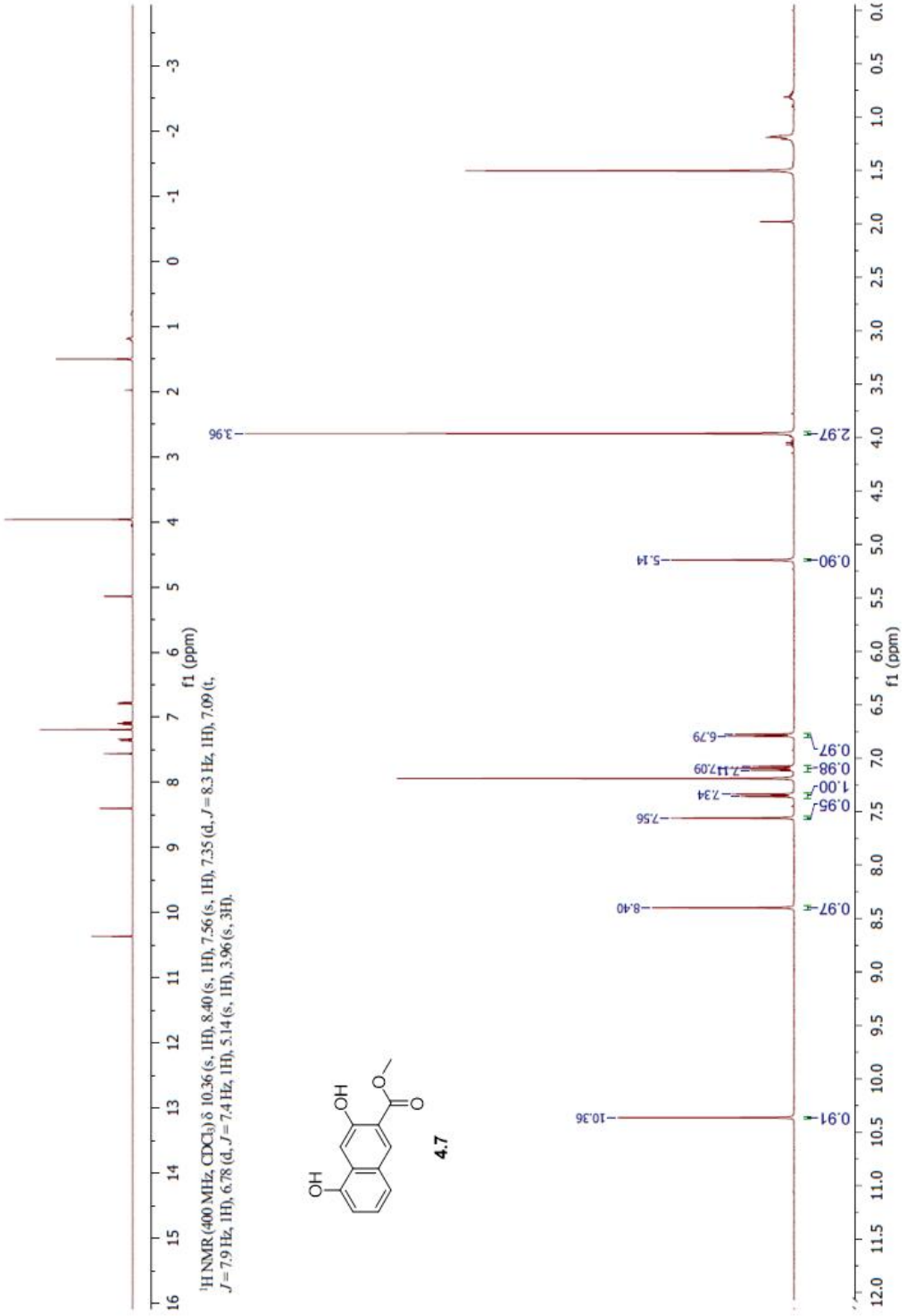

4.7 ^{1}H NMR Spectra

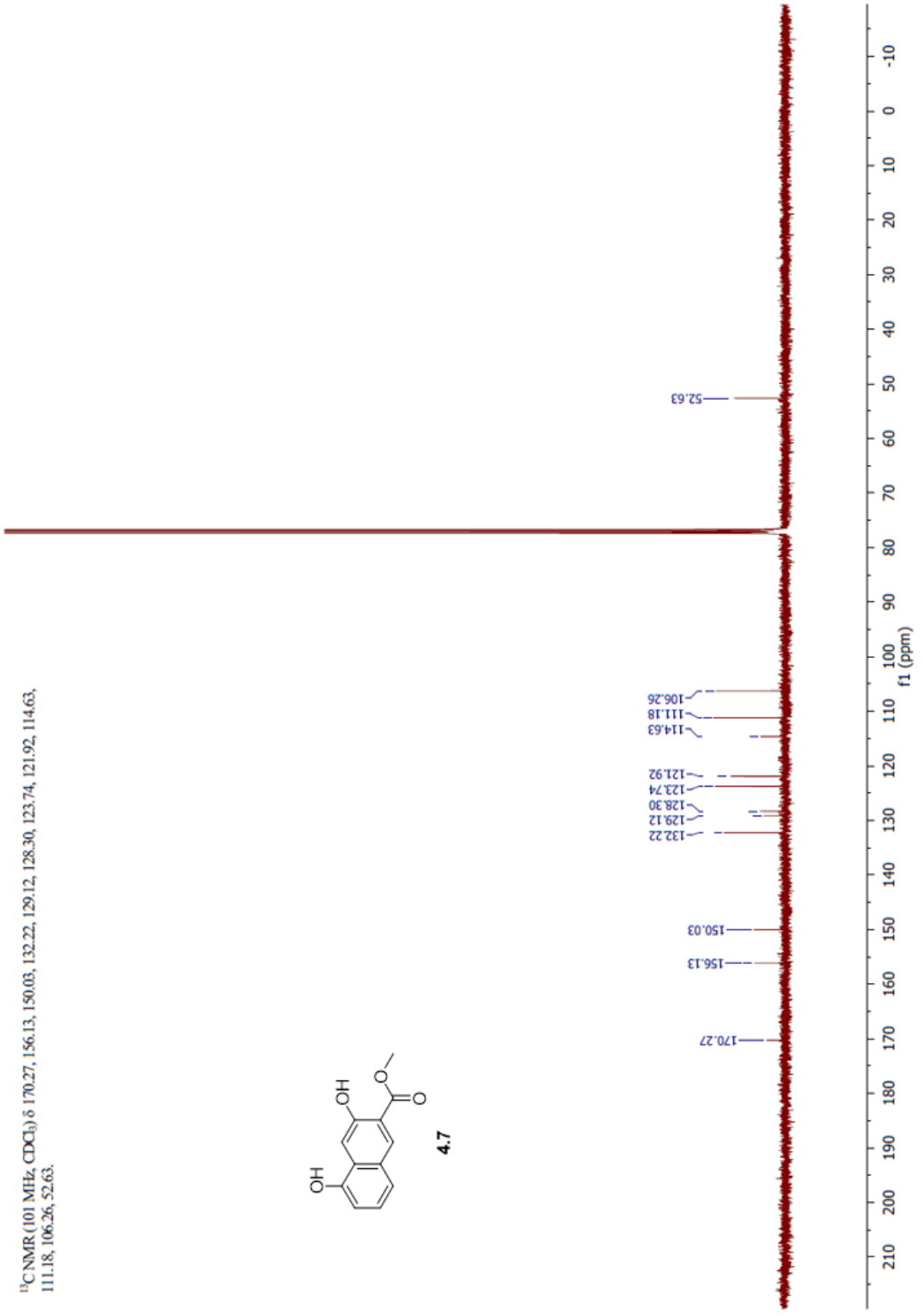

4.7 ^{13}C NMR Spectra

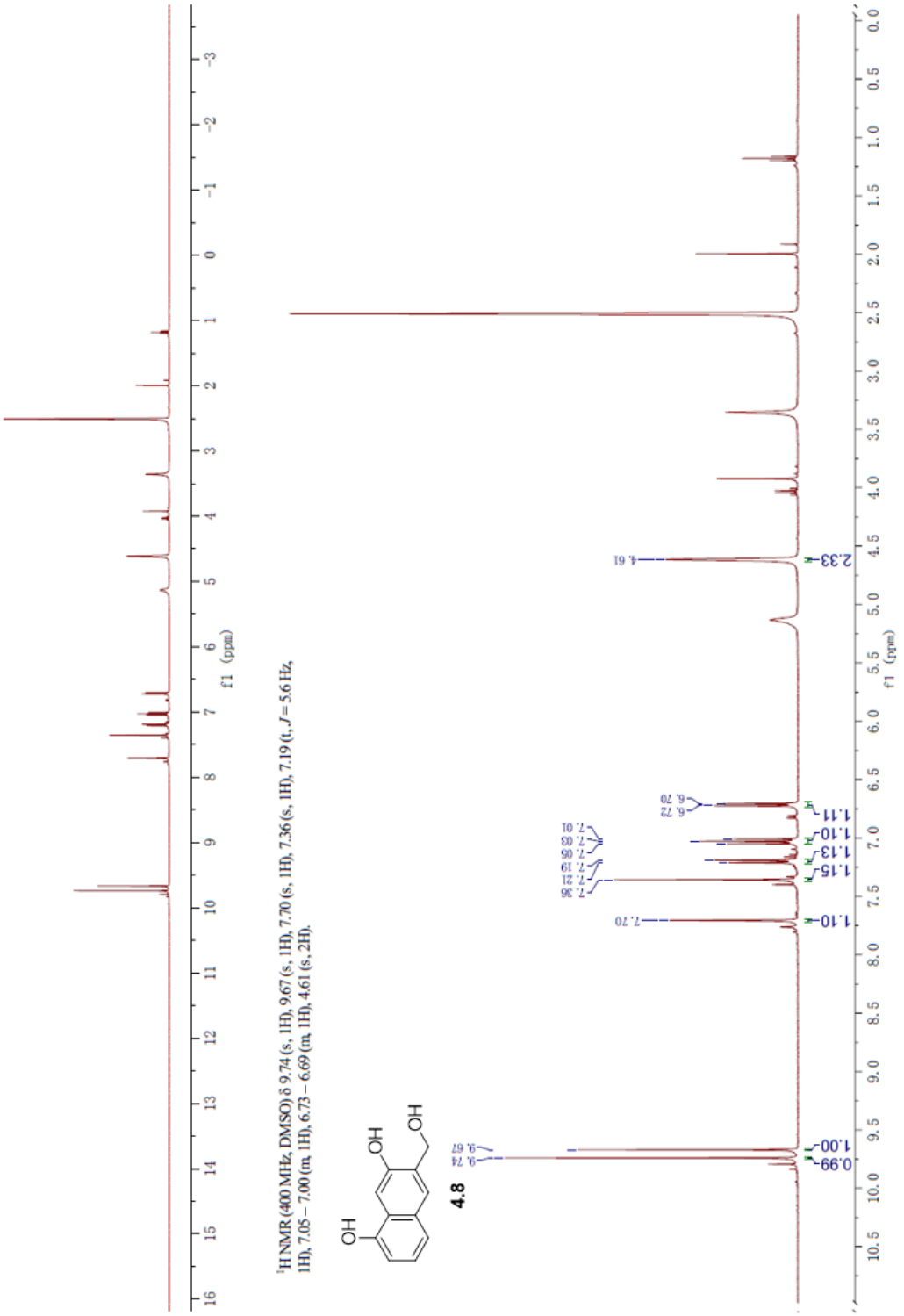

4.8 ^{1}H NMR Spectra

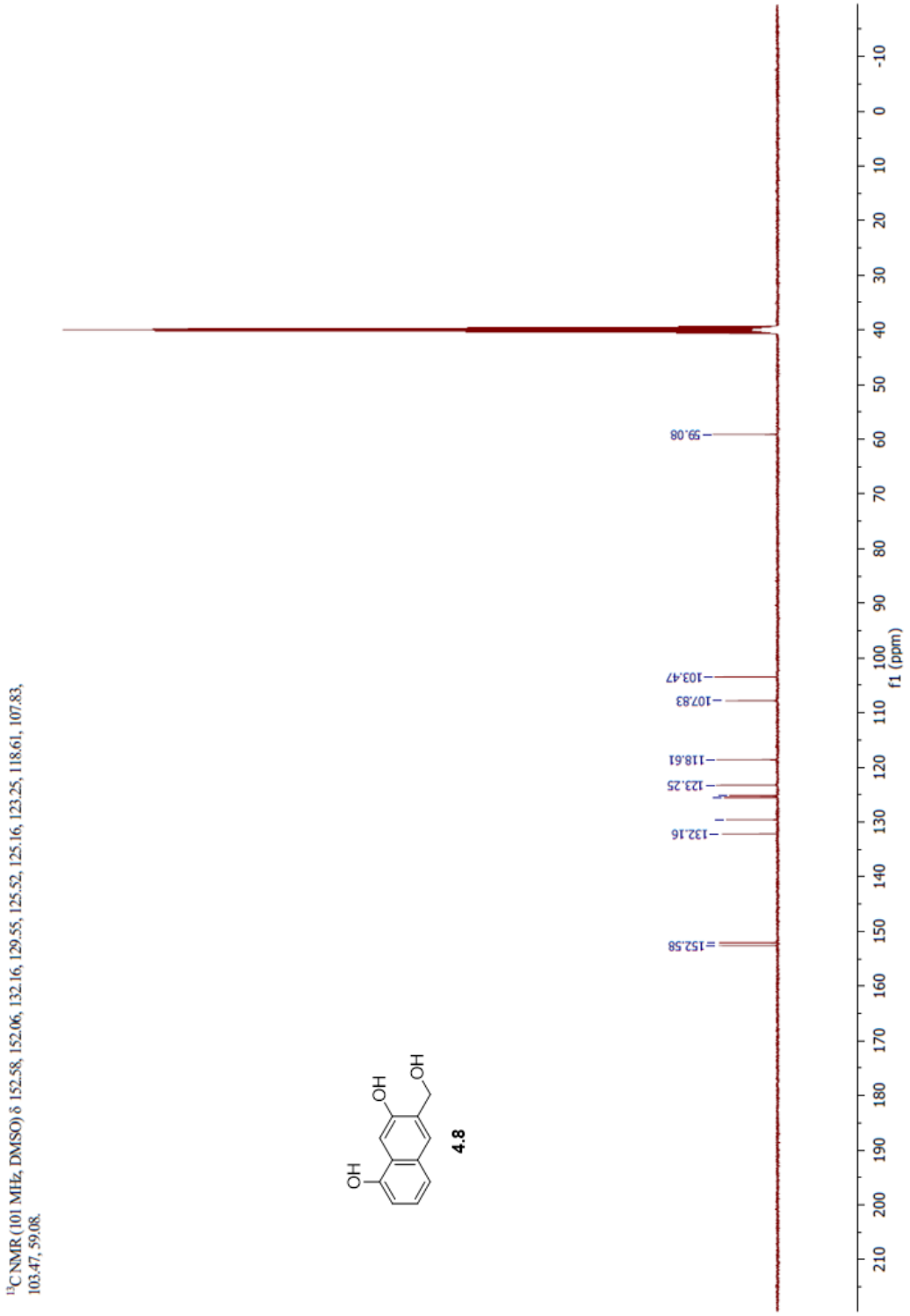

4.8 ^{13}C NMR Spectra

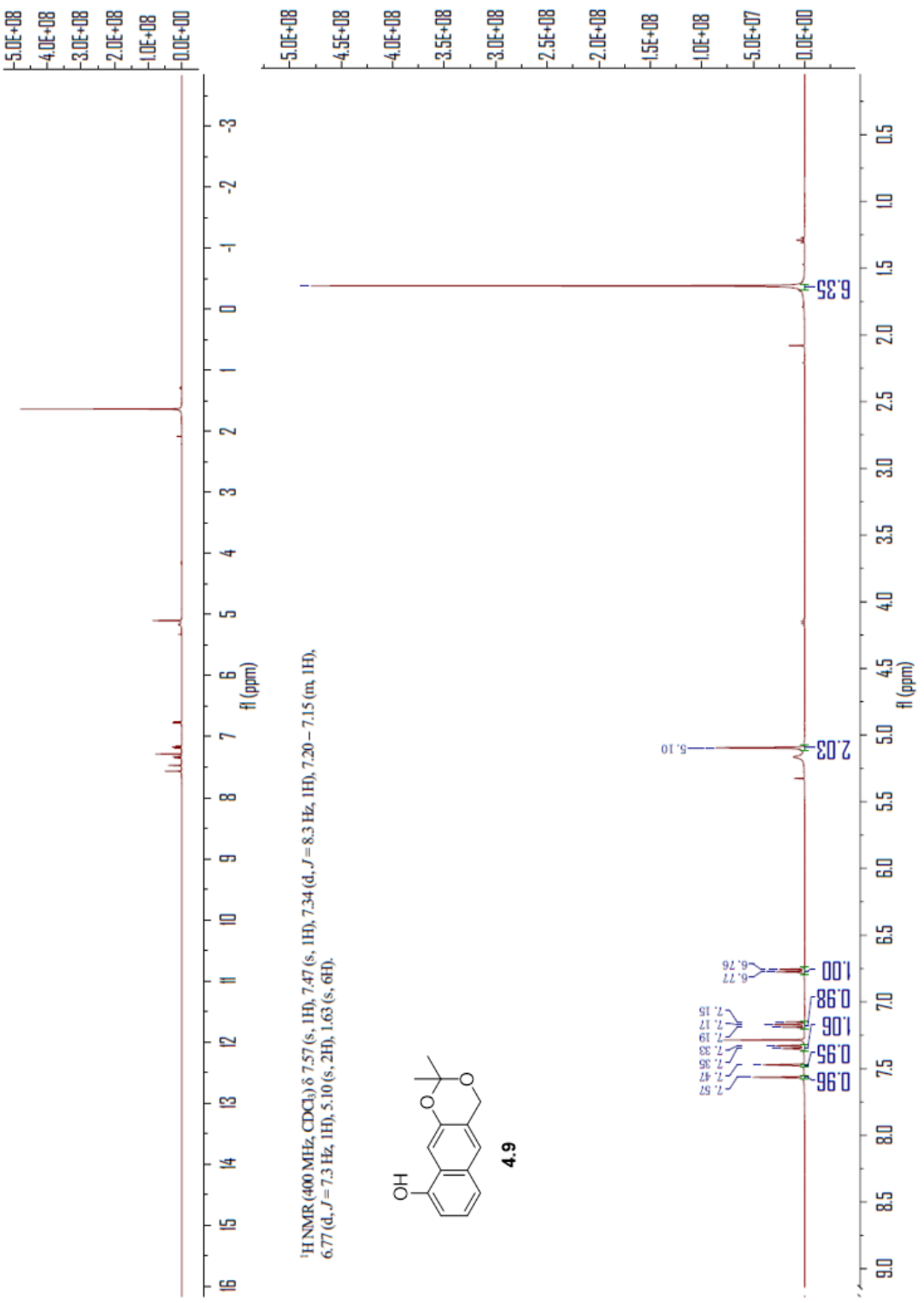

4.9 ^{1}H NMR Spectra

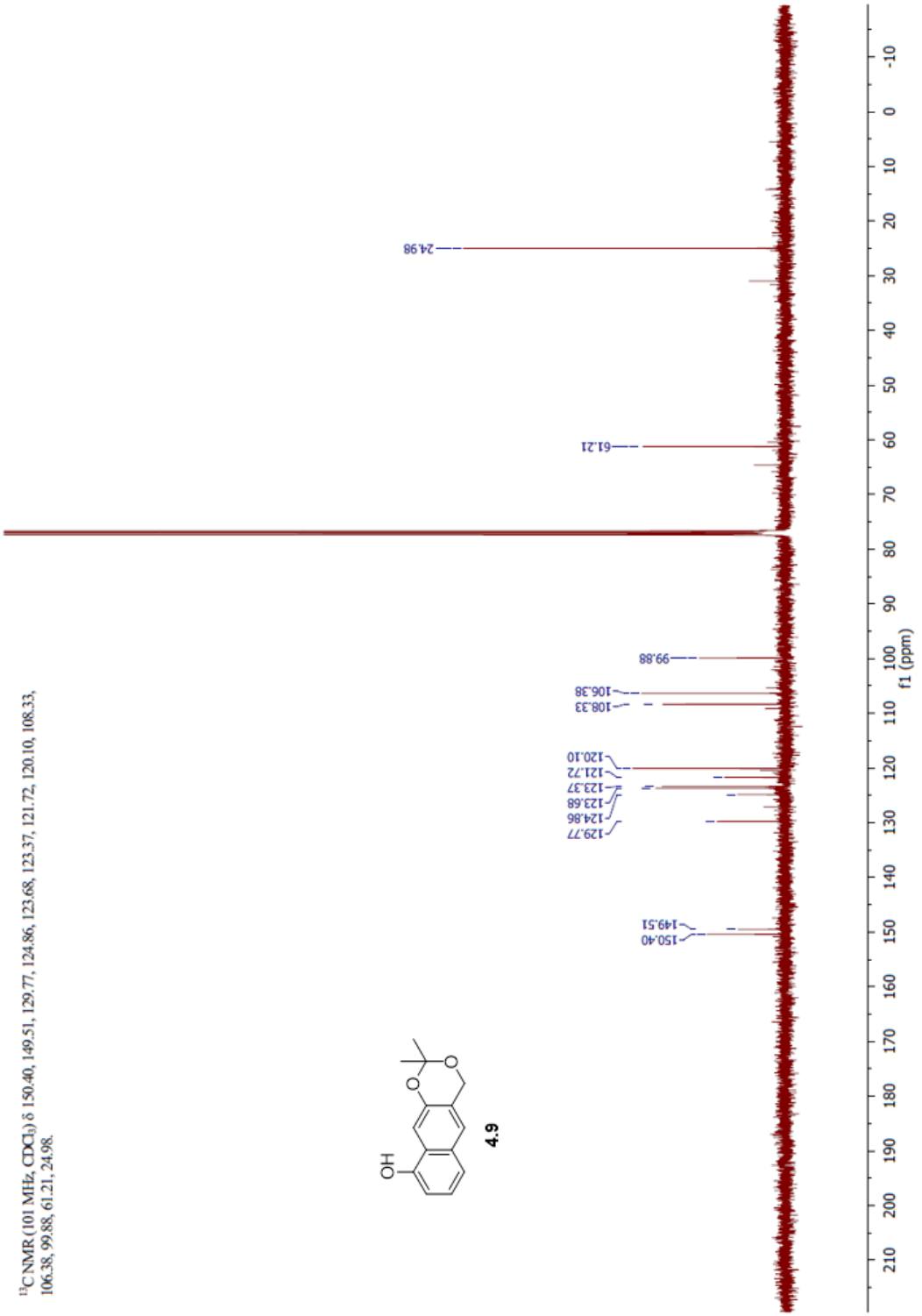

4.9 ^{13}C NMR Spectra

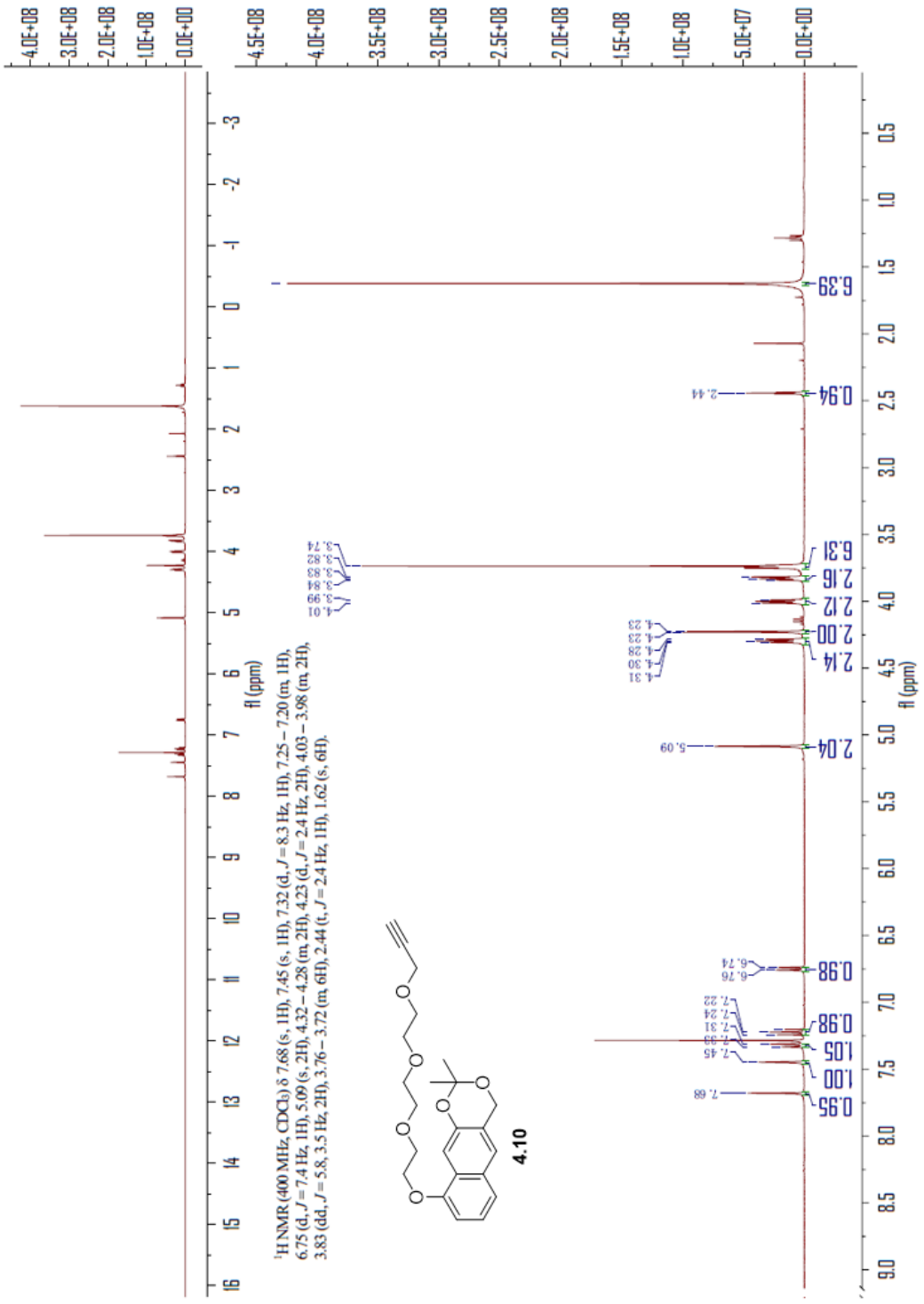

^{1}H NMR (400 MHz, $CDCl_3$) δ 7.68 (s, 1H), 7.45 (s, 1H), 7.32 (d, J = 8.3 Hz, 1H), 7.25 – 7.20 (m, 1H), 6.75 (d, J = 7.4 Hz, 1H), 5.09 (s, 2H), 4.32 – 4.28 (m, 2H), 4.23 (d, J = 2.4 Hz, 2H), 4.03 – 3.98 (m, 2H), 3.83 (dd, J = 5.8, 3.5 Hz, 2H), 3.76 – 3.72 (m, 6H), 2.44 (t, J = 2.4 Hz, 1H), 1.62 (s, 6H).

4.10 ^{1}H NMR Spectra

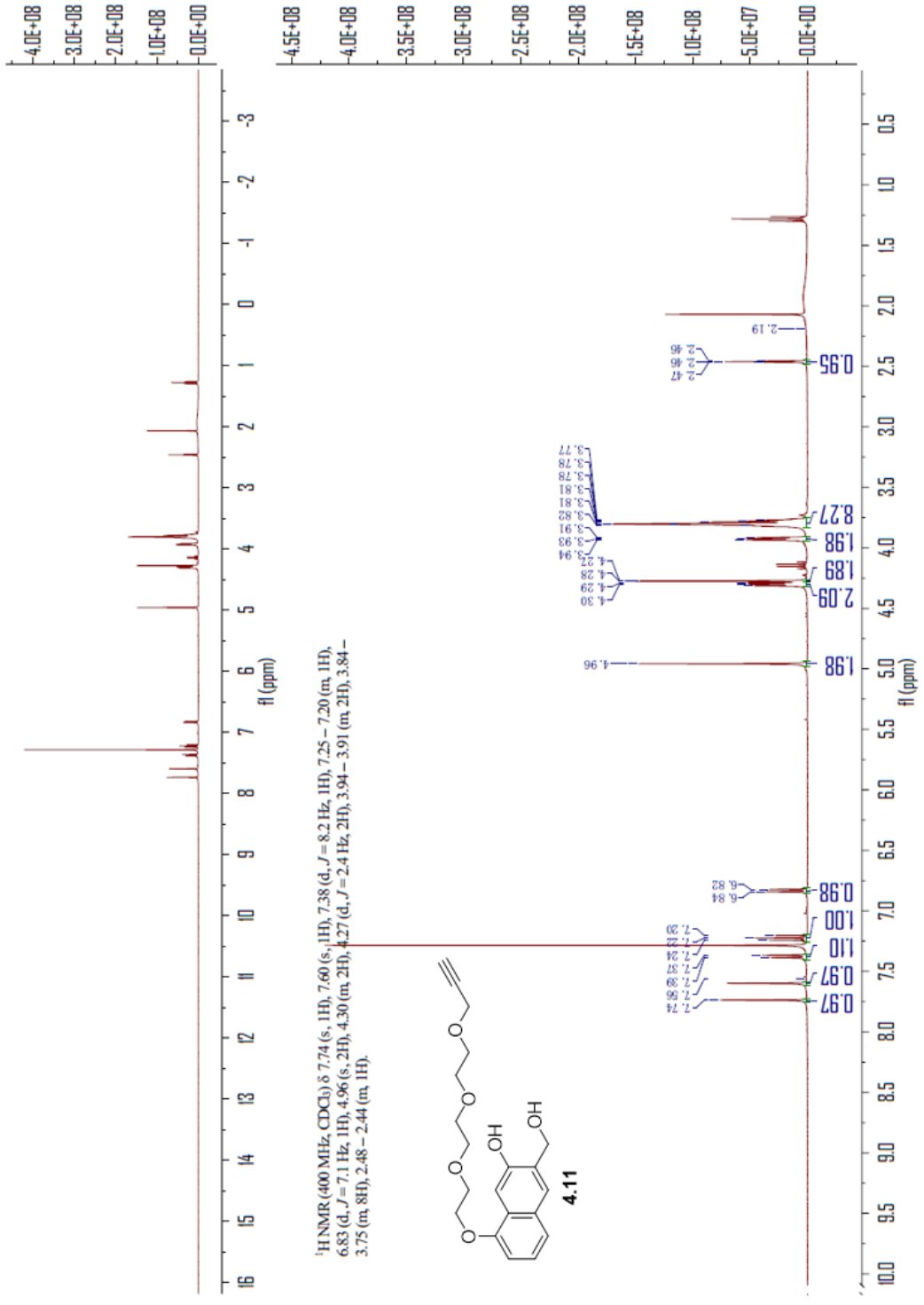

4.11 ^{1}H NMR Spectra

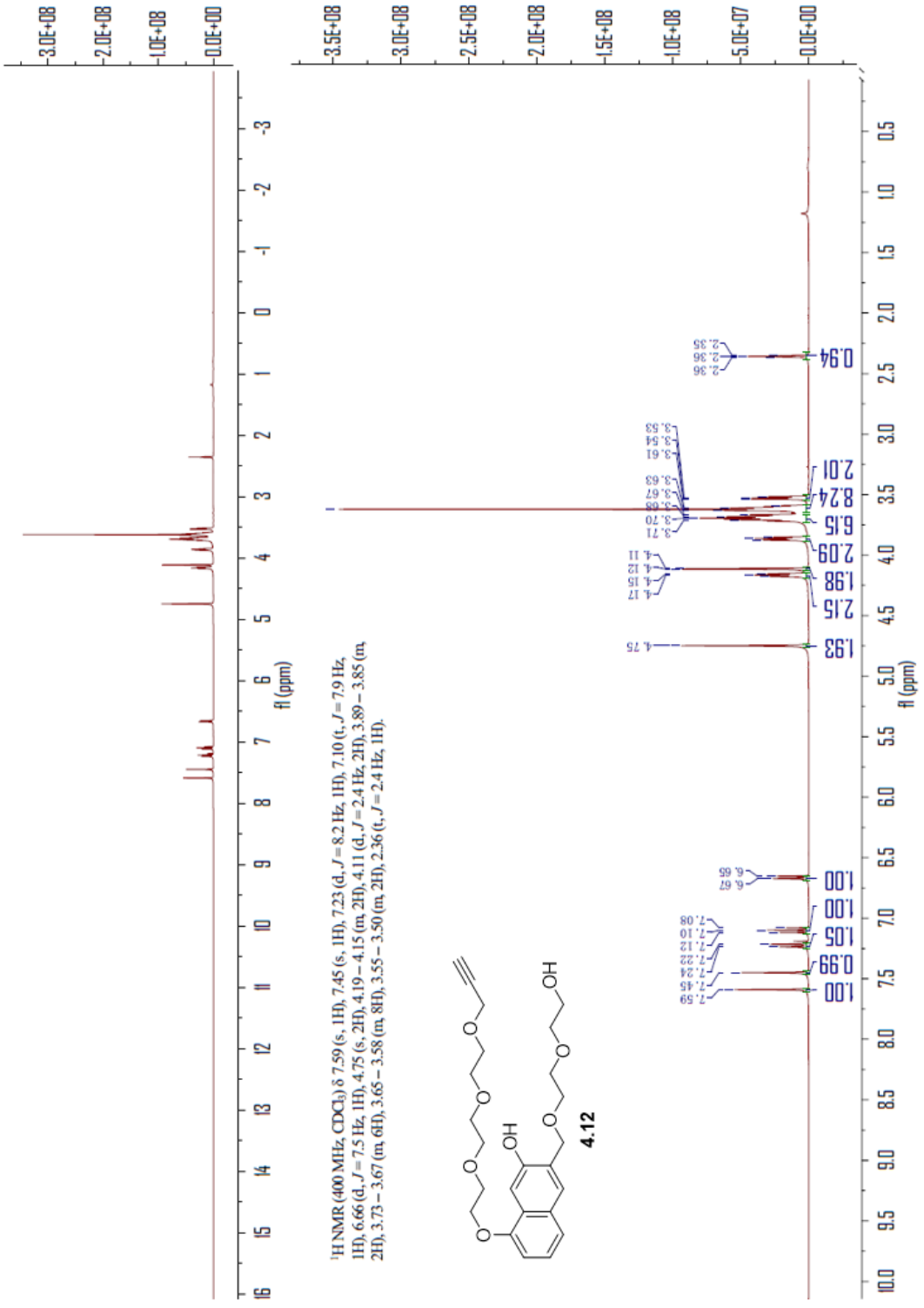

4.12 ^{1}H NMR Spectra

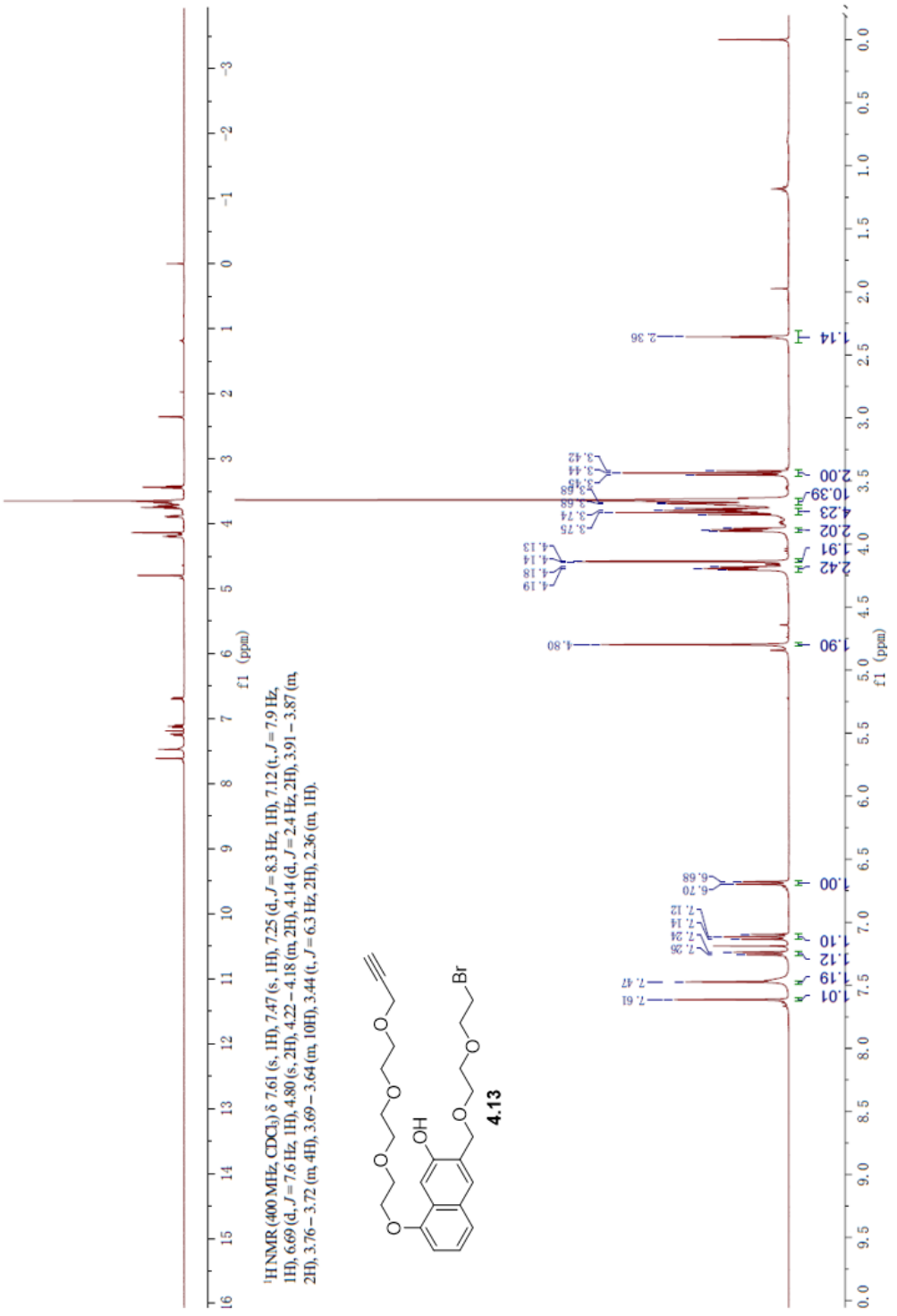

4.13 ^{1}H NMR Spectra

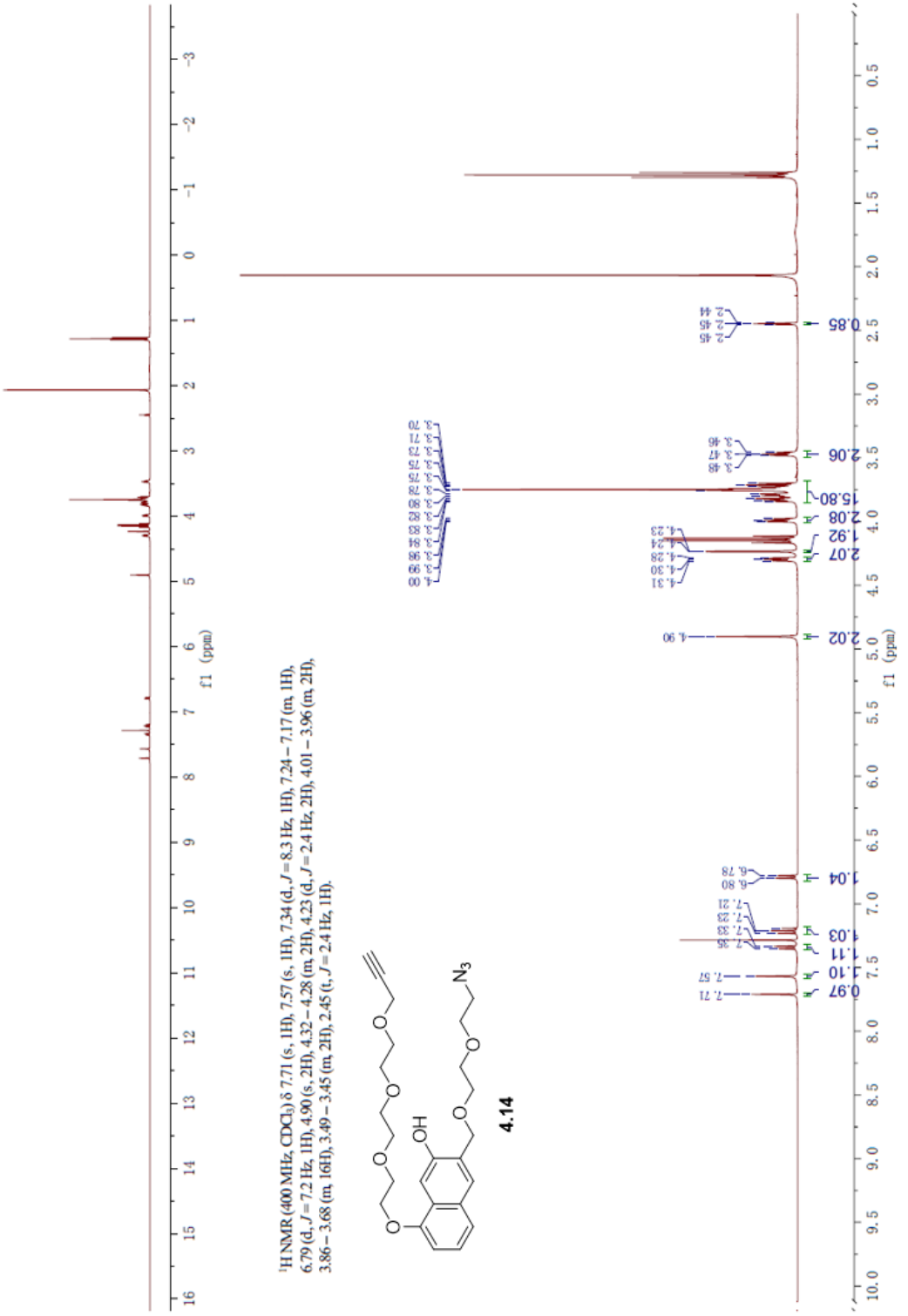

4.14 ^{1}H NMR Spectra

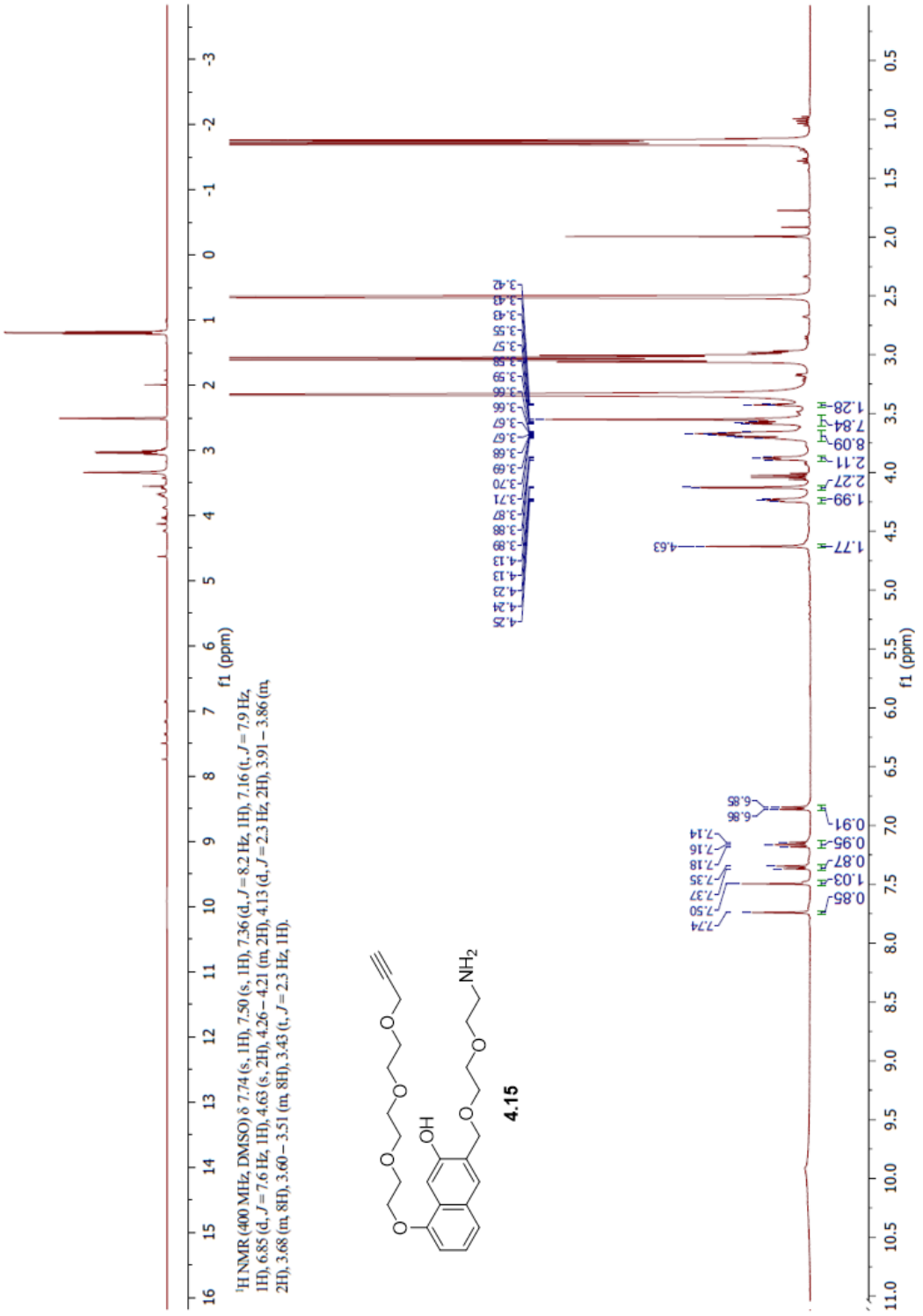

4.15 ^{1}H NMR Spectra

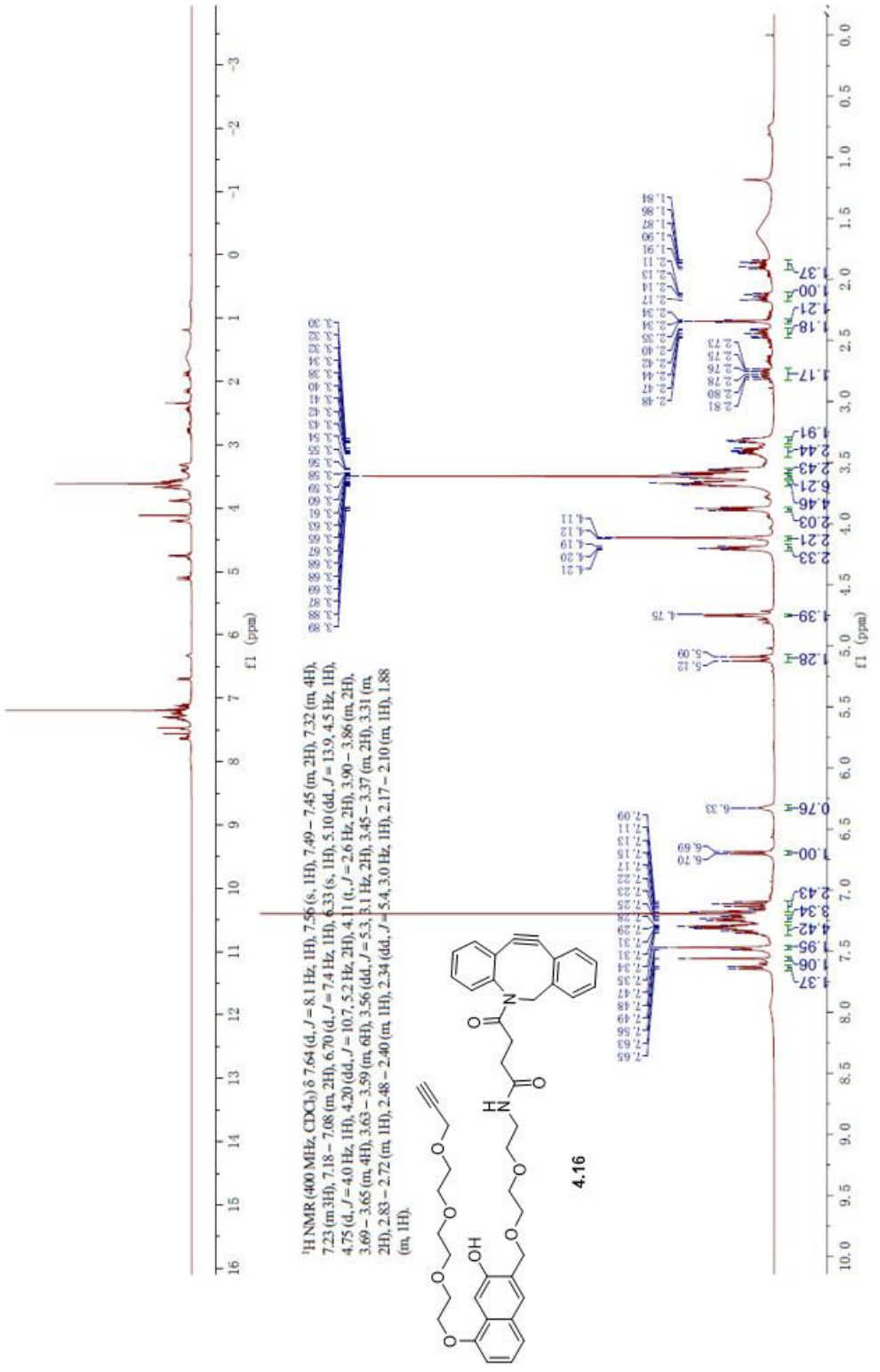

4.16 ^{1}H NMR Spectra

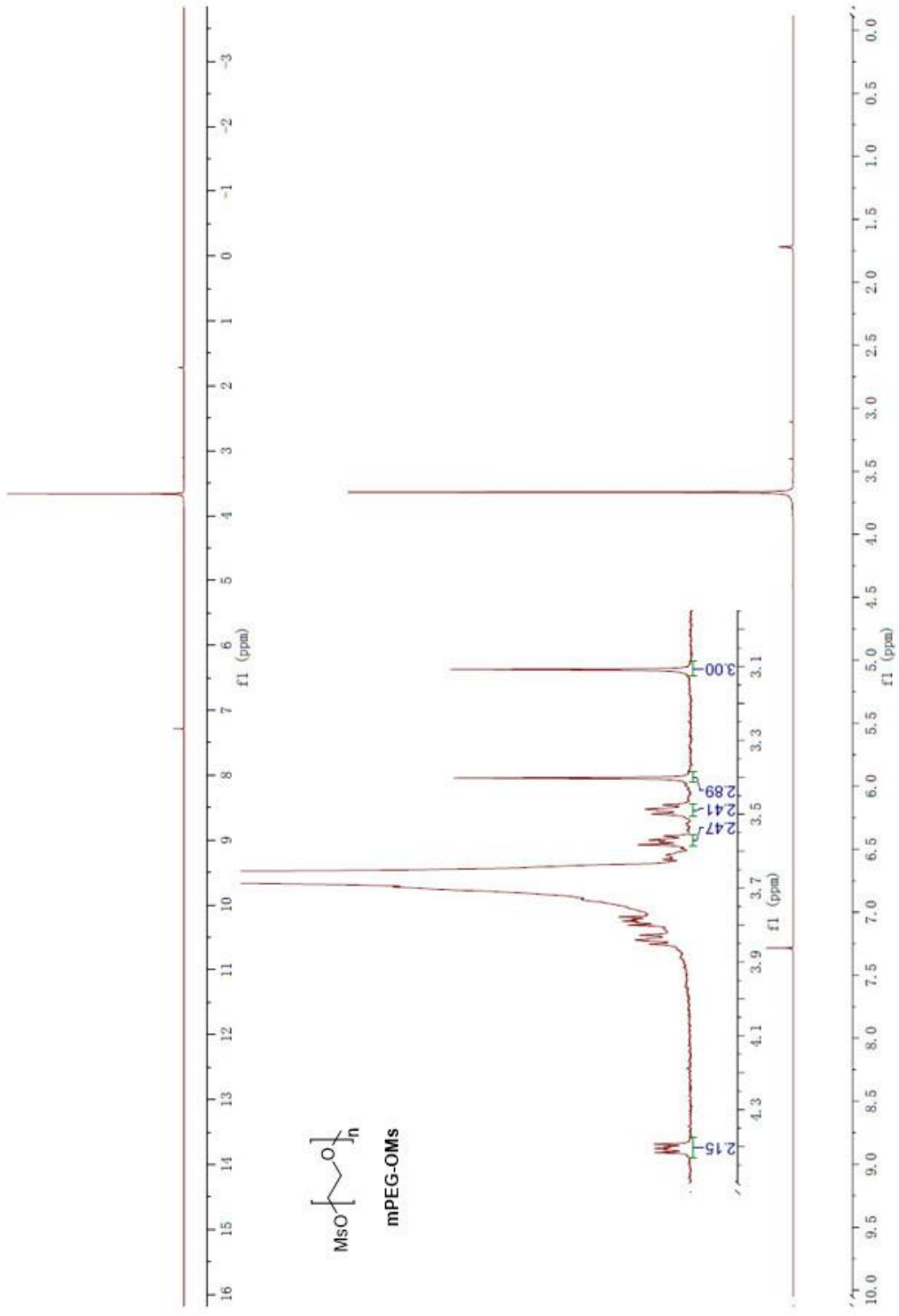

mPEG-OMs ^{1}H NMR Spectra

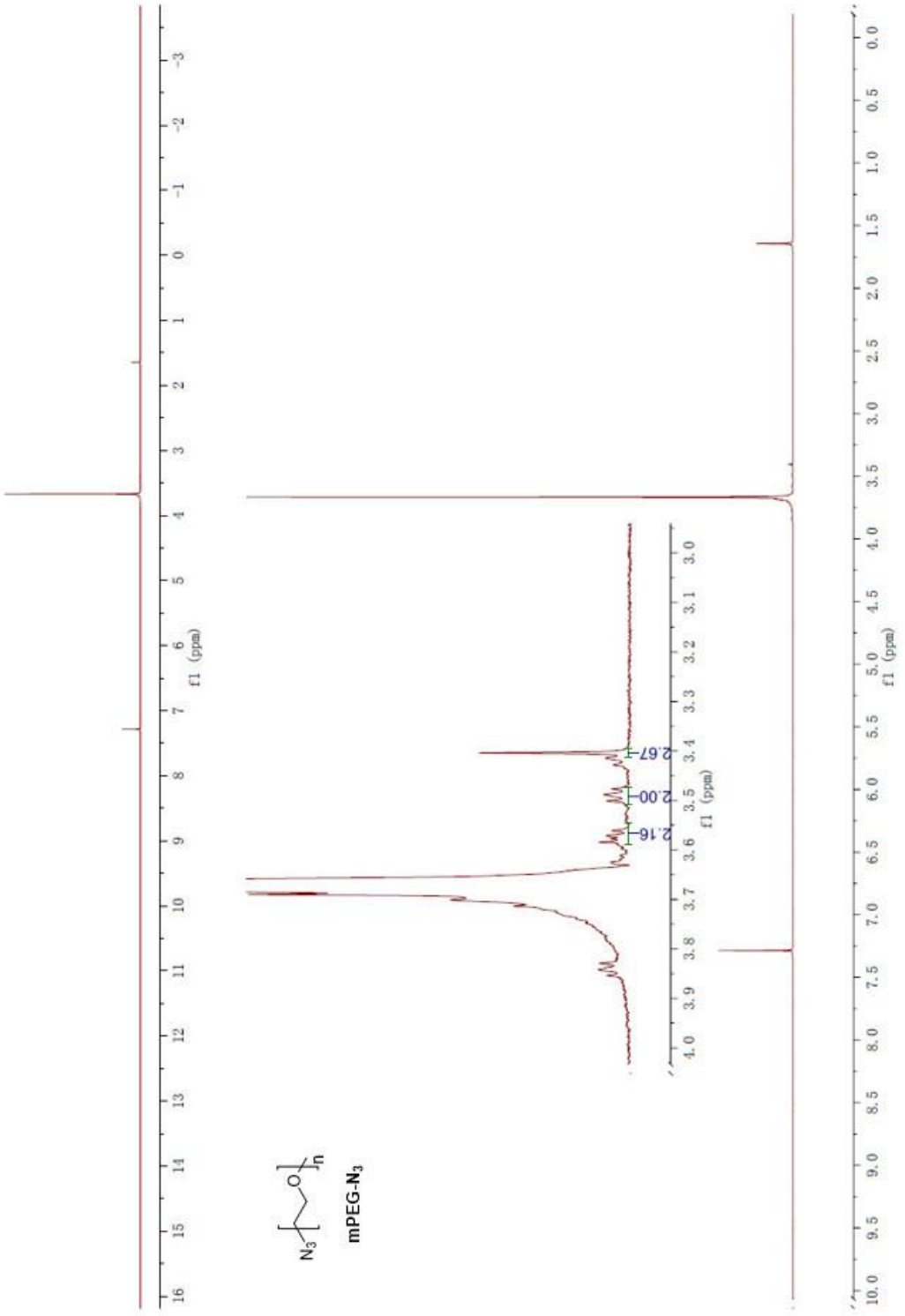

mPEG-N$_3$ ^{1}H NMR Spectra

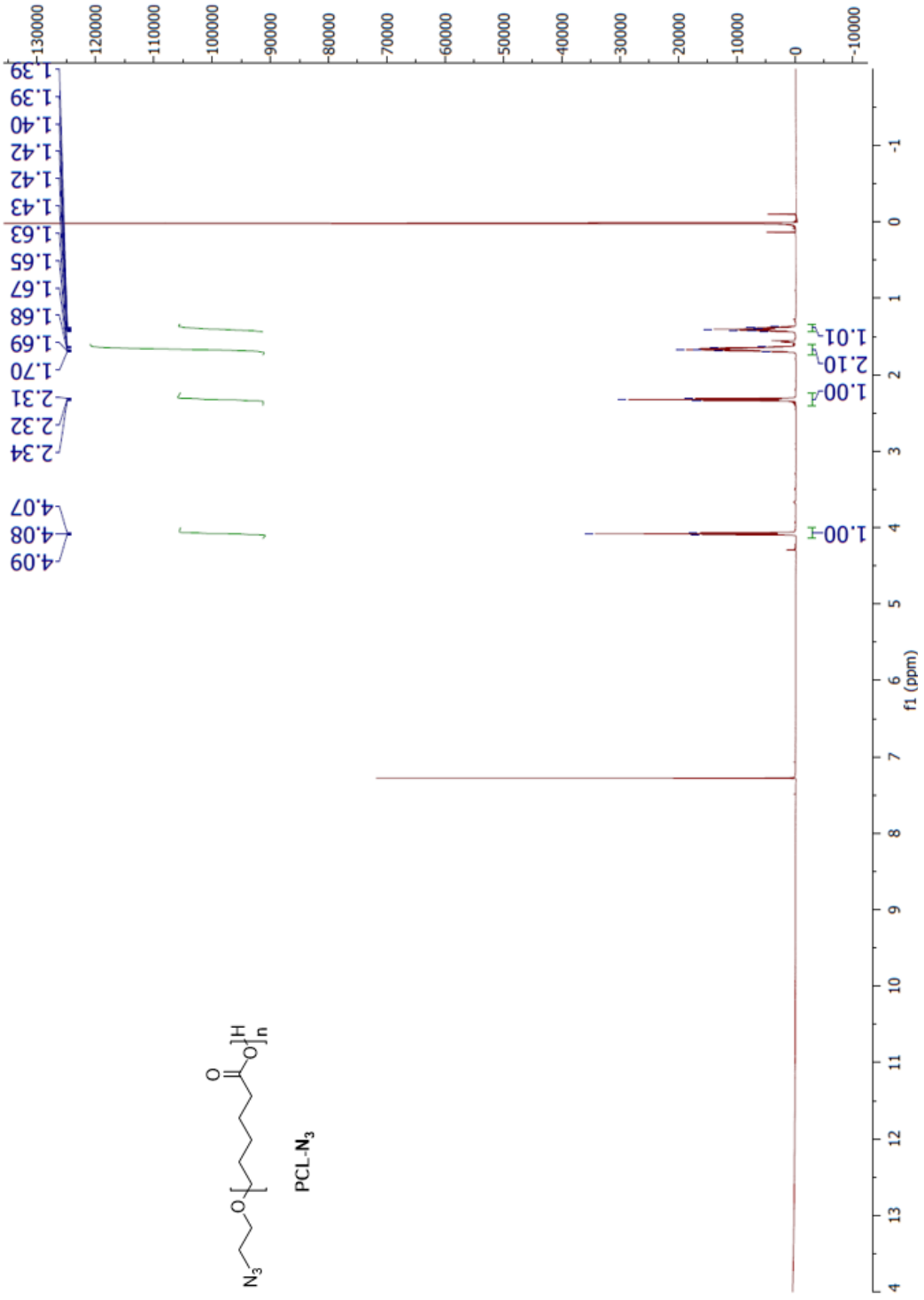

PCL-N$_3$ ^{1}H NMR Spectra

2. ESI-MS Spectra

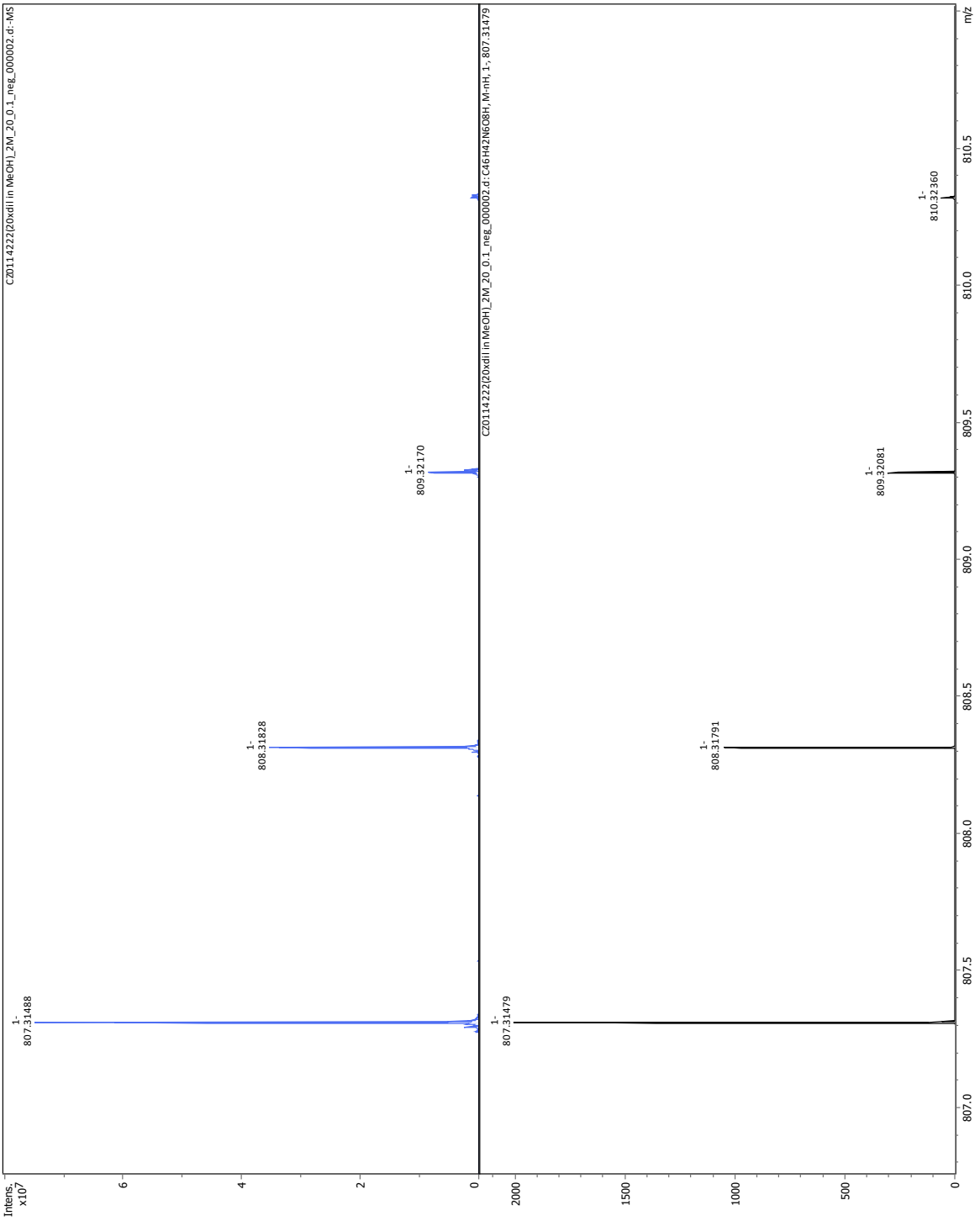

2.1 ESI-MS Spectra

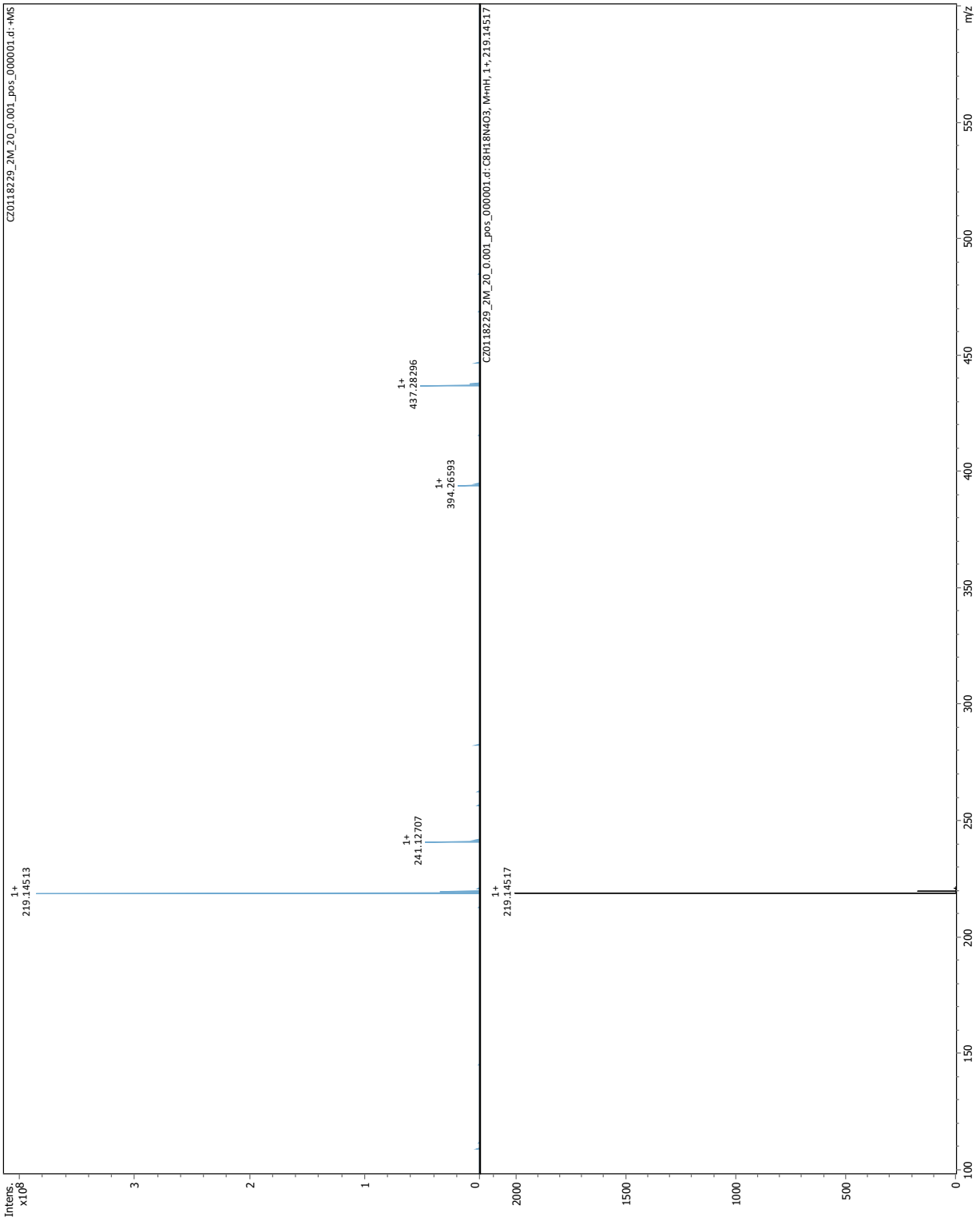

2.11 ESI-MS Spectra

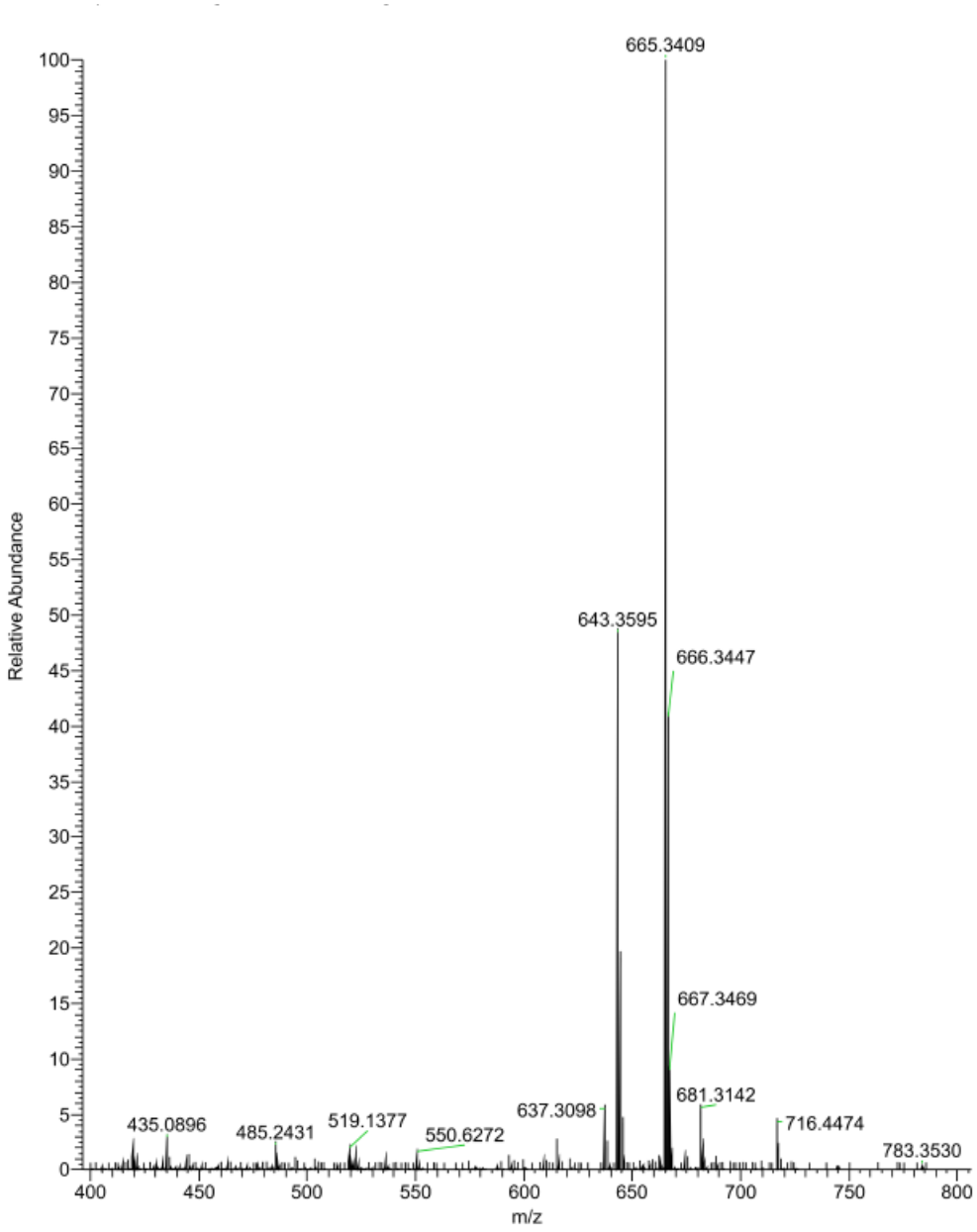

2.12 ESI-MS Spectra

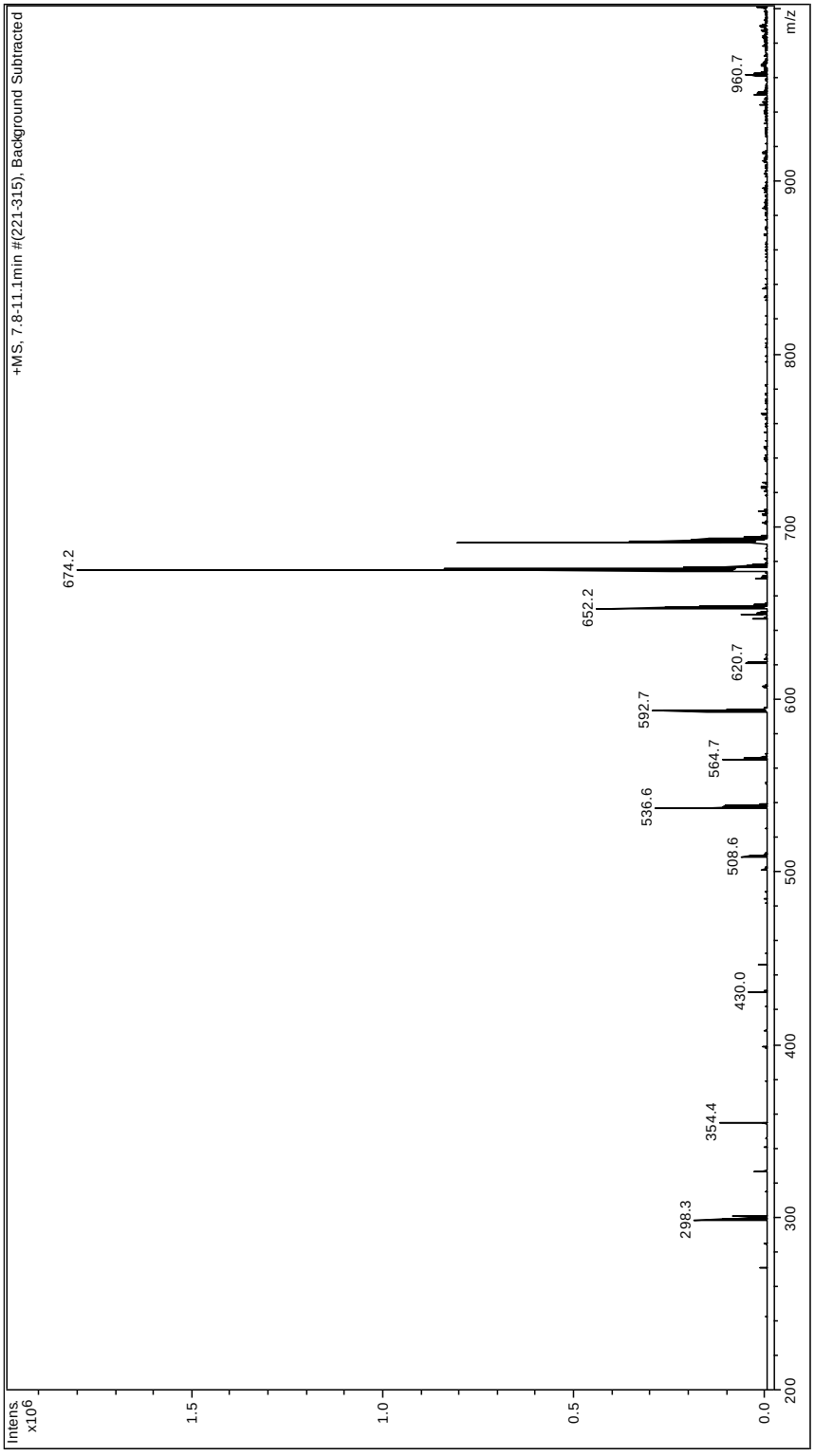

3.6 ESI-MS Spectra

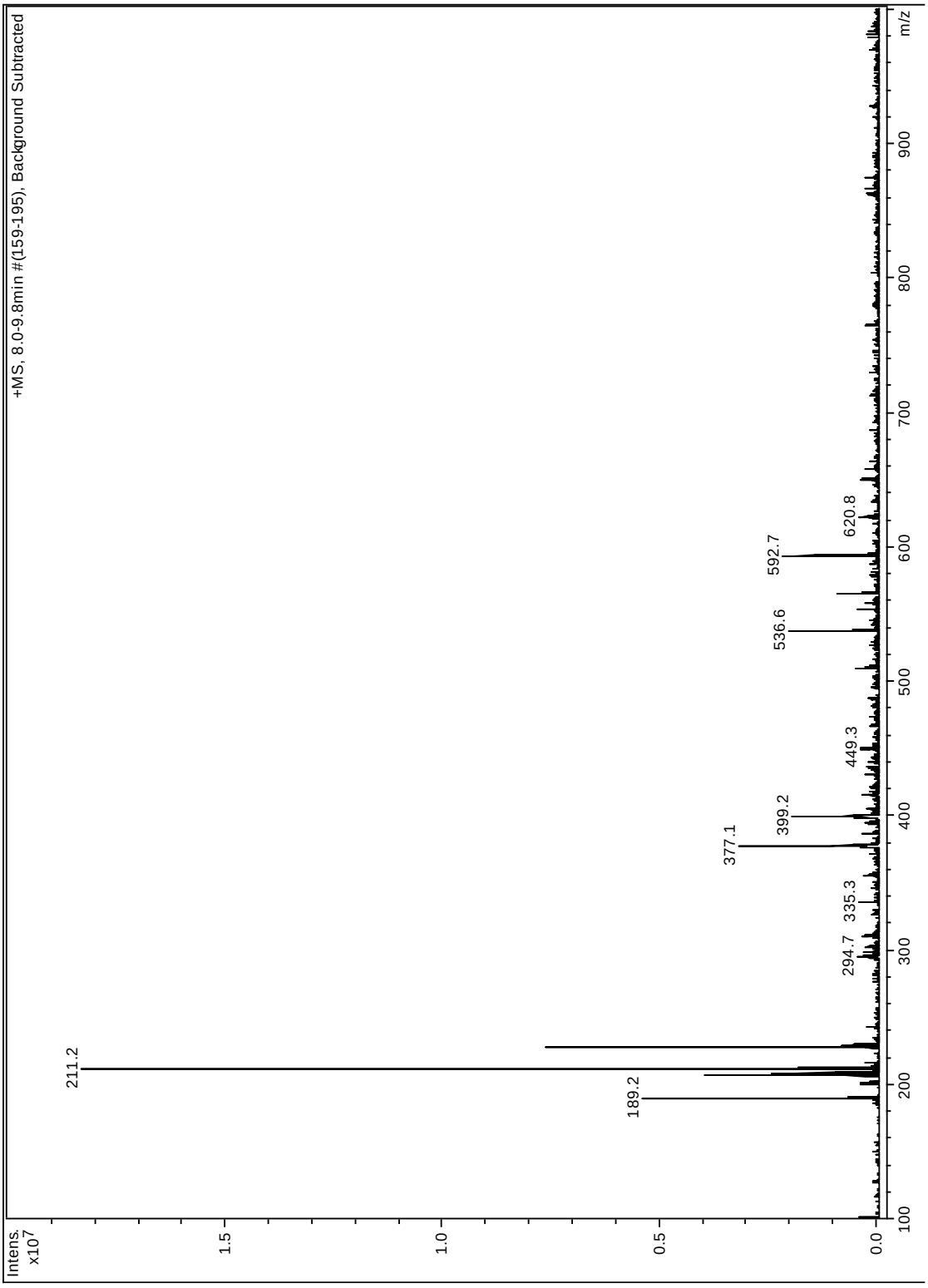

4.5 ESI-MS Spectra

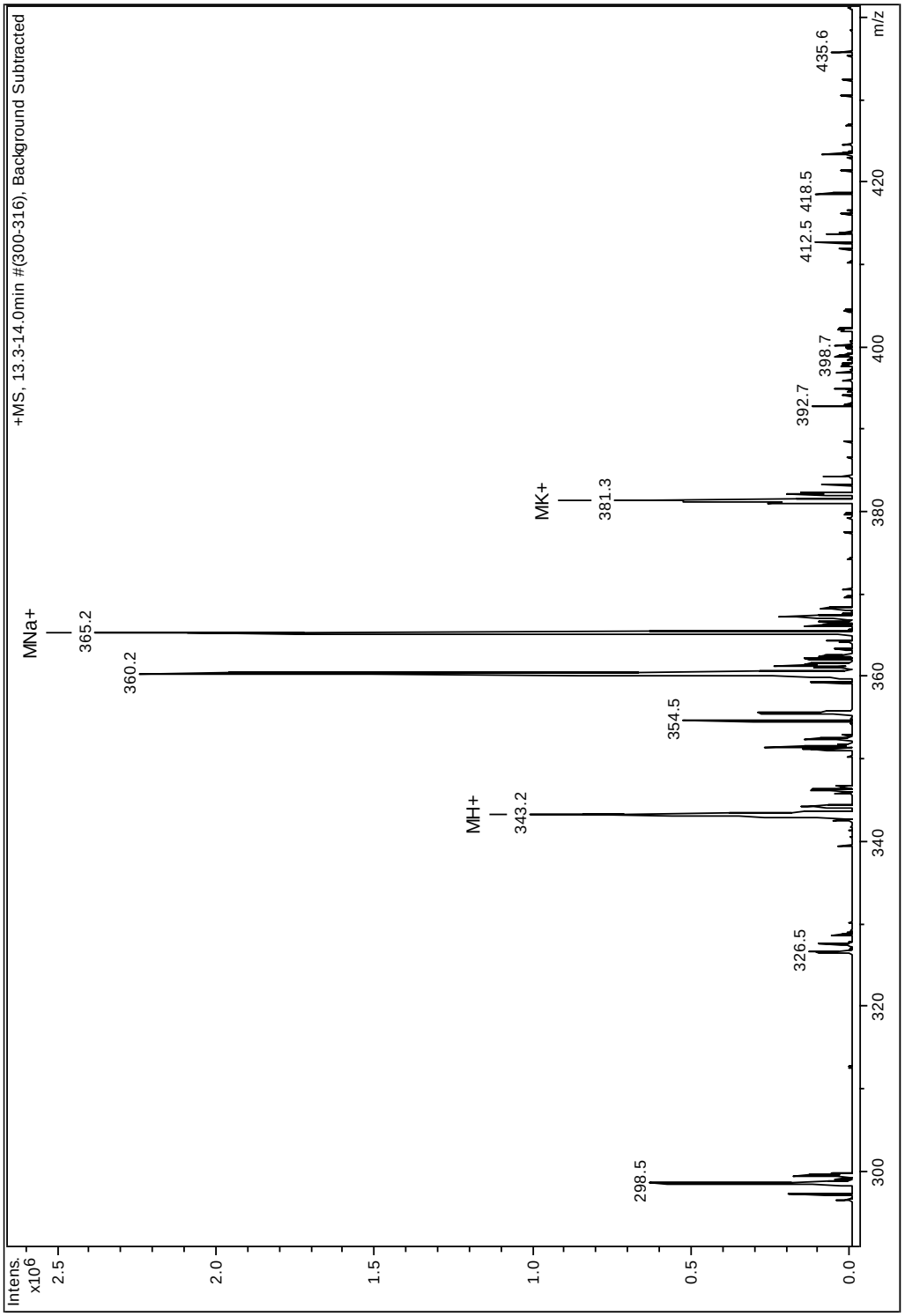

4.6 ESI-MS Spectra

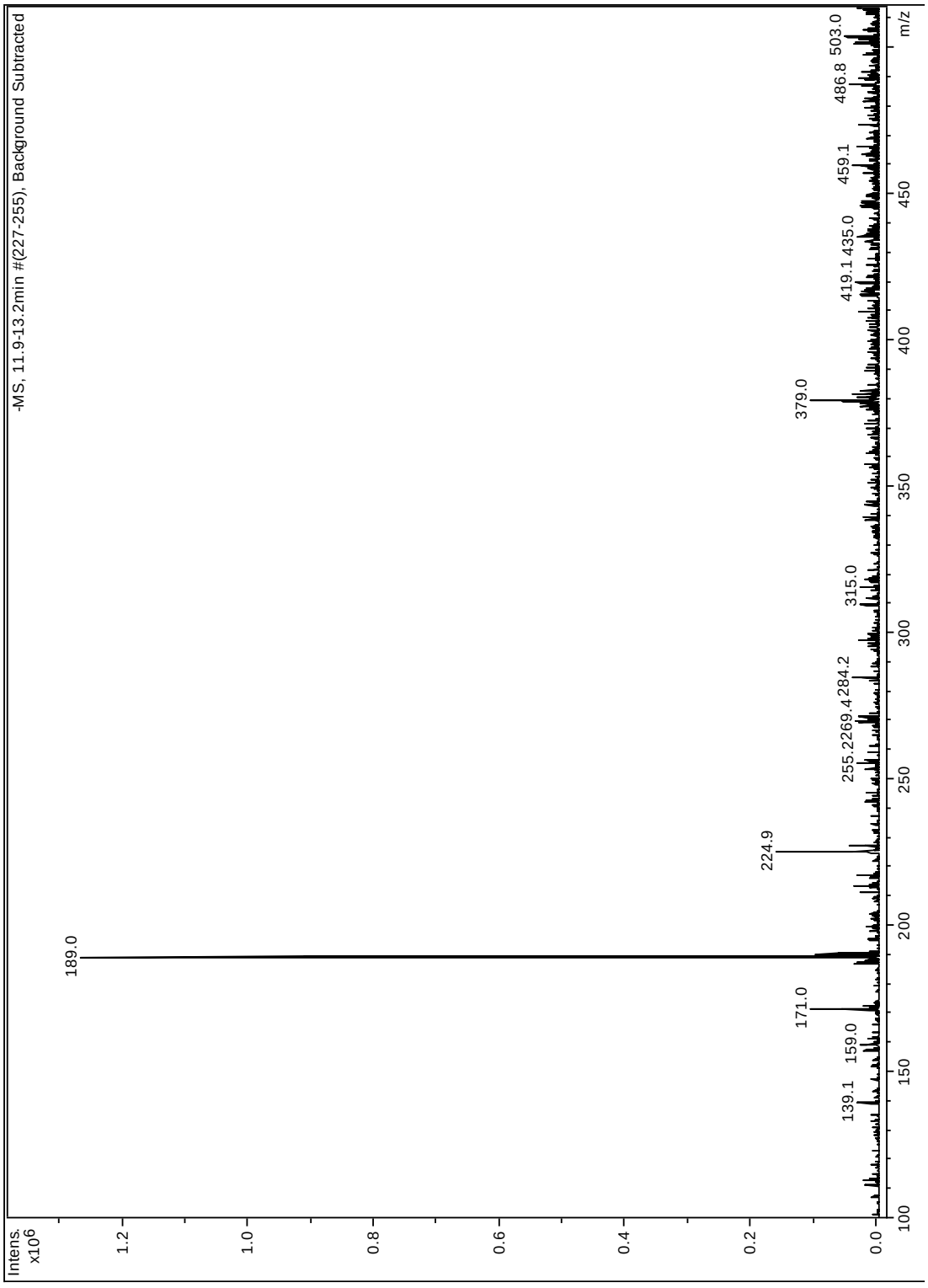

4.8 ESI-MS Spectra

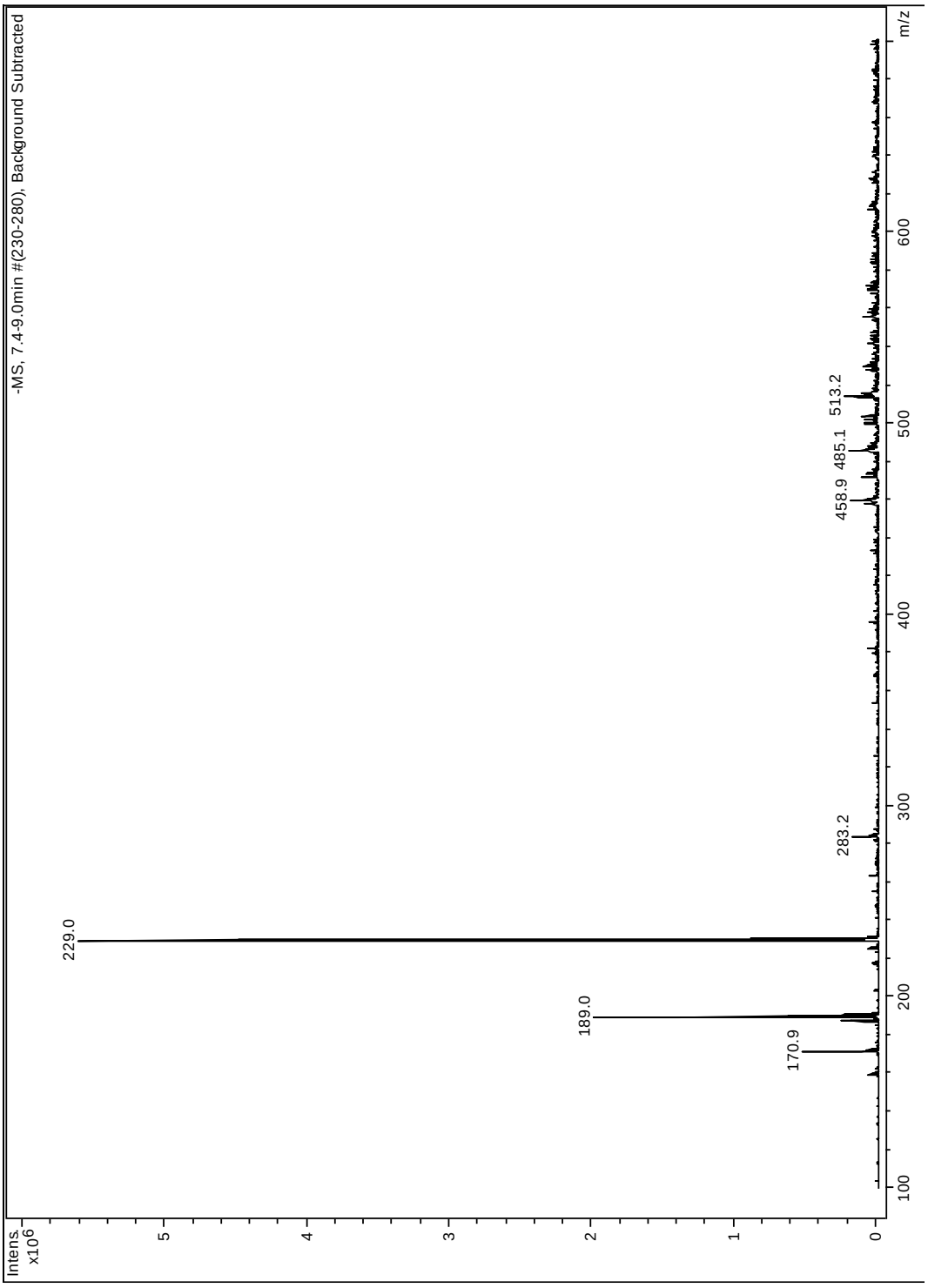

4.9 ESI-MS Spectra

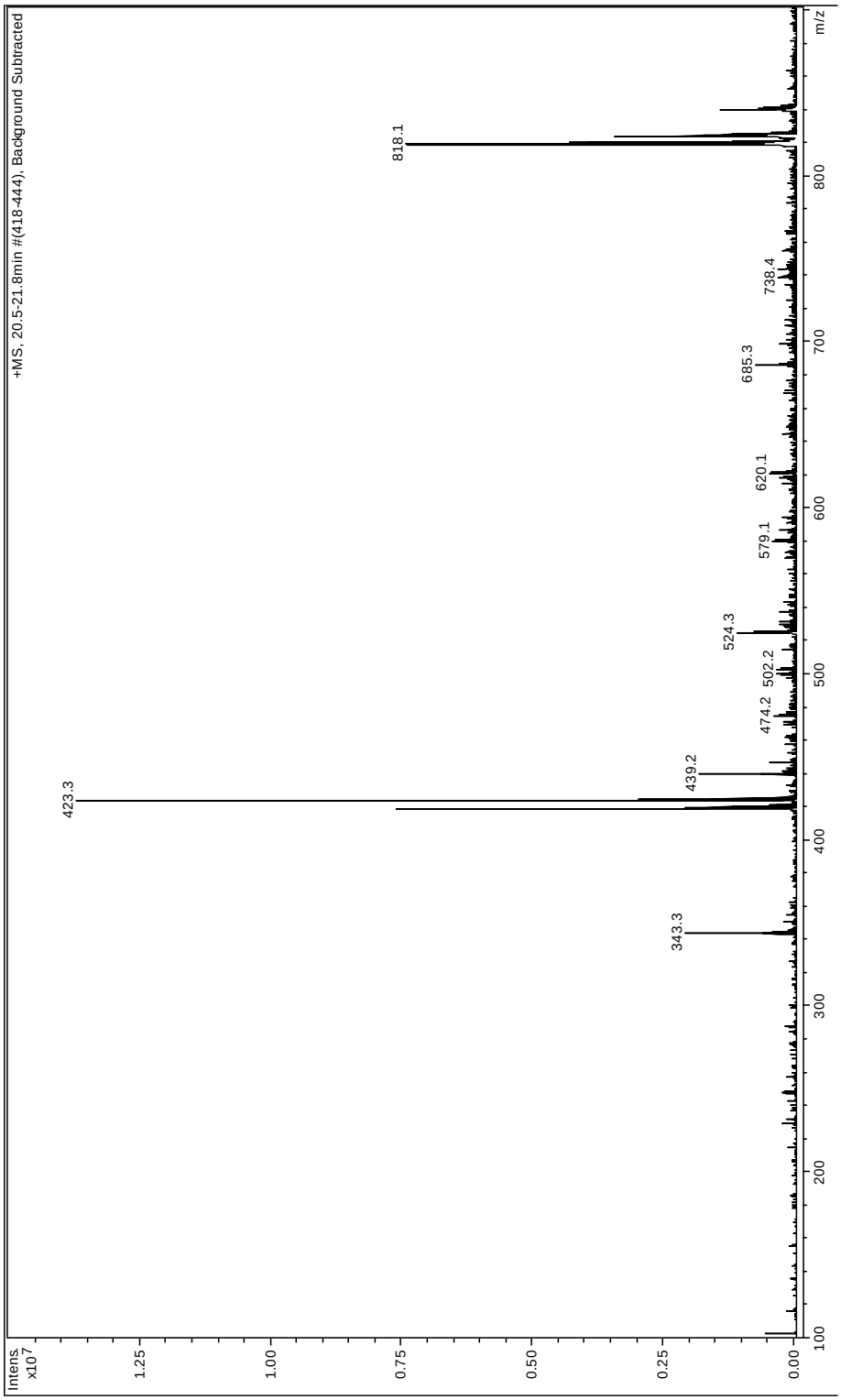

4.10 ESI-MS Spectra

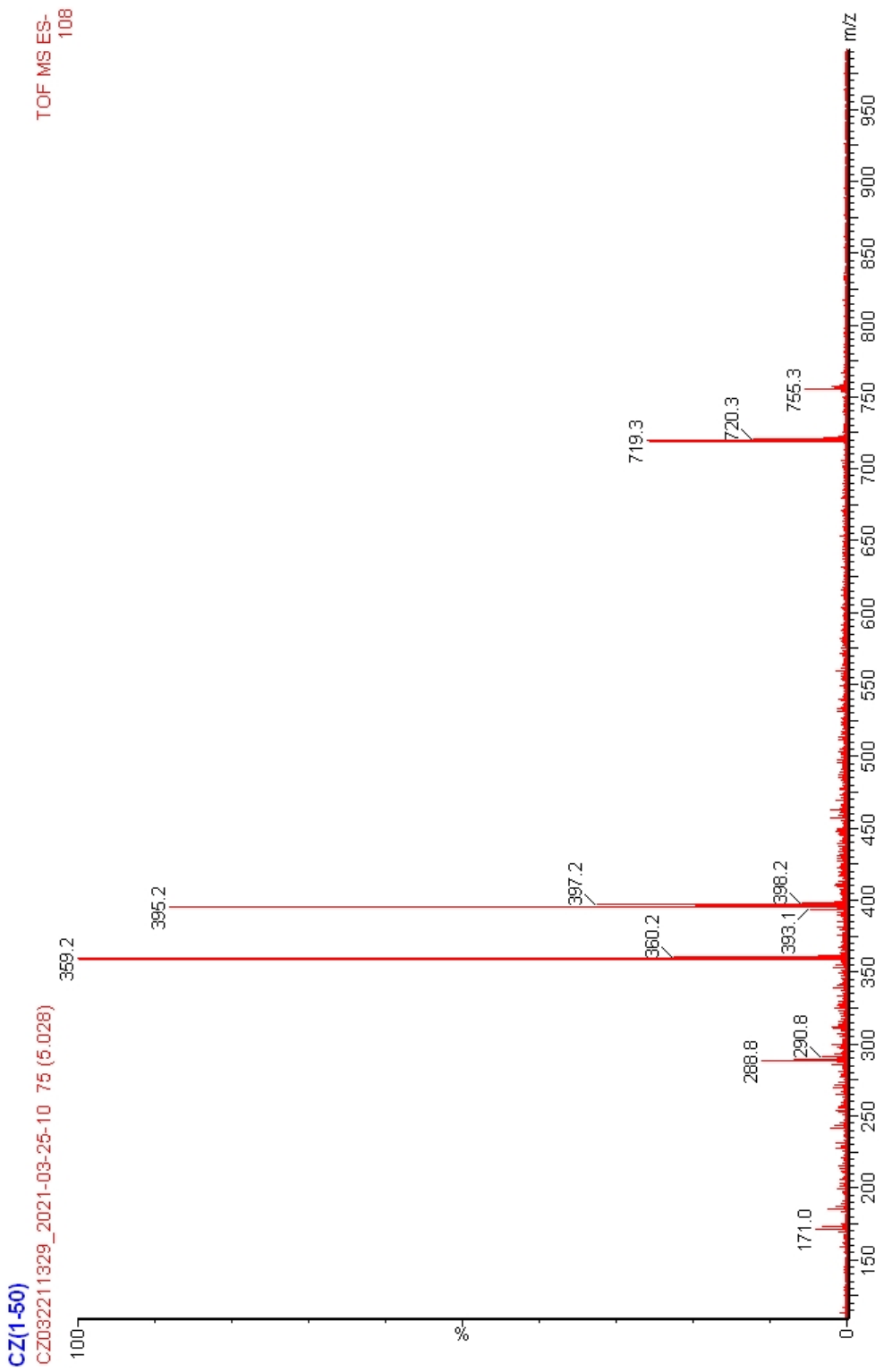

4.11 ESI-MS Spectra

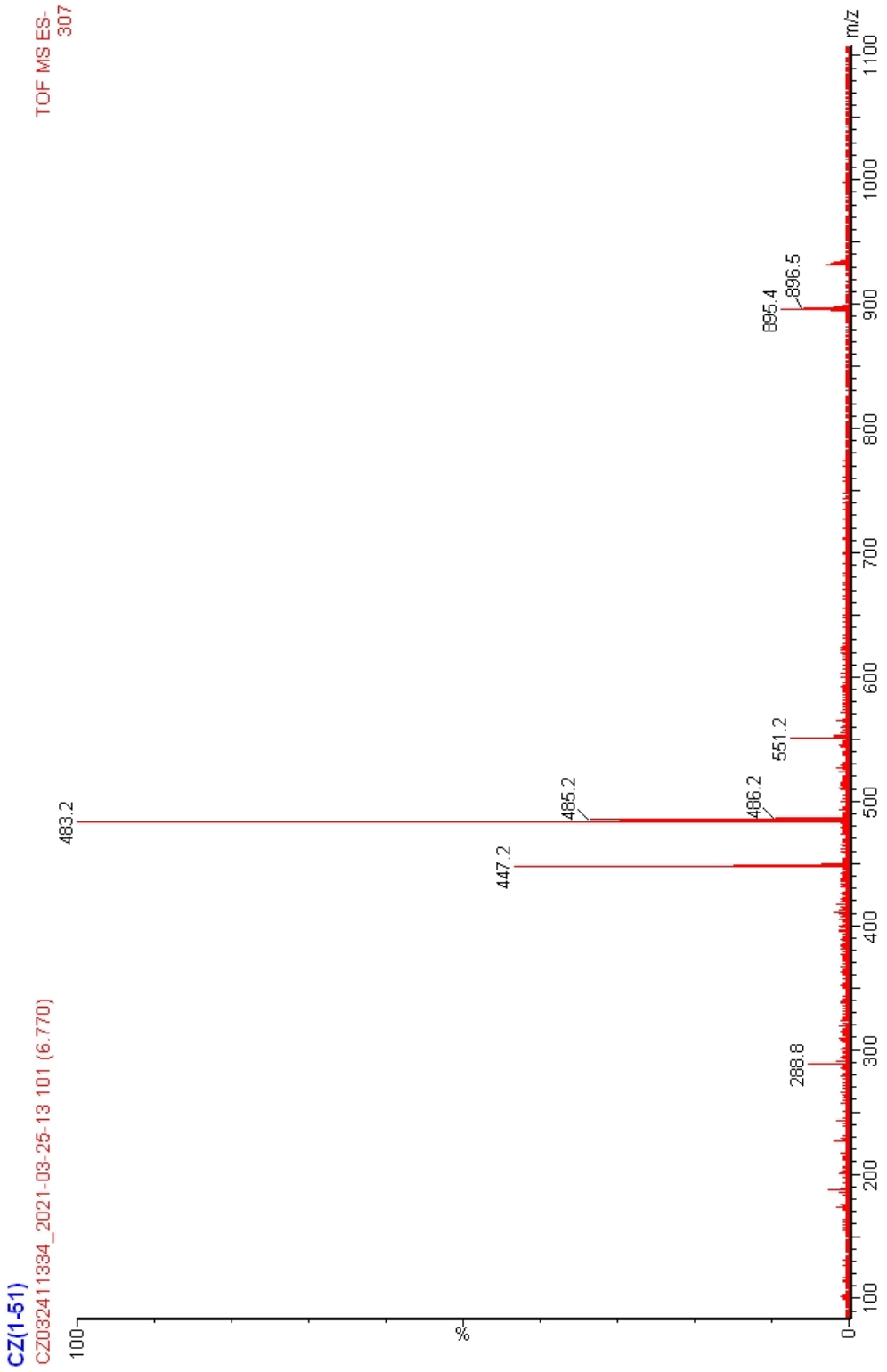

4.12 ESI-MS Spectra

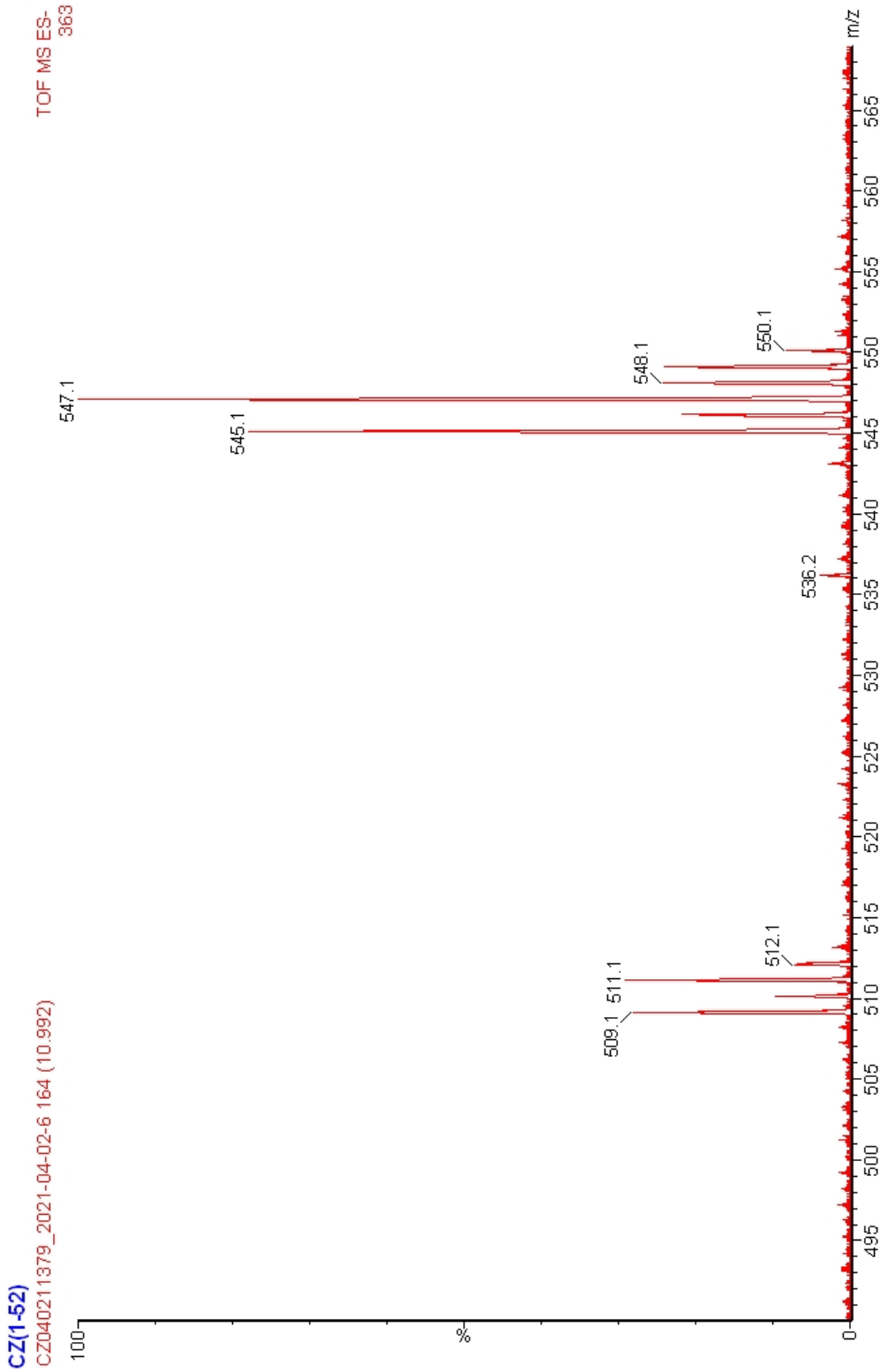

4.13 ESI-MS Spectra

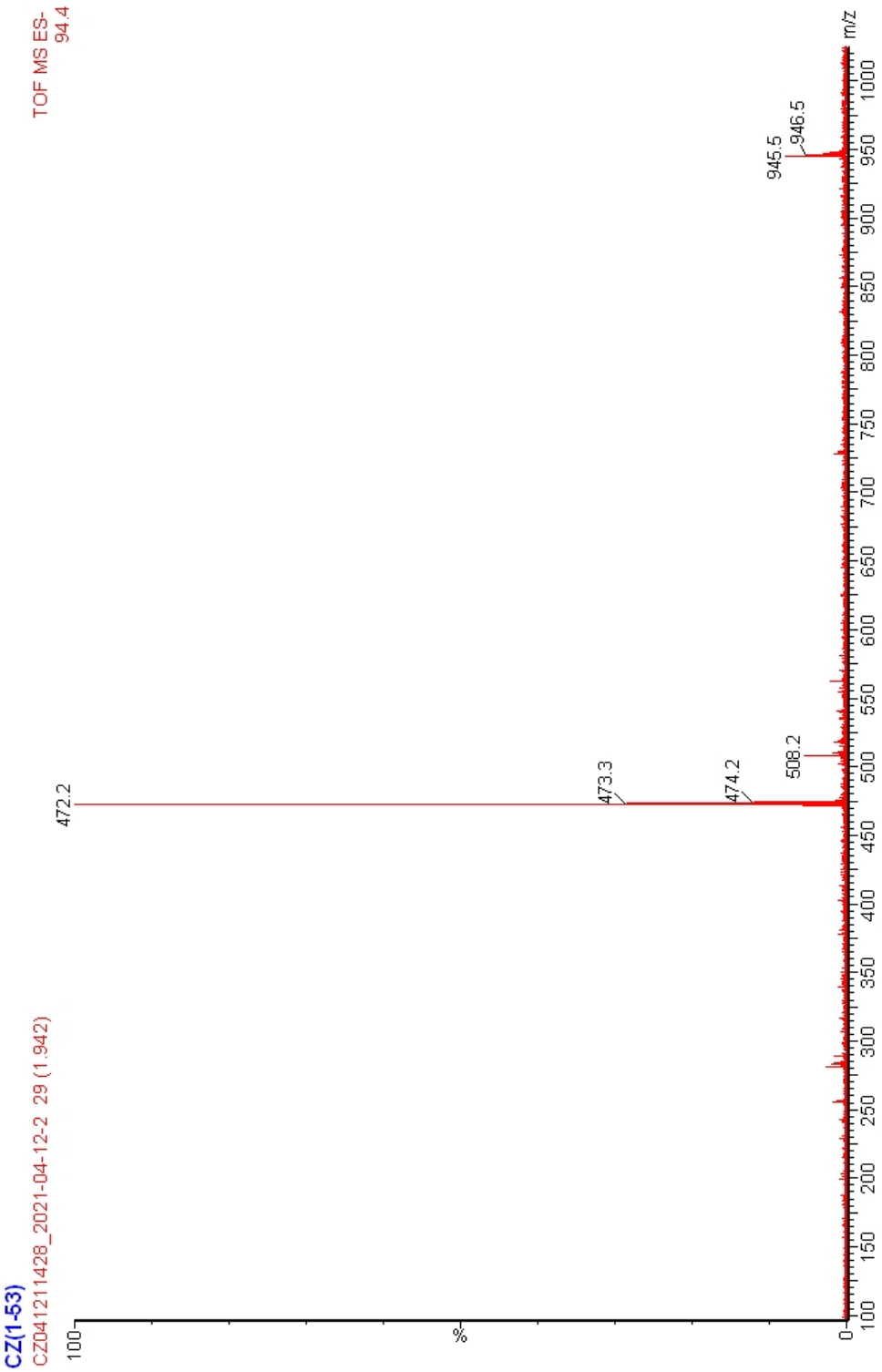

4.14 ESI-MS Spectra

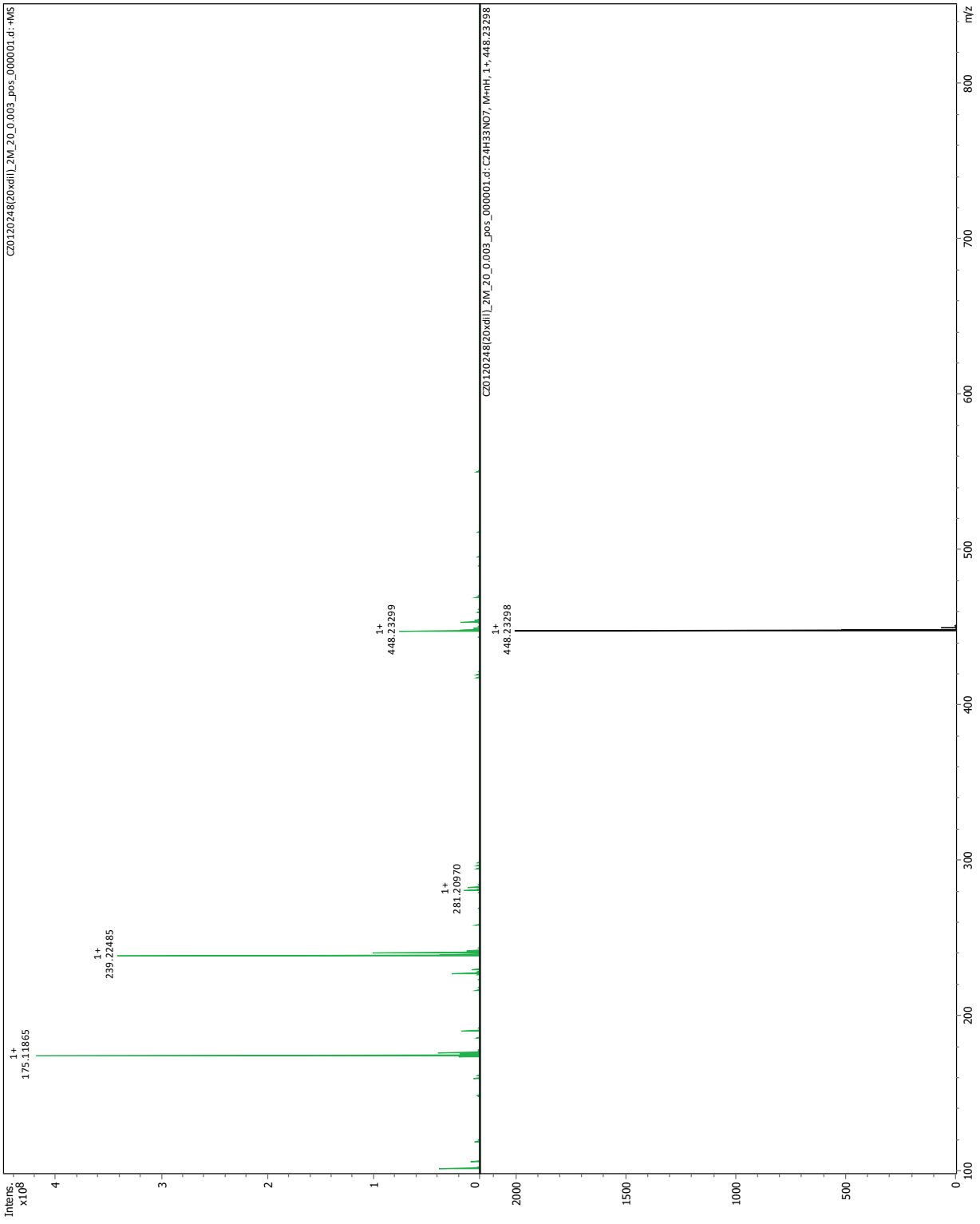

4.15 ESI-MS Spectra

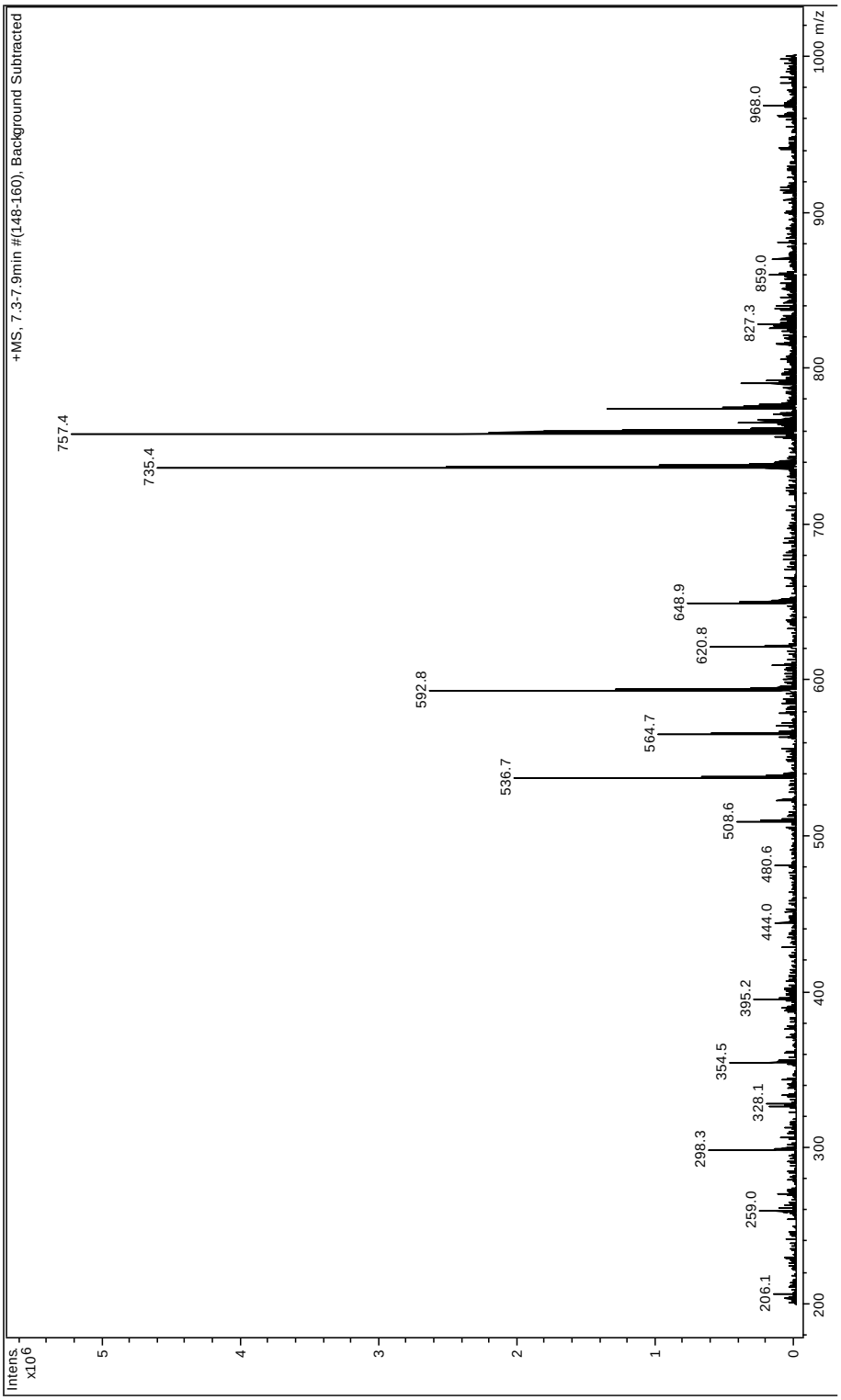

4.16 ESI-MS Spectra

3. Ultraviolet-Visible Spectra

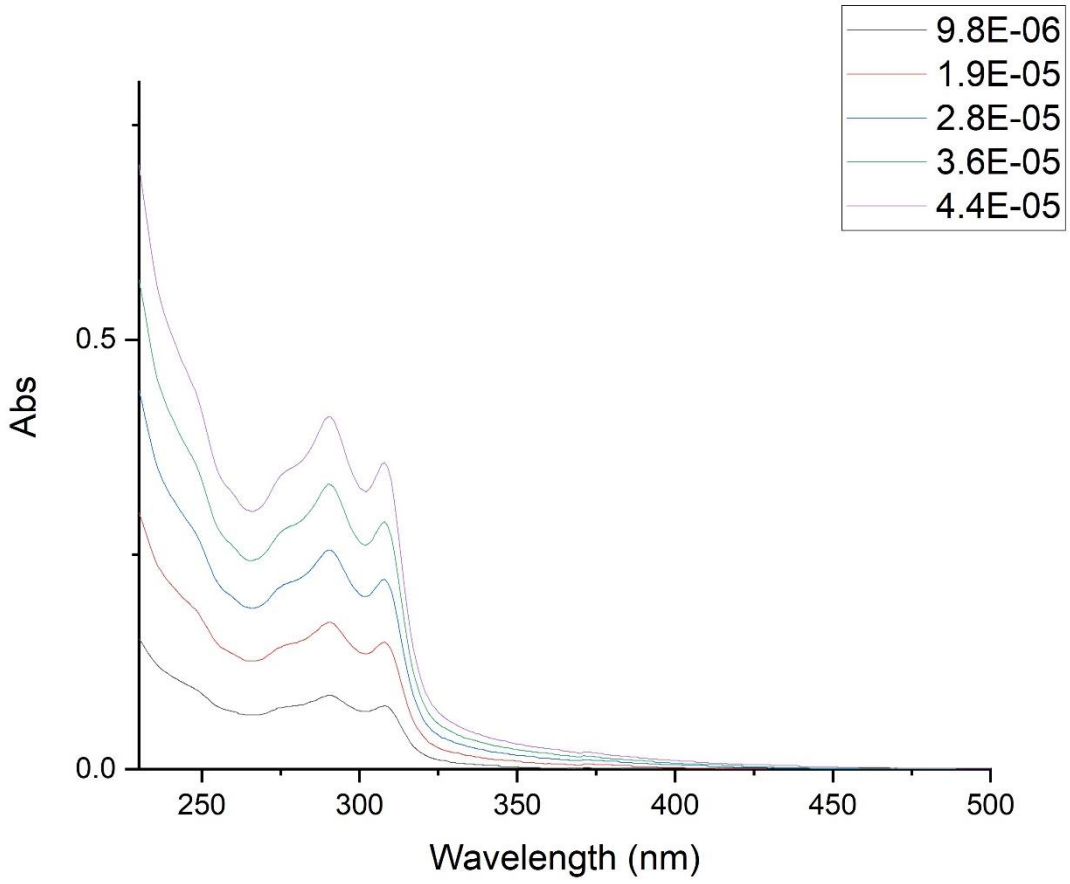

Figure S. 1 UV–Vis Absorption Spectra of Bis-ADIBO 2.1 in DI Water

Table S. 1 Extinction Coefficient of bis-ADIBO 2.1

Wavelength (nm)	Extinction Coefficient ($M^{-1} \cdot cm^{-1}$)
290	9330.4 ± 47.4
310	7680.8 ± 48.9
321	2075.8 ± 11.6

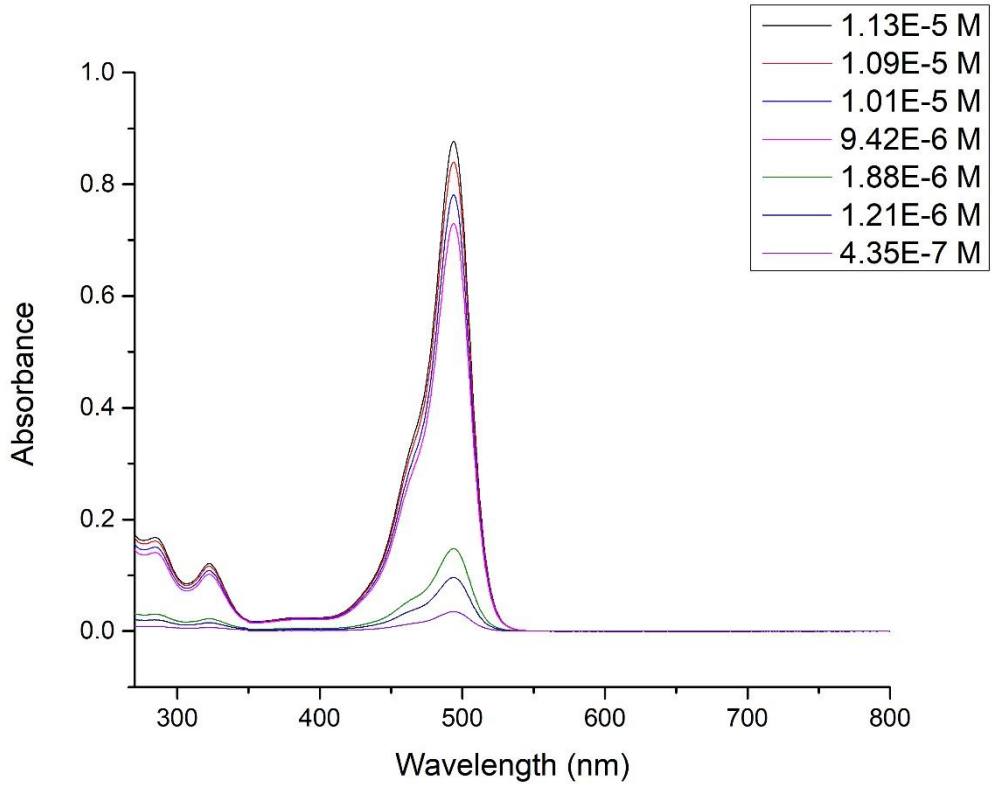

Figure S. 2 UV–Vis Absorption Spectra of 5-FAM-azide in 0.1% DMSO/Phosphate Buffer

Table S. 2 Extinction Coefficient of 5-FAM-azide in 0.1% DMSO/Phosphate Buffer

Wavelength	Extinction Coefficient ($M^{-1} \cdot cm^{-1}$)
493 nm	77003.5 ± 175.5

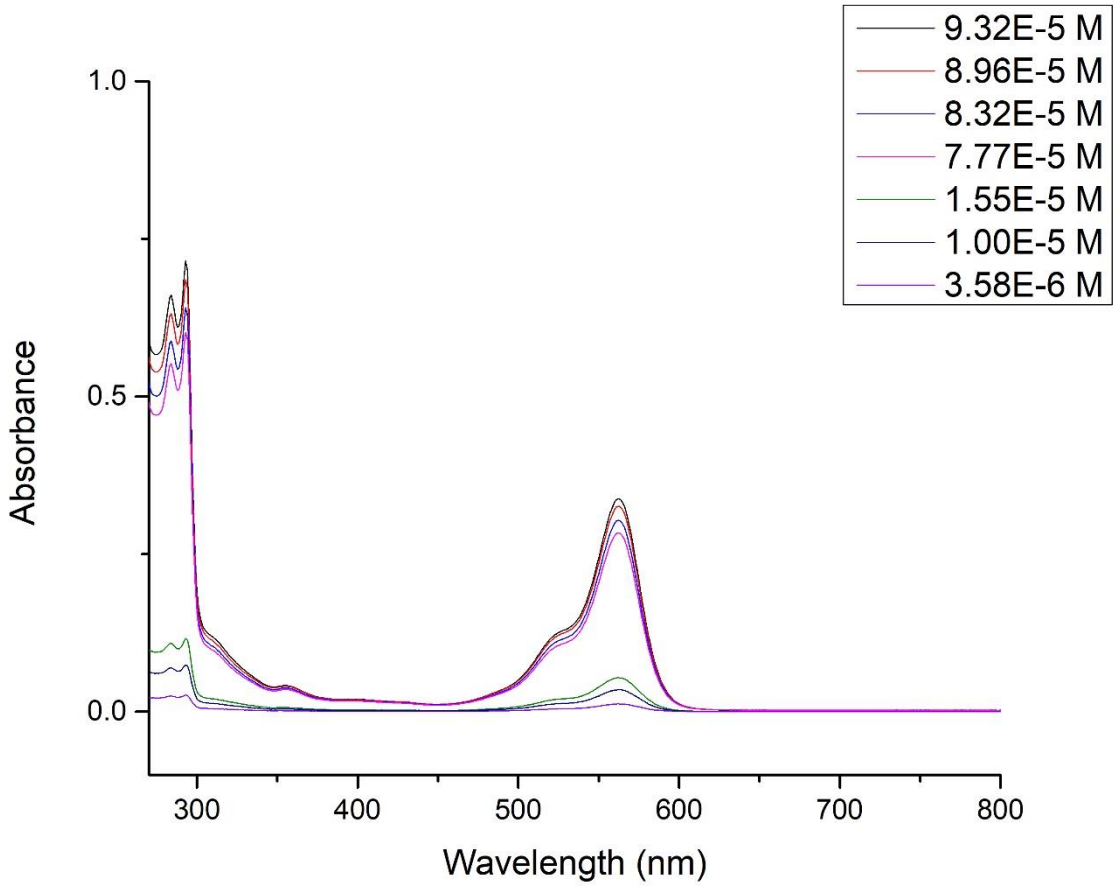

Figure S. 3 UV–Vis Absorption Spectra of 2.12 in 0.2% DMSO/HCl/H_2O (pH = 3.23)

Table S. 3 Extinction Coefficient of 2.12 in 0.2% DMSO/HCl/H_2O (pH = 3.23)

Wavelength (nm)	Extinction Coefficient ($M^{-1} \cdot cm^{-1}$)
560	3603.9 ± 11.5

4. IR Spectra

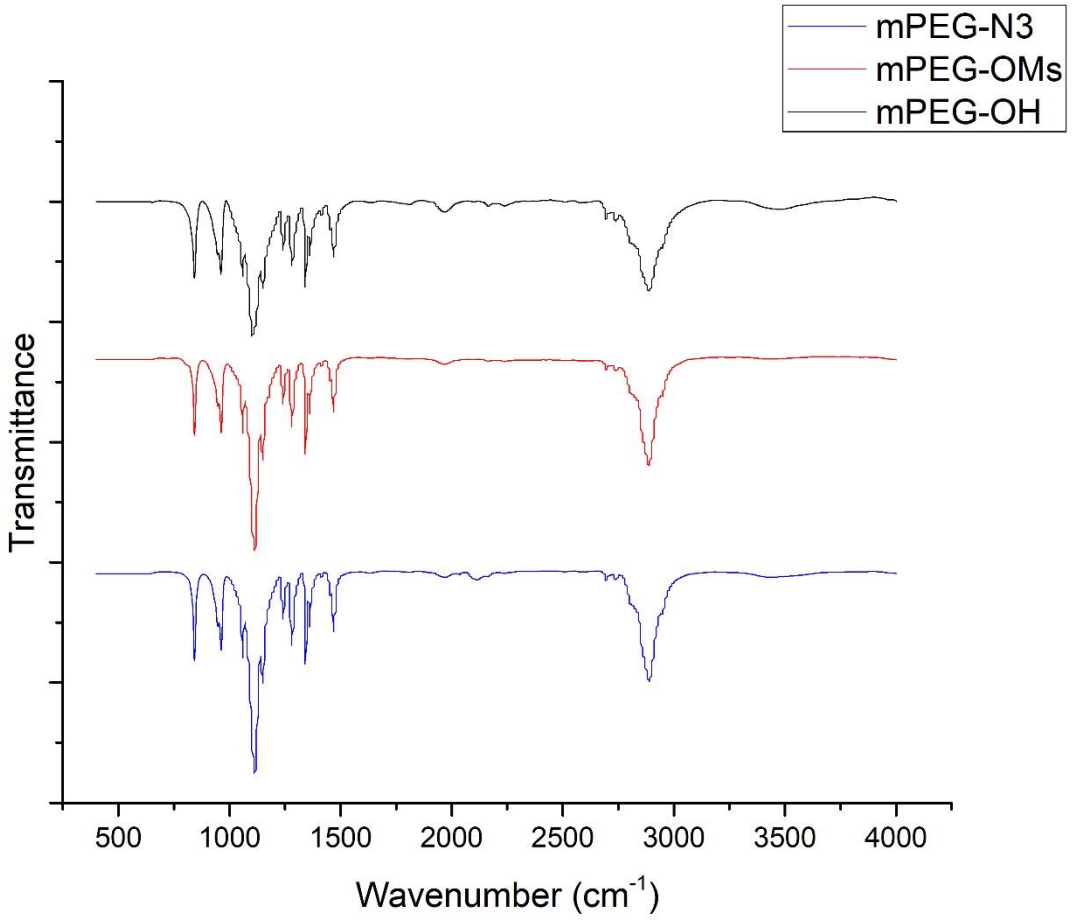

Figure S. 4 IR Spectra of mPEG-OH, mPEG-OMs, mPEG-N_3

5. GPC Graph

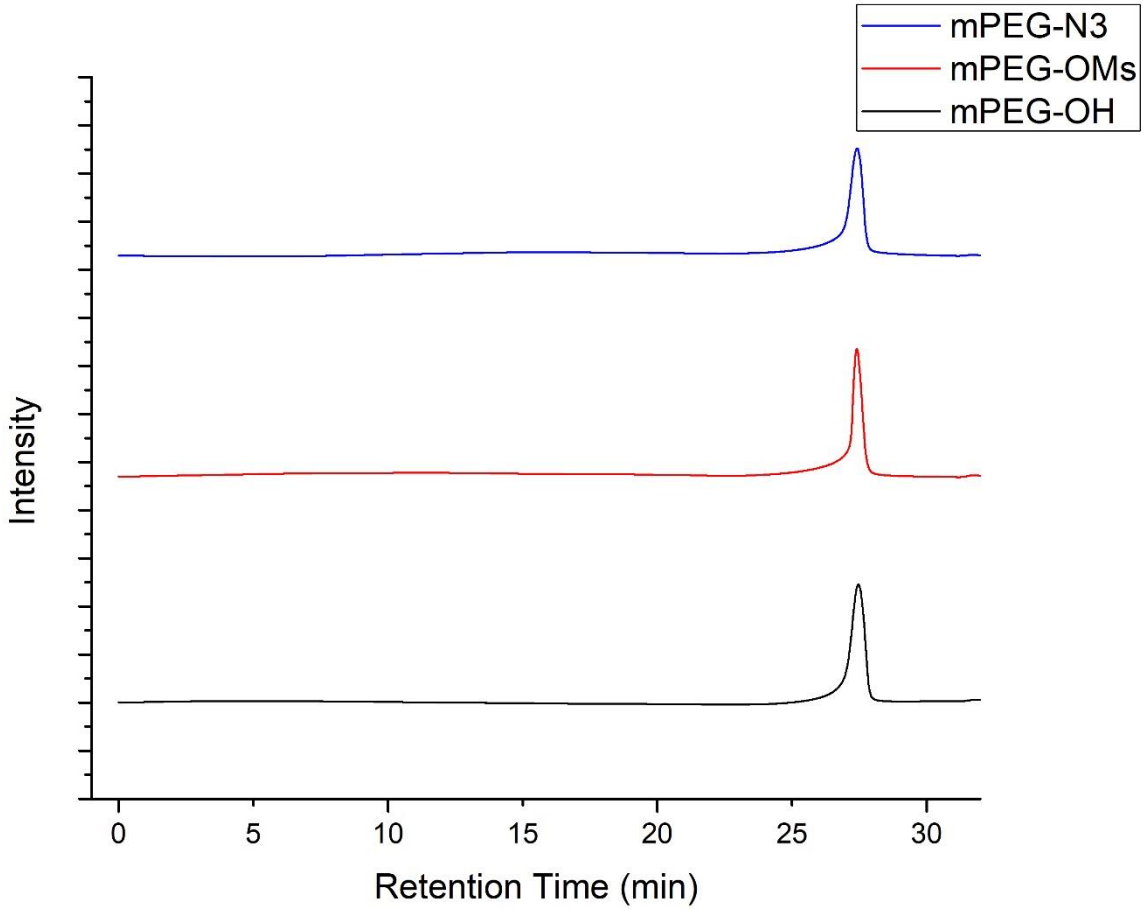

Figure S. 5 GPC Spectra of mPEG-OH, mPEG-OMs, mPEG-N_3

6. Elementary Analysis

Table S. 4 Alg-A Elementary Analysis

	Degree of substitution	Purity
Alg-A1	15.53%	73.98%

Alg-A2	19.62%	78.84%
Alg-A3	23.70%	75.69%